DOI: 10.15477/SZE.MMTDI.2015.002

Orsolya Katalin Kegyes-Brassai

Earthquake Hazard Analysis and Building Vulnerability Assessment to Determine the Seismic Risk of Existing Buildings in an Urban Area

PhD Dissertation

Supervisor: Professor Dr. Richard P. Ray PhD
Department of Structural and Geotechnical Engineering
Faculty of Engineering Sciences, Széchenyi István University, Győr, Hungary

Interdisciplinary Doctoral School of Engineering
Faculty of Engineering Sciences, Széchenyi István University, Győr, Hungary

2014

DOI: 10.15477/SZE.MMTDI.2015.002

Declaration

Name:	Orsolya Katalin Kegyes-Brassai
Email:	kegyesbo@sze.hu
Title of the dissertation:	Earthquake Hazard Analysis and Building Vulnerability Assessment to Determine the Seismic Risk of Existing Buildings in an Urban Area
Supervisor:	Professor Dr. Richard P. Ray PhD
Department:	Department of Structural and Geotechnical Engineering Faculty of Engineering Sciences, Széchenyi István University, Győr, Hungary
Year:	2014

I hereby declare that this PhD dissertation was written by me and that I used only the designated references. All information in this document has been obtained and presented in accordance with academic rules and ethical conduct. I also declare that, as required by these rules, I have fully cited and referenced all material and results that are not original to this work indicating the source.

Győr, 1st of September 2014 _____

Orsolya Katalin Kegyes-Brassai
PhD candidate, senior lecturer

DOI: 10.15477/SZE.MMTDI.2015.002

Acknowledgement

First of all, I would like to extend my appreciation to my supervisors. Dr. Béla Csák introduced me to the world of research and encouraged me to deepen in questions of earthquake engineering. With his supervision I spent my first years focusing on the topic of plastic hinges, finally I have found my very specific topic of earthquake risk analysis. Many thanks to Dr. Richard P. Ray for his valuable help in professional questions and encouragement throughout the last two years of this risk analysis project, which I have started in September 2012. I would like to express my appreciation to the head of department Dr. Róbert Szepesházi, who stayed by me and helped during the PhD candidate period.

I am expressing sincere gratitude to Péter Tildy, scientific fellow of Hungarian Geological and Geophysical Institute, who arranged the instrumentation for MASW measurements, and who taught me the basics and interpretation of this technique. I would like to thank to Gabriella Mohácsiné Simon, head of the North Transdanubian Environmental Protection and Water Management Inspectorate for allowing me to go through hydrogeological registers free, gathering information about strata for research purposes.

I would like to thank to my fellow Ph.D. students Zsolt Szilvágyi, Ákos Wolf and János Szép, who helped me during this research with enthusiasm and support. I would like also to thank my coworkers for taking off some of the education duties and my students for data collection, and especially to Gábor Radics, who helped me with data arrangement.

Finally, my sincere thanks to my husband and children for their support and patience during the last years. I would like to express my gratitude to my mother who took care unselfish of my children, and to my father, Dr. Csaba Kegyes, who was not only a grandfather playing with the kids, but also an expert in earthquake engineering answering my never-ending questions.

The data collection of the research was partly supported by Széchenyi István University within the framework of TÁMOP 4.2.2. B-10/1-2010-0010 application within the period 1st of September and 28th of December 2012.

Data processing of the research was supported by the European Union and the State of Hungary, co-financed by the European Social Fund in the framework of TÁMOP 4.2.4. A/2-11-1-2012-0001 ‘National Excellence Program’ from 1st October 2013.

DOI: 10.15477/SZE.MMTDI.2015.002

Summary

Determining the earthquake risk of buildings in a town or settlement has lately become a more prominent issue. The research can provide important data for governments, authorities, disaster management and insurance companies to better understand risks to many buildings and engineering systems rather than a single building. By this assessment process they can make better decisions about remedial actions, insurance underwriting, and evacuation and rescue. This research addresses the rapid evaluation of a large number of similar buildings in the area of Győr, Hungary. The steps involve: determination of the hazard, assessing building stock, and computing vulnerability.

In order to determine the earthquake hazard of the area, the vulnerability of the buildings, and the earthquake risk of the city, a very large database is needed. Concerning data collection, two very important expectations must be fulfilled: (1) the data should be accurate and suitable for the given goals; and (2) the assessment must be performed within an acceptable period of time and within a modest budget. One goal of the research is to develop methods of data collection that fulfill the above requirements in order to give a reproducible chain of processes for risk analysis. Other goals of the research focus on data processing and in determining and performing validation.

Additionally, shear wave velocity profiles have been determined for many areas within Győr. Extensive use of historical boring logs allowed for correlations and reasonable extrapolation of soil performance throughout the area. This has led to a pattern of soil layer distributions and delineates several different soil zones for Győr. Compared to more simplified profile standards from building codes, it can be clearly seen that the different levels of hazard concerning Győr are apparent, even though almost all of the region belongs to soil category C based on EC8 (European Committee for Standardization, 2013).

Another task of the research was to categorize buildings and assess their seismic vulnerability. This was accomplished through visual screening methods which were then verified by more detailed push-over analysis of typical buildings. Based on building vulnerability characteristics, the city districts have been divided further into smaller zones.

Finally the overall seismic risk of the designated area has been evaluated based on different scenarios. Two maps; one depicting seismic hazard, the other displaying building vulnerability have been overlaid resulting in a detailed zonation of seismic risk. Based on this visualization, engineers can better plan to make improvements to infrastructure, determine insurance rates for protection, and plan for emergency activities in case of a seismic event.

DOI: 10.15477/SZE.MMTDI.2015.002

Summary in Hungarian

Városok vagy települések épületeire vonatkozó földrengéskockázat meghatározása az utóbbi években előtérbe került feladatkör. Erre a témakörre irányuló kutatás fontos adatokat szolgáltathat a kormányzatok, a hatóságok, a katasztrófavédelem és a biztosítók számára, hogy jobban megértsék több épület és mérnöki szerkezet együttes kockázatát nemcsak egy különálló épülettét. Ez az értékelési folyamat lehetővé teszi, hogy jobb döntéseket hozzanak a megelőző tevékenységekben, a biztosítások megkötésekor illetve mentés esetén. A kutatás nagyszámú hasonló épület gyors elemzését mutatja be Győr területén. A lépések a földrengés veszélyeztetettség, épületállomány értékelését és szeizmikus sérülékenység meghatározását foglalják magukba.

Ahhoz hogy egy terület veszélyeztetettsége, az épületek sérülékenysége és a város földrengéskockázata meghatározható legyen, egy hatalmas adatbázisra van szükség. Az adatok gyűjtése kapcsán két nagyon fontos elvárásnak kell eleget tenni: a megadott célokhoz igazodóan az adatok pontossága megfelelő kell, hogy legyen, egy elfogadható időtartamon belül, mindezek mellett alacsony költségvetéssel. A kutatás egyik célja, hogy az előbbi követelményeknek megfelelő adatgyűjtési módszereket kifejlessze, hogy a földrengéskockázat egy megismételhető folyamat láncolatát adja meg. A kutatás másik célja az adatfeldolgozásra, az ellenőrzési módok meghatározására és azok végrehajtására összpontosít.

A kutatás egyrészt minden fúrás esetében meghatározza a nyíróhullámok terjedési sebességét összehasonlítva a mért adatokkal, azért, hogy a talajrétegek eloszlásának mintázata azonosítható legyen, valamint Győr különböző talaj zónái körülhatárolhatóak legyenek. A szabványokkal összehasonlítva egyértelműen látszanak a különböző veszélyeztetettségi szintek Győrben, annak ellenére, hogy Győr teljes területe C talajosztályba sorolható az EC8 szerint.

Másrészt a kutatás csoportosítja és elemzi az épületeket épületsérülékenység szempontjából. Szemrevételezési módszerek és a tipikus épületek részletesebb *„pushover”* elemzésének összehasonlítása a következő lépés. A városrészek tovább oszthatóak kisebb zónákra sérülékenységi jellemzők alapján.

Különböző szcenáriók alapján lett meghatározva a kijelölt terület földrengéskockázata. A veszélyeztetettséget ábrázoló és az épületek sérülékenységét bemutató két térkép egymás fölé helyezése a földrengéskockázat részletes zónáit eredményezi. Ez a képi megjelenítés megalapozhatja a mérnökök infrastruktúrát érintő fejlesztéseit, a védelemhez szükséges biztosítási arányok meghatározását és földrengés eseményre vonatkozó katasztrófavédelmi tervek készítését.

DOI: 10.15477/SZE.MMTDI.2015.002

Table of contents

DOI: 10.15477/SZE.MMTDI.2015.002

DOI: 10.15477/SZE.MMTDI.2015.002

DOI: 10.15477/SZE.MMTDI.2015.002

DOI: 10.15477/SZE.MMTDI.2015.002

DOI: 10.15477/SZE.MMTDI.2015.002

Chapter 1. Introduction

Recent earthquakes throughout the world with a high number of casualties and enormous devastation proved that natural disasters should not be ignored. Preventive (pre-event) approaches have received greater attention recently since post-event evaluation methods are effective only in areas of regular seismic activity. Research in earthquake hazard mitigation has focused on evaluating possible damage scenarios for different magnitude events (Luco, et al., 2007) (Committee on National Earthquake Resilience, 2011).

Although seismic events are rare in many places, they are characterized by high exposure and their economic and social effects cannot be neglected. The vulnerability increases with extending urban areas. As long as accurate forecast methods concerning earthquakes are not available the only alternative is to decrease vulnerability in urban areas. To reduce the potential damage, a comprehensive assessment of the seismic risk followed by a package of relevant remedial measures is needed. This requires an analysis of potential losses in order to make recommendations for prevention, preparedness and response.

Hungary has experienced destructive earthquakes in the past; most significant was the event of 1763 in Komárom (Varga, 2014) with estimated intensity of IX, and an intensity of VII-VIII in Győr according to European Macroseismic Scale (Grünthal ed., 1998). Another large earthquake affecting Győr happened in 1850 with an intensity of VII. Although such events are very rare, their intensity is comparable to the major earthquakes such Northridge earthquake (California 1994) with an intensity of IX according to Modified Mercalli Intensity Scale (Southern California Earthquake Center, 2001), being the second costliest disaster in US history after Hurricane Katrina (Martinez, 2014).

The goals of the research are: to present the process of seismic risk evaluation of a town; to integrate local site effects to previously determined seismic hazards (GeoRisk Earthquake Engineering Ltd., 2006); to examine the vulnerability of the built environment focusing on residential and public buildings; and finally to combine the results and map risk scenarios to aid in the mitigation process. The designated area to perform seismic risk assessment is Győr, being the sixth largest city of Hungary with an important regional economic and political role. Since no major damaging earthquake has occurred in Győr recently, vulnerability functions from observed damage patterns are not available. Therefore a simple and fast evaluation method is proposed suitable for the assessment of local soil effects and evaluation of a large number of buildings.

DOI: 10.15477/SZE.MMTDI.2015.002

1.1. Research context

Assessment and management of earthquake risk requires several disciplines and different aspects to evaluate. Risk is defined as the expected loss (of lives, persons injured, property damaged, and economic activity disrupted) due to particular hazard for a given area and reference period. Based on mathematical calculations, risk is the product of hazard and vulnerability. Different approaches have suggestions for further clarification of the formula, taking into account exposure or costs. Considering earthquakes, the process of risk evaluation consists of several steps performed in parallel.

One line of the research deals with paleoseismic study to identify historical and recent seismicity of the area, identifying potential sources, usually along fault systems, for probabilistic hazard assessment. The next step focuses on the simulation of strong ground motions for regional hazard assessment. Ground motion attenuation models are calibrated based on observed strong motion recordings and on theoretical computations taking into account realistic models for wave propagation as well as possible seismic source zones. Further research takes into account local site effects and will result in a microzonation for the evaluated area based on data of the local soil conditions and field testing of the soil properties.

Another line of research focuses on the built environment. It requires a comprehensive database of buildings and other structures, lifelines and natural features that may be susceptible to failure during a seismic event such as hillsides, river channels, and coastlines vulnerable to tsunami or seiche activity. Vulnerability functions are established for these features, describing the expected damage as a function of the seismic input. The results of these studies are then mapped, allowing for visualization of the expected damages from different earthquake scenarios. Use of a GIS-based system has become essential in urban disaster management, since most data has a spatial component and also changes over time.

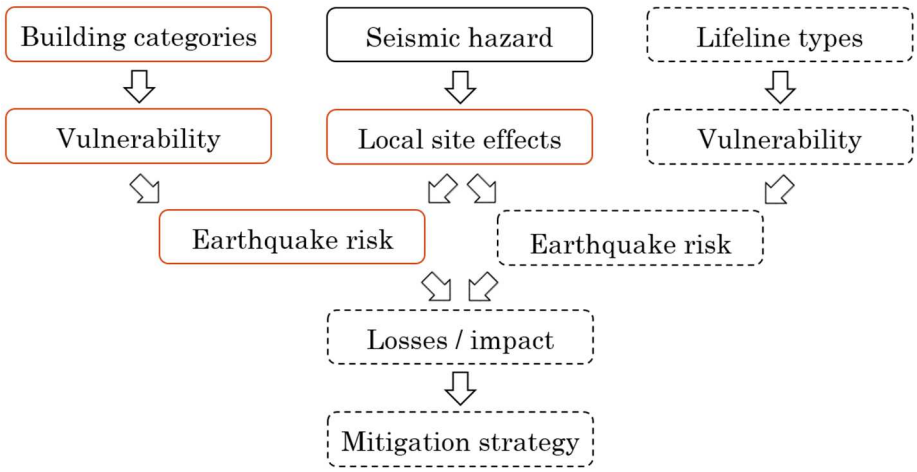

1.1. Figure: Flowchart of the method

DOI: 10.15477/SZE.MMTDI.2015.002

Figure 1.1 represents the methodology of risk assessment. The steps concerning the research about risk assessment of Győr are indicated with red solid lines. Parallel or further possible investigations are indicated with dashed lines.

1.1.1. Actuality of the theme

SHARE (a Collaborative Project in the Cooperation program of the Seventh Framework Program of the European Commission) has published the European Seismic Hazard Map showing the 10% exceedance probability in 50 years for Peak Ground Acceleration in 2013. This map provides the recent achievements concerning seismic hazard assessment in Europe and highlights that higher values of expected earthquakes can happen throughout Europe in the future. One of the SHARE members, F. Cotton, warns the public that greater earthquakes should be expected than e.g. the historical earthquake in Basel 1356, which destroyed a part of, France, Switzerland and Germany (Szentendrei, 2013).

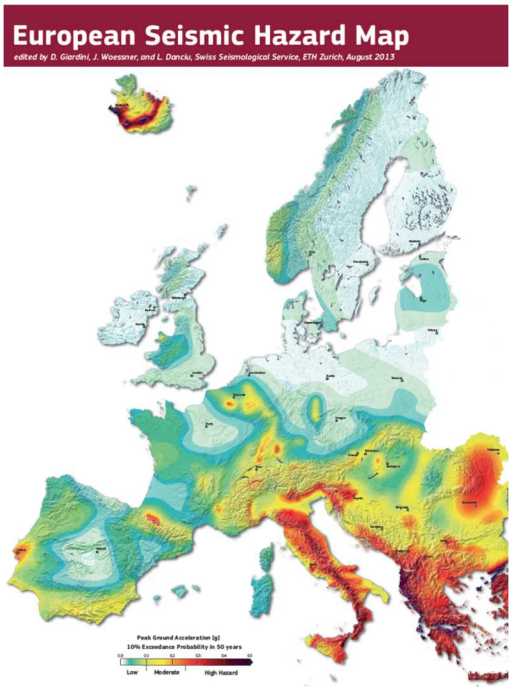

1.2. Figure: European Seismic Hazard Map 2013 (Giardini, et al., 2013)

The Basel earthquake in 1356 can be characterized with a 6.3 magnitude and an intensity of IX on EMS scale. The seismic hazard of the Basel region is comparable to that of Mór - fault (close to Győr), and 1356 Basel earthquake is comparable to the 1763 Komárom earthquake. Seismic risk of Basel has been investigated recently, a seismic microzonation of Basel was performed in 2012 (Wenk & Fäh, 2012) and vulnerability assessment of buildings has been carried out in the year 2000 (Lang & Bachmann, 2004).

Beside the SHARE project; several others have been funded by the European Commission in order to evaluate seismic hazard, vulnerability and risk across Europe. These topics have become more important in the last 10 to 20 years. Ongoing projects (NERIES, 2006-2010) (SYNER-G, 2009-2012) emphasize this is a topic the research community works on worldwide. The NERIES project provided an initial set of tools for services in the context of seismic hazard and risk, in addition to improving access to seismological data and infrastructure across Europe. SYNER-G focused on systemic seismic vulnerability and risk analysis of buildings, lifelines and infrastructures providing e.g. the Fragility Function Manager to visualize and assess fragility functions for buildings and infrastructures.

DOI: 10.15477/SZE.MMTDI.2015.002

1.1.2. Importance of the research

Scientists around the world have made a great effort concerning seismic hazard assessment, vulnerability evaluation and risk management in order to mitigate the consequences of a possible earthquake. The next quote clearly states the importance of the work in seismic risk assessment: *"The fundamental role of the seismic risk assessment for the society is to provide all the information for each community or organizations to support the risk mitigation decision-making. These decisions are generally related to the likelihood and significance of structural collapse to the life-safety or business interruption. Hence a high risk of structural collapse is not accepted by the current standards and there are various methods available for making decisions to reduce that risk."* (ETH Zurich, 2013)

It is high time for Hungarian scientist and engineers to pick up the pace with the scientists in Europe and to determine the seismic risk of those major cities, which have experienced destructive earthquakes in the past. This research about the seismic risk of the city of Győr is trying to set an example concerning this important topic.

1.1.3. Hungarian overview

Seismicity in the Pannonian Basin is more moderate compared to seismicity of surrounding areas, and is particularly difficult to decide whether the epicenters occur at isolated places or along elongated zones when the statistical significance of the data is so low.

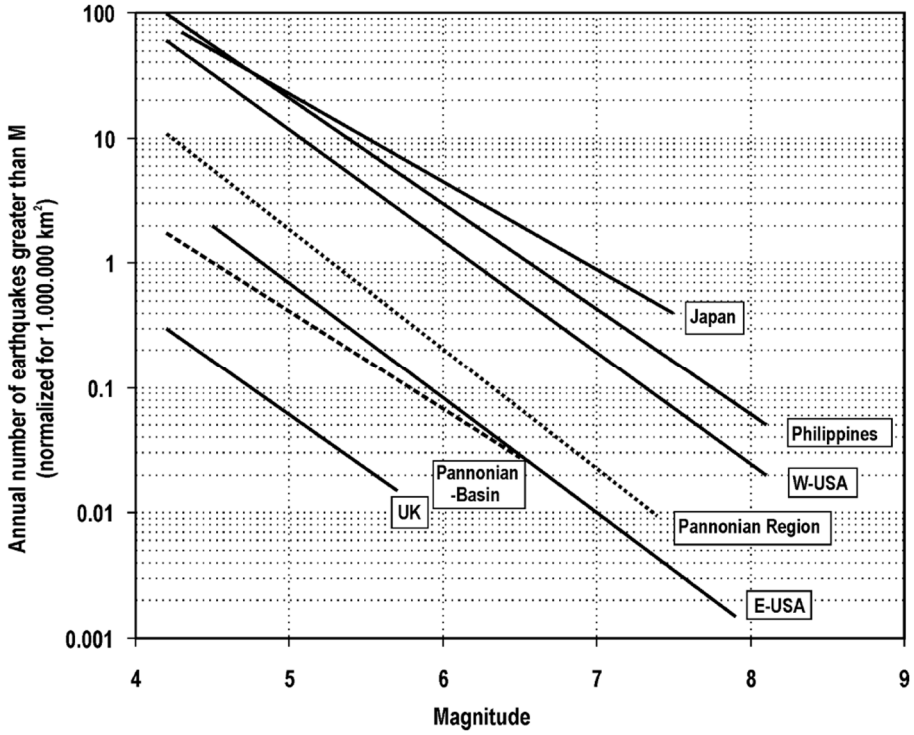

1.3. Figure: Annual number of earthquakes in seismically different parts of the World (Tóth, et al., 2002)

The recent high quality of earthquake observations and epicenter determinations compared to historical assessments show that recent earthquakes, in general, lie near to clusters of historical activity. It can be stated that at several individual locations earthquakes occur repeatedly. For example the Komárom and Mór area produced significant activity during a specific, but limited, period of time. Moderate seismicity does not necessarily equate to a moderate size of earthquakes: reports of major earthquakes often refer to heavy building damage and liquefaction (e.g. 1763 Komárom earthquake). These observations indicate that magnitude 6.0–6.5 earthquakes are possible but infrequent in the Pannonian Basin. Stronger present-day activity has been detected in the north-eastern part of the Transdanubian Mountains and at the Danube Bend. (Horváth, et al., 2009)

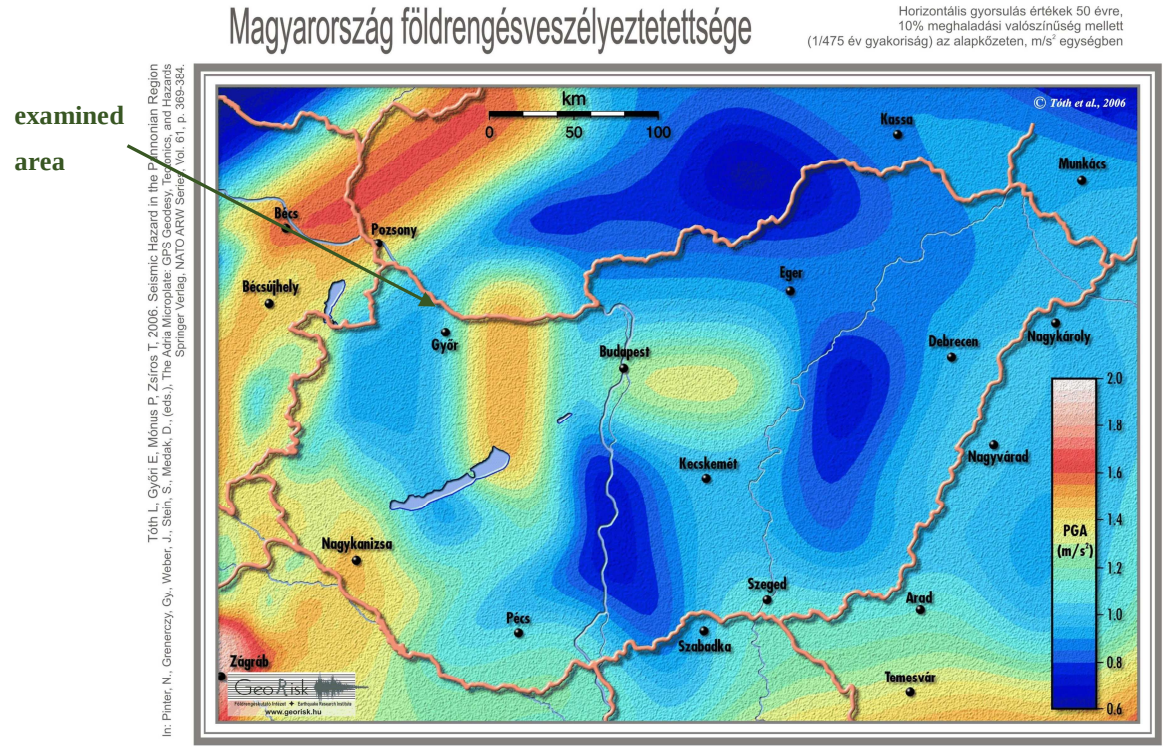

1.4. Figure: Seismic Hazard Map of Hungary (GeoRisk Earthquake Engineering Ltd., 2006)

The Seismic Hazard Map of Hungary (Figure 1.4) has been created by Tóth et al. (2006) and it is an attachment of the Hungarian National Annex of EC8 (European Committee for Standardization, 2013). The map shows that the level of ground motion in the most hazardous areas of Hungary ranges between 0.12-0.15 g PGA (i.e. Peak Horizontal Ground Acceleration) at bedrock with 10% probability of exceedance (GeoRisk Earthquake Engineering Ltd., 2006). The range 0.12-0.15 g translates to PGA = 9.807×0.12 = 1.177 m/s^2 and 9.807×0.12 = 1.471 m/s^2. It displays the ground shaking (PGA) to be reached or exceeded with a 10% probability in 50 years, corresponding to the average recurrence of such ground motions every 475 years,

DOI: 10.15477/SZE.MMTDI.2015.002

as prescribed by the national building codes in Europe for standard buildings. This hazard is comparable to seismic hazard of other European countries, where attention was given to assessing and managing risk in order to mitigate the consequences of such an event.

Nevertheless, little attention has been paid to these questions in Hungary; there is even a debate between engineers that the values of PGA should be reduced with 0.7 in the National Annex of EC8 (Dulácska, 2009). Compared to the European Seismic Hazard Map, it can be clearly seen that the values of PGA in the Seismic Hazard Map of Hungary are lower than the recently published PGA values of European Seismic Hazard Map. The difference e.g. at Mór-fault is more than 25%: it is 0.15 g according to the Seismic Hazard Map of Hungary and more than 0.2 g according to European Seismic Hazard Map. Even in case of Győr (Figure 1.5) the value can be higher than 0.12 g based on European Seismic Hazard Map (0.13-0.14 g). The suggestion of reducing the PGA by 0.7 could cause the buildings to be designed only to an expected PGA of 0.084 g in case of Győr and 0.105 g in case of Komárom compared to 0.2 suggested by the SHARE researchers. It should be even emphasized that the values of hazard maps are based on probabilistic approach and offer an average value, which means that there is a chance of occurrence of quakes with even higher values.

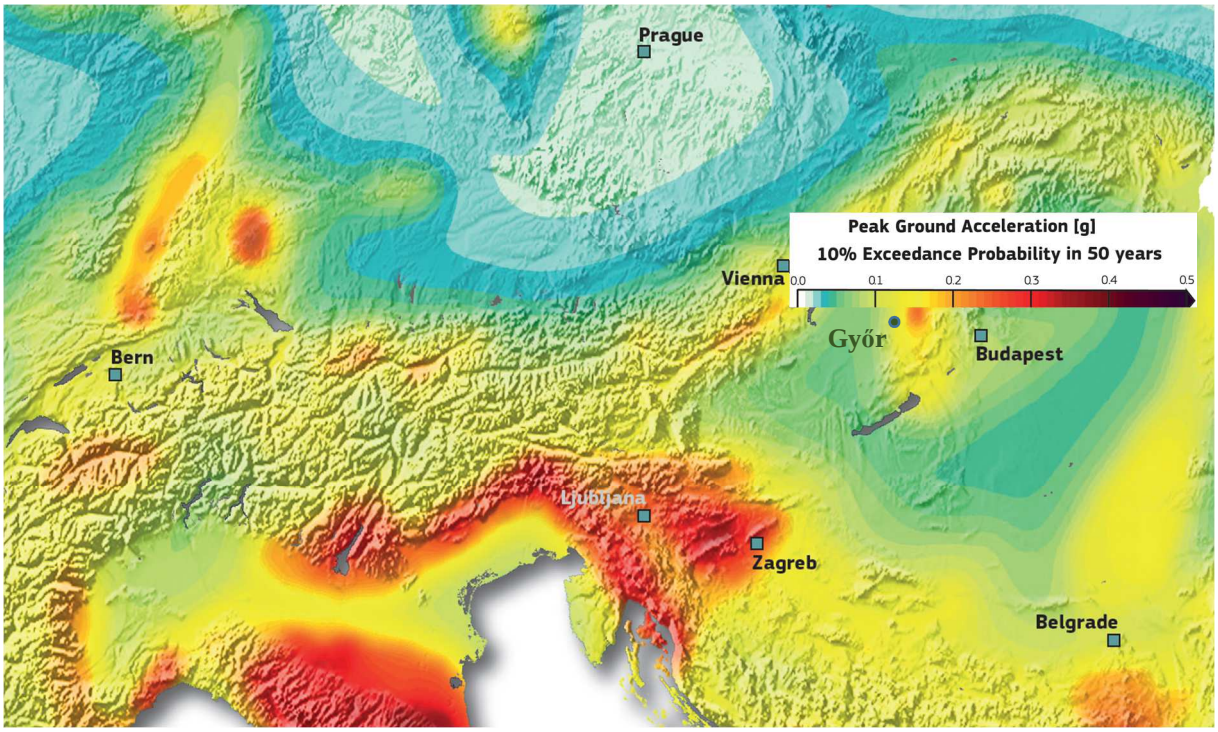

1.5. Figure: Part of European Seismic Hazard Map 2013 (Giardini, et al., 2013)

Taking a closer overview of the area other hazards connected to earthquakes should be evaluated. Liquefaction occurs in loose to medium dense saturated granular soil when earthquake shaking level that is strong enough to generate excess porewater pressure; reducing

DOI: 10.15477/SZE.MMTDI.2015.002

the effective stress in the soil nearby to zero and causing loss of support for buildings, soil embankments and other structures relying on its support. Based on the research of Győri et al. (2004) there is a considerable liquefaction potential in some parts of Hungary; Győr is included in these regions. (Figure 1.6)

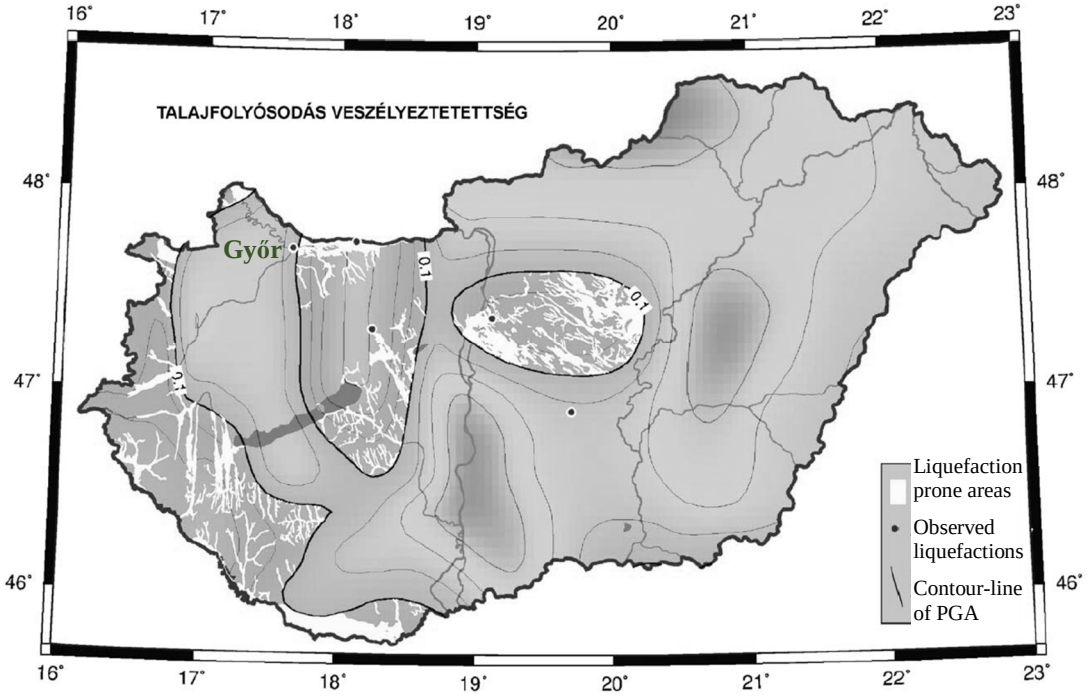

1.6. Figure: Liquefaction hazard of Hungary (Győri , et al., 2004)

The results of seismic hazard assessments are further used by engineers to appropriately design any type of building, thus the results are widely used and important information. Taking into account the Hungarian situation according to seismic risk, the other major issue is related to the built environment. It is important to note that a greater part of Hungarian buildings were not designed to resist earthquake loads. The first buildings to be designed taking into account the seismic loads were the large panel cast buildings in the seventies. The rest of the buildings of this era and earlier were designed only to resist wind load.

The seismic hazard, vulnerability, and earthquake risk is underestimated by both engineers and authorities or is not properly quantified as indicated in the next quotation. From a risk management point of view the seismic risk is considered very low, as stated on the homepage of Győr-Moson-Sopron County Emergency Management Directorate. *"The county in terms of earthquake risk does not include itself among the hazardous counties." "Experience has shown that magnitude 2 to 3 earthquakes on the Richter scale occur only in 120 or 180 years. It is therefore concluded that the county is not seismically hazardous, but definitely has to be considered."* (Győr-Moson-Sopron County Emergency Directorate, 2014) This fact underlines the necessity of the hazard and vulnerability assessment of major cities (at least).

DOI: 10.15477/SZE.MMTDI.2015.002

1.2. Background

Calculating earthquake risk requires the cooperation of several disciplines. To narrow down the focus, the earthquake risk affecting buildings can be calculated with the help of two bordering disciplines: seismology and engineering. Based on data obtained by seismological studies and earthquake engineering research, regional hazard assessment and microzonation maps can be constructed. They consider the local site effects and a significant database of buildings with computed vulnerability. Earthquake risk can be assessed as:

$$\text{RISK} = \text{HAZARD} \times \text{VULNERABILTY} \tag{1.1}$$

The "multiplication" of Eq. 1.1 should be considered a convolution of two large sets of data: the earthquake hazard data which describes the intensity and probability of an earthquake event and the vulnerability data that estimate the performance of a variety of building types to different levels of seismic loading taking into account different factors respectively (Table 1.1). The risk is then the proportion of buildings that are likely to fail (considered as collapse, structural damage, or loss of operation).

1.1 Table: Factors to be considered at hazard analysis and vulnerability assessment

Factors affecting earthquake hazard:	Factors affecting building vulnerability:
• type of soil; • thickness of layers; • lateral variation of layers; • dynamic properties of strata; • local site effect; • the potential of liquefaction; • master faults; • historical earthquakes, etc.	• construction system and period; • quality of materials, workmanship; • regularity in plan and elevation; • position of the building; • adjacent buildings; • changes in function; • previous damages, state of the building; • dynamic characteristics, etc.

To obtain an overall view concerning the expected damage beside the vulnerability analysis of a region or a settlement the vulnerability analysis of lifelines and industrial facilities should be performed and socioeconomic effects should be taken into account.

1.2.1. Research problems

Two widely different approaches exist to determine the risk of an earthquake; one considers the effect of previous earthquakes, listing the damaged buildings and casualties. The other offers a method to evaluate possible damages prior to an event. The latter method facilitates prevention by gathering information about the state of the building stock and the expected damages, so the authorities can strengthen the most vulnerable buildings in order to mitigate risk.

The challenge with this method is that many uncertainties must be taken into consideration. In order to determine earthquake risk within towns a fast and simple method should be developed. Otherwise it would be very time-consuming and require too much expert participation.

The steps are the following:

- determine the hazard intensity and the probability of occurrence of an earthquake,
- assess the building stock for resistance to earthquake loading.

With given input parameters of subsoil and PGA (peak ground acceleration) and the estimated vulnerability, the damage based on building classes can be obtained, and various risk scenarios can be derived.

1.2.2. Research objectives

This research addresses the rapid evaluation of a large number of similar buildings in the area of Győr. The steps include determination of the hazard, assessing building stock, and computing vulnerability by different methods.

Objectives concerning the research are:

- review the literature concerning seismic hazard;
- review the literature about vulnerability and earthquake risk assessment;
- study the geographical and geomorphological formation of the investigated territory;
- study the tectonics of the area;
- study the development of the city;
- determine the typical building construction periods;
- collect data about the soil profiles within and around Győr in order to determine the seismic hazard of the town;
- collect data about the building stock of Győr in order to determine the vulnerability of the buildings;
- develop data collection and validation procedure in a very specific Hungarian context;
- analyze soil parameter data to define the effect of local soil profiles;
- analyze building data to determine their vulnerability;
- divide the area of study into zones of similar hazard level;
- evaluate the levels of seismic risk to the selected building stock;
- develop the methodology for seismic risk analysis of a town, taking into account local soil effects and behavior of the buildings.

In order to achieve the goals of the research it was necessary to construct a method to fulfill the requirements of being accurate enough but reach the aims within an acceptable period of time using little resources. Compared to other methods, it should give a more accurate overview of the local site effects and should take into account the factors that contribute to the dynamic behavior of the buildings.

1.2.3. Motivation

The seismicity of Pannonian region is moderate. Earthquakes causing light damages occur every year, while stronger, more damaging magnitude 5 quakes happen about every 20 years and the return period of magnitude 6 events is about 100 years (Tóth, et al., 2006). The focal depth of earthquakes is between 6 and 15 km below ground level in the Pannonian region. With this earthquake hazard level, Hungary ranks with the medium-hazardous countries.

Since events that cause damage occur only every 15-20 years, there is very little data concerning how buildings and other facilities will perform under such conditions. Anecdotal data from previous events suggest that the damage can be significant. Considering the historical increase in Győr, and other similar towns, in building height, mass, and unsupported span distances, and one must seriously consider the possibility of a much higher seismic vulnerability in newer (post 1900) construction. Of course, building material technology has advanced as well, but there is no evidence that such an advance automatically translates to a safer structure under seismic loading.

Predicting the likely consequences of an earthquake to a city or an individual facility is generally covered by the scientific field of earthquake risk assessment, a relatively young discipline. It requires the expertise and knowledge of a number of research areas such as:

- seismology, seismic hazard assessment,
- geology and tectonics,
- geotechnical and structural (earthquake) engineering,
- other connecting fields, like:
    - urban land-use planning,
    - insurance industry,
    - disaster management.

It is a challenge to get expertise in these areas to generate reliable estimates of expected physical damage in case of an earthquake. Further research could focus on the economic and social losses that are connected to the damages. Motivation of this work is to contribute to the prevention of future losses in the capital of Western Transdanubia region.

DOI: 10.15477/SZE.MMTDI.2015.002

1.3. Outline

The structure of the thesis follows two parallel lines of the research: one is the assessment of seismic hazard, the other is the investigation of building vulnerability. First data collection is presented, then data processing for both research lines, finally these lines are combined in risk evaluation.

1.3.1. Available and collected data

For seismic risk assessment, data is needed concerning the soil stratigraphy and built environment in accordance with the objectives of the research. The greatest challenge of this project was the lack of data and financial support. Nevertheless, the data should be accurate and suitable for the given goals and accomplished within an acceptable period of time. The mentioned TÁMOP support was not enough to cover the costs of borings, CPT tests nor information about buildings. Therefore sources had to be found where the information is hidden or had to be organized into a coherent whole. First, a checklist was developed about building properties, and with the help of trained staff (in this case, students) information about more than 5000 buildings was gathered. Next, the idea came from one colleague to check the hydrogeological registers for soil layer information. Graciously donated CPT data and MASW measurements performed with the help of Péter Tildy served the basis for soil properties examination. Data collection methods will be presented more deeply in Chapter 5.

1.3.2. Research methodology

The research methods consisted of:

- Hazard activities
    - collecting historical soil data throughout Győr;
    - processing and validating historical soil data with present day information;
    - measuring soil shear wave velocity at selected locations;
    - extending shear wave velocity estimates throughout the city by correlating measured data to historical data;
    - modeling site response by one dimensional response analysis;
    - comparing response analysis to code (EC8) profiles;
    - using site response analysis to determine seismic demand;
- Vulnerability activities
    - designing methods to collect building data then actually collecting it;
    - processing and validating building data;
    - analyzing typical buildings to generate vulnerability functions;
- Risk activities
    - comparing seismic demand to vulnerability to determine risk;
    - mapping risk for different areas of the city and scenarios.

DOI: 10.15477/SZE.MMTDI.2015.002

1.3.3. Dissertation Structure

First, literature concerning seismic hazard, vulnerability and earthquake risk assessment is reviewed in the context of application to the assessment process, presented in Chapters 2 and 3 with international and Hungarian examples.

Second, a more detailed description of geologic formations, the tectonics and geomorphology of the area and its influence on the near-surface seismic behavior is presented in Chapter 4. Additionally, information on the built environment with respect to construction methods, materials and their evolution with time are evaluated throughout the town region. These formed the base of the preparation of the checklist and further building investigation.

A great part of the work has been in processing the data and in determining and performing validation in Chapter 6. The MASW method was used to measure v_s (shear wave velocity) profiles of the various soil types in and around Győr. CPT data, using empirical relations based on Wair et al. (2012) allowed further v_s profiles to be generated (Wair, et al., 2012). A regression technique to determine the variation of v_s parameters with depth allowed a more general application of shear wave profiles and delineation of soil zones. Based on the zoning, one-dimensional site response analyses were applied and compared to EC8 standards.

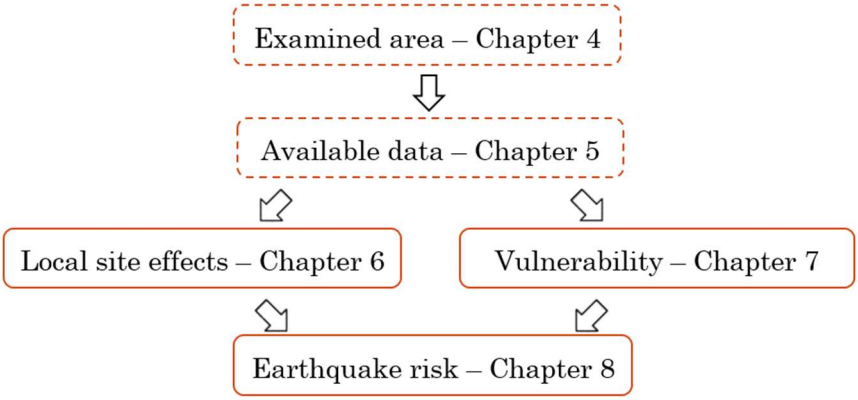

1.7. Figure: Structure of the dissertation

Next, the research deals with the built environment with emphasis on residential and public buildings. Method of building classification and evaluation of their seismic performance is presented in Chapter 7. Visual screening, lateral force analysis, spectrum approach and push-over methods are discussed.

Finally Chapter 8 presents the evaluation of the overall seismic risk on the designated area based on different scenarios. Two maps, one depicting seismic hazard, the other displaying building vulnerability were overlaid resulting in a detailed zonation of seismic risk. Based on this visualization, engineers can better plan to make improvements to infrastructure, determine insurance rates for protection, and plan for emergency activities in case of a seismic event.

DOI: 10.15477/SZE.MMTDI.2015.002

Chapter 2. Theoretical background

Earthquakes are naturally occurring, vibratory ground motions, resulting from a number of causes including tectonic ground motions, volcanism, landslides, and so on. Most common cause of earthquakes is tectonic-related, caused by the fracture and sliding of crust along faults. Earthquakes initiate a number of phenomena, called seismic hazards, which can cause significant damage to the built environment. These include ground shaking as the most dominant effect, ground rupture, and various kinds of ground failure (liquefaction, landslides). Further damages might occur as secondary effects, such as fires following the earthquake, etc.

Seismic hazard is the potential threat to human society that is caused due to earthquakes. Neither the earthquakes nor the secondary effects can be prevented. Generally, seismic hazard assessment attempts to quantify the level, intensity and frequency of ground shaking and the probability of occurrence.

The aspect of whether something is closely connected to seismic hazard or not is described by **exposure**. Due to vulnerability, several aspects are subject to potential seismic risk: e.g. people can be injured or killed by earthquake effects; functionality can be impaired or lost. Financial consequences are related to business interruption, repair costs of damaged buildings, and repair or replacement costs of the critical infrastructure.

Vulnerability represents the link between building or structural damage and the earthquake effects and defines loss as a function of ground shaking, which are specific to different elements of the built environment. These functions can be developed statistically, analytically or based on expert opinions. From a probabilistic point of view, fragility functions can be derived defining the probability of some undesirable result as a function of ground shaking levels. Analogous vulnerability functions can provide a damage factor, given the intensity of the earthquake.

Seismic risk refers to the social and economic consequences resulting from earthquakes. Seismic risk assessment implies the identification and characterization of the potential seismic hazard and evaluation of existing conditions of exposure and vulnerability. The risk can be expressed in absolute terms such as the risk of collapse or in probabilistic terms, such as estimate of damage and economic loss or casualties.

Seismologists, geologists, and engineers work together to assess the potential seismic hazard and vulnerability to develop appropriate measures and remedies, so that e.g. buildings do not collapse during an earthquake.

DOI: 10.15477/SZE.MMTDI.2015.002

2.1. Seismic hazard

"Earthquake is a term used to describe both sudden slip on a fault, and the resulting ground shaking and radiated seismic energy caused by the slip, or by volcanic or magmatic activity, or other sudden stress changes in the earth." (US Geological Survey, 2014) The hypocenter or focus is the point within the earth where an earthquake rupture starts and the projection of it on the Earth surface is the epicenter. The released energy creates seismic waves that propagate from hypocenter in every direction causing the lithosphere to shake.

The severity of this ground motion depends on different factors, such as geologic and topographic conditions of the area, initial frequency content of the vibration, and the directionality of the fault release. The size of an earthquake determines the potential damage level if a populated area is involved. The first methods for characterizing the size of earthquakes were based on qualitative descriptions of the effects of the earthquakes. With the development of modern instrumentation, a number of quantitative measures have been developed to describe the size of earthquakes: some expressing the size of earthquake at its source, some describing the intensity of the seismic event on the surrounding territories affected by an earthquake.

The oldest measure of earthquake size is macroseismic intensity or **intensity** offering a qualitative measure of the effects of a seismic event based on observed damage and human reactions near and further away from the epicenter. Commonly used intensity scales around the world are the Modified Mercalli Intensity Scale (MMI) used mainly in US (Wood & Neumann, 1933), European Macroseismic Scale (EMS) applied in Europe (Grünthal ed., 1998) and the Seismic Intensity Scale developed by JMA in Japan (Japan Meteorological Agency, 1996). Historical events were described by these or former intensity scales offering valuable information about the rates of recurrence of earthquakes of different size in various locations, serving as a basis for evaluating the likelihood of seismic hazards.

Magnitude is a quantitative measure of the released energy that characterizes the relative size of an earthquake. Magnitude is based on measurement of the maximum motion recorded by seismographs. There are different scales for measuring magnitude, such as local magnitude (ML) commonly referred to as Richter magnitude, surface wave magnitude (MS), body wave magnitude (MB) and moment magnitude (MW). The first three scales have limited range and applicability and cannot be used in case of large earthquakes. The moment magnitude (MW) scale, is uniformly applicable but is more difficult to compute than the other types. (Tóth & Mónus, 2011)

The increment of the released energy does not result in the same rate of increasing ground-shaking characteristics. For describing the important characteristics of strong ground motion quantitatively, other ground motion parameters are essential. Many parameters have been proposed to characterize the amplitude, frequency content and duration of an earthquake.

The most commonly used single parameter to describe the horizontal motion is the **peak ground acceleration** (PGA or PHA) giving the largest change in velocity recorded by a particular accelerogram. The vertical component of acceleration (PVA) is assumed to be a percentage of the PGA according to codes. PGA does not provide information about the frequency content and duration of the motion, so additional parameters are needed. Other parameters are the peak ground velocity (PGV or PHV), peak ground displacement (PGD) or effective design (or peak) acceleration (EPA). (Kramer, 1996)

If the earthquake takes place in a region where instruments are installed, the entire time history of the earthquake can be recorded and analyzed. Generally this is done with a strong motion seismograph, which measures and records three components of shaking (N-S, E-W, vertical) usually as acceleration for the 1-2 minutes of strong shaking. The time history is digitized and stored for later processing. These time histories may consist of 1.000 -20.000 values spaced 0.001-0.01 seconds apart.

Using Fourier analysis, the amplitude or the phase can be plotted versus frequency, expressing the frequency content of a motion very clearly obtaining a Fourier spectrum. Other spectra describing the frequency of a shake is the power spectrum and response spectrum, being a very powerful tool, since the dynamic response of structures is very sensitive to the frequency of the motion. The **response spectrum** describes the maximum response of single-degree-of-freedom (SDOF) systems to a particular input motion as a function of the natural frequency (or natural period) and damping ratio of the SDOF system. Spectral acceleration (S_a), spectral velocity (S_v) and spectral displacement (S_d) are, respectively, the absolute maximum acceleration, velocity and displacement values of the response of a SDOF system. Spectral parameters are the predominant period, bandwidth, central frequency, shape factor, etc. (Kramer, 1996)

2.1 Table: Ground motion characteristics described by parameters *(Kramer, 1996)*

Ground Motion Parameter	Ground Motion Characteristic		
	Amplitude	Frequency Content	Duration
PGA	×		
Predominant period		×	
Duration			×
Arias intensity	×	×	×

Duration is also a parameter describing strong motion, related to the time needed for release of accumulated strain energy. Other ground motion parameters taking into account the duration are: rms acceleration (a_{rms}), arias intensity (I_a) obtained by integration of intensity over the entire duration, cumulative absolute velocity (CAV), velocity response spectrum intensity (VSI) or acceleration spectrum intensity (ASI). (Kramer, 1996) These different parameters describe different characteristics of the ground motion. Some offer only a single value; while others take into account two or even three features (Table 2.1).

Seismic hazard analysis and seismic building design rely on characterization of the ground motion by the above described parameters and predictive relationships. **Seismic hazard analysis** involves the quantitative estimation of ground-shaking hazard at a particular site. Two principal approaches exist which may be referred to as *deterministic* and *probabilistic* seismic hazard assessment. Both approaches are based on geological and seismological data, but the final definitions of seismic hazard are fundamentally different.

Deterministic seismic hazard analysis (DSHA) involves the development of a particular seismic scenario upon which a ground motion hazard evaluation is based. The steps for deriving DSHA consist of:

1. Identification and characterization of all earthquake sources identifying the geometry of each source and earthquake potential.
2. Determination of distance expressed as epicentral or hypocentral distance, choosing the events closest to the examined area.
3. Selection of the expected earthquake assuming the strongest level of shaking, described in terms of magnitude.
4. Expressing the hazard at the site in terms of the ground motion parameters (PGA, PGV, or S_a) obtained from predictive relationships.

DSHA provides evaluation of worst-case ground motions, but no information on the likelihood of occurrence in terms of time, space and size. (Oliveira & Campos-Costa, 2006)

Probabilistic seismic hazard analysis (PSHA) uses a probabilistic approach, taking into account uncertainties in the size, location, and recurrence of earthquakes, even the variation of ground motion characteristics. The steps for deriving PSHA consist of:

1. Determination of the hypocenter distribution around the source assuming uniform probability to each source zone, implying that earthquakes are equally likely to occur at any point within the source zone. Combined with the source geometry, the corresponding probability distribution of source-to-site distance can be obtained.
2. Characterization of the seismicity for each source zone specifying the earthquake recurrence relationship.
3. Use of predictive relationships to evaluate the ground motion at the site caused by quakes of any possible size, occurring at any possible point in each source zone.

DOI: 10.15477/SZE.MMTDI.2015.002

4. Evaluation of energy attenuation to obtain the ground motion parameter with a given probability during a particular time period taking into account the uncertainties.

Limitations concerning PSHA also exist especially with larger return periods or higher magnitudes than available data. (Oliveira & Campos-Costa, 2006)

An essential element in both deterministic and probabilistic seismic hazard analyses is the ability to estimate strong ground motion from a specified set of seismological parameters. This estimation is carried out using a ground motion relation referred to as an attenuation relation. An attenuation relation is a mathematical equation that relates a given strong-motion parameter to one or more parameters of the earthquake source, wave propagation path and local site conditions; referred to as seismological parameters. (Figure 2.1)

Combination of the two methods can be found in recent applications, exploiting the advantages and avoiding limitations of both methods. The 1990 edition of Uniform Building Code (UBC97) and NEHRP Recommended Provisions for Seismic Regulations for New Buildings takes into account both methodologies. Two series of maps are overlaid, one contouring the spectral ordinates using PSHA, and the values of the deterministic approach are used in case of lower values offering an upper bound. (Bommer, 2002)

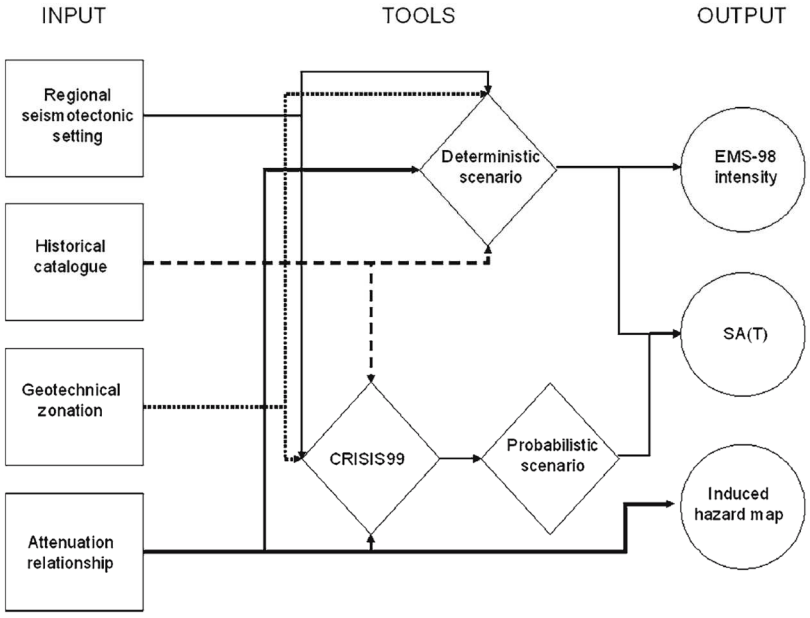

2.1. Figure: Flowchart by Faccioli showing the main ingredients of the approach proposed for earthquake hazard assessment in urban areas (Faccioli, 2006)

Seismic hazard obtained by PSHA or DSHA uses ground motion parameters with a given exceedance probability referenced to rock. That layer of the strata is considered rock in which the shear wave velocity is more than 700 m/s (Bisztricsány, 1974). In the previously mentioned SHARE models the hazard values are referenced to a rock velocity equal to 800m/s. Seismic waves propagate through different geological formations affecting the characteristic of

the waves, producing different effects on the ground motion at the ground surface, amplifying selectively different wave frequencies. These complex phenomena are known as soil effects. It has been recognized that earthquake damage is generally larger over soft sediments than on firm bedrock outcrops. This is particularly important because most of urban settlements have occurred along river valleys over such soft surface deposits. The local topography can also modify the characteristics of waves, causing more damage to structures / buildings located at hill tops than those located at the base. . Soil effects and topographic effects are known as local site effects. **Local site conditions** describe the type of deposits that lie beneath the site. They are usually described in terms of shear-wave velocity and sediment depth, representing physical quantities that can be related directly to the dynamic response of the underlying geological deposits.

Microzonation is the identification of separate individual areas having different potentials for hazardous earthquake effects. Seismic microzoning applies the local ground response, becoming a useful tool for cost effective risk mitigation. The geological description and interpretation of data is required to perform a microzoning assessment. (Roca, et al., 2006)

2.2. Vulnerability to earthquakes

Major cause of losses during an earthquake is strongly related to the deficient seismic performance of the built environment. Catastrophic events with high socio-economic impact occurred at the end of the 20th Century, including those parts of the world (e.g. Northridge and Kobe Earthquake) where earthquake engineering studies and seismic design code preparations are priority tasks. New standards and regulations have been applied to new structures from the beginning of 21st Century, which represent only a small part of existing structures. In Hungary this is true also, just as it is in other parts of the world. Many existing buildings, portions of infrastructure and other structures might fail to resist the strong ground motion caused by an earthquake and thus sustain some degree of damage. Primary damage can vary from minor cracking to total collapse. Some building types are more vulnerable than others, but even when a building sustains no structural damage, the contents of the building may be severely damaged. Since other forms of damage and loss are generally defined as a function of primary structural damage, the starting point is to find out the expected damage due to a likely strong ground motion. If the uncertainty of seismic hazard is considered, e.g. in a probabilistic way, various intensity levels of ground motions could be applied and the vulnerability of structures evaluated for more scenarios, resulting in a more complete vulnerability analysis.

DOI: 10.15477/SZE.MMTDI.2015.002

Vulnerability is the possibility of damage or loss of structures due to a seismic event; it is the characteristic of the structures and it can be expressed in probabilistic or statistical terms. A vulnerability assessment is the process of identifying, quantifying, and prioritizing (or ranking) the vulnerabilities in a system, and can be performed according to the following steps:

- cataloguing assets and resources in a system;
- assigning quantifiable value and importance to those resources;
- identifying the vulnerabilities or potential threats.

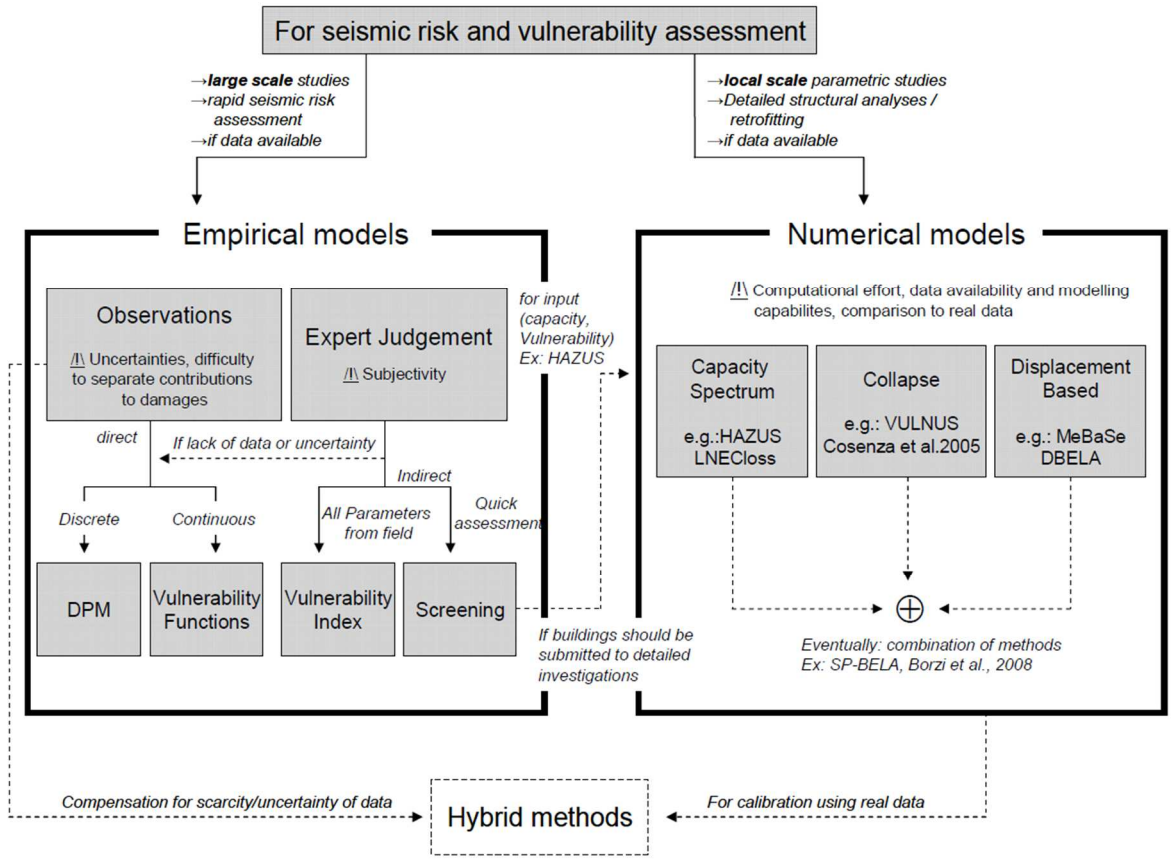

2.2. Figure: Schematic representation of the classical models for seismic vulnerability derived by ENSURE project (Foerster, et al., 2009)

Vulnerability can be determined with the help of different methods. The selection of the methods depends on the objective of the study, the required results and on available data, and can be grouped according to the space scale considered for analysis: e.g. urban level or building level, etc. (Foerster, et al., 2009). Large-scale approaches are based on empirical methodologies and local scale assessments are performed using some detailed numerical analyses (Figure 2.2). As these methods are getting more complex, they become more accurate, but also more expensive, requiring higher computational and evaluation effort. Vulnerability assessment can be performed after or before an earthquake with different aims: either to determine retrofitting measures or to estimate expected damage for prevention purposes respectively.

DOI: 10.15477/SZE.MMTDI.2015.002

2.2.1. Empirical assessment methods

Vulnerability as an input parameter to earthquake scenarios requires evaluation of a large building population in a rather short period of time using a simple method, which describes the seismic performance of the buildings adequately. There are different methods to analyze the vulnerability of buildings: methods used during the post-earthquake study as well as analytical or numerical methods. Vulnerability can be determined by observation or based on expert opinions; usually based on post-earthquake studies. Other methods offer a possibility to estimate the possible damages before an earthquake occurs. (Calvi, et al., 2006)

Empirical methodologies are widely used to quickly assess the seismic risk on a large scale or to sort out structures that need more detailed analysis. Dolce et al. (1995) classified methodologies for the evaluation of structural vulnerability in four groups (Dolce, et al., 1995):

1. direct, which assesses in a simple way the damage caused in a structure by a given earthquake;
2. indirect, which determines first a vulnerability index of the structure and then assesses the relationship between damage and seismic intensity;
3. conventional, which is essentially a heuristic method, introducing a vulnerability index independent of the damage prediction;
4. hybrid, which combines elements of the previous methods with expert judgments.

One of the basic tasks in determining vulnerability of structures is the classification of buildings and infrastructure from the point of view of earthquake risk. The classification worked out by researchers (Vaseva & Kostov, 2002) and agencies e.g. EMS (Grünthal ed., 1998) is largely based on inspections of structural systems, possibly the time of construction and the proximity to earthquakes.

Observed vulnerability refers to assessments based on statistics of past earthquake damage. In the case of observed vulnerability (Castano & Zamarbide, 1992) (Haddar, 1992) (Porro & Schraft, 1989) the damage is defined with the repair cost as a ratio of the replacement cost or the amount of loss of all affected elements considering the number of casualties as a ratio of their value. The relation between damage and earthquake intensity is valid only for the region where it was developed.

The vulnerability of structures can also be evaluated through **expert opinions**. Experts have to estimate the expected percentage of damage caused by a given intensity, which are implied in macroseismic scales. These scales are used to evaluate the possible damage after an earthquake assuming a complete observed damage data base. Researchers are applying this technique also in studies prior to an earthquake (Fäh, et al., 2001).

Score assignment procedures aim to identify seismically hazardous structures by identifying structural deficiencies. The vulnerability index and screening methods gather quantitative information, by using vulnerability assessment forms including parameters, such as quality of materials, type of foundations, number of stories, state of conservation, or stiffness of the structure. Depending on the parameter's value, a score is attributed to each feature to quantify the level of damage according to the severity of potential ground motion (Calvi, 1999). Potential structural deficiencies are identified from observed correlations between damage and structural characteristics (FEMA, 2002) (Mouroux, et al., 2004) (Fukuyama, et al., 2001). The main objective of these procedures is to determine whether a particular building needs a more detailed investigation or not. The advantage of score assignments with respect to observed data or expert opinions is that it allows for updating the vulnerability function following a modification to the building structure.

Whitman et al. (1974) proposed the use of **damage probability matrices** for the probabilistic prediction of damage to buildings from earthquakes based on 1600 building data from the 1971 San Fernando earthquake. Several recent applications (Applied Technology Council, 1985) estimate loss based on damage probability matrices expressing in a discrete form the probability P_{ij} of reaching a level of damage i for a given earthquake intensity j and class of buildings (Whitman, et al., 1974) as shown in Table 2.2.

2.2 Table: Format of damage probability matrix proposed by Whitman et al. *(Calvi, et al., 2006)*

Damage State	Structural Damage	Non-structural Damage	Damage Ratio (%)	Intensity of Earthquake				
				V	VI	VII	VIII	IX
0	None	None	0.00- 0.05	10.4	-	-	-	-
1	None	Minor	0.05- 0.30	16.4	0.5	-	-	-
2	None	Localized	0.30- 1.25	40.0	22.5	-	-	-
3	Not noticeable	Widespread	1.25- 3.50	20.0	30.0	2.7	-	-
4	Minor	Substantial	3.50- 4.50	0.2	47.1	92.3	58.8	14.7
5	Substantial	Extensive	7.50-20.00	-	0.2	5.0	41.2	83.0
6	Major	Nearly total	20.00-65.00	-	-	-	-	2.3
7	Building condemned		100.00	-	-	-	-	-
8	Collapse		100.00	-	-	-	-	-

The **vulnerability function** is the vulnerability of buildings to various levels of ground motion, plotting the expected damage to a building or a class of buildings as a function of the ground motion. Spence et al. (1992) introduced the parameterless scale of intensity (PSI) to derive vulnerability functions (Figure 2.3) based on the observed damage of buildings using the MSK damage scale, solving the problem of discrete macroseismic intensity values (Spence, et al., 1992). PSI can be converted to PGA using empirical correlation functions.

DOI: 10.15477/SZE.MMTDI.2015.002

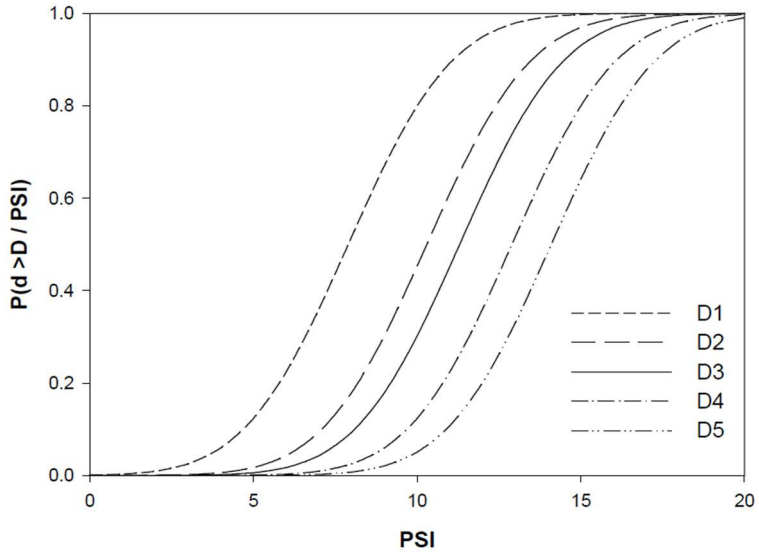

2.3. Figure: Vulnerability curves produced by Spence et al. (1992) for bare moment-resisting frames using the parameterless scale of intensity (PSI); D1 to D5 relate to damage states in the MSK scale (Spence, et al., 1992)

Fragility curves (Figure 2.4) describe the probability of reaching or exceeding different states of damage given peak building response (Oropeza, et al., 2010). Building class fragility curves are functions that describe the probability of a building belonging to a certain building class of reaching or exceeding a particular damage grade given a median value of the PSHA demand parameter (e.g. spectral displacement/acceleration, PGA or PGD) that corresponds to the threshold of the damage state and by the variability associated with that damage state. The fragility curves of a building class take into account the variability associated with the vulnerability function of a building class.

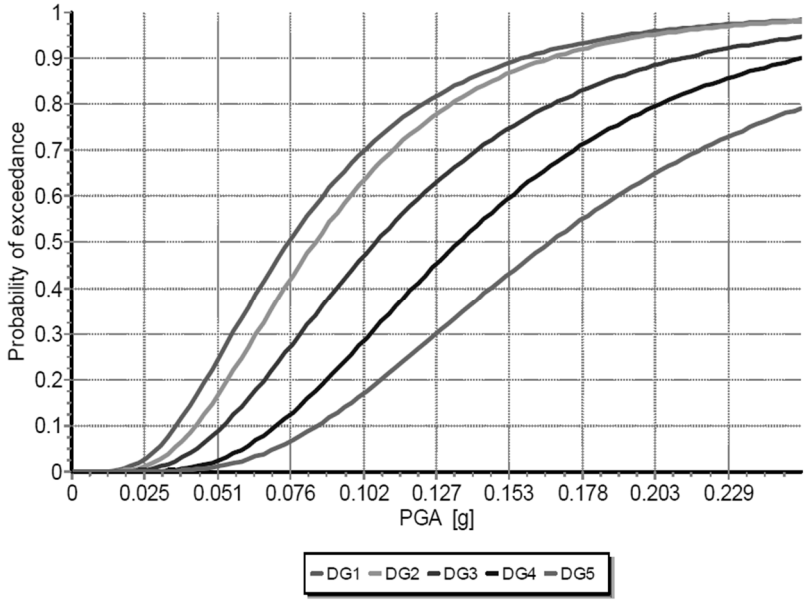

2.4. Figure: Harmonized (by SYNER-G project) fragility function set of unreinforced masonry (Oropeza, et al., 2010) (Pitilakis, et al., 2011)

DOI: 10.15477/SZE.MMTDI.2015.002

2.2.2. Structural analysis methods

Detailed analyses are the most time-consuming evaluation of vulnerability. Engineers may use several structural analysis methods to estimate building vulnerability to seismic loading. These methods apply equally to zones of strong, moderate, or weak seismicity. They are simply ways to quantify the ability of a structure to resist an earthquake event.

Typically, an engineer will use a method appropriate to the purpose at hand: if the building is not critical, is located in a low-seismicity zone, and is easily strengthened by standard methods with little increase in cost, a simple method of analysis is appropriate. If the building is a critical structure, located in a strong seismic zone, and requires considerable re-design and reconstruction to withstand anticipated loadings, a more sophisticated approach is necessary. The primary decision by the engineer is which method of analysis and what kind of data is necessary to adequately evaluate this building under seismic conditions.

The design/analyze cycle for the engineer can follow many paths. These analyses correspond to the methods of design: linear static analysis (lateral force method); modal response spectrum analysis which is a linear dynamical analysis; pushover analysis, an increasingly popular non-linear static analysis; and a fully non-linear time-history dynamic analysis. Listed below are common methods to estimate building resilience, in order of increasing sophistication and time spent on analysis and design by the engineer.

2.2.2.1 **Lateral Force Method** applies additional lateral forces to the structure and the model is analyzed as a static load case. The magnitude and location of additional lateral forces are based on the intensity of the earthquake and geometry and mass of the structure considered. Beams and columns are sized so that they remain in the elastic state.

2.2.2.2 The approach of **Elastic Response Spectrum Method** is similar to (2.2.2.1) in that it assumes elastic behavior of the structure. However, the fundamental period of the structure is either estimated (empirical formulae) or computed (eigenvalue extraction or Rayleigh Ritz calculation). Based on the fundamental building period and anticipated earthquake spectrum, lateral forces are amplified (or reduced) based on the level of agreement between earthquake spectra and building frequency.

2.2.2.3 **Modal Response Method** assumes the structure will respond as a combination of harmonic motions determined from eigenvalue/eigenvector extraction or other methods. It considers additional vibration modes and frequencies that the structure may undergo during an earthquake. The contribution of each of these modes to the response of the structure is scaled according to its mass participation factor. The material behavior is still elastic. The

earthquake record may be converted to frequency domain by Fast Fourier Transform (FFT) and the various components superimposed to determine final response. Damping is often modeled as a Rayleigh damping since the formulation is much easier to compute.

2.2.2.4 In case of **Elastic Time History Analysis** earthquake acceleration records are applied to the base of the model and response is computed. This may be a useful first step since locations where there may be high stress are revealed. This method is often used with nonlinear methods.

2.2.2.5 **Method of Complex Response** is a very popular method for studying soil-structure interaction during an earthquake. It is similar to modal methods, but uses a complex-valued stiffness matrix to mimic material damping. The stiffness of soil and structural elements may be reduced due to increased strain levels and the system re-evaluated, therefore it is called an equivalent linear method. Calculations are performed in the frequency domain after earthquake histories are converted via FFT. Strain levels are evaluated by inverse FFT and examining the strain time histories of all the elements. The stiffness reduction is applied and the model is re-evaluated until computed strains converge.

2.2.2.6 **Pushover Analysis** method has become very popular to determine the non-linear capacity of a building to lateral forces. The basis of analysis is a static, deflection controlled approach. As the structure is pushed over, its resistance increases to a peak value, then declines to a residual value. Values of deflection vs. base shear are often compared to displacement response spectra, or seismic demand curves. The method is computationally efficient for determining nonlinear, plastic behavior of structures. Modifications and refinements to this method will be discussed in a following section.

2.2.2.7 **Nonlinear Time History Analysis** represents the most accurate and challenging method to evaluate structural response to earthquake loading. The earthquake acceleration record is used as input to the base of the model and the structure's deformation, stiffness, damping, hinge formation and changes in geometry are all evaluated. The analysis is usually performed using a suite of earthquake records to gain a more complete picture of the building's performance and areas of weakness. Since the analyses are so time consuming, other analyses are usually performed first to aid in dimensioning beam and column elements and specifying connection details.

No matter which method is chosen, there must be a set of criteria that will allow the engineer to determine if the structure performs well or poorly. These criteria may be top story deflection, story drift, base shear, formation of plastic hinges, collapse progression, residual strength, energy absorption, or others dictated by specific codes or standards of practice.

2.3. Risk assessment

Risk assessment is the determination of quantitative or qualitative value of risk and a recognized threat or hazard, requiring calculations of two components of risk: the magnitude of the potential loss, and the probability that the loss will occur. Risk is resulting from the convolution of hazard and vulnerability (Eq.1 in Section 1.2). Acceptable risk is a risk that is understood and tolerated because the cost or difficulty of an effective countermeasure exceeds the expectation of loss. This idea is incorporated in seismic design codes, namely different performance levels are defined. Since it is not possible to modify the seismic hazard to reduce the risk, emphasis should be laid on the study of vulnerability and vulnerability reduction as a measure of damage/loss mitigation, i.e. risk reduction.

The primary structural damage might not only trigger secondary damages, but also cause loss. Financial losses are primarily the restoring costs, but loss of function can also lead to secondary forms of loss, such as loss of revenues due to business interruption, unemployment, loss of market share etc. Recent publications according to ENSURE (Foerster, et al., 2009) also incorporate other components such as the coping capacity, the deficiencies in preparedness, the lack of resilience, etc. Equations listed below are some of the existing definitions for risk:

$$\text{RISK} = \text{HAZARD} \times \text{VULNERABILTY} \times \text{EXPOSURE (UNDRO, 1979)} \quad (2.1)$$

$$\text{RISK} = \text{HAZARD} \times \text{VULNERABILTY} \times \text{EXPOSURE} \times \text{k (TCG, 2001)} \quad (2.2)$$

where the coefficient k is expressing the population density and the socio-economic significance of the function of the buildings.

$$\text{TOTAL RISK} = \text{HAZARD} \times \text{VULNERABILTY} \times \sum \text{elements at RISK (Alexander, 2002)} \quad (2.3)$$

where the risk is the probability that some given elements may sustain a particular level of loss while total risk means the sum of predictable casualties, damages and losses.

$$\text{RISK} = (\text{HAZARD} \times \text{VULNERABILTY})/\text{coping CAPACITY (Villagrán De León, 2006)} \quad (2.4)$$

"Whatever the definition of risk, it should include the potential effects of correlative impacts (socio-economic impacts on employment, production, etc.) or induced effects (hazardous industries impacts, dams collapses, fires and explosions, etc.) and the human or social dimension through the analysis of vulnerability factors (demographic, social organizational, political, educational and cultural aspects). Hence, risk assessment requires a multi-disciplinary approach that accounts not only for physical impacts, but also for less quantifiable factors, such as social, environmental, organizational and institutional factors." (Foerster, et al., 2009) The definition of ENSURE goes beyond the objective of this research, but in future may be considered to extend the risk evaluation of Győr into this direction.

DOI: 10.15477/SZE.MMTDI.2015.002

Chapter 3. State of the Art

According to Coburn and Spence the last decade of 20th Century was *"the costliest decade on record in terms of disaster management, due to such (1994 Northridge, 1995 Kobe, 1999 Koaceli) seismic events, placing unprecedented pressure on the insurance industry in particular, and changing its views of earthquake protection"* (Coburn & Spence, 2002). This triggered the huge increase in research concerning different steps of risk assessment, lessons learned from those devastating earthquakes improved the understanding how the manage, mitigate and work towards the prevention. These events highlighted the possibility of seismic hazard not only in earthquake prone areas, but also in middle hazardous regions initiating several projects to assess the risk of densely populated cities.

3.1. Existing methods

This part of the thesis presents the existing methods used in assessment earthquake hazard, building vulnerability, and seismic risk.

In the US the engineering/technical side of the assessment process has evolved for about 20 years. The adoption of a performance-based design approach has been underway since 2000 by the Pacific Earthquake Engineering Research Center (PEER, formerly known as EERC). It is a consortium of universities, government, and industry working to "*develop, validate, and disseminate performance-based seismic design technologies for buildings and infrastructure to meet the diverse economic and safety needs of owners and society*". Part of the performance-based earthquake engineering (PBEE) approach is shown in the unifying equation to represent the performance-based design methodology (Stewart, et al., 2001):

$$v(DV) = \iint G\ DV|DM|dG\ DM||\ dv(IM) \tag{3.1}$$

where

G soil shear modulus;

DV a Decision Variable that can be understood and used by owners/policy makers (e.g. cost, down time, etc.);

DM a Damage Measure representing the performance of the structure under consideration (e.g. displacement ductility for buildings, building settlement for foundations);

IM an Intensity Measure of the ground motion (e.g., spectral acceleration, duration);

$dv(IM)$ Derivative with respect to IM of the Poisson rate of IM exceeding some threshold value;

$v(DV)$ Poisson rate of DV exceeding some threshold value.

Equation 6 means that relationships can be constructed between parameters representing damage to structures (DMs) and ground motions (IMs), as well as between decision variables (DVs) and damage measures (DMs). For simple structures, it may be possible to derive closed form solutions for the conditional probabilities of DM/IM and DV/DM. However, for unique and complex structures, such relations will likely involve structure-specific simulations utilizing carefully chosen ground motion parameters, or suites of time histories, sophisticated structural analysis models, and a more comprehensive (economic and social) basis for decision-making.

The risk assessment process has broadened to include other impacts as well (Tate, et al., 2010). Any number of natural and man-made hazards can be integrated into the same geo-spatial model. Additional dimensions to vulnerability can include: emergency response, social and economic status of the affected population, general health conditions, age, gender and race. Such vulnerabilities are measured differently than structural survival in earthquakes, but the methodologies and decisions are very similar. The concept of geo-spatial multi-hazard risk assessment is presented below in Figure 3.1.

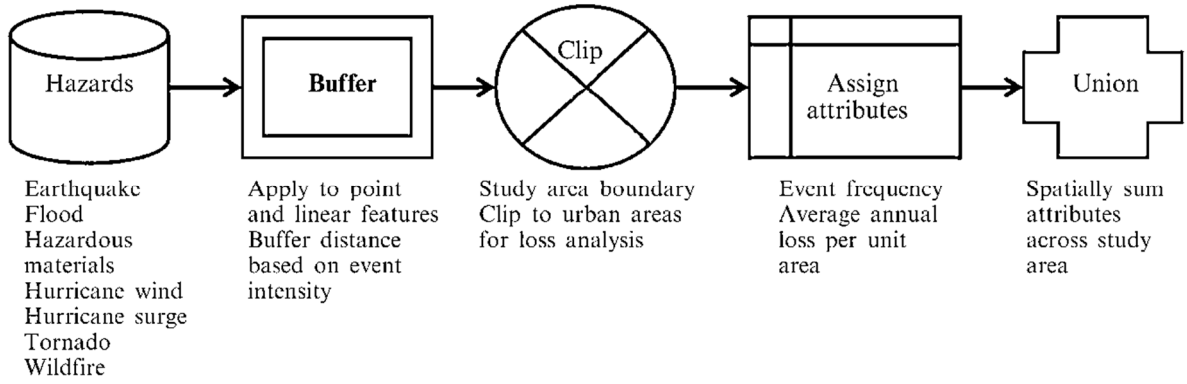

3.1. Figure: Integrated Geospatial Hazard flowchart (Tate, et al., 2010)

3.1.1. Risk assessment framework

One of the most-utilized risk assessment frameworks is HAZUS. Several other assessment methodologies from Japan, India, China, as well as the EU use a similar approach. It is specifically configured for the US with an extensive database of building stock, earthquake hazard, and economic information already in place. The system can be used “manually” unfortunately it requires ARCGIS version 10.0.1, which was not available during this research due to software purchasing restrictions. However, since it is the basis for most structured risk assessment systems, a brief description follows.

Acknowledging the need to develop a standardized approach to estimating losses from earthquake and other hazards, Federal Emergency Management Agency (FEMA, 2013) with

DOI: 10.15477/SZE.MMTDI.2015.002

the cooperation with the National Institute of Building Sciences, first released HAZUS in 1997 followed by an updated version in 1999. HAZUS is a tool government officials and others can use for earthquake-related mitigation, emergency preparedness, response and recovery planning, and disaster response operations. The methodology in HAZUS covers many aspects and incorporates state-of-the-art approaches for:

1. characterizing earth science hazards including ground shaking, liquefaction, and landslides;
2. estimating damage and losses to buildings and lifelines;
3. estimating fires following earthquake;
4. estimating casualties, displaced households, and shelter requirements; and,
5. estimating direct and indirect economic losses.

HAZUS is built upon an integrated GIS platform that produces regional profiles and estimates of earthquake losses. The methodology addresses the built environment, and categories of losses, in a comprehensive manner. It is composed of seven interdependent modules shown in Figure 3.2. This modular approach allows different levels of analysis to be performed, ranging from estimates based on simplified models and default inventory data to more refined studies based on detailed engineering and geotechnical data for a specific study. A brief description of each of the seven modules is presented below. Detailed technical descriptions of the modules can be found in the HAZUS technical manual (FEMA, 2013).

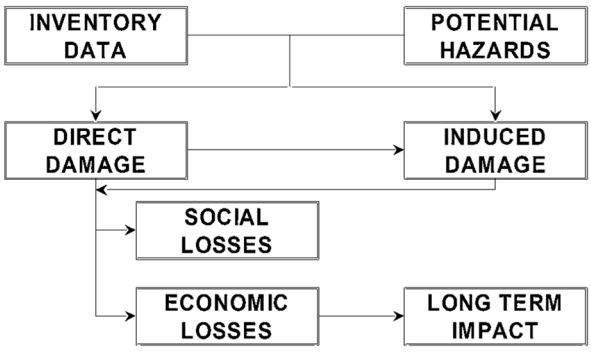

3.2. Figure: HAZUS modules (FEMA, 2013)

Module 1: The **Potential Earth Science Hazard (PESH)** module estimates ground motion and ground failure (landslides, liquefaction, and surface fault rupture). Ground motion demands in terms of spectral acceleration (S_a) and peak horizontal ground acceleration (PGA) are typically estimated based on the location, size and type of earthquake, and the local geology. For ground failure, permanent ground deformation (PGD) and probability of occurrence are determined. GIS-based maps for other earth science hazards, such as tsunami and seiche inundation, can also be incorporated.

Module 2: Inventory and Exposure Data built into HAZUS is a US national-level basic exposure database that allows a user to run a preliminary analysis without having to collect any additional local data. The general stock of buildings is classified by occupancy (residential, commercial, etc.) and by model building type (structural system and material, height). The default mapping schemes are state-specific for single-family occupancy type and region-specific for all other occupancy types. They are age and building-height specific. The four inventory groups are:

1. general building stock,
2. essential and high potential loss facilities,
3. transportation systems, and
4. utilities.

The infrastructure within the study region must be inventoried in accordance with the standardized classification tables used by the methodology. These groups are defined to address distinct inventory and modeling characteristics. Default population data is usually based on the census. Estimates for building exposure are based on default values for building replacement costs (dollars per square foot) for each model building type and occupancy class, in addition to certain regional cost modifiers. This data was drawn from Dun and Bradstreet and RS Means who are building cost estimation service providers.

Module 3: Direct Damage module provides damage estimates for each of the four inventory groups based on the level of exposure and the vulnerability of structures (potential for damage at different ground shaking levels). For HAZUS, a technique using building fragility curves based on the inelastic building capacity and site-specific response spectra was developed to describe the damage incurred in building components (Kircher, et al., 1997).

Since damage to nonstructural and structural components occurs differently, the methodology estimates both damage types separately. Nonstructural building components are grouped into drift-sensitive and acceleration-sensitive components. For both essential facilities and general building stock, damage state probabilities are determined for each facility or structural class.

Damage is expressed in terms of probabilities of occurrence of specific damage states, given a level of ground motion and ground failure. Five damage states are identified - none, slight, moderate, extensive and complete.

Module 4: Induced Damage is defined as the secondary consequence of an event. This fourth module assesses dams and levees for inundation potential, and hazardous materials sites for release potential. Fire following an earthquake and accumulation of debris are also assessed.

DOI: 10.15477/SZE.MMTDI.2015.002

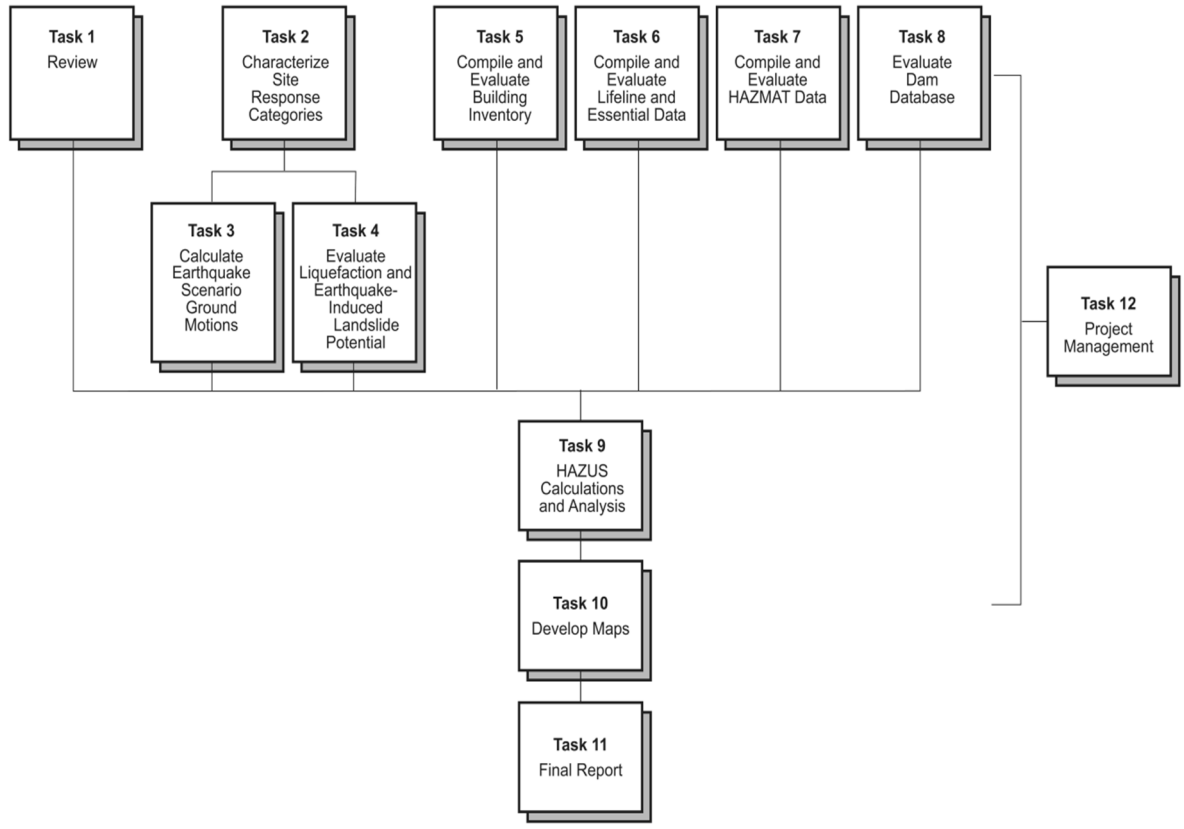

3.3. Figure: Typical Earthquake Hazard Assessment Tasks (FEMA, 2013)

Module 5: Direct Social Losses are estimated in terms of casualties, displaced households, and short-term shelter needs. The output of the casualty module includes estimates for four levels of casualty severity (minor to dead) by time (2:00 a.m., 2:00 p.m., and 5:00 p.m.) for four population groups (residential, commercial, industrial, and commuting). Casualties, caused by secondary effects such as heart attacks or injuries while rescuing trapped victims, are not included. Homelessness is estimated based on the number of structures that are uninhabitable, which in turn is evaluated by combining damage to the residential building stock with utility service outage relationships.

Module 6: Direct Economic Losses are estimates that include structural and nonstructural damage, costs of relocation, and losses to business inventory, capital-related losses, income losses, and rental losses.

Module 7: Indirect Losses module evaluates the long-term effects on the regional economy from earthquake losses. The outputs in this module include income change and employment change by industrial sector. A typical HAZUS-based study may include the tasks listed below. Note each task may be simple or complex in its treatment of data and analyses.

For this study, most of the work focused on Tasks 2,3,5,9 and 10 (Fig.3.3). Relevant literature review is given in the following sections.

DOI: 10.15477/SZE.MMTDI.2015.002

3.1.2. Soil classification procedure

The main goal of soil classification is to obtain the most important properties of a tested soil sample, right after classification, using experience collected about each group. To reach this goal, soil classification must be based on these most important and most typical properties and parameters.

The naming of soils is related to the particle composition and the importance of the particle-water relations. Granular soils are classified based on their particle size distribution, because their behavior is determined by particle composition. Cohesive soils are classified based on their plasticity index, as their behavior is determined mainly by particle-water relations. The larger fraction gives the name of granular soils according to former Hungarian soil classification. The following fraction(s) (containing "enough" of it) gave the attributive.

The Soil and Rock Logging, Classification, and Presentation Manual of Caltrans offers procedures for soil and rock description, identification, classification, and preparation of boring logs. It gives a very detailed classification of different soil types. (Caltrans, 2007)

The new European Standards of soil classification was introduced recently based on EN ISO 14688-1:2002. The standard establishes the basic principles for identification and classification of soils on the basis of those material and mass characteristics commonly used for soils for engineering purposes. Basic soils are soils with uniform grading (Table 3.1).

3.1. Table: Particle size fractions *(European Committee for Standardization, 2002)*

Soil fractions	Sub-fractions	Symbols	Particle sizes [mm]
Very coarse soil	Large boulder	LBo	> 630
	Boulder	Bo	> 200 to 630
	Cobble	Co	> 63 to 200
Coarse soil	Gravel	Gr	> 2,0 to 63
	Coarse gravel	CGr	> 20 to 63
	Medium gravel	MGr	> 6,3 to 20
	Fine gravel	FGr	> 2,0 to 6,3
	Sand	Sa	> 0,063 to 2,0
	Coarse sand	CSa	> 0,63 to 2,0
	Medium sand	MSa	> 0,2 to 0,63
	Fine sand	FSa	> 0,063 to 0,2
Fine soil	Silt	Si	> 0,002 to 0,063
	Coarse silt	CSi	> 0,02 to 0,063
	Medium silt	MSi	> 0,0063 to 0,02
	Fine silt	FSi	> 0,02 to 0,0063
	Clay	Cl	≤ 0,002

DOI: 10.15477/SZE.MMTDI.2015.002

3.1.3. Local site effects and microzonation techniques

Microzonation is the identification of separate individual areas having different potentials for hazardous earthquake effects with respect to some geological and geophysical characteristics of the sites. Seismic microzonation is the process of estimating the response of soil layers under earthquake excitations and thus the variation of earthquake characteristics on the ground surface. The site response of the ground motion may vary in different locations of the city according to the local geology. A seismic zonation map for a whole country may, therefore, be inadequate for detailed seismic hazard assessment of the cities. Microzonation provides the basis for site-specific risk analysis, and for the mitigation of earthquake damages.

There is a great deal of literature concerning effects of soils on the amplification or attenuation of seismic shaking. Seed and Idriss (1971) presented a summary of soil effects as observed from damage patterns during the 1964 Alaska, 1964 Niigata, and 1971 San Fernando earthquakes (Seed & Idriss, 1971). While liquefaction was a primary focus of their work, much of the performance data demonstrated the influence of soil properties on building damage as well. A very dramatic example of the influence of soil conditions was presented by Zeevaert (1986, 1991) on the 1985 Michocán Mexico City Earthquake (Zeevaert, 1986) (Zeevaert, 1991). Similar work on the Loma Prieta-San Francisco earthquake (NRC, 1994) reinforced the concept of soil amplification.

Shown in figure 3.4, from Srbulov (2003) are the results of 66 different case studies and the influence of soil amplification. The boxes represent a large number of records while the dots are less-extensive studies.

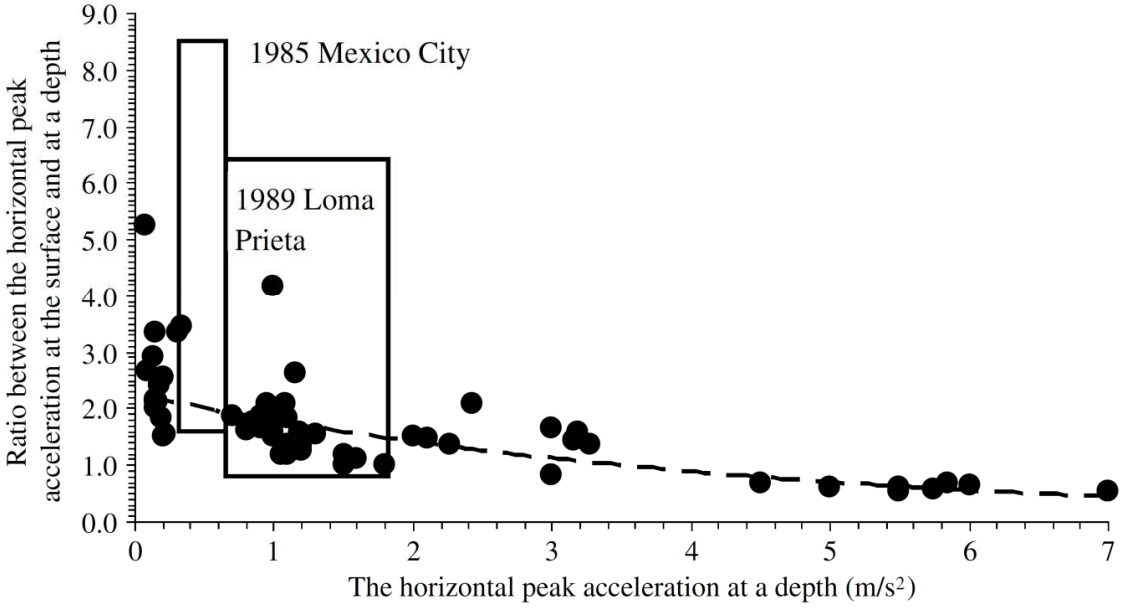

3.4. Figure: Amplification due to soil layers from 66 case studies (Srbulov, 2003)

Similar work has been summarized by Kramer (1996) and Boore (2007), on the various interactions of earthquake source, travel through the lithosphere, and arrival at the surface where interaction with structures takes place (Kramer, 1996) (Boore, 2007).

The effects of topographic irregularities and alluvial basin geometry on ground motions can be significant. Ridges, canyons and ground slopes tend to shake differently from horizontal ground because seismic energy can be focused within their physical boundaries. Topographic effects were observed at a number of ridges in California during the 1971 San Fernando (ML = 6.4) earthquake (Trifunac & Hudson, 1971), during earthquakes in Matsuzaki in Japan (Jibson, 1987), and a small hill in Tarzana, California, during the 1994 Northridge earthquake (Bouchon & Barker, 1996). Many large cities are located on or near alluvial valleys, the effect of basin geometry on ground motion is of great interest. The softer deposited alluvial soils can trap body waves and cause some incident body waves to propagate through the alluvium as surface waves (Vidale & Helmberger, 1988). These waves can produce stronger shaking and long durations.

There are several methods proposed to investigate the behavior of soft sedimentary structures to excitation of seismic waves. Dynamic characteristics of site such as predominant period (Teves-Costa, et al., 2001), amplification factor (Giovinazzi, 2009) are appropriate for seismic microzonation purpose. Average shear wave velocity is the most applied parameter in microzonation (Bauer, et al., 2007), used in several international projects, such SHARE (Lemoine, et al., 2012), Risk-UE (Faccioli, 2006), ROSRINE (Nigbor, et al., 2001).

Recent researches use different techniques to estimate the dynamic soil properties: 1) experimental methods, such as standard spectral ratio (Borcherdt, 1970), H/V noise ratio or "Nogishi-Nakamura" technique (Nakamura, 1989)and borehole data, microtremor techniques (Perrin, et al., 2010); 2) numerical methods, such as one-dimensional (Teves-Costa, et al., 2001) or two-dimensional response analysis. Bard and Gariel (1986) used an analytical approach to study the two-dimensional response of alluvial valleys, and compared to the assumption of one-dimensional wave propagation. The one-and two-dimensional amplification functions at the center were quite similar, which indicates that one-dimensional analyses would be appropriate in that area (Bard & Gariel, 1986). These methods have their advantages and disadvantages, experimental methods require large financial support and manpower, while numerical methods are very sensitive to initial soil data. Those methods achieving a higher accuracy are more time consuming. The main advantage of numerical models rest in their flexibility to assess the uncertainty in the seismic response of a site, given the imperfect knowledge regarding the mechanical and geometrical characteristics of the considered site. (Lacave, et al., 1999)

DOI: 10.15477/SZE.MMTDI.2015.002

3.1.4. Classification and possible damage estimation of buildings

The **European Macroseismic Scale** offers a simple differentiation of the resistance of buildings to earthquake generated shaking (vulnerability) in order to give a robust way of differentiating how the buildings may respond to earthquake shaking. The Vulnerability Table (Table 3.2) categorizes in a manageable way the strength of structures, taking both building type and other factors into account. Subdivision of structures marked with letters from "A" to "F" were determined roughly based on different levels of vulnerability and not based on architectural point of view. (Grünthal ed., 1998)

3.2. Table: Vulnerability Table of EMS *(Grünthal ed., 1998)* (full table in Annex)

Type of Structure		Vulnerability Class A B C D E F
MASONRY	rubble stone, fieldstone	
	adobe (earth brick)	
	simple stone	
	massive stone	
	unreinforced, with manufactured stone units	
	unreinforced, with RC floors	
	reinforced or confined	

The same degree of shaking may destroy an adobe building and may not have much effect on a well-constructed modern building. Vulnerability is defined taking into account the material of the structure, the condition of the building, and also other factors such as:

- state of disrepair,
- quality of construction,
- irregularity of building shape, level of earthquake resistant design (ERD),
- etc.

For each building type, the Vulnerability Table gives a line showing the most likely vulnerability classes, and also the probable range shown as a dashed line. The position of a particular building along this line has to be found by taking into account other factors contributing to the vulnerability of the building.

Damage grades from 1 to 5 represent the increase of shaking describing classes of damage, which can be easily distinguished. Different types of building response and failure are illustrated for both masonry and reinforced concrete buildings.

FEMA 155 (FEMA, 2002) offers also a rapid visual screening (RVS) method providing an approach to classify surveyed buildings into two categories: those acceptable as to risk to life safety or those that may be seismically hazardous and should be evaluated in more detail by a design professional experienced in seismic design. For classification purposes the seismic-lateral-load-resisting system of buildings should be identified.

3.3. Table: Building Classification of FEMA 155 *(FEMA, 2002)*

Building Type	
W1:	Light wood-frame residential and commercial buildings smaller than or equal to 5,000 square feet
W2:	Light wood-frame buildings larger than 5,000 square feet
S1:	Steel moment-resisting frame buildings
S2:	Braced steel frame buildings
S3:	Light metal buildings
S4:	Steel frame buildings with cast-in-place concrete shear walls
S5:	Steel frame buildings with unreinforced masonry infill walls
C1:	Concrete moment-resisting frame buildings
C2:	Concrete shear-wall buildings
C3:	Concrete frame buildings with unreinforced masonry infill walls
PC1:	Tilt-up buildings
PC2:	Precast concrete frame buildings
RM1:	Reinforced masonry buildings with flexible floor and roof diaphragms
RM2:	Reinforced masonry buildings with rigid floor and roof diaphragms
URM:	Unreinforced masonry bearing-wall buildings

The RVS procedure of FEMA 155 was designed to be implemented without performing structural analysis calculations. It utilizes a scoring system that requires the user to

- identify the primary structural lateral-load-resisting system (Table 3.3) scoring with a basic structural score;
- identify building attributes that modify the seismic performance expected of this lateral-load-resisting system, such as score modifiers concerning code of design, height and irregularity of the building, soil conditions.

The RVS procedure can also be used for ranking a community's seismic rehabilitation needs; designing seismic hazard mitigation programs for a community; developing inventories of buildings for use in regional earthquake damage and loss impact assessments; planning post-earthquake building safety evaluation efforts; and developing building specific seismic vulnerability information for purposes such as insurance rating, decision making.

3.1.5. Methods for vulnerability evaluation

Calvi et al. (2006) summarize the development of vulnerability assessment methodologies, emphasizing that *"One of the main ingredients in a loss model is an accurate, transparent and conceptually sound algorithm to assess the seismic vulnerability of the building stock and indeed many tools and methodologies have been proposed over the past 30 years for this purpose."* (Calvi, et al., 2006)

There are different methods to analyze the vulnerability of the buildings: methods used during the post-earthquake study or analytical or numerical methods. Vulnerability can be determined by observation or based on expert opinions; these usually are used at post earthquake studies. Other methods offer a possibility to estimate the possible damages before an earthquake occurs.

Score assignment methods have been successfully applied recently to seven European cities in the RISK-UE European project (Mouroux, et al., 2004). In Japan, the JBDPA (Japanese Seismic Index Method, JBDPA, 1990) describes three seismic screening procedures to estimate the seismic performance of a building: a seismic performance index (strength, ductility, etc.), time-dependent deterioration of the building and a seismic judgment index for safety of structure (Fukuyama, et al., 2001).

In the case of observed vulnerability (Haddar, 1992) (Porro & Schraft, 1989) (Castano & Zamarbide, 1992) the damage is defined with the repair cost as a ratio of the replacement cost or the amount of loss of all affected buildings considering the number of casualties as a ratio of their value. The relation between damage and earthquake intensity is valid only for the region where it was developed.

Another method is to ask experts to estimate the expected percentage of damage caused by a given intensity, which are implied in macroseismic scales. These scales are used to evaluate the possible damages after an earthquake (Fäh, et al., 2001).

Analytical approaches are based on identification of collapse mechanisms yielding the equivalent shear capacity (Benedetti & Pezzzoli, 1996). The vulnerability is expressed as the critical acceleration causing the mechanism to take place. In the case of visual screening and score assignment, the structural deficiencies are identified and scores for different deficiencies are calibrated by experts (Calvi, 1999).

Detailed analyses are the most time consuming evaluation of vulnerability. These analyses correspond to the methods of structural analysis and design. They were presented in Chapter 2.

DOI: 10.15477/SZE.MMTDI.2015.002

3.2. International examples of earthquake risk evaluation

There are several methods from the last 20-25 years to estimate seismic risk. Some methods are based on local previously observed earthquake damages, some try to evaluate the future loss based on building typology. Some methods give seismic risk as a function of financial loss (casualties and replacements cost of damaged structures), other determine the risk by only engineering aspects, such as the probability of damage to structures.

3.2.1. Mendoza City (1992), Argentina

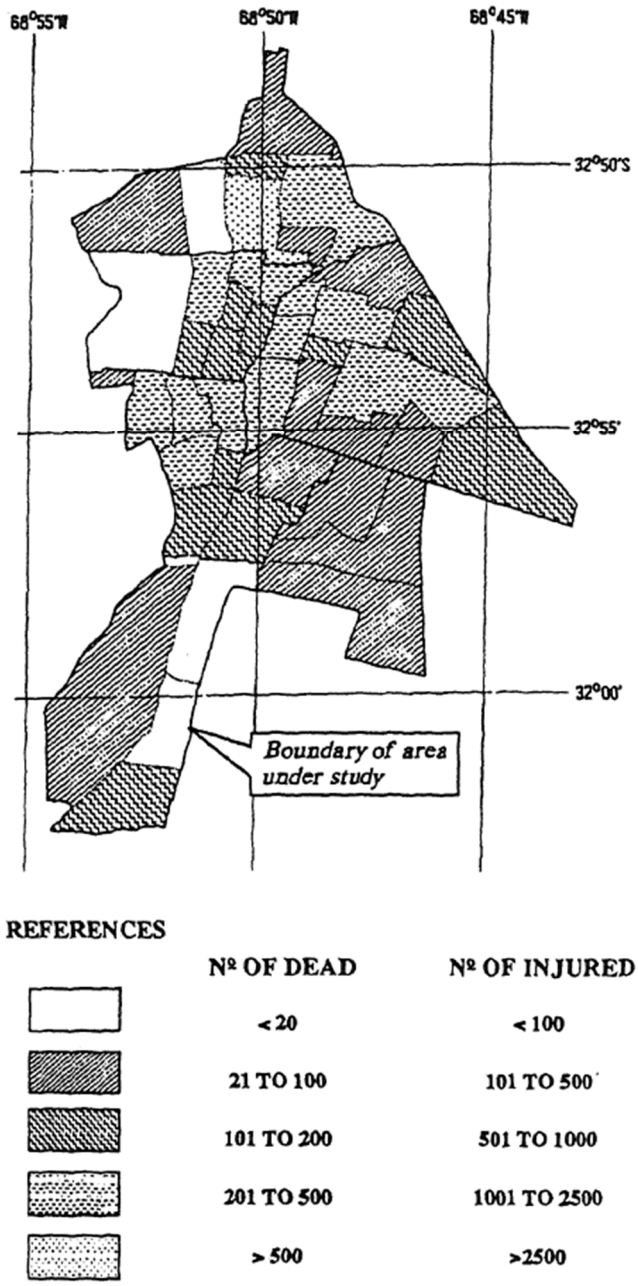

A seismic risk reduction program was carried out for Mendoza province with a population of 1.4 million inhabitants. Probabilistic seismic hazard maps were obtained from attenuation relationships and soil conditions. Construction types were determined by the Cadastral Information Bank. Population density distribution was also surveyed. Seismic vulnerabilities were determined for different probable damage states and loss distributions, using three characteristic earthquakes, corresponding to 10% probability of exceedance for periods of 10, 50 and 250 years. Damage assessment focused on possible collapses using the number of casualties or homeless people as damage indicator (DI) based on 1985 Mendoza earthquake (Fig. 2.6). (Castano & Zamarbide, 1992)

3.5. Figure: Probable human loss distribution (Castano & Zamarbide, 1992)

$$DI = \frac{number \text{ of seriously } damaged\ constructions\ of\ one\ construction\ type}{total\ number\ of\ constructions\ of\ the\ same\ construction\ type} \quad (3.2)$$

3.2.2. Case of Algeria (1992)

After 1980 El-Asnam and 1989 Tipaza earthquake vulnerability functions were determined for different structures based on observed vulnerability (Haddar, 1992). The seismic risk definition of UNDRO (Eq. 2.1) was adapted to obtain seismic risk:

$$\text{RISK} = \text{HAZARD} \times \text{VULNERABILTY} \times \text{SPECIFIC LOSS} \quad (3.3)$$

Specific loss is expressed in terms of monetary units, human loss or damage to property.

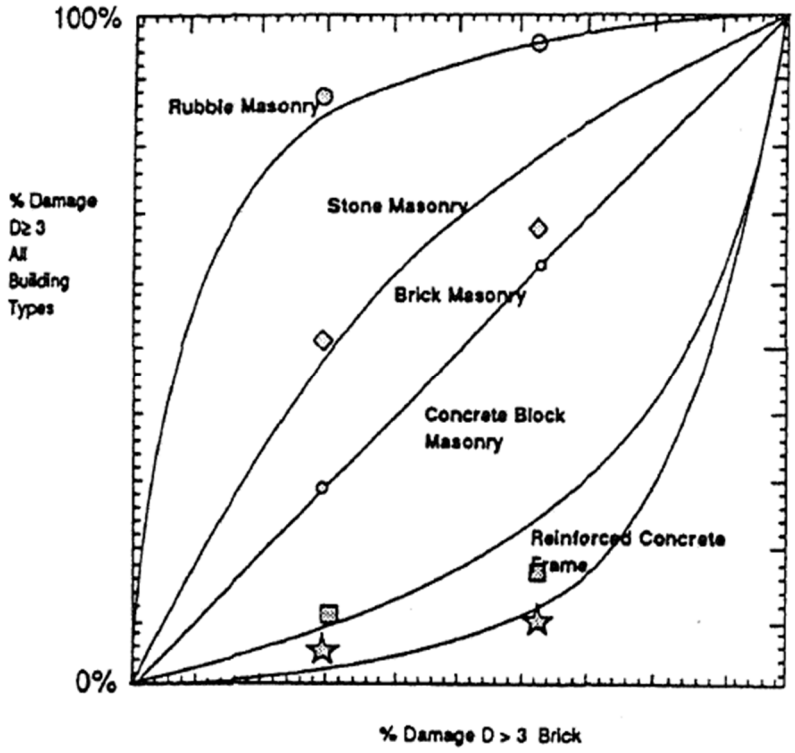

3.6. Figure: Earthquake damage distribution of all building types in Tipaza (Haddar, 1992)

3.2.1. Japan method (2000): Tokyo, Kobe, etc.

The study of seismic risk assessment of urban cities in Japan proposed a methodology to estimate potential seismic risk of towns based on their regional characteristics. Regional characteristics included macro information such as topography, climate, location of active faults, regionally dependent building types and their seismic capacity, experience of past earthquake disasters, background history of urban development, inter-city traffic system, accessibility from neighboring cities, etc. (Lee, et al., 2000)

$$CL(t,n) = \{FS_t(n) - Min[FS_t(n)]\} \times 10/MFS_t(n) \quad (3.4)$$

where

$CL(t,n)$ Class value of each city [$0 \leq CL(t,n) \leq 10$]

$FS_t(n)$ Factor score of each city in each category (t)

$MFS_t(n)$ $Max\{FS_t(n) - Min[FS_t(n)]\}$,

t: category, n: City ID

DOI: 10.15477/SZE.MMTDI.2015.002

Scores of each city are calculated with

$$R(n) = \sum CL(t,n) \tag{3.5}$$

where

$R(n)$ Score of potential seismic risk

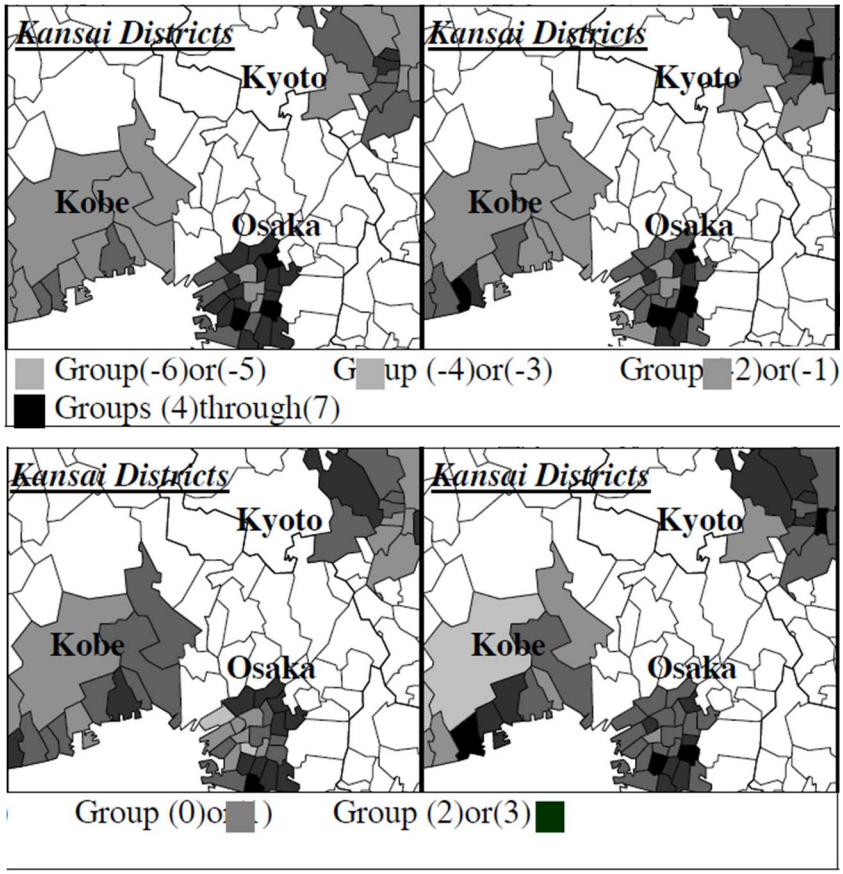

3.7. Figure: Estimated potential seismic risk: a) Risk of damage to buildings b) Risk of fire c) Capability of rescue within intra-city d) Capability of building reconstruction (Lee, et al., 2000)

3.2.2. Scenarios for Basel (2001), Switzerland

The project presented a rapid technique based on the European Macroseismic Scale (Grünthal ed., 1998) including both a qualitative and quantitative approach to model building damage in urban areas for deterministic and probabilistic earthquake scenarios, based on a microzonation study and the inventory of buildings in the area. The method was applied to the city of Basel, an area with a high density of population and industry, also famous for its earthquake history. For a vulnerability assessment, the goal was to generate a detailed map of the distribution of building damage expected for the occurrence of a scenario earthquake. Different scenario earthquakes were assumed: the first corresponded to an event with a regional intensity VII-VIII, which has a return period of 475 years (10% probability of exceedance in 50 years) used in building codes. The second event simulated the 1356 Basel earthquake with an intensity of IX in the city. The varying intensity values were computed in the different areas

DOI: 10.15477/SZE.MMTDI.2015.002

of the city using the results of a microzonation study. With the approximation knowledge of the building types (taxonomy in Annex) and their distributions within the city, and by assuming vulnerability curves based on EMS98, overall damage was determined in the city districts, as well as the percentage of buildings with very heavy damage and destruction. (Fäh, et al., 2001)

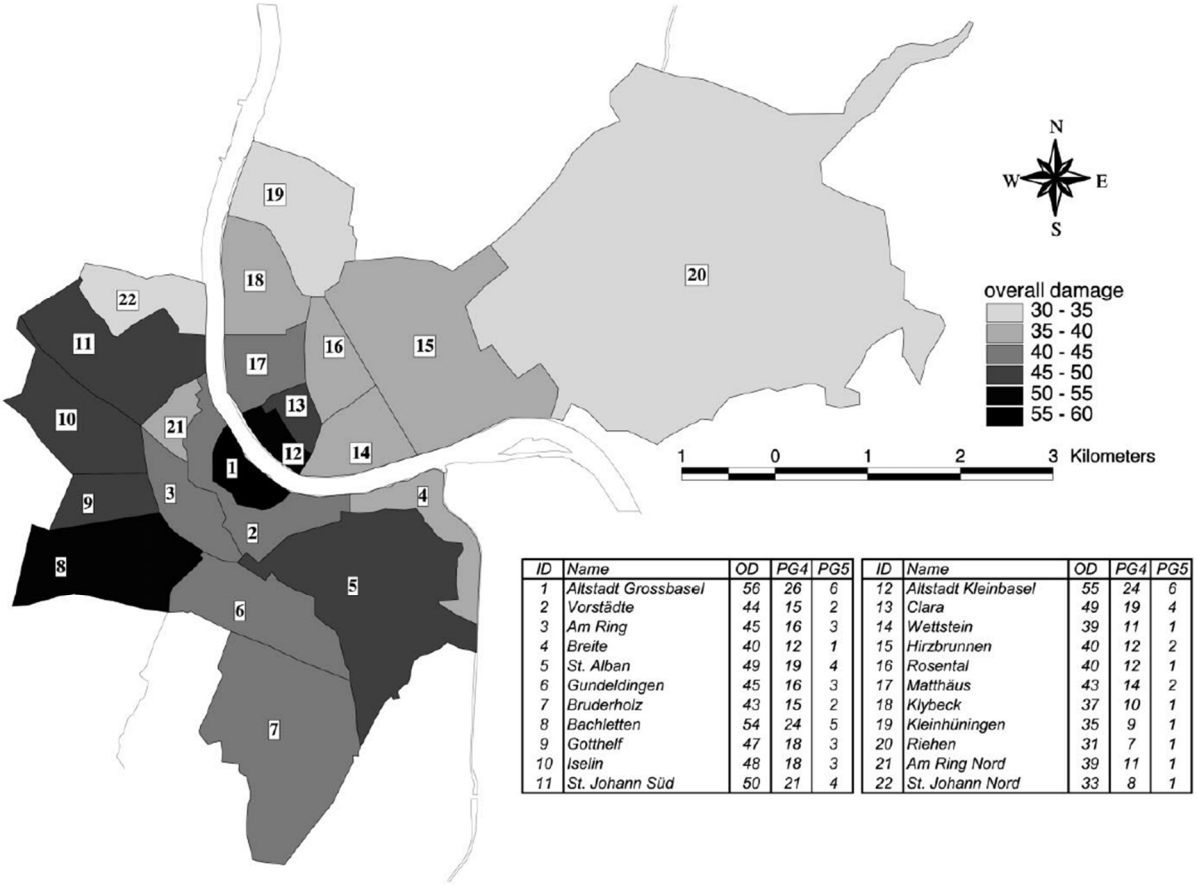

ID	Name	OD	PG4	PG5	ID	Name	OD	PG4	PG5
1	Altstadt Grossbasel	56	26	6	12	Altstadt Kleinbasel	55	24	6
2	Vorstädte	44	15	2	13	Clara	49	19	4
3	Am Ring	45	16	3	14	Wettstein	39	11	1
4	Breite	40	12	1	15	Hirzbrunnen	40	12	2
5	St. Alban	49	19	4	16	Rosental	40	12	1
6	Gundeldingen	45	16	3	17	Matthäus	43	14	2
7	Bruderholz	43	15	2	18	Klybeck	37	10	1
8	Bachletten	54	24	5	19	Kleinhüningen	35	9	1
9	Gotthelf	47	18	3	20	Riehen	31	7	1
10	Iselin	48	18	3	21	Am Ring Nord	39	11	1
11	St. Johann Süd	50	21	4	22	St. Johann Nord	33	8	1

3.8. Figure: Damage scenario in Basel assuming an earthquake similar to the 1356 Basel earthquake with an intensity of IX. The values in the table are the percentage for the overall damage (OD), the percentage of buildings with damage grades 4 and 5 (Fäh, et al., 2001)

3.2.3. Risk-UE project (2004): Barcelona (ES), Bitola (FYROM), Bucharest (RO), Catania (IT), Nice (FR), Sofia (BG), and Thessaloniki (GR)

The European RISK-UE project was launched in 1999, at the end of the International Decade for Natural Disaster Reduction (IDNDR), and commenced in January 2001 and ended in 2004. The project involved the assessment of earthquake scenarios based on the analysis of the global impact of one or more plausible earthquakes at city scale, within a European context. *"The primary aim of these scenarios was to increase awareness within the decision-making centers of a city, of the successful appropriation of the problems caused by a seismic risk and of the implementation of Management Plans and Plans of Action to effectively reduce this risk."* (Mouroux, et al., 2004) Work Packages completed by the project are:

DOI: 10.15477/SZE.MMTDI.2015.002

- WP01: European distinctive features, Geographic Information System inventory (GIS), database and building typology (taxonomy in the Annex);
- WP02: Seismic hazard assessment, at both regional and local level (based on peak ground acceleration);
- WP03: Urban system analysis. Highlighting weak points under normal conditions, during crisis and recovery periods;
- WP04: Vulnerability assessment of current buildings;
- WP05: Vulnerability assessment of old town centers, historical monuments and buildings;
- WP06: Vulnerability assessment of lifeline facilities and essential structures;
- WP07: Seismic risk scenarios.

3.9. Figure: WP03 results for the city of Thessaloniki: analysis of the commercial zones in the center town (Mouroux, et al., 2004)

Vulnerability assessment of buildings were performed using a traditional, so-called macroseismic or statistical methods based on a large number of samples retrieved from previous earthquakes, particularly those in Italy, Greece, Romania and the former Yugoslavia.

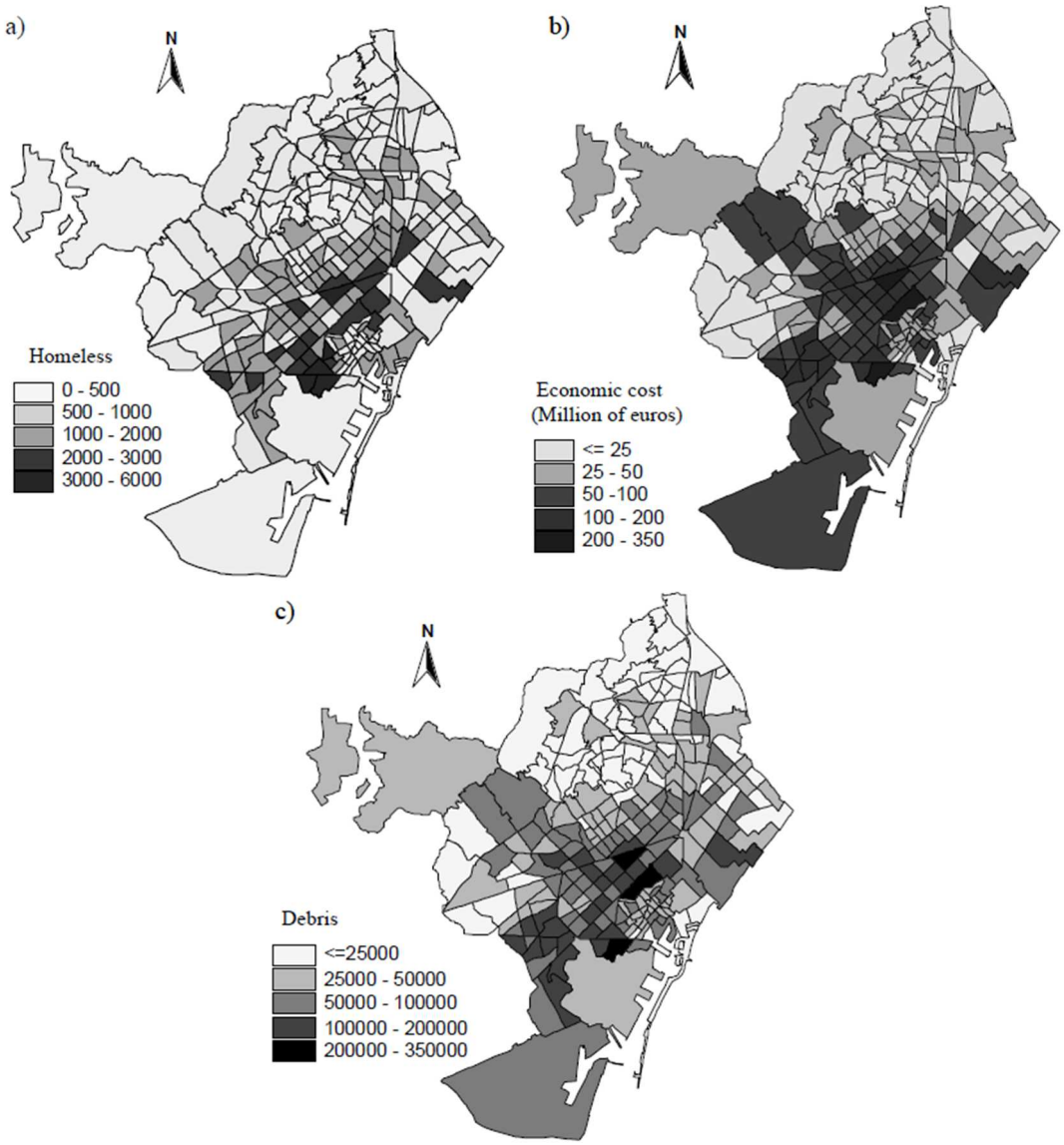

3.10. Figure: (a) Homeless (b) Total economic cost in millions of Euros (c) Debris volume (tons) generated for probabilistic hazard scenario of Barcelona (Lantada, et al., 2010)

3.2.4. Metropolitan area of Lisbon (2008), Portugal

Seismic scenario simulators were developed in order to determine earthquake scenario with different modules similar to FEMA: source geodynamics, wave propagation from source to site, classification of the objects under analysis (building stock, networks), vulnerability of each classified object, inventory and cartography of the existing objects, measure of the impact of an event, selection of the Lisbon earthquake scenario. Geological profiles were obtained at different locations, and extrapolation to other locations was based on the geological mapping interpretation.

Typology classifications of buildings were determined. For the building stock in Portugal three different approaches were developed using a) Census data when working in large areas; b) individual enquires when studying small or limited geographical areas; c) mixed individual enquiry with aerial object recognition. (Oliveira, 2008)

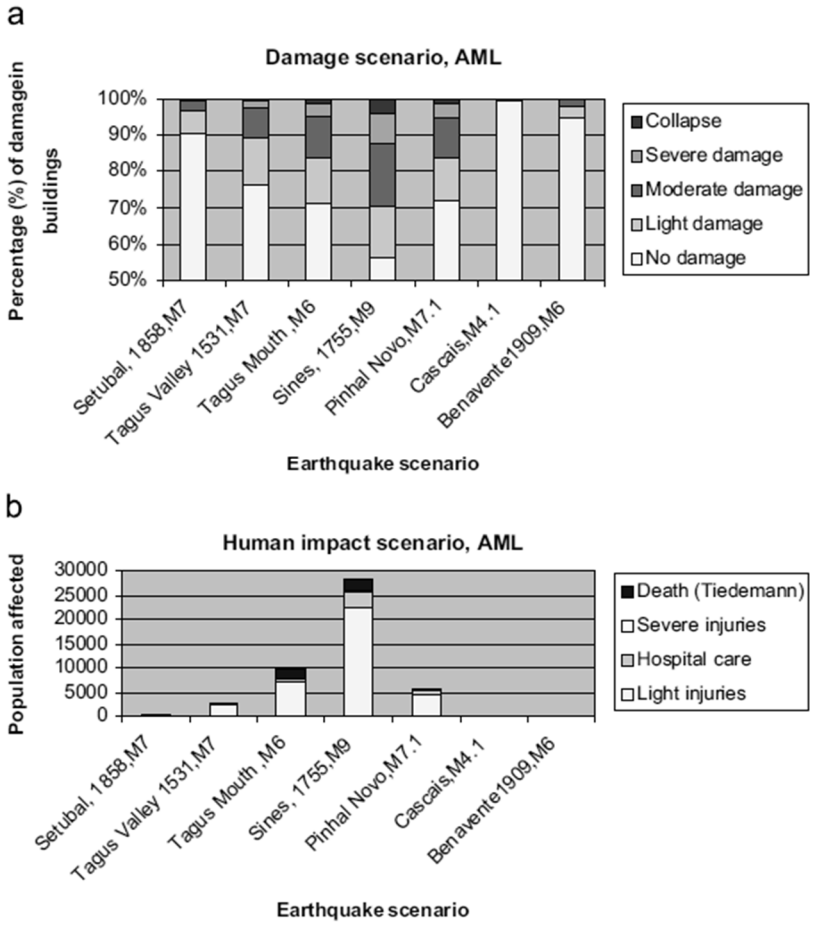

3.11. Figure: Impact of several events in the metropolitan area of Lisbon: (a) in the building stock; (b) in the population (Oliveira, 2008)

3.2.5. Case study for Denizli (2008), Turkey

The study aimed to carry out a seismic risk assessment for a typical mid-size city based on building inventory from a field study. An inventory was conducted by trained observers to obtain building properties in a selected region of Denizli. Parameters that are known to have some effect on the seismic performance of the buildings during past earthquakes were collected during the inventory studies. The inventory includes data of about 3,466 buildings on 4,226 parcels. The evaluation of inventory data provided information about the distribution of building stock according to structural system, construction year, and vertical and plan irregularities. Casualty and shelter needs were estimated for the scenario earthquakes. The damage assessment (Figure 3.12) and loss studies showed that significant casualties and economic losses can be expected in future earthquakes. (Inel, et al., 2008)

DOI: 10.15477/SZE.MMTDI.2015.002

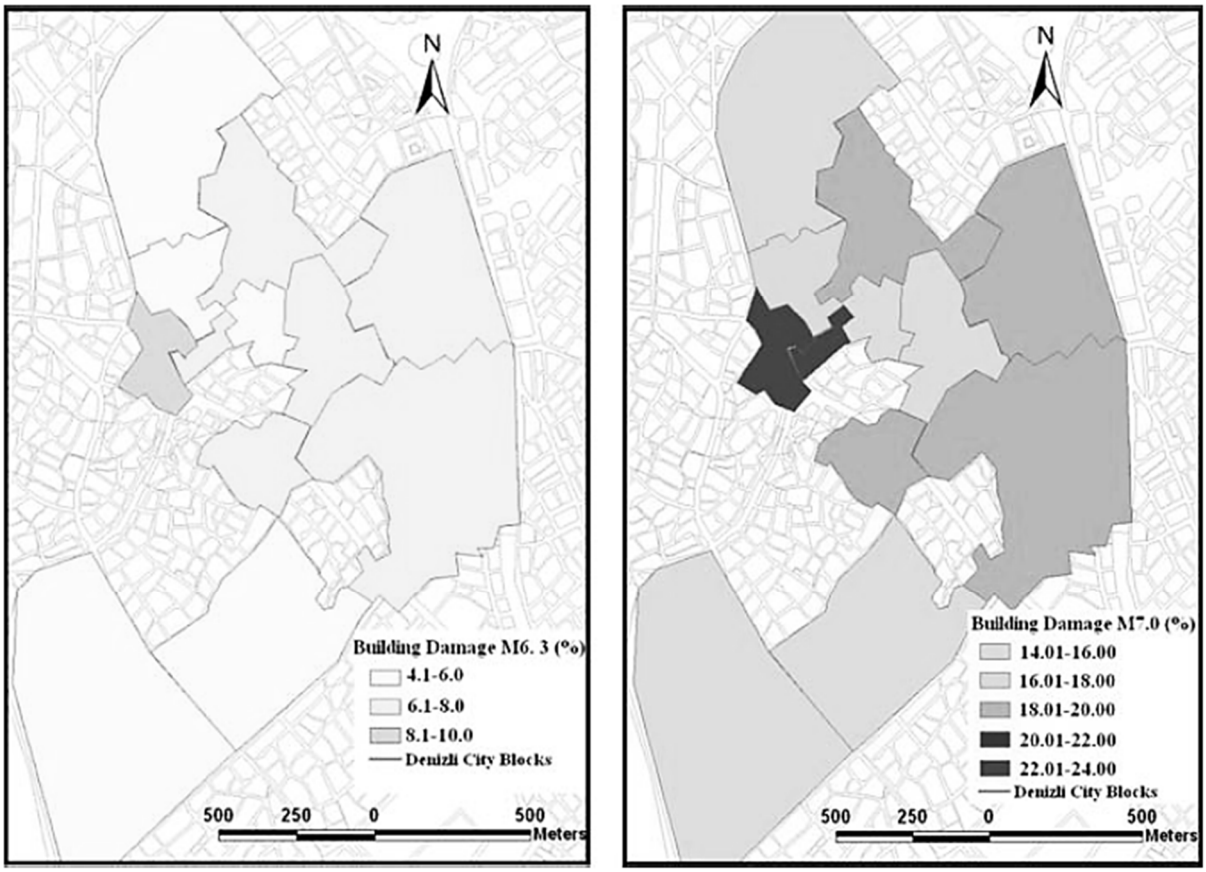

3.12. Figure: Distribution of extensively damaged plus collapsed building ratios (%) in the selected region of Denizli (Inel, et al., 2008)

3.2.6. New Jersey State Hazard Mitigation Plan (2014), US

The New Jersey Standard HMP was initially adopted in April 2005. As required under Disaster Mitigation Act of 2000 (DMA 2000), the Plan focuses on natural hazards that pose great risk to the state including flooding, hurricane, earthquake, etc. *"Hazard mitigation is specifically meant to break the cycle of damage, reconstruction, and repeated damage."*

Section 5.5 deals with the risk assessment concerning earthquakes. The profile includes a detailed description of the geological makeup of soils in the area, and the fault systems. The vulnerability assessment includes the results of probabilistic Hazards US Multi-Hazard (FEMA, 2013) earthquake models to estimate potential losses to the updated state building and critical facility/infrastructure inventory (Table 3.1):

- number of people that may potentially be injured and/or killed by an earthquake depending on the time of day the event occurs (2:00 a.m., 2:00 p.m. and 5:00 p.m.);
- direct building losses to repair or replace the damage caused to the building.

A building's construction determines how well it can withstand the force of an earthquake (taxonomy in the Annex). (Tetra Tech, Inc., 2014)

DOI: 10.15477/SZE.MMTDI.2015.002

3.4. Table: Earthquake Estimated Potential Losses to Buildings (Structure and Contents) HAZUS-MH Probabilistic Scenarios *(Tetra Tech, Inc., 2014)*

County	100-Year MRP	500-Year MRP	1,000-Year MRP	2,500-Year MRP
Atlantic	$0	$12,284,628	$51,781,912	$225,109,153
Bergen	$809,531	$171,687,912	$687,673,786	$2,899,261,622
Burlington	$0	$43,471,185	$185,484,958	$842,902,037
Camden	$0	$45,983,158	$190,847,704	$902,972,070
Cape May	$0	$5,401,287	$22,472,592	$104,494,337
Cumberland	$0	$7,695,787	$31,606,422	$141,318,997
Sussex	$0	$22,368,750	$86,739,266	$333,863,404
Union	$62,000	$66,788,422	$290,714,217	$1,327,112,754
Warren	$0	$13,624,734	$54,712,697	$215,873,326
Total	**$2,690,859**	**$1,129,303,379**	**$4,711,346,212**	**$20,302,123,551**

Source: Default general building stock data in HAZUS-MH v. 2.1
Notes: Building losses include structural and non-structural damage estimates.
MRP = Mean Return Period

3.2.7. The City of New York – Hazard Mitigation Plan (2014), US

New York City's original HMP was published in 2009. It includes non-natural hazards along with natural hazards, and addresses the climate change.

3.5. Table: Number of Buildings Damaged from Earthquakes by Return Period for New York City *(Hazard Mitigation Unit, 2014)*

Recurrence Interval	Construction Type	Slight	Moderate	Extensive	Complete	Total Damaged	% of Buildings Damaged
100-year	Unreinforced Masonry	0	0	0	0	0	0.00%
	Total	**0**	**0**	**0**	**0**	**0**	**0.00%**
250-year	Unreinforced Masonry	3,100	1,100	100	0	4,300	2.27%
	Total	**5,800**	**1,500**	**200**	**0**	**7,500**	**0.70%**
500-year	Unreinforced Masonry	11,300	4,800	800	100	17,000	8.98%
	Total	**26,000**	**7,500**	**1,000**	**100**	**34,600**	**3.22%**
1,000-year	Unreinforced Masonry	21,300	11,100	2,500	400	35,300	18.64%
	Total	**66,600**	**22,000**	**3,600**	**400**	**92,600**	**8.63%**
2,500-year	Unreinforced Masonry	35,600	25,900	8,500	2,100	72,100	38.08%
	Total	**159,300**	**69,600**	**15,900**	**2,600**	**247,400**	**23.05%**

Chapter 9 of New York HMP deals with the risk assessment concerning earthquakes. Soil types are determined by the National Earthquake Hazard Reduction Program (NEHRP), seismic hazard is given by Modified Mercalli Intensity Scale (MMI) and peak ground acceleration (PGA). Building typology is determined based on the New York City Construction Codes. Potential damages related to five damage states are presented for return periods of 100, 250, 500, 1000 and 2500 years. (Hazard Mitigation Unit, 2014)

DOI: 10.15477/SZE.MMTDI.2015.002

3.3. Hungarian studies concerning seismic risk analysis

Seismic hazard assessment dates back to 1960s motivated by industrial purposes, and first probabilistic seismic hazard map was prepared by Zsíros in 1985 (Zsíros, 1993). Basic source for earthquake seismic hazard assessment is the Hungarian Earthquake Catalogue (Zsíros, 2000). The current Seismic Hazard Map of Hungary (GeoRisk Earthquake Engineering Ltd., 2006) is presented in Figure 1.4.

Another aspect of the risk assessment is vulnerability. Vulnerability assessments were performed only in the case of the nuclear power plant in Paks by T. Katona (Katona, 2001). Other vulnerability assessment studies have been performed concerning typical masonry and RC buildings in the last years (Kegyes-Brassai, 2003) (Kegyes-Brassai, 2004a) (Kegyes-Brassai, 2004b) (Kegyes-Brassai, 2006) (Kegyes-Brassai, 2007).

Besides the research presented in this thesis, risk assessment studies were performed on the Downtown Budapest (Gribovszki, et al., 2010) and Debrecen (Gribovszki & Panza, 2004) by Gribovszki at al. It should be noted that these researches were mainly focusing on deterministic seismic hazard combined with hybrid technique. To obtain seismic risk maps, risk was calculated by determining the difference between the maximum amplitude frequencies of S_a of synthetic seismograms, and the estimated eigenfrequencies of buildings at every 0.1 km^2 of the Downtown, taking into account only the height of the building.

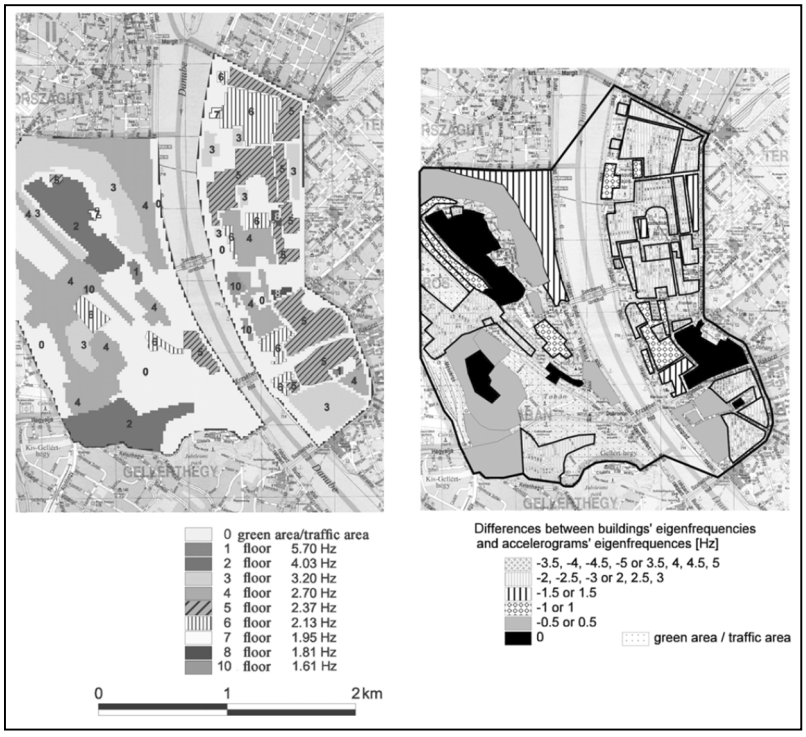

3.14. Figure: Eigenfrequencies of the buildings and the difference between the maximum amplitude frequencies of S_a, and the estimated eigenfrequencies of the buildings – the value zero means the most hazardous buildings (Gribovszki, et al., 2010)

At six buildings macroseismic noise measurements were performed in order to determine the eigenfrequencies of the buildings. The developed seismic risk map of Downtown show that buildings situated on hilly western part of the city have higher risk than the eastern plain part. (Gribovszki, et al., 2010)

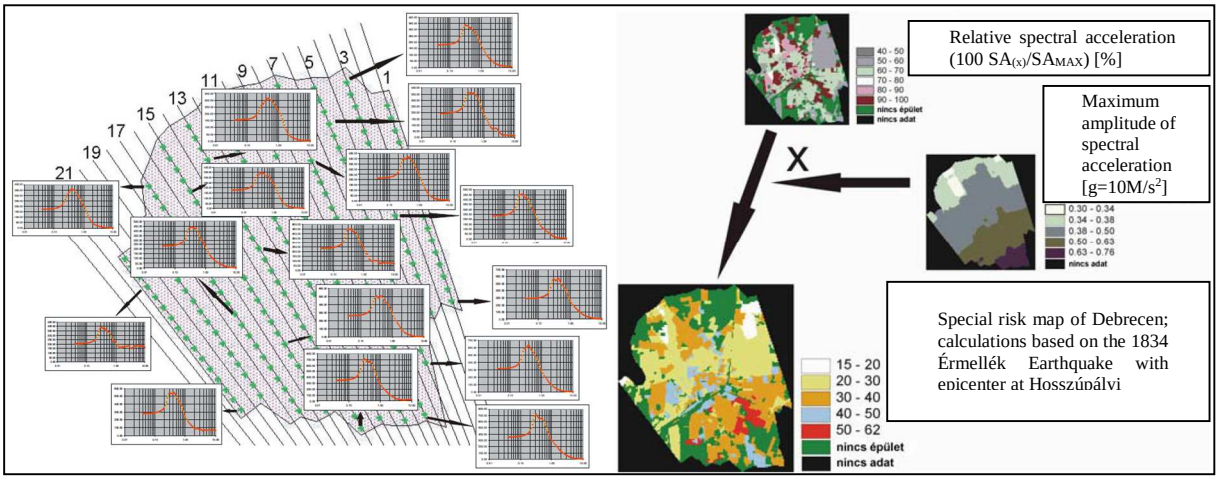

3.15. Figure: Spectral acceleration diagrams from synthetic seismograms and the steps of the earthquake risk map in Debrecen (Gribovszki, 2005)

The research concerning Debrecen offers new results in seismic hazard evaluation. Concerning vulnerability, only the height of the buildings is considered in order to estimate the eigenfrequencies. The risk map developed for Debrecen presents only a relative degree of damage of the buildings compared to each other resulting in a relative scale. As far as the map was developed from the spectral acceleration values is not suitable to show the values of expected peak ground acceleration in case of a selected area of the city. (Gribovszki, 2005)

Recently published National Emergency Risk Evaluation by National Directorate General for Disaster Management, Ministry of Interior adapts the results of the previous mentioned research about the seismic risk of Budapest (Gyenes, 2011). Surprisingly it contradicts the former quoted (in Section 1.1.3) statement of Győr-Moson-Sopron County Emergency Management Directorate, which definitely underestimates the seismic risk in Győr-Moson-Sopron County (Győr-Moson-Sopron County Emergency Directorate, 2014). National Emergency Risk Evaluation suggests that microzonation of densely populated areas with higher values of assets should be performed, for example in case of county towns. In the case of areas with higher seismicity, like Budapest, Berhida-Várpalota-Mór, Komárom-Győr, Kecskemét, Eger, Jászberény and Debrecen, the local site effects should be taken into account not only the values offered by regional hazard maps. Assessing seismic risk would highly contribute to the damage prevention and could provide valuable information for emergency management. This suggestion matches the goals of this project concerning Győr (Kegyes-Brassai & Ray, 2013).

DOI: 10.15477/SZE.MMTDI.2015.002

Chapter 4. Examined area

Győr was chosen to be the examined area for seismic risk analysis because it is the most important city of northwest Hungary. The city is the sixth largest in Hungary, and it is the capital of Győr-Moson-Sopron County and Western Transdanubia region; an important economic, industrial, ecclesiastic, educational, cultural and sports center. It is often referred to as the City of Associations or Meetings and has become a vital industrial link with Germany, Austria, Slovakia and Czech Republic.

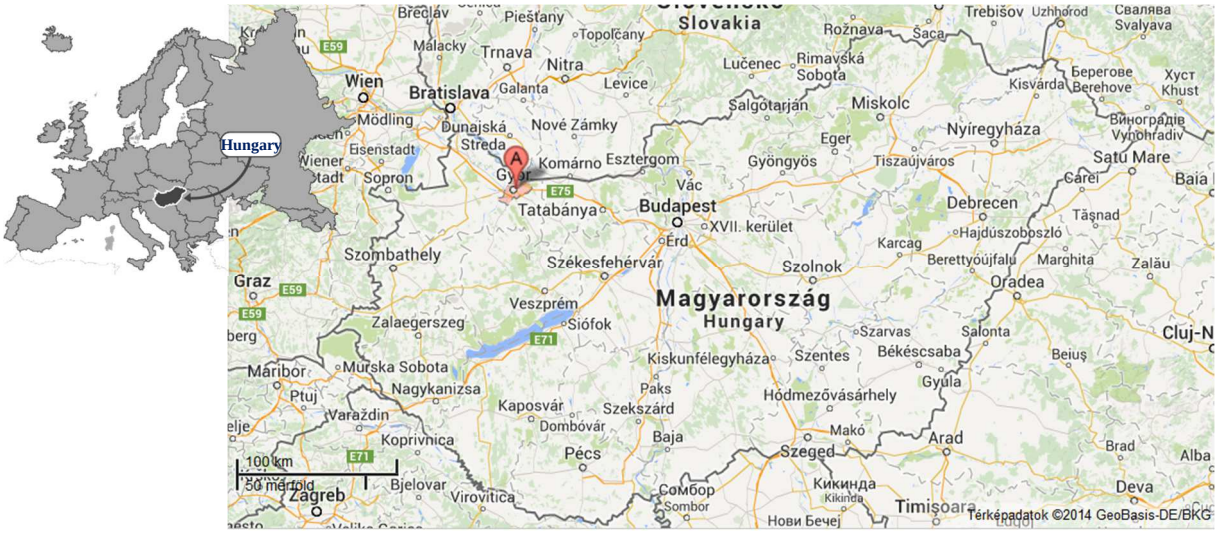

4.1. Figure: Győr is situated in northwestern part of Hungary (Google Map, 2014)

4.1. City of Győr

The dynamically developing city lies halfway between Budapest and Vienna, on one of the most important roads of Central Europe with an excellent accessibility. The city is located at latitude 48°41’ and longitude 17°38’ (Göcsei, 2005). Győr is also referred to as the City of Waters as it lies on the banks of river Rába, at the confluence of the Moson-Danube, the Rába and the Rábca; not far from the main channel of the Danube. It is rich in thermal water as well. Győr is Hungary's second richest town in historic buildings outside Budapest. Characteristic corner-balconies and narrow lanes, churches, museums are all reminders of a historic past, mainly situated in the center of the town.

4.2. Figure: Arial view of the Downtown (Civertan, 2014)

DOI: 10.15477/SZE.MMTDI.2015.002

4.1.1. General information

The development of the town enhance the understanding of the geological and soil conditions that are closely related to the urban layout, the periods, and the structure of the buildings. This emphasized the importance of historical, archeological, geographical knowledge about the city, so the research focused on these aspects too.

The most important factors that explain the existence of the city are connected with its geographical endowments and its location close to the Moson-Danube, the tributary of the main branch of the Danube. Along the southern part of the Danube, on the right bank was established an important transport route, which lead from the central part of Carpathian Basin through the Little Hungarian Plain to the west, through the Western Gate, an opening between the Alps and Carpathian Mountains before Vienna (Borbíró & Valló, 1956). The line for this route was explained by the fact that many rivers confluence to the Danube on the northern side, and only one obstacle had to be overcome on the southern part: the Rába and Rábca at one place: their confluence to the Moson-Danube at Győr. Other important routes branched off toward Sopron (Scarbantia), following Rába toward Szombathely (Savaria) Graz and Italy, toward Veszprém (Cimbria) and Székesfehérvár (Alba Regia).

The significance of this node contributed to the development of the settlement. Győr was inhabited at least from the 5th Century A.D. (Figure 4.3(a)). The present-day Downtown known as Arrabona was settled during Roman times, which is a flood-free terrace suitable for a fortress. Its significance increased during the Turkish occupation, when Győr became the most important border castle of Hungary. After the Turkish era, the suburb regions started to develop e.g. Újváros. In the 18th Century the southern parts were resettled, and new parts, such Sziget, became settled and Győr was raised to the rank of free royal city.

4.3. Figure: Settled parts of Győr in 3rd (a) and 13th Century (b), and around 1855 (c) (Borbíró & Valló, 1956)

On 28th June of 1763 a devastating earthquake destroyed some part of the buildings, even the Püspökvár (Bishop's Castle) suffered serious damages. (Winkler, et al., 2006)

DOI: 10.15477/SZE.MMTDI.2015.002

At the end of Napoleonic wars the fortress was destroyed by French engineers. As shown in Figure 4.3 (c) the outlook of Győr was changed, because it lost its military role and took on a new industrial and trading role from the beginning of 19th Century with fast expansion of the town (Nádorváros, Révfalu).

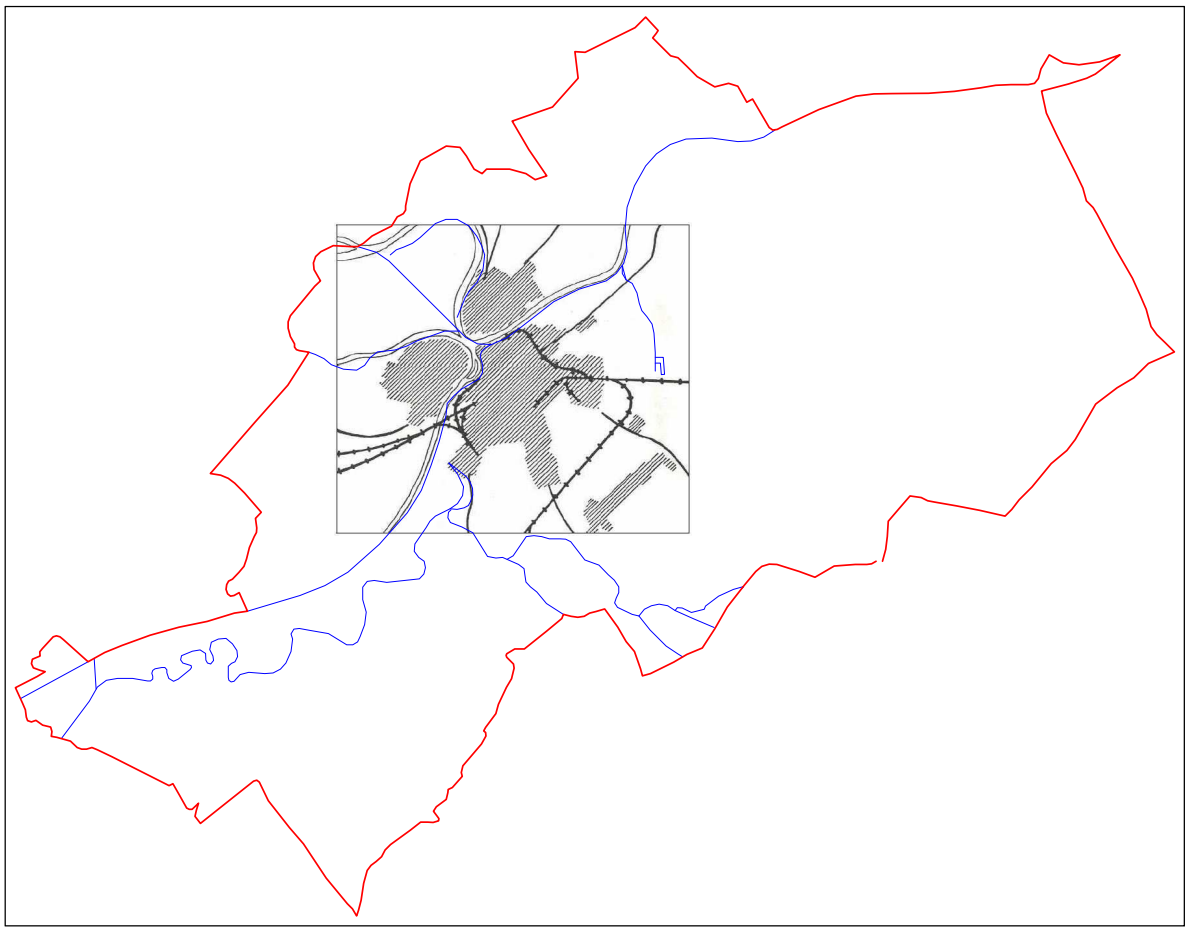

4.4. Figure: Extension of the city in 1910 and nowadays (Borbíró & Valló, 1956) (border of the city based on Google Maps)

The significance of waters at Győr changed through decades (Göcsei, 2005). Sometimes the river Rába and the Moson-Danube protected the castle, other time it had an important transportation task concerning the grain trade, since Győr was the country's largest grain trading and exporting center. Surface water and a high water table in every era could provide the city water supply, even for industrial needs too at the beginning of industrialization in the 19th Century. After the Second World War, deep drilling brought to the surface thermal water which can be used for recreation and medical purposes.

As an important industrial city, it suffered a lot of bombing and destruction during the Second World War, mainly affecting the bridges, railways and industrial buildings. Reconstruction started after the war. Parallel with the expansion of the population, construction

of dwelling houses started, mainly in Nádorváros in the years 1960-1971. The development of town districts as Adyváros and Marcalváros with large panel system buildings erected during 1970-1989 along with the reconstruction of Downtown. After 1990, a gradual migration started moving out from the denser areas into single family houses or apartment houses. Nowadays, the city of Győr has absorbed surrounding villages that have become the suburb-urban area of the town such as Ménfőcsanak, Gyirmót, Győrszentiván, Kisbácsa, etc.

The population of the city was constant over the past 20-25 five years, with more than 120 000 residents. Due to the latest census, Győr is the sixth largest town in Hungary with 131 564 residents (Hungarian Central Statistical Office, 2012. 01. 01). This increase is due to the migration concerning work opportunities (Rechnitzer, et al., 2014). After the building and textile industries were ruined at the end of 20th Century the town recovered in the mid-nineties. New types of industries recognized the geographical potential of the city. Due to economic and industrial development, Győr has become the second major city after Budapest in terms of economic competitiveness (HHP Contact Tanácsadó Kft., et al., 2011).

The fact that Győr is one of the largest cities in Hungary with leading cultural and economic role emphasizes the need for evaluation of seismic risk of the city, being very important because of the large number of living and non-living values. In case of the built environment, not only the residential buildings but also the huge number of monuments should be taken into account. Since residential buildings represent the largest percentage of building stock in Győr, this research focuses mainly on residential buildings.

4.1.2. Previous earthquakes

The seismicity of the Pannonian region is moderate. Earthquakes causing light damage occur every year, while stronger, more damaging magnitude 5 quakes happen about every 20 years and the return period of magnitude 6 events is about 100 years (Tóth, et al., 2006). The focal depth of earthquakes is between 6 and 15 km below ground level in the region. The distribution of earthquakes is diffuse; however, there are certain areas where the occurrence is more concentrated, e.g. at the surroundings of Komárom-Mór-Berhida, known as Móri-trench.

The largest earthquake in Hungary occurred in the city of Komárom in 28th of June 1763 with an estimated magnitude of 6.3, there were 63 casualties in Komárom and 4 in Győr. Overall more than 100 victims were reported. The taller (2-3 story high) ecclesiastic and noble buildings with more complex structure, typical for that age, suffered serious damage, both in Komárom and Győr, while the buildings of common people with only a ground floor made of adobe and timber survived the quakes (Varga, 2014). Remedial measures were applied after the

earthquake: the construction of 2-3 story high buildings were forbidden by authorities. Later damaging events happened in 1783, 1806, 1822, 1841, 1851, and 1857.

Based on the very detailed damage catalogue for mitigation purposes, Varga et al (2001) were able to determine the epicenter for the 1763 quake assuming a 10 km focal depth: 25 km from Győr and 10 km from Komárom on the line connecting the two towns (Varga, et al., 2001). Based on the 24% buildings destroyed, 30% seriously damaged, and 18% requiring reconstruction, the intensity can be assumed to be IX on the EMS (European Macroseismic Scale).

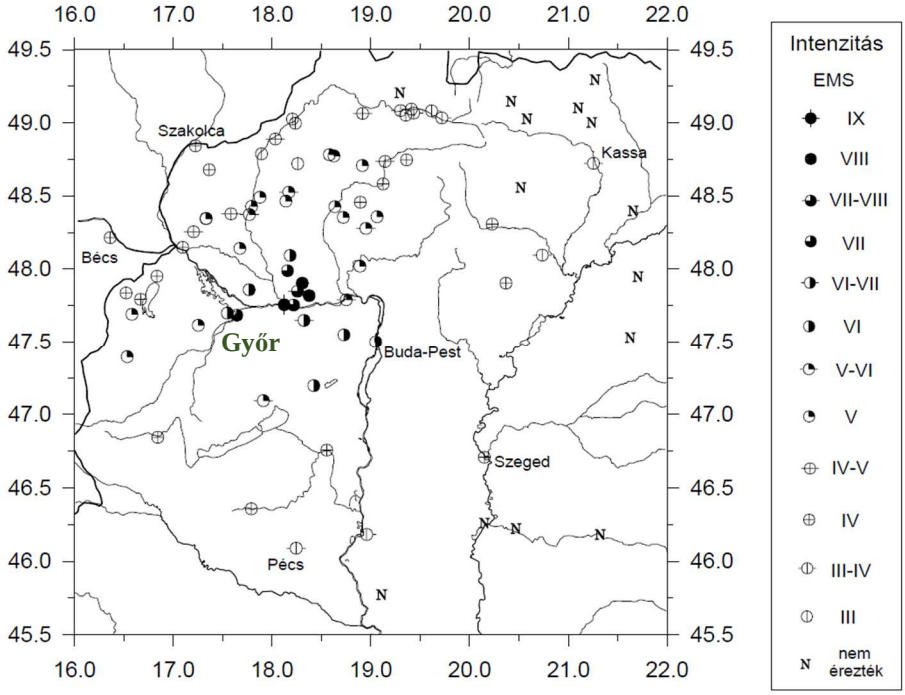

4.5. Figure: Distribution of intensities in 1763 earthquake at Komárom (Zsíros, 2000)

In Győr, the shaking affected mainly the inner city; clerical buildings were seriously damaged, but there remained no houses without some extent of loss in the Downtown region. This would translate to an EMS between VII – VIII on a scale from I to XII (Figure 4.5).

4.6. Figure: The painting from Mainzell (Austria) depicts the damages buildings in Győr suffered in the 1763 earthquake, even the tilted steeple can be recognized (Varga, 2014)

DOI: 10.15477/SZE.MMTDI.2015.002

The hazard map of Hungary (Figure 6.1, discussed later) illustrate that there are regions with higher earthquake hazard, such as the Móri-trench. Aerial distance between Győr and Móri-trench is about 60 km. Historic data show that major earthquakes of this area had significant effect on buildings, causing damage not only in Komárom, but also in Győr.

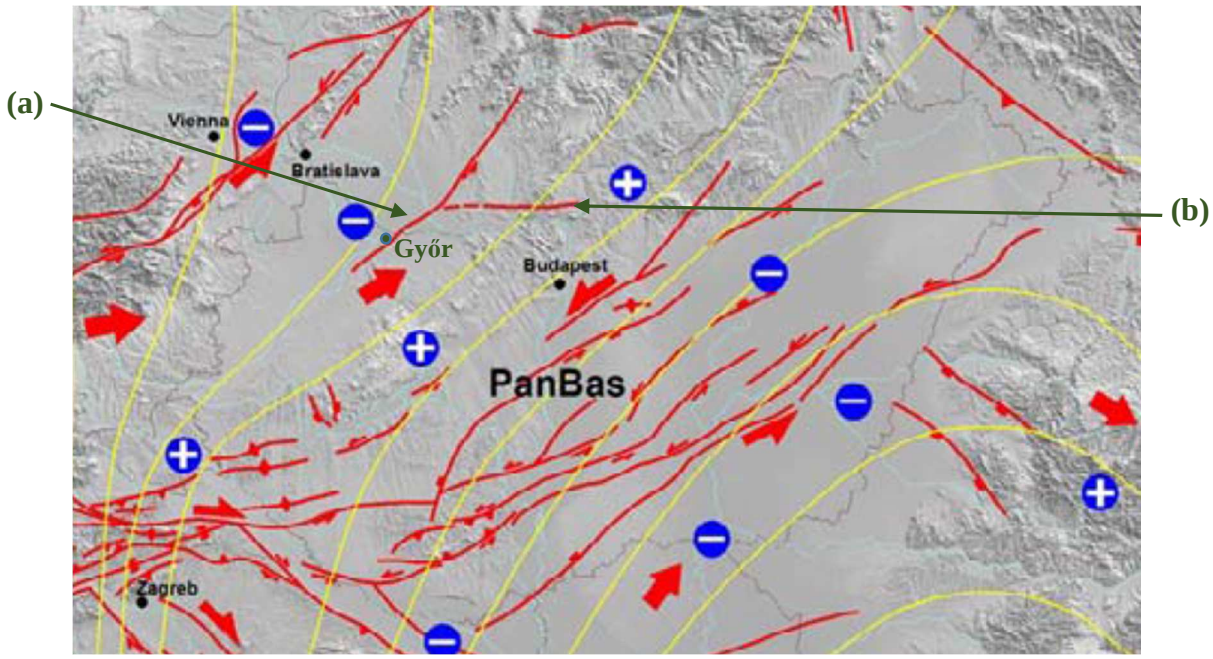

4.5. Figure: Neotectonics of Pannonian region (Bada, 2005)

Other significant faults contribute to the hazard concerning Győr. One of the lineaments lies beneath the Rába River, called Rába line (Figure 4.5 (a)) and meets the Diósjenő-Őgyalla or Hrubanovo fault (Figure 4.5 (b)) beneath Danube River close to Győr. Recorded earthquakes with epicenter at Győr mainly occur due to the above mentioned faults.

The following figure shows the annual number of earthquakes related to their magnitude. Horváth et al. (2003) states based on the diagram, that the seismic activity of the Pannonian region is increasing (Horvát & Bada, 2003). Present research collected the historical earthquakes with epicenter at Győr (listed in Table 4.1) and features about the shakes in the vicinity of Győr.

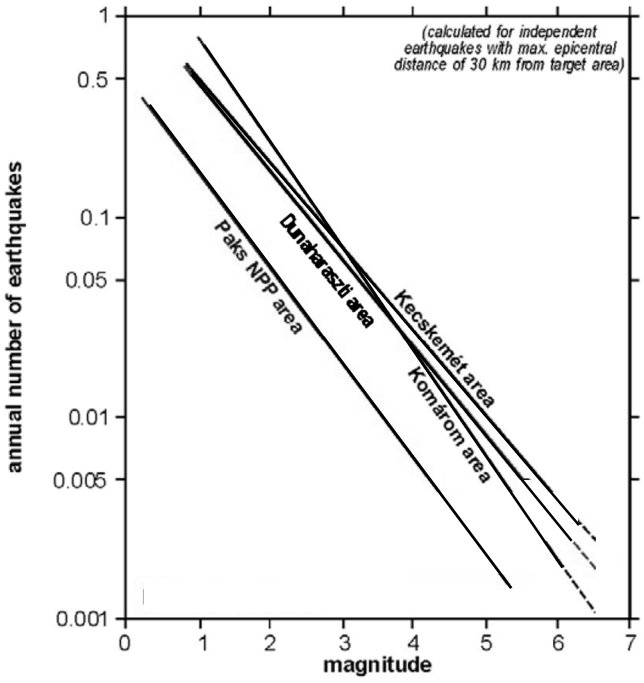

4.6. Figure: Frequency distribution of earthquakes for some seismogenic zone in Hungary (Varga, 2001)

4.1 Table: Earthquakes with epicenter at Győr collected from Hungarian Earthquake Catalogue *(Zsíros, 2000)*

Date	Latitude	Longitude	Depth [km]	Magnitude	Intensity	Place
1700. 02. 11.	47.68	17,65		3,5	5,0	Győr
1754. 10. 21.	47.68	17,65		3,5	5,0	Győr
1758. 08. 07.	47.68	17,65		3,2	4,5	Győr
1763. 08. 04.	47.68	17,65		2,2	3,0	Győr
1763. 08. 09.	47.68	17,65		3,2	4,5	Győr
1765. 02. 05.	47.68	17,65		2,9	4,0	Győr
1765. 02. 21.	47.68	17,65		2,9	4,0	Győr
1768. 01. 05.	47.68	17,65		3,9	5,5	Győr
1768. 09. 20.	47.68	17,65		2,2	3,0	Győr
1768. 10. 29.	47.68	17,65		2,2	3,0	Győr
1779. 04. 02.	47.68	17,65		2,9	4,0	Győr
1779. 04. 02.	47.68	17,65		2,9	4,0	Győr
1781. 10. 07.	47.68	17,65		2,9	4,0	Győr
1786. 02. 29.	47.68	17,65		2,9	4,0	Győr
1850. 10. 07.	47.41	17,38		4,9	7,0	Győr
1850. 10. 29.	47.41	17,38		3,5	5,0	Győr
1860. 04. 13.	47.41	17,38		2,2	3,0	Győr
1914. 02. 04.	47.68	17,65		2,9	4,0	Győr
1921. 05. 04.	47.70	17,81		3,5	5,0	Győr
1990. 08. 22.	47.77	17,57	8	2,9	4,0	Győr
1993. 07. 12.	47.71	17,67	8	2,8	3,5	Győr

The importance of the city as a regional center, the number of inhabitants and the closeness to the above-mentioned fault system, emphasizes the necessity of its earthquake risk analysis of Győr. Registered events with the epicenter around Győr and its vicinity were determined during this research (based on Hungarian Earthquake Catalogs):

- in the period of 456 to 1810 the number of registered earthquakes within a 100 km radius based on historical data is 216, in 151 cases magnitude and intensity values were determined: estimated magnitude value range between 2.2-6.3 and intensity based on EMS between III.-IX.;
- in the period of 1811 to 1910 the number of registered earthquakes within a 100 km radius based on historical data is 315, in 240 cases magnitude and intensity values were determined: estimated magnitude value range between 1.5-4.9 and intensity based on EMS between II.-VII.;
- in the period of 1911 to 2013 the number of registered earthquakes within a 100 km radius based on historical data is 2028, in 1953 cases magnitude and intensity values were determined: estimated magnitude value range between 0.8-5.2 and intensity based on EMS between II.-VIII..

DOI: 10.15477/SZE.MMTDI.2015.002

4.2. Site data

In order to understand the characteristics of the soil conditions in Győr it is necessary to examine the wider environment and what factors contributed to its geological development. One part of the research deals with the effect of local soil, so the background had to be investigated thoroughly. *"Topography is one of the most important factors in the geographical environment. Its configuration, origin, as well as past, present and future development is decisive for the character and course of the evolution of drainage, soils, flora, fauna and human settlements."* (Schweitzer, 2009)

4.2.1. Geographical data

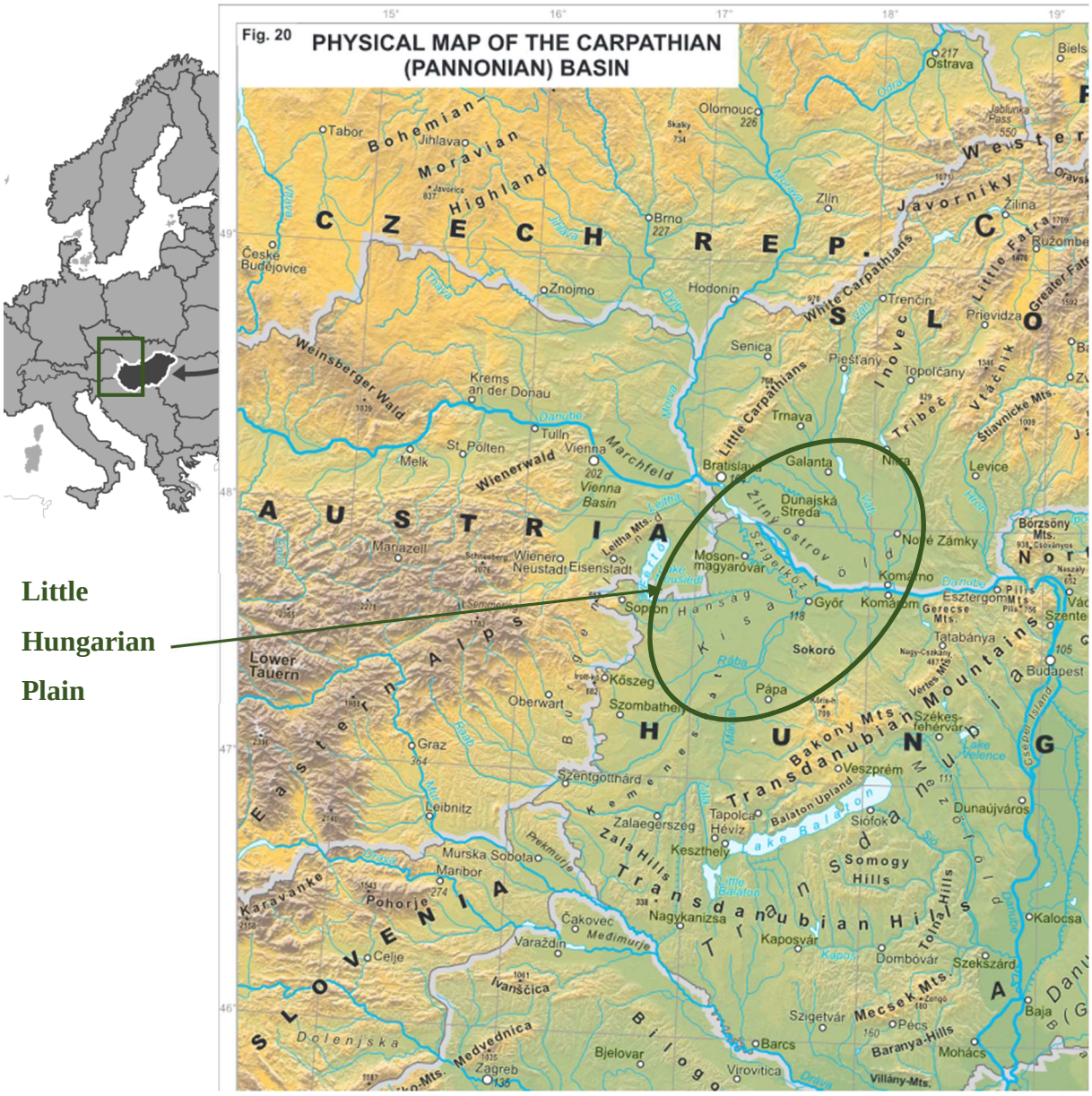

4.7. Figure: Section of the Physical Map of the Carpathian (Pannonian) Basin by Keresztesi at al. (Schweitzer, 2009)

Győr is situated in the eastern part of Little Hungarian Plain (Kisalföld in Hungarian), which is an extensive basin occupying the northwestern part of Transdanubia in northwestern Hungary, and extending into Austria and Slovakia. The Little Hungarian Plain is a depression located in the northwestern part of the Pannonian Basin, bordered by the Transdanubian Mountains: Bakony and Vértes on the south and Gerecse on the east, the North-Western Carpathians (Little Carpathians) to north in Slovakia and the Eastern Alps (Leitha Mountains) to west in Austria. It has an area of approximately 9,000 square km. Its territory is divided by the main branch of the Danube. The greater part of it (north of the river as Danubian Lowland) belongs to Slovakia, the rest is situated in Hungary. Smaller micro regions of The Little Hungarian Plain are: Seewinkel, Neusiedl Basin, Győr Basin (formed by marshy lowland of Fertő-Hanság, Szigetköz (Small Detritus), Moson Plain, Rábaköz (Rába Interfluve)), Marcal Basin, Komárom-Esztergom Plain and Csallóköz (Great Detritus).

Győr can be found just at the intersection of Győr Basin, Marcal Basin, foothills of Bakony and Komárom-Esztergom Plain determining the soil conditions of the city districts belonging to different geological formations.

4.2.2. Hydrology of the area

The Danube River serves as major drainage for Little Hungarian Plain in the direction from west to east. The climate is relatively dry, but abundant water comes from the surrounding highlands. On the Hungarian side, the Rába River and its tributaries drain the connecting section through Győr, while on the Slovakian side, the system of the Vág River confluence to the Danube at Komárno (Komárom).

Water is a very important geofactor in the life of Győr, which played an important role not only in geographical formation, but also in the urban development of the town (Göcsei, 2005). The three major rivers can be found even in the coat of arms of Győr: Moson-Danube, Rába and Rábca, but even the Great Danube has a huge influence on the city. The confluence of the Moson-Danube to the Great Danube is only few kilometers away from the city, and in case of floods can have an impact on the city (e.g. floods in 1954, 2013).

After the Danube reaches the Little Hungarian Plain it changes, getting a lower stream flattening, slowing and meandering into many branches, laying down sediments and filling up the riverbed (Alföldi, 2009). Before its regulation, it would often flood due to alluvial reefs. The permeable gravel and sand layers of Szigetköz and Csallóköz are highly sensitive to the water level of the Danube. It was regulated in three steps between 1886 and 1894: secondary water regulation, construction of flood protection dikes and reconciliation of inland water.

DOI: 10.15477/SZE.MMTDI.2015.002

The most significant river of Győr is Moson-Danube, which played an important role defending the fortress at Győr in the old times, nowadays separates the districts of the town. It branches off the Great Danube at Oroszvár and Dunacsuny (two settlements in Slovakia) and after 125 km on the southern part of Szigetköz confluences into the Danube at Vének (about 10 km distance from Győr city center). In Győr it picks up the Rábca and Rába, therefore the amount of water increases and becomes navigable. The 1883 flood destroyed the buildings in two settlements Sziget and Révfalu (nowadays districts of Győr), so regulation of Moson-Danube took place at the time as Danube regulation, maintaining the navigable feature of the river. The Rajka sluice was built in 1907, in order to avoid floods coming from Austrian region with Danube, but there remain still flooding risk because of Rába River and the backwater flooding of Danube. Further regulation of Moson-Danube consisted of the building of Industrial Channel (Ipari csatorna) between 1913 and 1924. After that in the eighties the cutoff of one of the river bends at Püspökerdő (Bishop's Forest) was dug adding a 2200 m long new bed for the river to serve as flood prevention, and offer sporting and recreation opportunities. The purpose of the Industrial Channel was to use for industrial shipping. The northern part was a side branch of the river at Kiskút (District of Győr) and southern part was incised in to one of the terraces in the direction of Komárom-Esztergom Plain. The old branch of the river can be seen on the old military maps. (Göcsei, 2005)

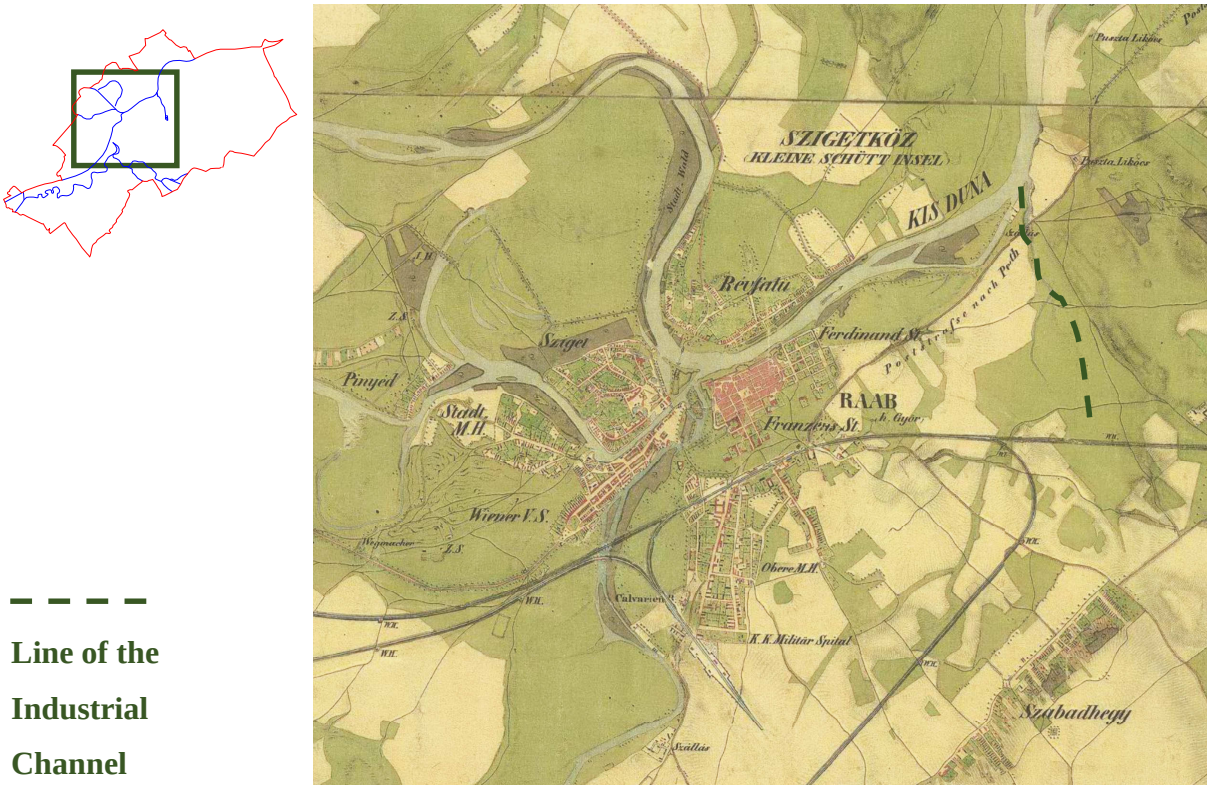

4.8. Figure: Győr on the historical maps of the Second Military Survey of Habsburg Empire made between 1806 and 1869 (Austrian National Archives & Arcanum Adatbázis Kft., 2014)

DOI: 10.15477/SZE.MMTDI.2015.002

The other major river is Rába, originating from Eastern Alps. It enters the Győr Basin at the town named Sárvár and flows on the right side of Rábaköz, which is the alluvial fan of the Rába. Because of the high altitude drop, Rába is rapid-flowing. Floods run down quickly, mainly when the melting of the snow coincides with heavy rain. The length of the river was shortened by 48 km using 48 cutoffs, and a new bed with 10 km length was created between Rábapatona and Győr during regulation in 1893. The old bed of Rába, just the Moson-Danube bend at Püspökerdő, become an abandoned channel. The Rába flows to the north in Győr and confluences the Moson-Danube at Downtown. (Göcsei, 2005)

Marcal River was regulated between 1890 and 1893, when its water was lead to the old Rába bed and entered the Rába at Győr. A sluice was built at Gyirmót (nowadays one district of the city), and the water of Marcal was redirected to enter Rába between Koroncó and Gyirmót in 1931-1932. Because of the changes, the name of the abandoned riverbed is Dead Marcal instead of Dead Rába on new maps (Göcsei, 2005). The stream of Pándzsa confluences the Dead Rába between Győr and Ménfőcsanak (nowadays a district of Győr). The Pándzsa originates in the Pannonhalmi hills, the foot of the Bakony Mountains.

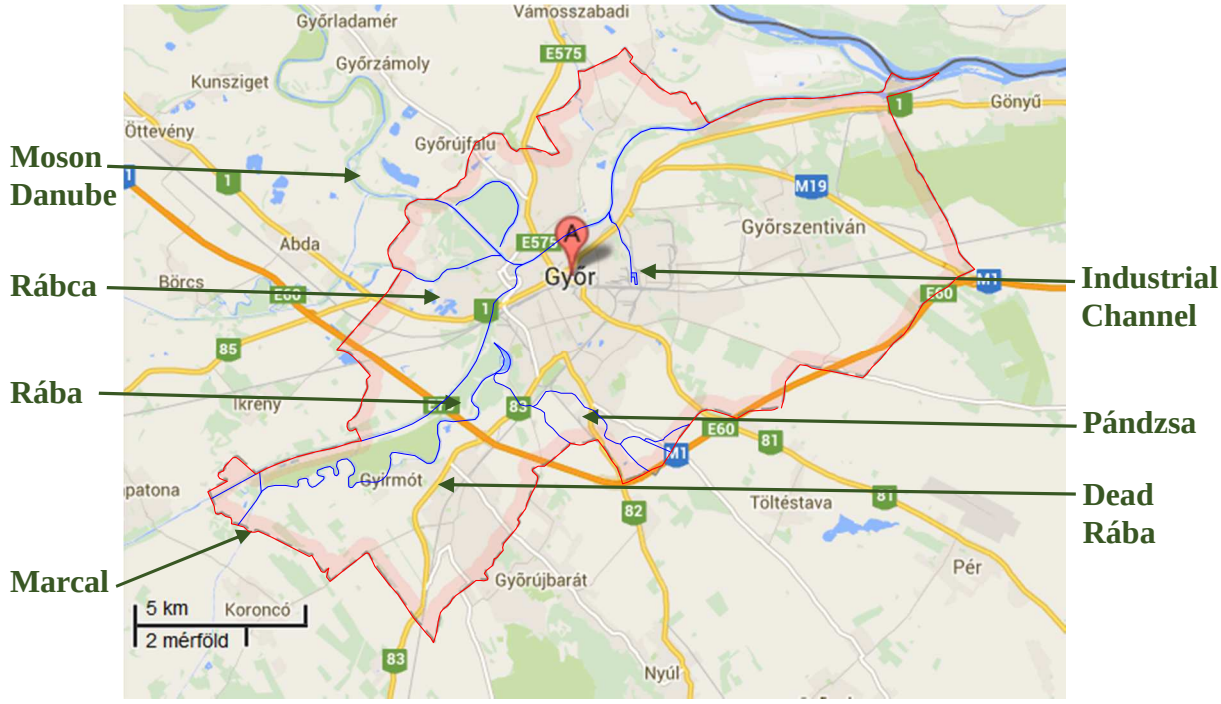

4.9. Figure: Rivers of Győr (Google Map, 2014)

Rábca River originates in Austria, it is named Répce on the upper section, and after the confluence of Small Rábca it is named Rábca. This river arrived in the city and formed two branches around Sziget (Island) in the bed of an old riverbed of Moson-Danube. Its original confluence was at Abda based on archival data (Borbíró & Valló, 1956). One of the branches

DOI: 10.15477/SZE.MMTDI.2015.002

was filled up in the year 1920, this way the island feature of Sziget disappeared. At the beginning of 21th Century the firth was relocated close to its original place, to Abda.

The goal of all regulation work in the 19th and 20th Century was to prevent floods in the city. Because of the above mentioned human intervention and the Gabčíkovo-Nagymaros Dam (Erdélyi, 1990) the water level decreased by the beginning of 21st Century by 65 cm at the confluence of Rába and 188 cm at the confluence of Moson-Danube. Recently a rehabilitation project started to control the level of the waters from ecological and urban view aspects: Moson-Danube is unable to carry further the suspended sediments of Rába and Rábca (Western Transdanubia Water Authority, 2014).

Groundwater conditions in the Győr Basin are very sensitive to the rivers. The depth of groundwater hardly reaches 2 m next to the Danube and is below 2 m next to the Moson-Danube (Marosi & Somogyi, 1990). There is a tendency of drawdown of the groundwater level due to the above mentioned human intervention (Szabó, 2005).

The groundwater is deeper than 2 m at most places in Győr, but into the direction of Pannonhalmi Hills it deepens even more from 5 to 15 m depth. The groundwater depth varies due to the distance from rivers, the water level of rivers and geomorphological aspects. The difference between the minimum and maximum level of groundwater surface is very diffuse in Győr, in the northern part of the city and next to the Dead Rába it is around 2.4-2.9 m, while on the southern part of the city is only 0.9 m. Even the level of the minimum groundwater level rises to the south, which is accountable for the higher ground surface level.

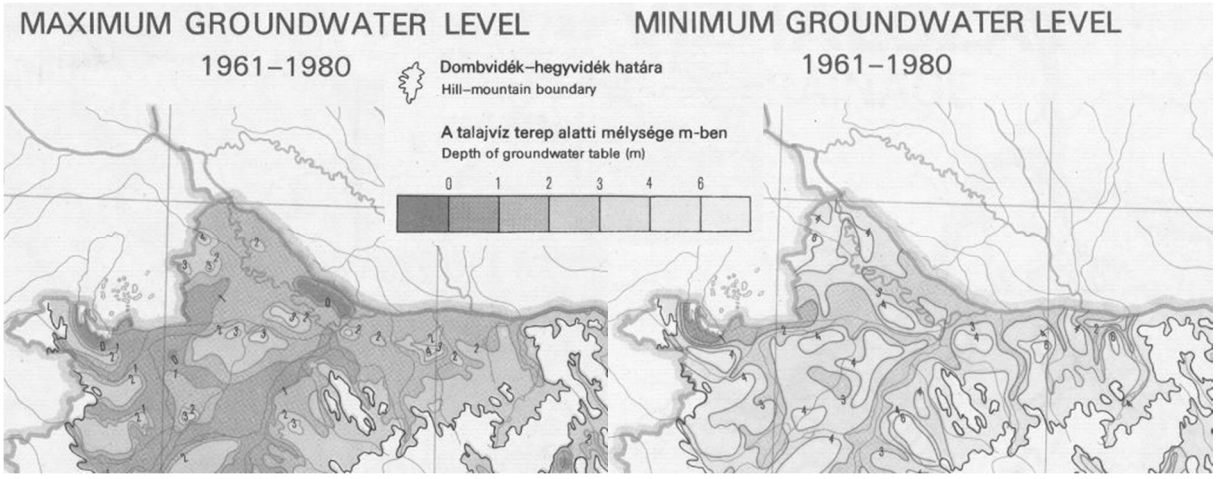

4.10. Figure: The depth of groundwater level at Győr varies between the maximum 2 m, and the minimum 3 to 4 m based on the National Atlas of Hungary (Cs. Deseő, 1989)

On the sketch about the geomorphological and water geography conditions of the ancient settled landscape can be clearly seen the changes of the Moson-Danube River and even the former Rába riverbed can be noticed before humans appeared (on the Figure 4.11).

DOI: 10.15477/SZE.MMTDI.2015.002

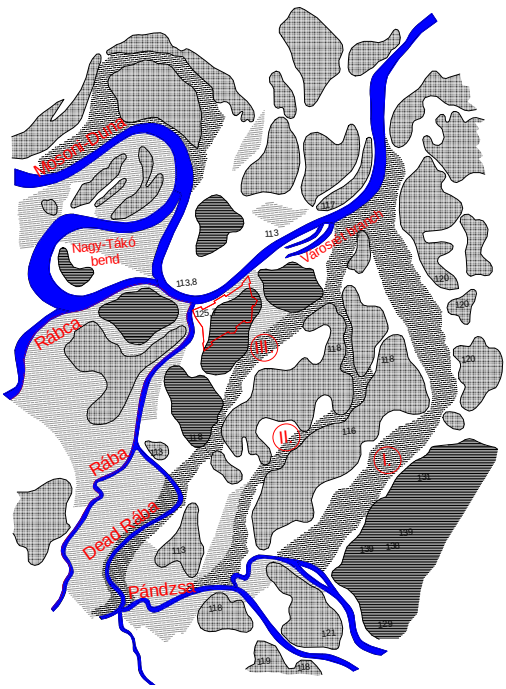

4.11. Figure: Redrawn after the illustration of Borbíró: ancient landscape of Győr area (Borbíró & Valló, 1956)

The original illustrations by Borbíró (Borbíró & Valló, 1956) was based on contour maps and archeological findings. It gives a good explanation on the forming of the settlement at this place. Natural defense lines were around the terraces and hills where the first traces of settlement can be found. From the west, only the Sziget arose from the bends of the Moson-Danube. South of this, the marshland of the Hanság Plain almost reached the line of the Rába. From the east, the border was the Moson-Danube. From the Dead-Rába and Pándzsa Stream three parallel lines of natural ditches ran to the direction of the Moson-Danube. These lines can be even recognized on recent contour maps. Other abandoned channels and flood terraces can be seen in satellite images from Google Earth.

4.2.3. Geology and tectonics of the Little Hungarian Plain

From a geological point of view Győr lies in the eastern part of the macro region of Little Hungarian Plain, which is a deflational lowland with a median altitude of 125 m a.B.s.l. (above sea level referred to Baltic Sea), a little higher than that of the Great Hungarian Plain. With attachment of the settlement of Ménfőcsanak in 1970 the city extends to the Pannonhalmi Hills, which is classified as part of the Transdanubian Mountains. Thus the formation of the area is related to these two large regions related to origin. (Göcsei, 2005)

The Little Hungarian Plain is properly plain only in its middle and north-central part. From north to south running hilly land between Lake Fertő and the Rába River called Rábaköz (Rába Interfluve) represents a huge alluvial fan with terraces and wide flood plains, made up of gravel during the Pleistocene times. The Marcal Depression is a subsidiary part of the Little Hungarian Plain, between Kemenesalja (southern part of Rábaköz) and the Bakony Mountain with Marcal River in the middle. Here are situated also the basalt-capped monadnocks: Mt. Somló (435 m) and Mt. Ság (291 m). The slight rise of Kemenesalja (Foot of Kemenes Rise) separates the Marcal Depression from the Győr Basin. The flood-plain accumulated by the Danube and its tributaries turns into slightly dissected, eroded lowlands and plains of medium elevation with terraces and outlier towards the marginal regions of the Kisalföld.

The 200 km long and 30–50 km wide southern marginal Transdanubian Mountains consist of gently undulating hilly country, dissected by deep valleys with a southwest–northeast strike. This upland between the depressions of the Little Hungarian Plain and the Great Hungarian Plain, is generally of low elevation, averaging between 400 and 500 m a.B.s.l. and consists mostly of Mesozoic limestone and dolomite rocks, and between the chain of horsts, sandstones gravel and clay deposits can be found of Late-Pliocene-Early-Pleistocene age. The present morphology was formed during the Quaternary period by fluvial erosion, tectonic movements and deflation processes. (Schweitzer, 2009)

The northern margin of the Little Hungarian Plain consists of similarly hilly country dominated by a thick loess cover. To the west of the plain can be found the West Hungarian Borderland macro region, including the isolated blocks of the crystalline range of the foothills of Eastern Alps (the Sopron, Kőszeg and Vas Mountains averaging between 400 and 550 m a.B.s.l.) descending to the gravel-covered alluvial plain through foothill slopes. (Göcsei, 2005)

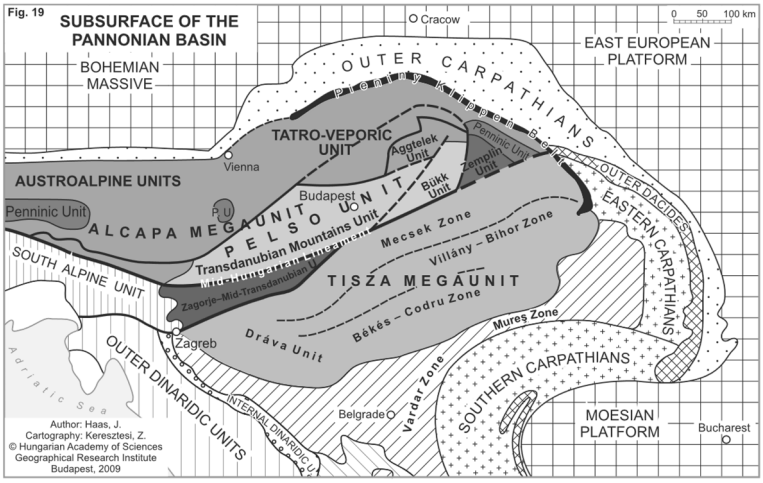

4.12. Figure: Present-day structure of the Pannonian Basin (Haas, 2009)

The pre-Neogene basement of the Carpathian Basin consist of structural units with different geologic history: Tisza Megaunit and Alcapa Megaunit overthrusted by European plate and Adriatic microplate (Fig. 4.12). The characteristics of this region are: large basin formation over thin, 22-32 km wide crust, high geothermal gradient (41–56°C/km) and high surface heat flow (80–120 mW/m^2), a thick lacustrine layer of Late-Miocene-Pliocene Pannonian Lake, above that Quaternary loess, sand and alluvial deposits. (Haas, 2009) The tectonics of the Carpathian basin is determined by the counterclockwise rotation of the Adria microplate and the north-northeast directed movement originating from the rotation (Földvary, 1988). Recently the neotectonic phase (Fig. 4.5) of the Pannonian Basin has been characterized by collision along the Alps-Dinarides belt, eastward extrusion of Alcapa, inclusion of Tisza Megaunit, and finally their collision with the Eastern Carpathians (Horváth, et al., 2009).

The Little Hungarian Plain is a lowland of the Pannonian Basin determined mainly by its Late Tertiary development. The tectonics of the basin sequence was controlled by their adaptation to the basement blocks moving differentially along the systems of faults developed during earlier Tertiary times (Földvary, 1988). The formation of the basin started in the second half of the Miocene. A Neogene sedimentary sequence directly overlies the crystalline basement. The oldest Neogene layers are thin. The Lower Pannonian sequence is even absent on the higher parts of the basin, mostly ranging between 200-300 m to 600-700 m. The thickness of upper Pannonian sediments reaches 1700-1800 m (Göcsei, 2005).

Submergence and basin formation of the Little Hungarian Plain began several million years ago. There was continual process of subsidence from Early Pannonian times to the present with the highest rate of subsidence in the Upper Pannonian starting in the southern part of the basin. The last part to subside was the crystalline basement block of Fertő-Hanság Depression, which might have started to sink in the Late Miocene. (Földvary, 1988) At the end of the Upper Pannonian, the fast sinking of the basin stopped, the inland sea receded, and then 100 m thick sand layers were deposited mainly by the ancient Danube and tributaries with a coarse gravel sediment on the top. Deposition and local submergence has continued on a smaller scale recently, and the Little Hungarian Plain is subsiding very slightly (Schweitzer, 2009).

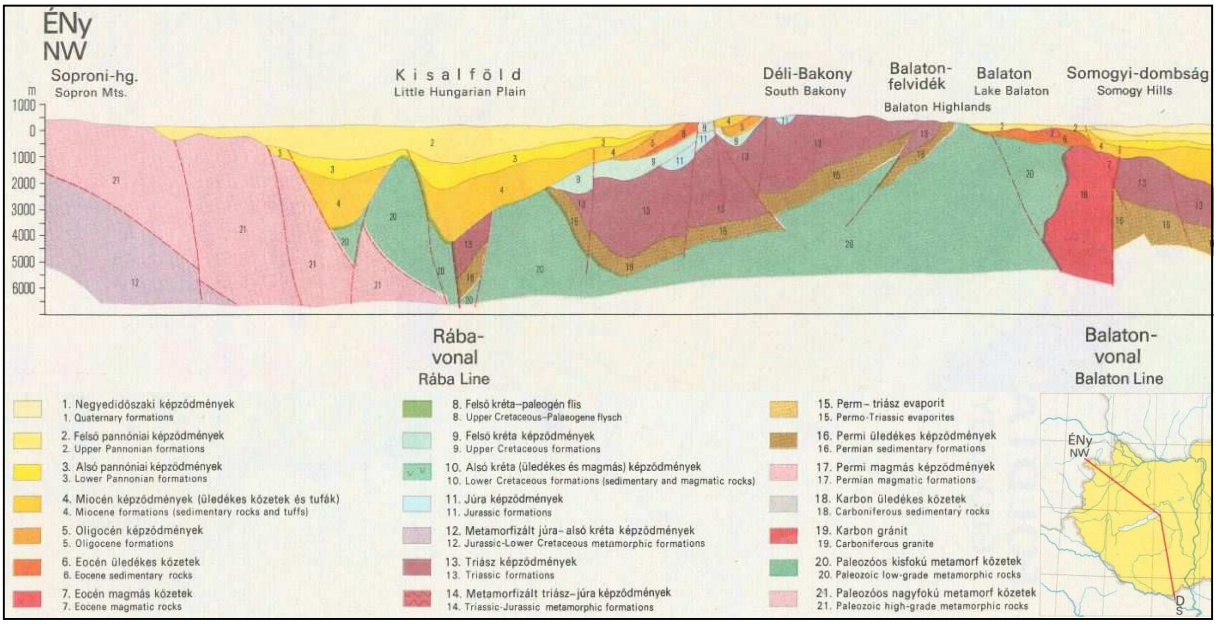

4.13. Figure: Part of the map of Geological Sections (Haas, 1989)

The most prominent tectonic lineaments in the basement determine the geological structure are the Rába Lineament, running from southwest to northeast, and the Danube or Hrubanovo Lineament with an exactly E-W direction (Figure 4.5), which separates two different geological units. Northwestward from this structural line the basement consist of

metamorphic rocks. It appears to be a continuation of the central zone to the East Alp formation sunken below the basin sediments, to a depth of 1500-2500 m in the central part of the Little Plain. Southeast from this the Mesozoic sequence can be found as the continuation of the Transdanubian Central Mountains. The difference between the two sides of the line suggests a strike slip structure. (Varga, et al., 2001)

All the rivers, even the Danube and the Rába and their tributaries flowed southward toward the Dráva River before the basalt volcanism in Late Pliocene. A ridge across the Hungarian Little Plain area was uplifted creating the present drainage pattern of the Hungarian Little Plain, forming the present-day Danube-Dráva watershed, with a narrow bar between the rivers Zala and Rába. These geomorphological conditions determined the eastward flow of the rivers entering the Hungarian Little Plain, instead of southward. (Földvary, 1988)

4.2.4. Geomorphology and soil profile conditions of Győr

The geologic formation of the surrounding area had a great influence on the geomorphologic conditions of the city. As mentioned above, Győr can be found at the meeting point of different landscapes: to the southwest can be found Marcal Basin, to the west Rábaköz, to northwest Szigetköz and Moson Plain as parts of Győr Basin, to the east the lowland of Komárom-Esztergom and in addition to the south the Pannonhalmi Hills belonging to the foothills of Transdanubian Mountains. The city is in a perfect urban location since it can be considered almost flat with non-floodable terraces, and only small areas to the south have differences in elevation larger than 25 m. The above Baltic Sea levels vary from 110-113 m from north to 132-145 m to south, Ménfőcsanak having the highest point with 168.9 m a.B.s.l.

The extended town has districts from each of the previously-mentioned landscapes; therefore, the soil profile of the area is quite diverse. The sediments of the Rába can be found on the southern parts of Győr. The alluvial fans of Danube lowland can be differentiated by age: the older sediments of Pleistocene on the terraces of Sashegy and Szabadhegy (nowadays districts of Győr) on the surface, while the younger sediments of Holocene after the sinking of Győr Basin with an even horizontal layer on the north of the city. (Göcsei, 2005)

Different elevations can be distinguished and separated easily from each other:

- low floodplain,
- high floodplain,
- shifted sand surfaces,
- II.a terrace (being one of the most important terraces of the city),
- II.b terrace,
- III. terrace,
- Pannonhalmi Hills (Figure 4.14). (Göcsei, 2005)

DOI: 10.15477/SZE.MMTDI.2015.002

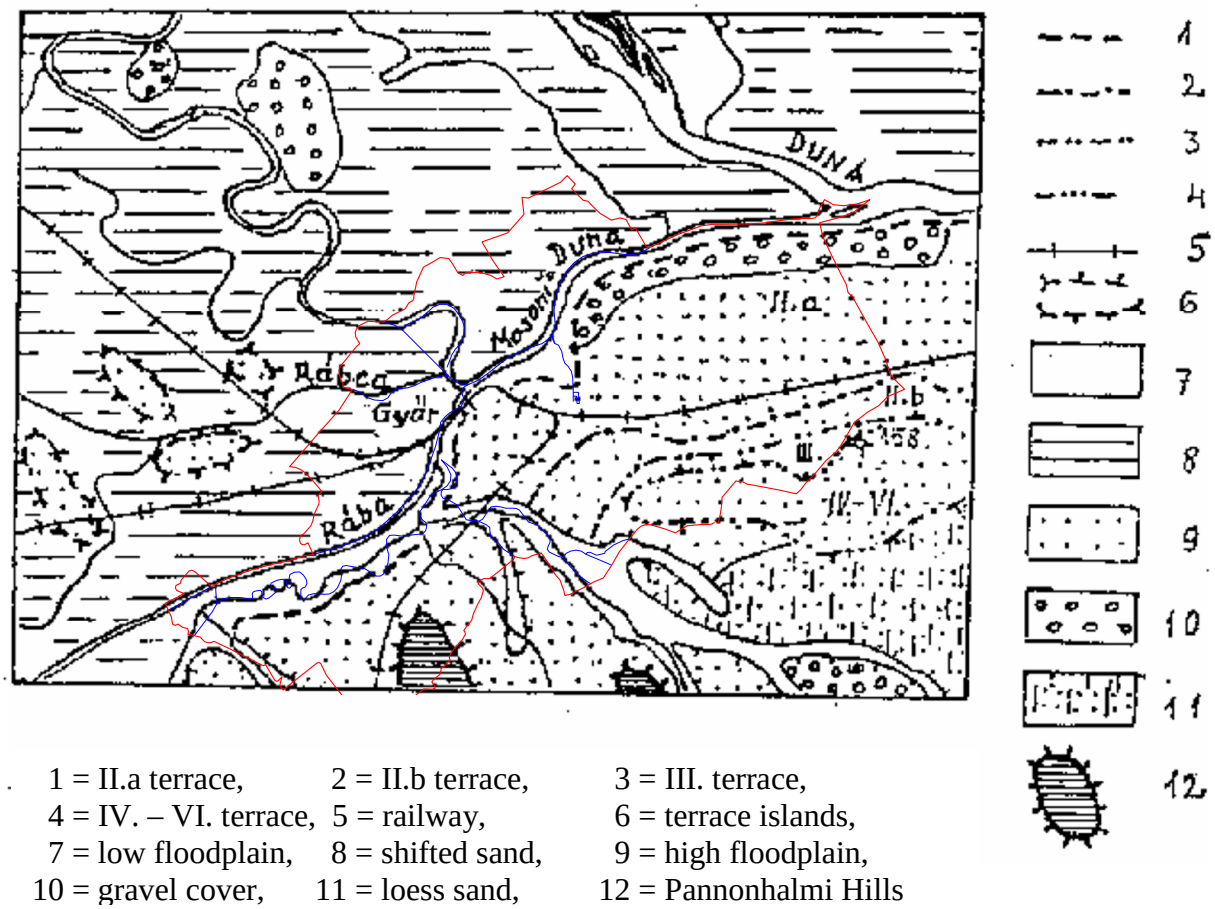

1 = II.a terrace, 2 = II.b terrace, 3 = III. terrace,
4 = IV. – VI. terrace, 5 = railway, 6 = terrace islands,
7 = low floodplain, 8 = shifted sand, 9 = high floodplain,
10 = gravel cover, 11 = loess sand, 12 = Pannonhalmi Hills

4.14. Figure: Terraces around Győr with the borders of the city (Göcsei, 2005)

The low floodplain areas vary in with along the watercourses. Those areas are listed here, which are inundated by river floods, or due to the high water level are covered by inland waters (e.g. to the north of the Danube and the west of Rába).

The high floodplain occupies large areas in marginal parts of the city. There can be found Holocene sediments of pale yellow mud, sandy mud, sometimes clay, clayey silt above sandy gravel layers.

Shifted sand surfaces can be found in the northern part of the Révfalu from Sáráspuszta trough Kisbácsa to Bácsa runs with 123 m a.B.s.l., 10 m higher than surrounding areas. The sand is running due to west winds disposition from the Moson-Danube riverbed at low water.

II.a Pleistocene terrace is the most important (formerly called City) terrace south of the Moson-Danube built up with three dunes: in the Downtown the Káptalan (Chapter) Hill (125 m), Kálvária (Calvary) Hill (113 m), and the site of Wagon Works and Spirit Works (latter eroded). A similar height of 117-120 m a.B.s.l. areas belong to II.a terrace starting from the dunes to the direction of II.b terraces, but with a different soil profile, since there are deeper (111-114 m) wet tracks running through it. In the earlier ages transport was only possible

because of shallows and higher spots. This terrace runs parallel to the Danube to the east toward Tata Ditch.

The II.b terrace arises from the main street of Szabadhegy (József Attila street) to the south, with an altitude of 130-132 m a.B.s.l., i.e. situated about 14 to 16 meters higher than Downtown. It stretches to the east as a narrow band with sandy silt and loess sand on the surface. The line between the II.b and II.a terraces is running above the ancient Rába riverbed (marked with I. on the Figure 4.11).

The III. terrace is extracting from Szabadhegy, it begins at Sashegy (145 m) and continues with the Kecskemét - tip (158 m). It is a narrow band extending eastward parallel to II.a and II.b terrace.

The northern part of Pannonhalmi Hills belongs to Győr since 1970 (after attachment of Ménfőcsanak). The hill is built of Pannonian sand, sandstone and clay hills falling below the sediments of Rába along fault lines at Ménfőcsanak. The highest projections of this area are: Rákóczi tree (183 m), Világosvár (167 m), Reiter (Reichter) (167 m). (Göcsei, 2005)

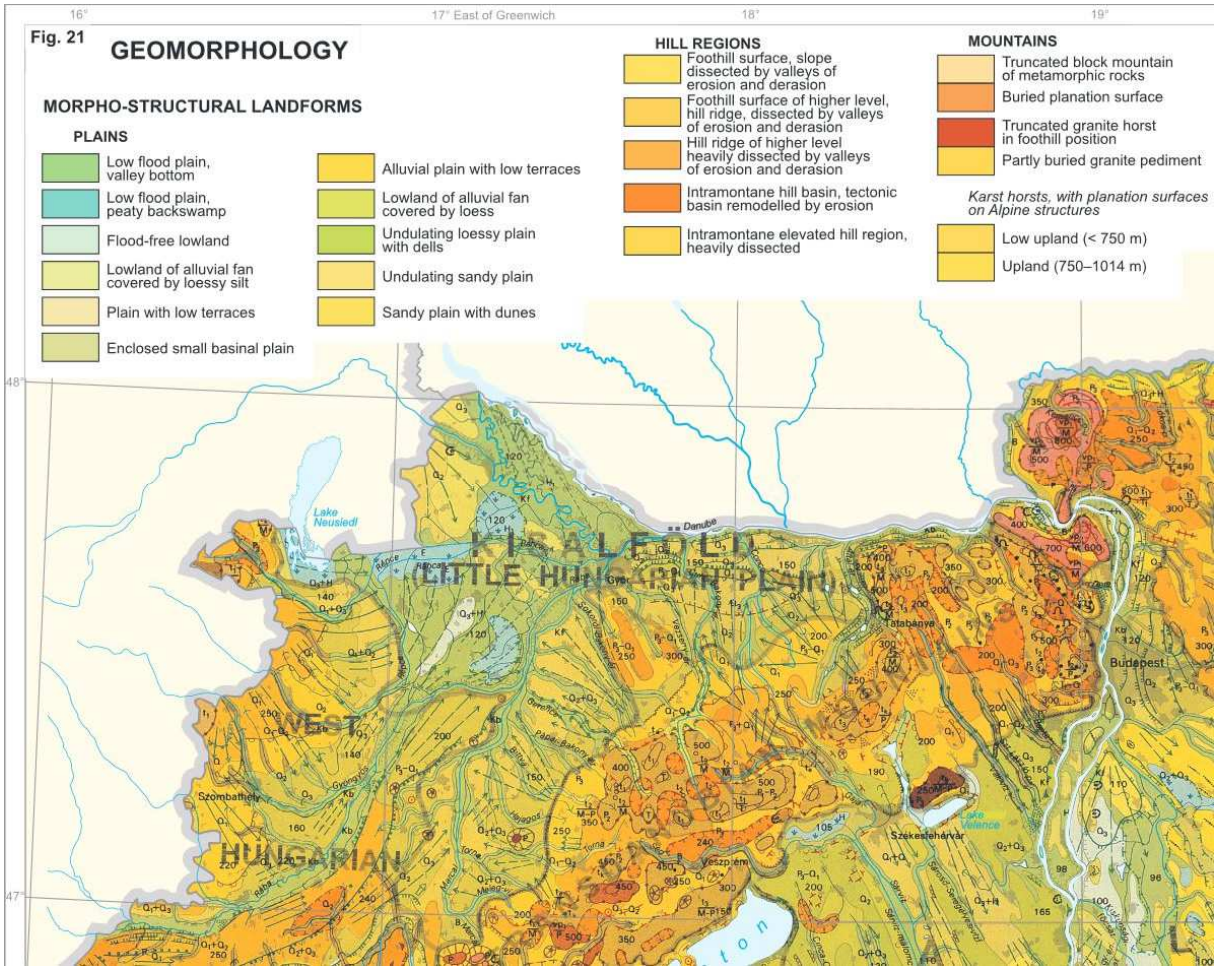

4.15. Figure: Section of the map the Geomorphology of Hungary Ádám et al. (Schweitzer, 2009)

DOI: 10.15477/SZE.MMTDI.2015.002

4.3. Built environment

Geomorphological conditions (Section 4.2.4) had a significant impact on the development and evolution of the town and takes effect even nowadays. The elevated flood-free terraces at the confluence of rivers offered a good possibility for the very first settlement, the Downtown (Belváros) is basically the oldest part of the city. The fact that the town is expanding to the south and east is basically due to the surface conditions. Surface water and the high water table in every era provided adequate water supply, also for industrial purposes. After the Second World War to the surface deep drilling brought to surface thermal water, which plays a role in medicine and tourism accounted for development of several part of the city.

The current city structure was the result of the merge of ten historical town parts. The historical Downtown (Belváros), the preterm and Late Middle Ages buildings, as well as the new and latest buildings form an organic urban structure. The suburb regions gradually built together with the historical city. Development of the urban areas were strongly influenced by the railway lines built in 19th Century. The industry was the key factor in the growth of several town districts such as Révfalu and Nádorváros in that time.

After the Second World War, the most striking developments took place in two areas: first, the neighborhood villages had been attached to the city, secondly the rapid industrial development led to the creation of new industrial areas between Downtown and Gyárváros (factory area). Accelerated urbanization enhanced the development of panel housing estates (Sziget, Gyárváros, Adyváros, József Attila lakótelep, Marcalváros). These panel estates formed a large contiguous zone in the last fifty years of the 20th Century. They were connected with small town and suburban residential areas. Bridges built over Rába and Danube connected the districts of the city. The establishment of the Transport and Telecommunication Technical College (nowadays known as Széchenyi István University) in Révfalu in the year 1968 had also influence on the urban development.

The transition period at the end of 20th Century brought again great changes. The economic crisis escalated, as a result, many former plant closed or new ones occupied previous sites. Concerning residential buildings the decline in housing construction was followed by parceling new areas and a more dense construction of the location of degraded houses.

The land use structure shows a transition between small town and big city: the historical Downtown has all the features of a city center, and no other developed district centers have the same functional variegation. Despite the dense panel districts and city center, the residential parts of the city are low-density residential areas with family houses, spreading still continues.

DOI: 10.15477/SZE.MMTDI.2015.002

The road network of Győr has basically a radial structure, passed by the motorway from south. Due to suburban and other sub-regional traffic there is significant road congestion in rush-hours. Recently, the main restructuring is the connection of the city districts, the development of the infrastructural system and the complex rehabilitation of several districts.

4.3.1. Districts

A total number of 21 city districts are grouped and presented according to the typical urban fabric. It can be differentiated between urban areas, housing estates, garden cities, and attached villages, recreational, industrial and commercial areas. (Table 4.2, 4.3, 4.4, 4.5)

4.2. Table: Territory distribution of the different functions of urban historical districts

HISTORICAL URBAN					TOTAL
Function of the area	**Belváros**	**Nádorváros**	**Újváros**	**Révfalu**	
economic, commercial, industrial	2.51%	30.23%	8.34%	1.49%	
special (cultural, educational, ecclesiastic)	69.79%	14.72%	5.94%	9.57%	
rural residential	-	7.69%	50.25%	36.97%	
garden city residential	-	29.74%	15.11%	34.49%	
urban residential	4.89%	12.46%	0.40%	0.14%	
Total area [ha]	**90.49**	**256.37**	**117.39**	**263.81**	***728***

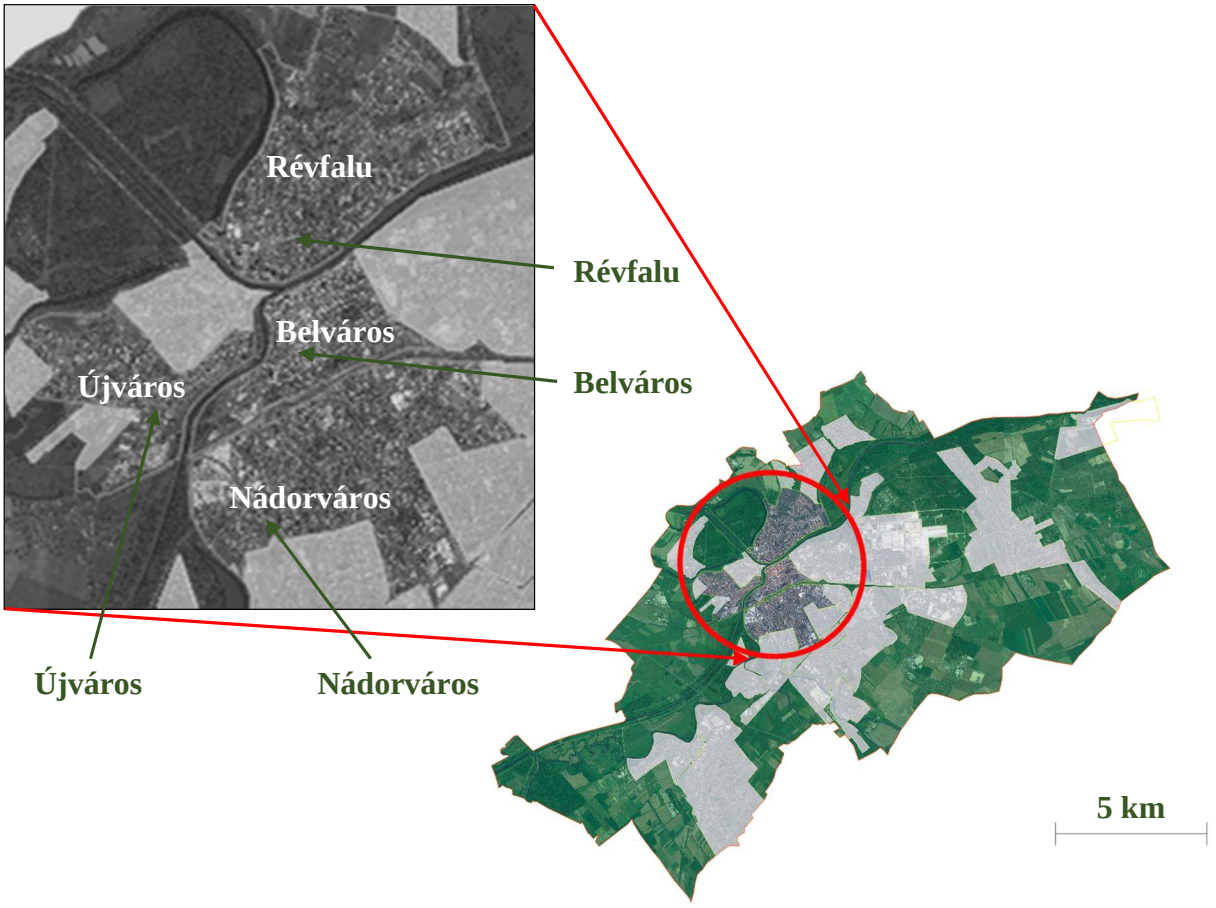

4.16. Figure: Historical urban districts of Győr

DOI: 10.15477/SZE.MMTDI.2015.002

The present structure of the **Downtown (Belváros)** (Fig. 4.16) preserves the structure of 16-17th Century. In the years following, the streets were lengthened and constructed in a similar way. The majority of buildings are one or two-story buildings, with a significant number of built in roof spaces turned into apartment houses. Typical are the enclosed courtyard formation. The area within the former city walls has a historic importance and is a protected area, both the structure and building stock should be preserved.

The structure of **Nádorváros** (Fig. 4.16) is essentially the continuation of the Downtown's chessboard-like system, complete concrescence of the two districts is prevented be the train-line crossing the city. In addition, two large areas around the Hospital and Frigyes army base, good, architectural-quality villa houses were built along Zryínyi Street. Nádorváros grew spontaneously with no clearly outlined boundaries.

Opposite to the Downtown lies **Révfalu** on the other side of Moson-Danube. Urbanization started after Révfalu was attached to Győr. The university buildings were built in the seventies having a clear influence on this part of the city. In this excellent waterfront location neighborhood can be found areas of family houses and a small area of social housing.

Újváros has an axis with housing estates and continues with an intensively built in area. Along the western parts there can be found family housing. (Fig. 4.16)

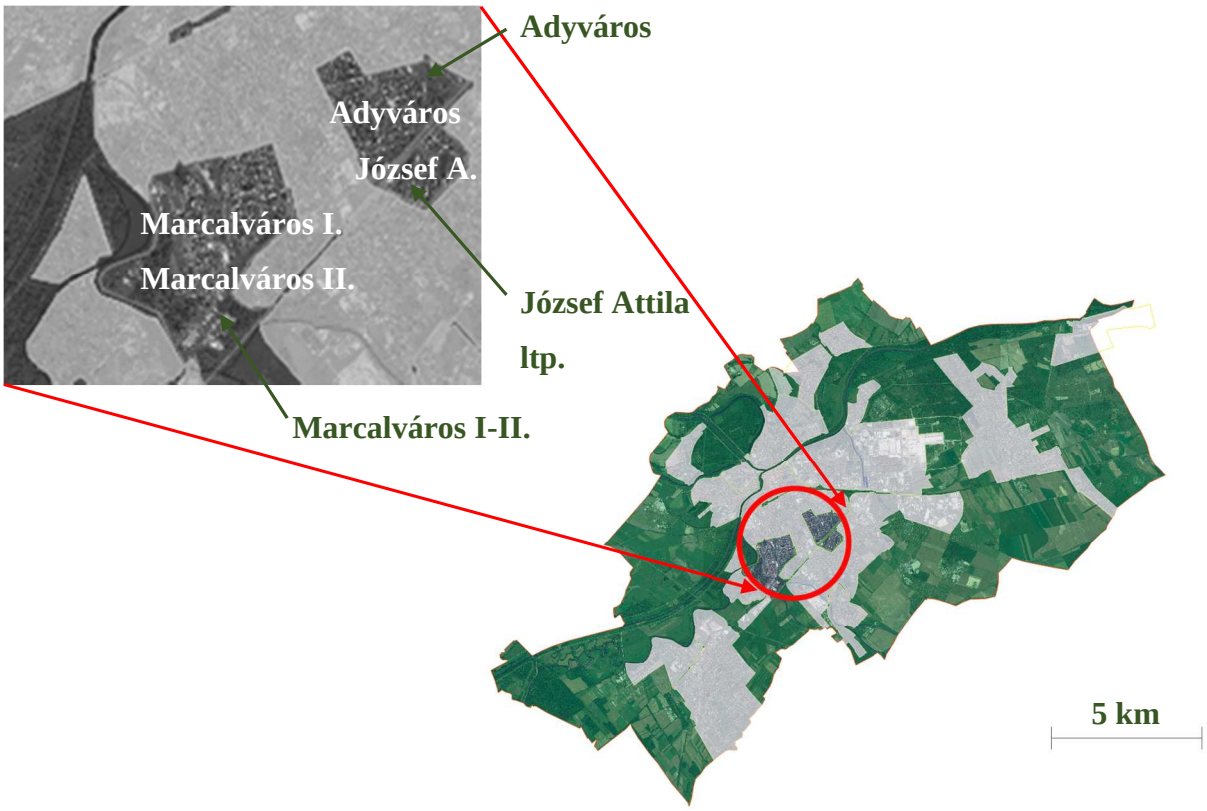

4.17. Figure: Housing estates of Győr

DOI: 10.15477/SZE.MMTDI.2015.002

4.3. Table: Territory distribution of the different functions of housing estates

HOUSING ESTATES					TOTAL
Function of the area	**Adyváros**	**Marcal-város I.**	**Marcal-város II.**	**József A. lt.**	
economic, commercial, industrial	1.98%	10.42%	8.28%	7.44%	
special (cultural, educational, ecclesiastic)	20.41%	22.56%	14.85%	-	
rural residential	0.24%	-	-	8.63%	
garden city residential	2.32%	6.83%	2.33%	1.17%	
urban residential	44.70%	32.46%	15.99%	47.16%	
Total area [ha]	**57.81**	**38.68**	**92.49**	**25.53**	***215***

These city districts with large reinforced concrete housing (Table 4.3) reflect different construction period: Adyváros: 1968-1970, József A. ltp. and Marcalváros I.: 1970-1980, Marcalváros II.: 1980-1990 (Fig. 4.17). Spatial distribution of the population is not uniform in Győr, nearly one-third of the inhabitants live in housing estates area (see Annex). The most populated districts are Adyváros and Marcalváros, a bedroom community, followed by Downtown and Nádorváros.

4.4. Table: Territory distribution of the different functions of garden cities

GARDEN CITIES					
Function of the area	**Gorkij-város**	**Sziget**	**Gyárváros 4.**	**Jancsifalu**	**Szabad-hegy**
economic, commercial, industrial	-	4.56%	3.54%	27.21%	6.43%
special (cultural, educational, ecclesiastic)	-	7.48%	1.81%	2.93%	3.71%
rural residential	100.00%	7.55%	51.56%	54.40%	47.17%
garden city residential	-	44.02%	23.91%	7.34%	26.94%
urban residential	-	9.15%	15.78%	8.12%	1.76%
Total area [ha]	**10.74**	**55.13**	**38.61**	**15.73**	**297.04**

4.18. Figure: Garden cities of Győr

DOI: 10.15477/SZE.MMTDI.2015.002

Garden cities of Győr are the oldest residential districts (Table 4.4). Sziget was attached to Győr in 1907, and the development of Gyárváros started at the beginning of 20th Century. Gorkijváros was built in after the Second World War. Szabadhegy was settled earlier, it can be seen on the maps of the Second Military Survey of Habsburg Empire (Fig. 4.8).

Features of these districts (Fig. 4.18) are that the most common building type are residential buildings with only a ground floor with one or two flats. More intensively built housing areas were constructed in the second part of the 20th Century with one or two-story height apartment houses. On the outer part of the cities appear the rural type houses.

4.5. Table: Territory distribution of the different functions of attached villages

ATTACHED VILLAGES					TOTAL
Function of the area	**Pinnyéd**	**Kisbácsa**	**Bácsa**	**Győrszentiván**	
economic, commercial, industrial	0.41%	-	1.84%	2.47%	
special (cultural, educational, ecclesiastic)	1.98%	-	2.40%	1.42%	
rural residential	58.45%	84.38%	85.82%	66.20%	
garden city residential	30.30%	1.16%	2.45%	2.30%	
Total area [ha]	**95.74**	**130.47**	**76.13**	**634.24**	
Function of the area	**Likócs**	**Kismegyer**	**Gyirmót**	**Ménfőcsanak**	
economic, commercial, industrial	17.51%	4.18%	3.05%	2.01%	
special (cultural, educational, ecclesiastic)	0.49%	2.15%	0.90%	1.74%	
rural residential	66.75%	55.37%	54.09%	75.19%	
garden city residential	-	6.92%	1.73%	5.04%	
Total area [ha]	**61.12**	**110.47**	**176.20**	**560.80**	***1,845***

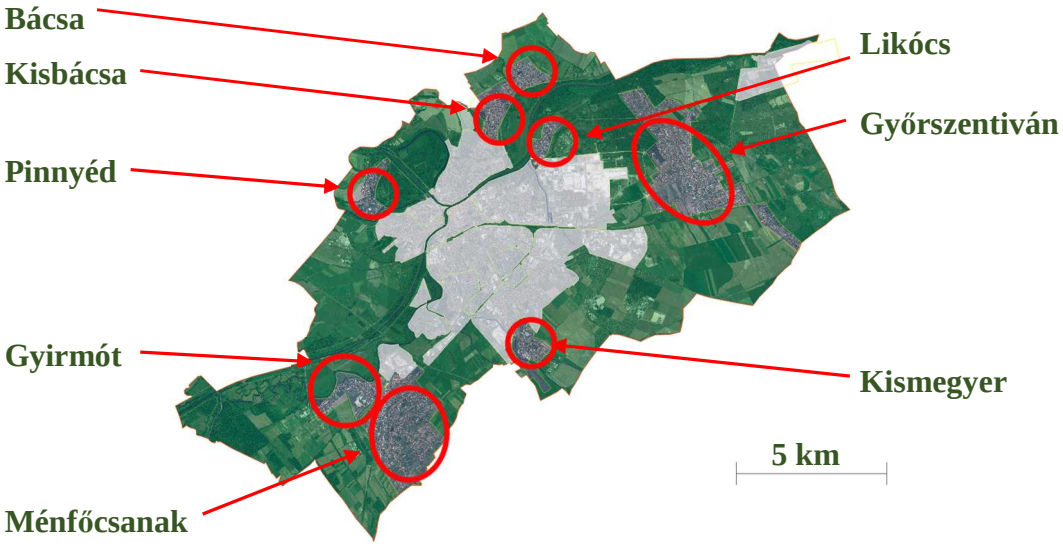

4.19. Figure: Attached villages of Győr

The rural character of the former villages attached to Győr was better preserved (Table 4.5) due to independence from the city because of the greater distance or natural barriers (rivers), and more recently artificial (roads) limits. Pinnyéd, Kisbácsa, Likócs and Kismegyer were attached to Győr in 1950s, Ménfőcsanak, Gyirmót and Győrszentiván in 1971.

DOI: 10.15477/SZE.MMTDI.2015.002

The typical residential buildings in this area are the single family houses. 75% of the buildings were built before 1990. New residential houses were built on newly designated areas of these districts with a more intensive structure including one or two story height apartment houses in the last 20 years.

4.20. Figure: Industrial and commercial areas of Győr

Fig. 4.20 shows the industrial and commercial districts of Győr.

4.3.2. Typical building structures

The research focused on the residential buildings representing the highest number of building stock in Győr. In case of residential buildings the most typical building structures are the unreinforced masonry loadbearing walls. Free standing buildings can be found in the urban city districts with a ground floor and 3-4 stories. The Downtown area has a typical pattern with closely constructed buildings, with different heights making them vulnerable in case of lateral dynamic forces. A huge number of residential buildings have a ground floor or at most one or two stories with one or two apartments in the areas of garden cities and attached villages. The horizontal structure of these masonry building depend on the time of construction. After the sixties came the increased use of reinforced concrete slabs, before that time wooden structures were typical.

One-third of the inhabitants live in reinforced concrete large panel housing areas with 4 or 10 story height buildings. Even though the number of these buildings are much less compared to masonry structures, they behavior is crucial in case of a seismic event. However, due to the unique nature of their construction, they are extremely difficult to analyze and assess for vulnerability. Evaluation of these structures was only an estimate and future research should focus on evaluating this type of structure ubiquitous to Central and Eastern Europe.

DOI: 10.15477/SZE.MMTDI.2015.002

Chapter 5. Data collection methods

In order to be able to determine the earthquake hazard of the area, the vulnerability of the buildings and the earthquake risk of the city, a very large database is needed. Concerning data collection, two very important expectations had to be fulfilled: the data should be accurate and suitable for the given goals while being developed in a reasonable period of time and a very modest budget. One goal of the research was to develop the method of data collection that fulfills the above requirement in order to give a reproducible chain of processes for risk analysis. The method may be used for further studies in Győr or other new studies in other towns.

5.1. Data for soil profiling of Győr

The seismic hazard map determined for Hungary by Tóth et al shows the level of ground motion expressed in PGA (peak ground acceleration) computed for bedrock expressed in m/s^2 with 90% probability of non-exceedance (Figure 1.4). The values on this map were implemented to the Hungarian National Annex of Eurocode 8. That means a single number for the whole city of Győr: 0.12g. Based on the literature, it can be clearly seen that parts of the town with different geomorphological and geological characteristics should behave differently in the case of a seismic event. One major part of the research deals with the determination of local soil effects due to the different soil strata below each city district. Two major sources were available concerning soil conditions for research purposes: research literature about the geology and geodynamics of the Little Hungarian Plain, presented mainly in Section 4.2, and data from borings.

5.1.1. Data from literature

The geological map series of the Little Hungarian Plain offer a broad view about the formation and lithology of the area. Data concerning Győr can be found on two sets of maps called Győr North and Győr South. The maps were determined from shallow borings (10 m deep) with a raster of approx.1000-1500 m, a few small depth borings (30-40 m deep) and one middle deep borings (with 400 m depth) for each set of maps. (Scharek & Tóth, 1994)

The number of borings for the entire territory of Győr is about 28 shallow, and 6 small depth. Considering only the intensely built area, this number drops to 6 shallow and 1 small depth boring. To achieve a higher resolution, further data is necessary. The geological map series offer a good overview about the wider area of Győr and the connections to the vicinity and the formation of sediments from different ages.

DOI: 10.15477/SZE.MMTDI.2015.002

The thickness of quaternary deposits ranges between 10-50 m in Győr, only in the southern part it decreases to 5-10 m. The basement of Pannonian deposits is between 3000-5000 m. (Further maps can be found in Annex.)

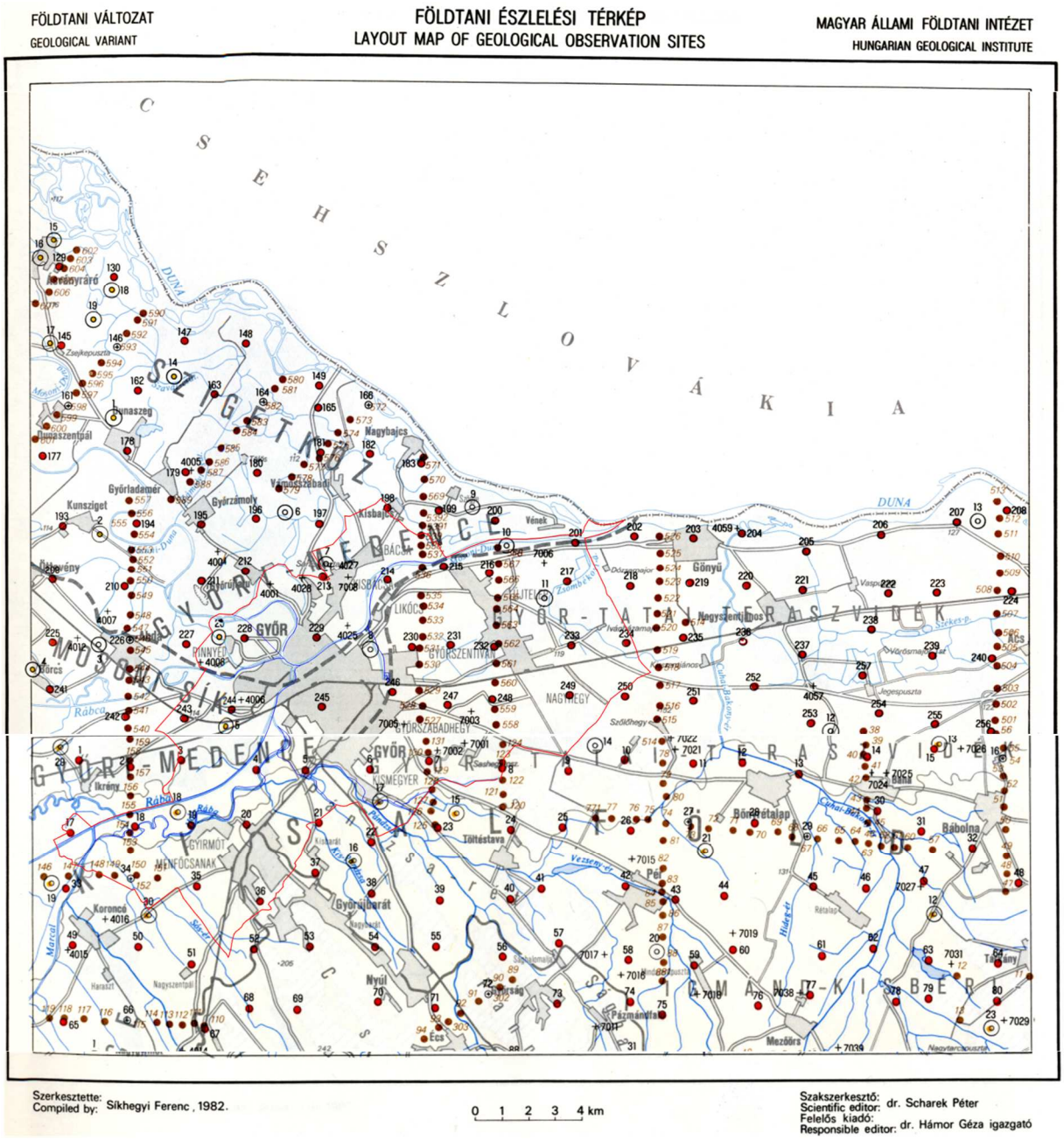

5.1. Figure: The compiled North and South Győr map and sectioned around the city based on the Layout map of geological observation sites (Scharek, 1990) (Scharek, 1991)

5.1.2. Boring data collection

In order to increase the density of data and enhance the accuracy of soil profiles, further borings were needed. The task was to locate the possible sources for further data. The Construction Geotechnical Database contains generally shallow borings that are much less than 30 m deep. The idea came to get permission from the North Transdanubian Environmental

DOI: 10.15477/SZE.MMTDI.2015.002

Protection and Water Management Inspectorate to use the soil profiles from the hydrogeological registers. On the territory of the investigated area, around 100 borings were available, from that 60 were picked for further study. The principle of selection was to cover adequately the study area with borings deeper than 30 m.

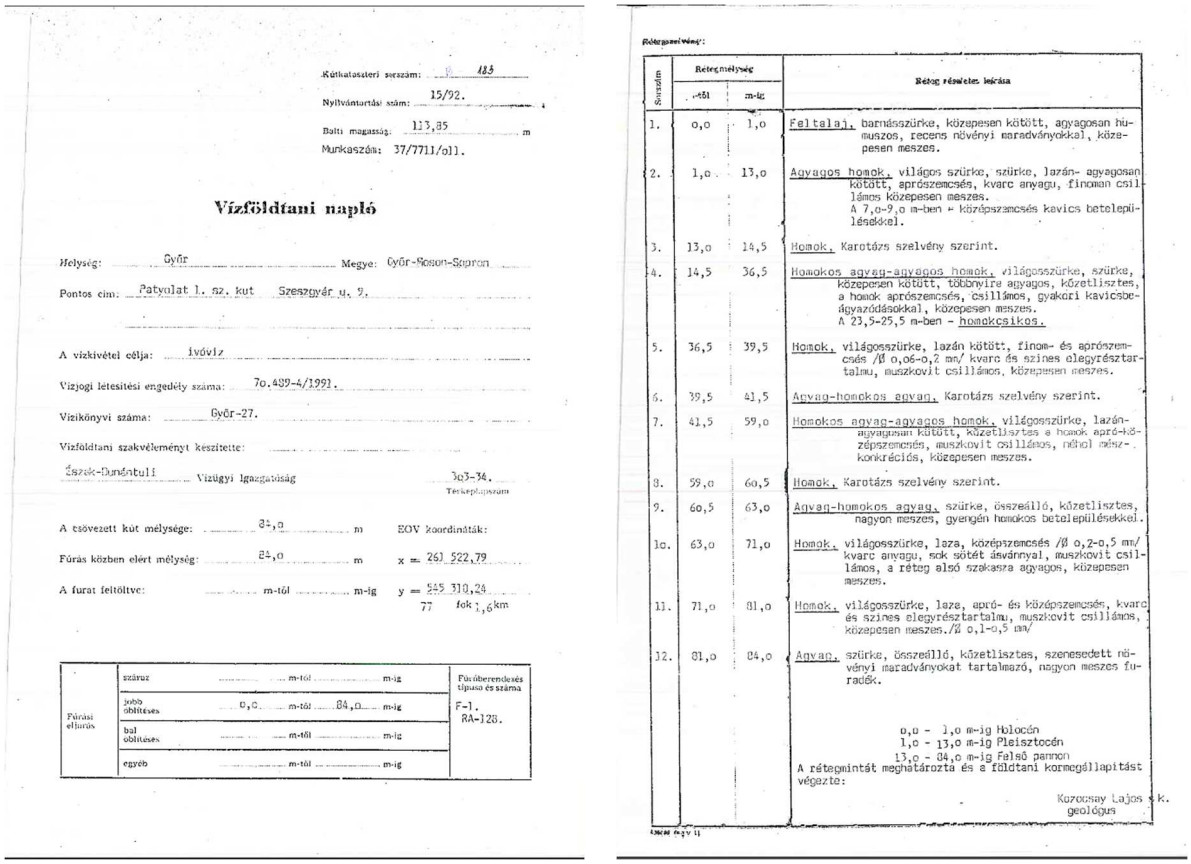

Kútkataszteri sorszám: 485
Nyilvántartási szám: 15/92.
Balti magasság: 113,85 m
Munkaszám: 37/7711/oll.

Vízföldtani napló

Helység: Győr Megye: Győr-Sopron-Szpron
Pontos cím: Patyolat I. sz. kút Szeszgyár u. 9.
A vízkivétel célja: ivóvíz
Vízjogi letesítési engedély száma: 7o.439-4/1991.
Vízikönyvi száma: Győr-27.
Vízföldtani szakvéleményt készítette:
Észak-Dunántúli Vízügyi Igazgatóság
Térképlapszám 3o3-34.

A tervezett kút mélysége: 84,o m EOV koordináták:
Fúrás közben elért mélység: 84,o m x = 261 522,79
A furat feltöltve: m-től m-ig y = 545 310,24
77 fok 1,6km

Fúrási eljárás: száraz m-től m-ig; jobb olditeres 0,o m-től 84,o m-ig; bal olditeres m-től m-ig; egyéb m-től m-ig
Fúróberendezés típusa és száma: F-1. RA-128.

Rétegsorleírás:

Sorszám	Rétegmélység m-től	Rétegmélység m-ig	Réteg részletes leírása
1.	o,o	1,o	Feltalaj, barnásszürke, közepesen kötött, agyagosan humuszos, recens növényi maradványokkal, közepesen meszes.
2.	1,o	13,o	Agyagos homok, világos szürke, szürke, lazán- agyagosan kötött, aprószemcsés, kvarc anyagu, finoman csillámos közepesen meszes. A 7,o-9,o m-ben - középszemcsés kavics betelepülésekkel.
3.	13,o	14,5	Homok, Karotázs szelvény szerint.
4.	14,5	36,5	Homokos agyag-agyagos homok, világosszürke, szürke, közepesen kötött, többnyire agyagos, közetlisztes, a homok aprószemcsés, csillámos, gyakori kavicsbeágyazódásokkal, közepesen meszes. A 23,5-25,5 m-ben - homokcsikos.
5.	36,5	39,5	Homok, világosszürke, lazán kötött, finom- és aprószemcsés /Ø o,o6-o,2 mm/ kvarc és szines elegyrésztartalmu, muszkovit csillámos, közepesen meszes.
6.	39,5	41,5	Agyag-homokos agyag, Karotázs szelvény szerint.
7.	41,5	59,o	Homokos agyag-agyagos homok, világosszürke, lazán-agyagosan kötött, közetlisztes a homok apró-középszemcsés, muszkovit csillámos, néhol mészkonkréciós, közepesen meszes.
8.	59,o	6o,5	Homok, Karotázs szelvény szerint.
9.	6o,5	63,o	Agyag-homokos agyag, szürke, összeálló, közetlisztes, nagyon meszes, gyengén homokos betelepülésekkel.
1o.	63,o	71,o	Homok, világosszürke, laza, középszemcsés /Ø o,2-o,5 mm/ kvarc anyagu, sok sötét ásvánnyal, muszkovit csillámos, a réteg alsó szakasza agyagos, közepesen meszes.
11.	71,o	81,o	Homok, világosszürke, laza, apró- és középszemcsés, kvarc és szines elegyrésztartalmu, muszkovit csillámos, közepesen meszes./Ø o,1-o,5 mm/
12.	81,o	84,o	Agyag, szürke, összeálló, közetlisztes, szenesedett növényi maradványokat tartalmazó, nagyon meszes furadék.

o,o - 1,o m-ig Holocén
1,o - 13,o m-ig Pleisztocén
13,o - 84,o m-ig Felső pannon
A rétegmintát meghatározta és a földtani kormegállapitást végezte:
Kuzcsay Lajos k. geológus

5.2. Figure: A sample of a Hydrogeological Register in Hungarian (with the permission from North Transdanubian Environmental Protection and Water Management Inspectorate to use for research purposes)

The chosen 60 hydrogeological registers originated from 1954 to 2008, with a depth varying between 25 and 2155.7 m. The depth and number of borings are presented in Table 5.1.

5.1 Table: Number and depth of borings concerning the hydrogeological registers

Depth [m]	25-30	30-50	50-100	100-200	200-400	400-700	2155.7
Number	1	8	15	13	9	3	1

The data was registered by various drilling supervisors, with different descriptions of soil layers mainly focusing on water quality and quantity. One challenge was to identify the soil types to be able to compare and group them. The other challenge was related to the location of borings. The names of the streets changed in the last 50 years, factories disappeared, and the given coordinates were not exact enough and some did not correspond to the site plans of the hydrogeological registers. After careful inspection and recalculation, the location of the borings are represented on Figure 5.3.

DOI: 10.15477/SZE.MMTDI.2015.002

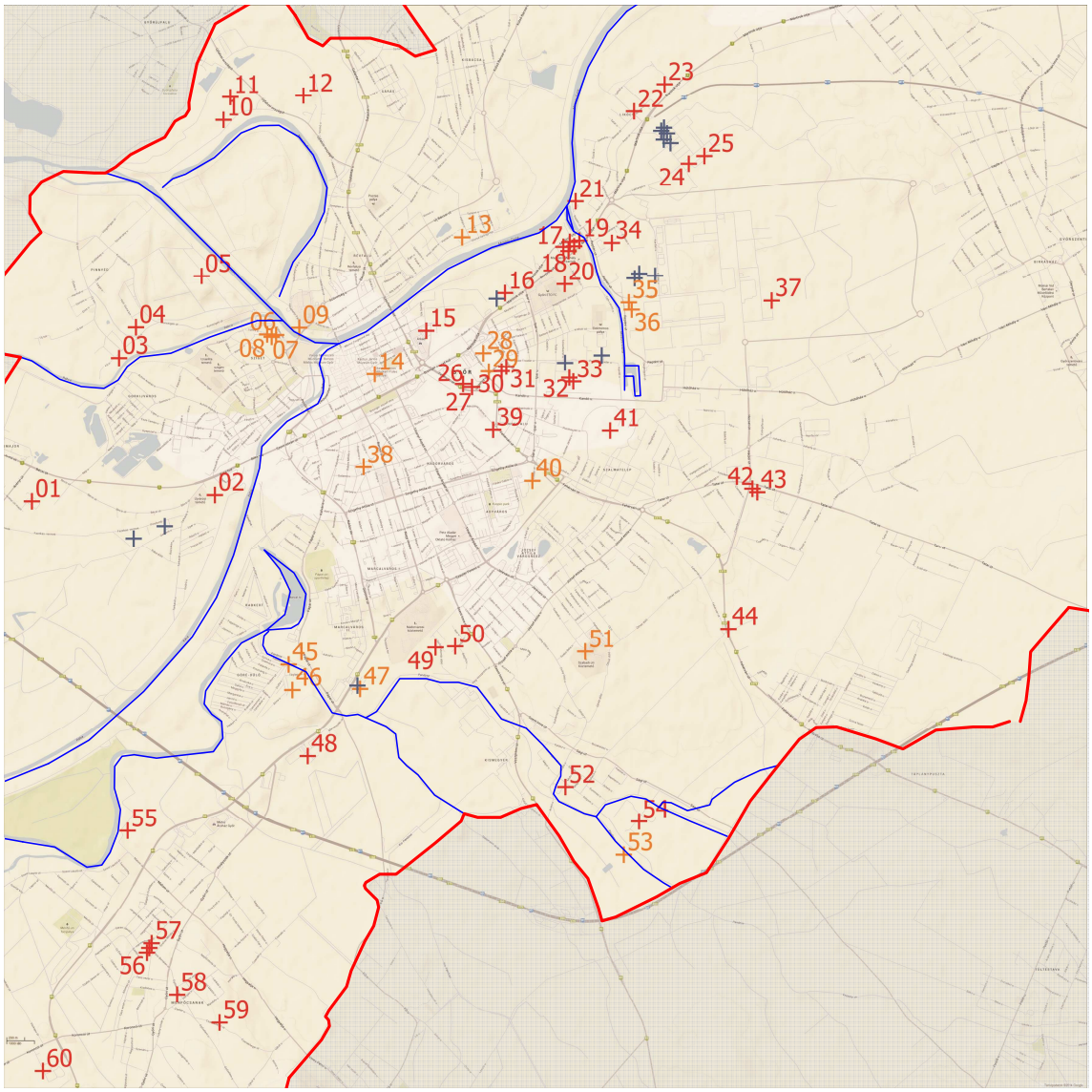

5.3. Figure: Borings from hydrogeological registers marked on the map of Győr numbered from 1 to 60 (borings without a number are shallower than 10 m, borings deeper than 30 m are marked red and orange, MASW were performed at borings marked orange)

The hydrogeological registers were mainly connected with water resources for different purposes: at Kiskút and Révfalu are those wells which supply the potable water for the city, the other wells support several industrial facilities.

5.1.3. MASW measurements and CPT data

The next step was to identify the dynamic properties of the different soil types. During the research, Multichannel Analysis of Surface Waves was performed at 11 places close to the original borings of the hydrogeological registers marked orange on Figure 5.3. Compared to conventional borehole sounding tests, it is less expensive and provides the subsurface shear wave velocity profile over a large area. At four locations, raw data from Cone Penetration Tests were offered by geotechnical companies, which ensured verification of the results.

DOI: 10.15477/SZE.MMTDI.2015.002

5.2. Data about buildings of Győr

Beside the earthquake hazard, the next major part the research focused on was the vulnerability of the buildings. Damage occurs from a seismic event only if the earthquake reaches inhabited areas. The question is of course, whether these buildings will suffer any damage in such cases or not. The condition, type of the structure, and year it was built all account for the vulnerability of the buildings.

5.2.1. Checklist and area of investigation

Based on literature concerning inventories for score assignment, and the knowledge about the most-used building construction of the area, a checklist was created. The points of the checklist can be grouped around three major topics: identification of the building, general data, and structural data about the building. The main questions of the checklist can be found in the Table 5.2. The whole questionnaire is attached to the Annex.

The investigated area was split into smaller regions, marked with letters (Figure 5.4 and Annex). The number of buildings was about 100 in each case, so a group of 5 to 6 trained staff was able to collect the data for an area in a relatively short time. After that, the data was uploaded on to an online interface with a total number of 5393 filled questionnaires.

5.2 Table: Points of the checklist for collection of building data

1. IDENTIFICATION OF THE BUILDING 1.1. Number of the building 1.2. Function 1.3. Two pictures of the building should be uploaded	
2. GENERAL DATA	**3. STRUCTURAL DATA**
2.1. Construction date	3.1. Structural system
2.2. State of the building	3.2. Later conversions
2.3. Relationship to adjacent buildings	3.3. Direction of structural system
2.4. Mass or elevation	3.4. Orientation (of the plane of street elevation)
2.5. Layout	3.5. Type of foundation
2.6. Form of the roof	3.6. Material of vertical structure (column, wall)
2.7. Basement	3.7. Material of horizontal structure, type of the slab
2.8. Number of stories (without basements and attic)	3.8. Material of roof
2.9. Attic is used for living space	3.9. Type of outer coverage

5.2.2. Trained staff versus experts

The trained staff consisted of second and third year architect and civil engineer students. The topics of the checklist were explained thoroughly. In order to validate the accuracy of the collected data 5% of the same buildings at 4 appointed areas were evaluated based on the same checklist by experts with more than 30 year expertise in earthquake engineering.

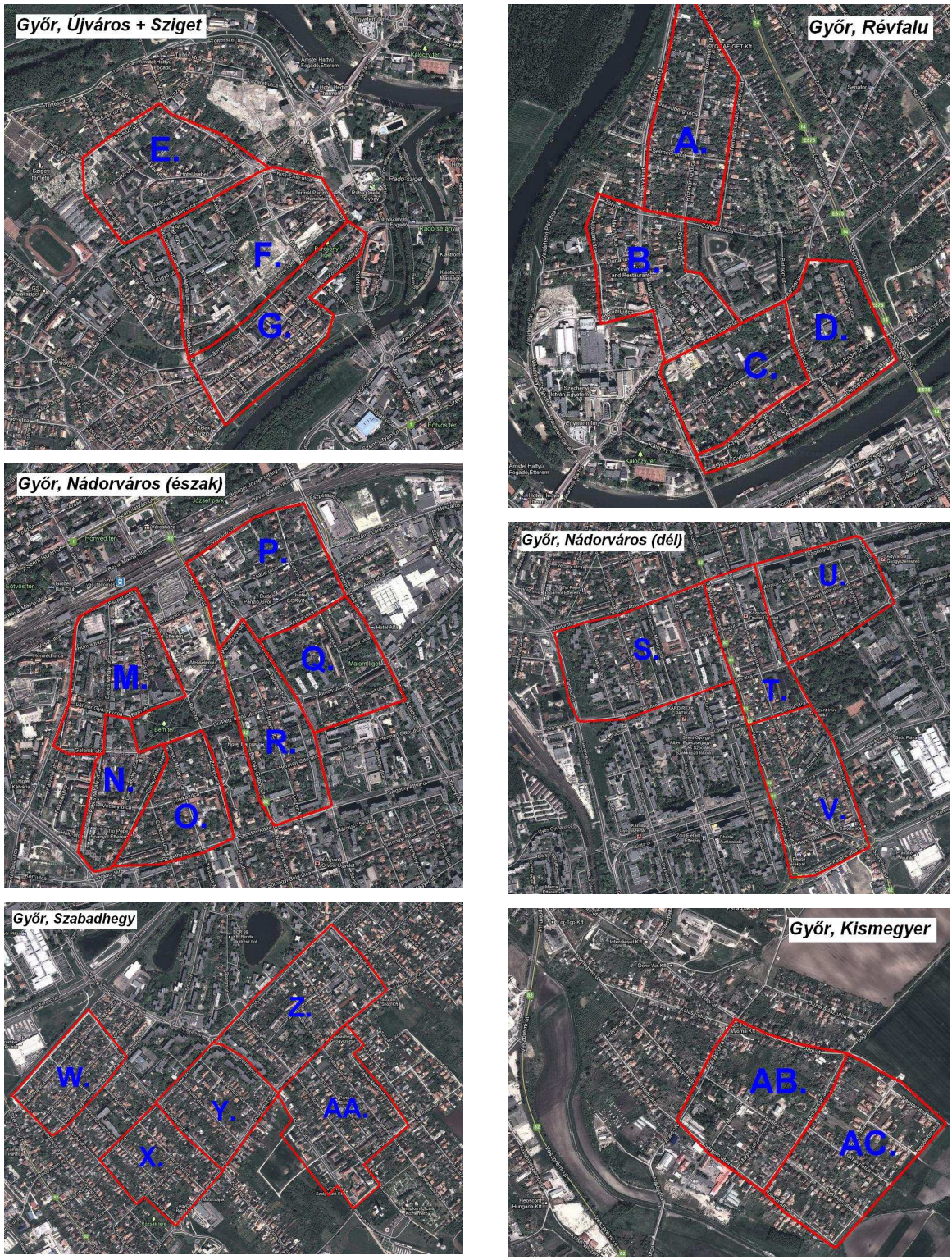

5.4. Figure: Examined areas of Győr (further areas can be found in Annex)

5.2.3. Plans of typical buildings

Finally, two major types of building construction were selected for further research. Masonry buildings and reinforced concrete buildings plans were gathered that were considered to be typical to this region. Vulnerability assessment of these buildings is presented in Ch. 7.

DOI: 10.15477/SZE.MMTDI.2015.002

Chapter 6. Earthquake hazard of the city

Based on the Seismic Hazard Map of Hungary (GeoRisk Earthquake Engineering Ltd., 2006) the level of ground motion is 0.12 g PGA at bedrock with 90% probability of non-exceedance (Figure 1.4). Based on EC 8 part 3, this value belongs to the Limit State of Significant Damage. According to Eurocode, three limit states (LS) should be taken into account for the evaluation of earthquake resistance of buildings, which form the basis for scenario preparation. In addition, a Confidence Factor (CF) can be varied based on knowledge level, such as limited (CF_{KL}=1.35× CF_{KF}), normal (CF_{KN}=1.2× CF_{KF}) or full (CF_{KF}). The values of PGA at bedrock are given according to different limit states and knowledge levels based on EC8 part 1, 2.1. (4) (European Committee for Standardization, 2013):

1. LS of Near Collapse (NC): 2475 years, corresponding to a probability of exceedance of 2% in 50 years; CF_{KF} 0.21 g, CF_{KN} 0.252 g, CF_{KL} 0.2835 g;
2. LS of Significant Damage (SD): 475 years, corresponding to a probability of exceedance of 10% in 50 years; CF_{KF} 0.12 g, CF_{KN} 0.144 g, CF_{KL} 0.162 g;
3. LS of Damage Limitation (DL): 225 years, corresponding to a probability of exceedance of 20% in 50 years; CF_{KF} 0.09 g, CF_{KN} 0.108 g, CF_{KL} 0.1215 g.

6.1. Seismicity of Győr and soil properties

As presented in Chapter 4 the area of Győr is at the meeting point of different geological structures, so further research concerning the local seismicity and soil conditions were performed in order to be able to differentiate between the very diverse territories of the city.

6.1.1. Earthquakes with epicenter close to Győr

There exists a very detailed catalogue of earthquakes concerning the territory of Carpathian Basin from antiquity until nowadays. The Hungarian Earthquake Catalogue contains data about historical earthquakes, earthquake records from the very beginning of seismology (after 1902) and recent data until 1995 (Zsíros, 2000). Nowadays records can be found in the annual edition of Hungarian Earthquake Bulletin. (Tóth, et al., 1996-2013)

The assorted data give a better overview about the seismicity of Győr. Data of earthquake records were organized in three categories: events with their epicenters at Győr, events within a 50-km radius around Győr and events with 100-km radius.

These data were evaluated first based on intensity, then on magnitude, the value ranges were determined for different periods of time according to historical data or registered data.

DOI: 10.15477/SZE.MMTDI.2015.002

Figure 6.1 shows the number of earthquakes around Győr within a 50-km radius (within 100 km is presented in Annex).

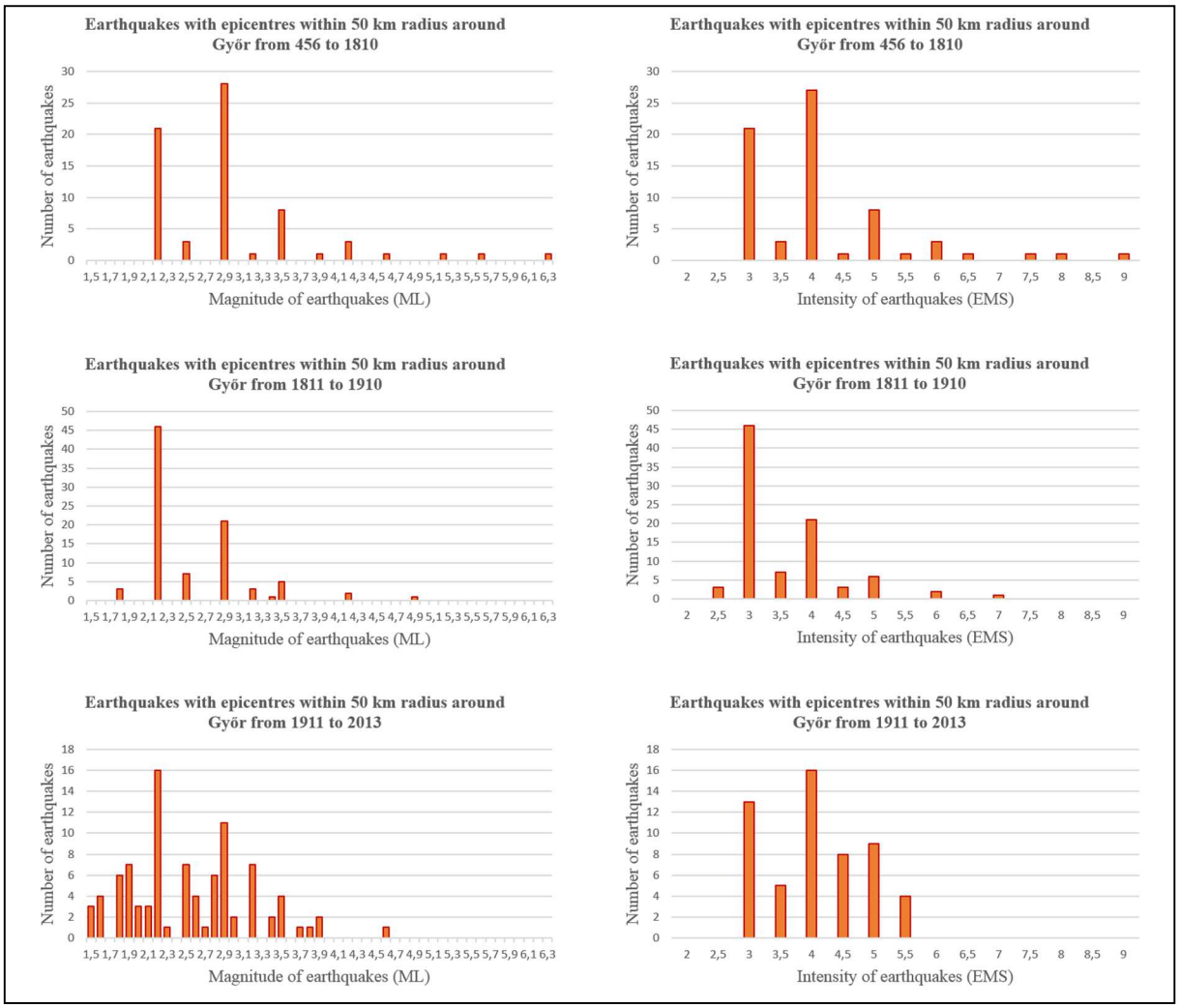

6.1. Figure: Number of earthquakes within 50 km radius around Győr

Table 6.1 summarizes the return period of earthquakes around Győr. Magnitude 3 and 4 earthquakes are quite frequent in this region, magnitude 4 and 5 earthquakes happen every 50 years close to Győr, and every 10 years within 100 km of the city. The return period of magnitude 5 and 6 events is about 100 years; this correlates with hazards determined by Tóth et al. (Tóth, et al., 2006) and underlines that the seismicity of the region has been underestimated (see quotation in Section 1.1.3) by Emergency Directorate (Győr-Moson-Sopron County Emergency Directorate, 2014).

6.1 Table: Return period of earthquakes with epicenter around Győr

Magnitude	Return period of earthquakes expressed in years	
	epicenters within 50 km radius	epicenters within 100 km radius
3-4	6-7	1-2
4-5	50	10
5-6	n.a.	100

DOI: 10.15477/SZE.MMTDI.2015.002

6.1.2. Soil data processing

The first step was processing the chosen 60 hydrogeological boring records (Table 5.1) and determining their location since the names of the streets have changed in the last 50 years, factories have disappeared, and the given coordinates were very inexact and often did not corresponded with the site plans of the hydrogeological records. Exact location of the borings could be determined based on archival and oral information gained from elderly colleagues. A software developed by Timár et al (Timár, et al., 2003) was used to convert stereo coordinates to EOV coordinates and the software developed by Papp (Papp, 2008) to identify the EOV coordinates in case of missing position offering direct connection with Google Maps (example in Annex).

The second step was to organize the borings according to city districts, then map the locations (Figure 5.3). After that, the upper 30 m of strata was discretized to a resolution of 20 cm. The descriptions by various drilling supervisors were made consistent with soil categories (Table 3.1). Categorization were based on the soil types: silt (Si), clay (Cl), fine sand (FSa), medium sand (MSa), coarse sand (CSa), fine gravel (FGr), medium gravel (MGr), coarse gravel (CGr). It was challenging to determine which category a soil type should be listed according to various descriptions.

The third step was grouping the borings based on their visible pattern organized by city districts (Figure 6.2) and the comparison to geological, geomorphological and historical data (presented in Section 4.2). Overlaying the maps (Figure 6.3) helped to delineate several zones with similar soil layers, identifying specific soil profiles related to each zone.

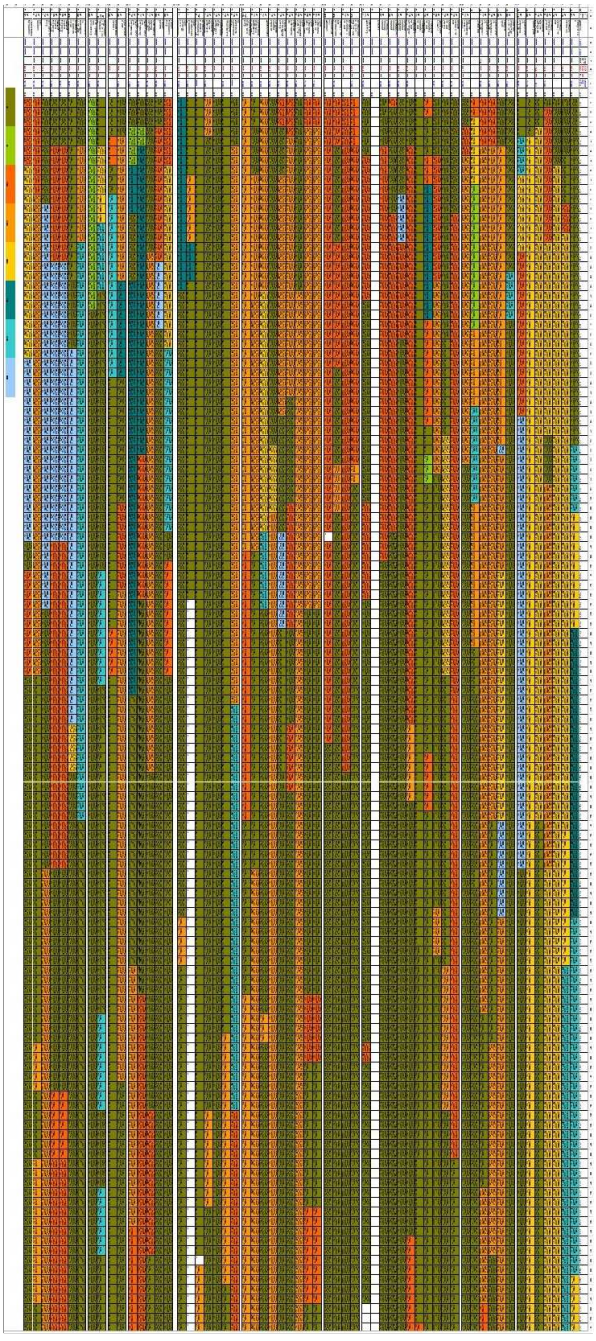

6.2. Figure: Soil layers of the upper 30 m organized by city districts, final version with legend can be found in Annex

DOI: 10.15477/SZE.MMTDI.2015.002

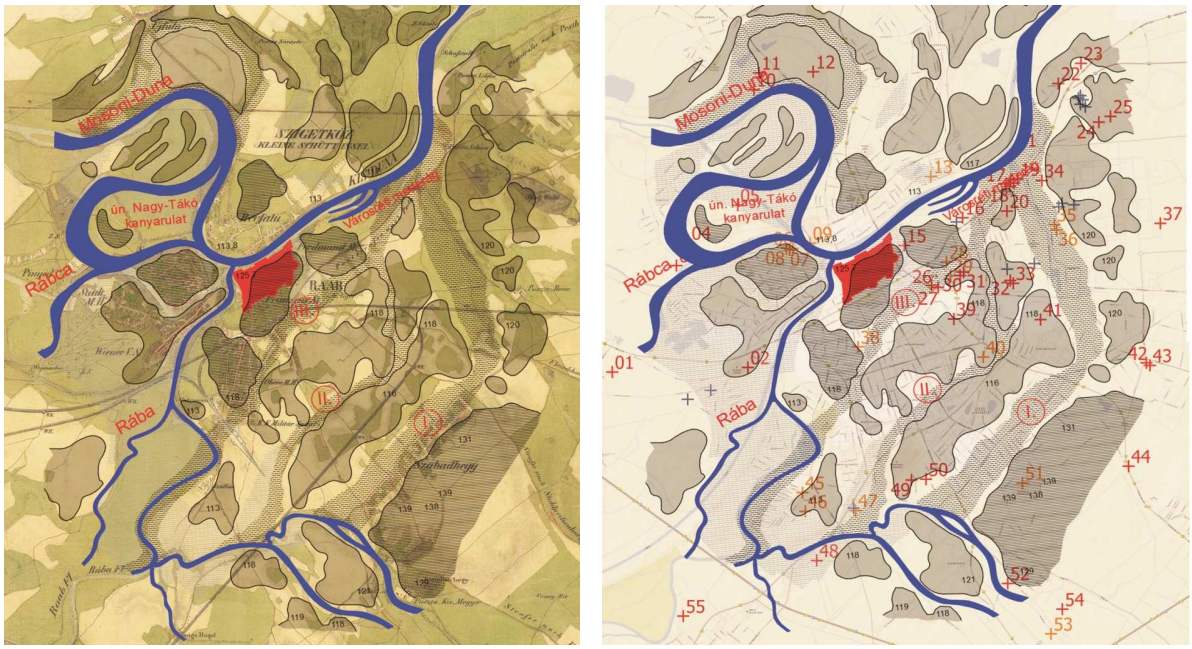

6.3. Figure: Overlaid maps: historical map of the Second Military Survey of Habsburg Empire made between 1806 and 1869 (Austrian National Archives & Arcanum Adatbázis Kft., 2014) and ancient landscape of Győr area redrawn after the illustration of Borbíró (Borbíró & Valló, 1956) and the numbered borings of hydrogeological registers

6.2. Shear wave velocity profile from MASW and CPT measurements

The stiffness of the soil at a site has a strong effect on the intensity of shaking delivered to the buildings at the surface. Variability in stiffness contributes to the large differences in ground motions over relatively short distances within sedimentary basins. Site effect studies are connected with the geodynamic characterization of the shallow layers, and can be grouped into three main categories (Bard, 1997): experimental, numerical and empirical. In the absence of macroseismic data or earthquake records, several methods can be used for obtaining information about the soil response in an area of study. Generally, it is the shear wave (S-wave) velocity that is the best indicator of the response at a given site. This is because the major contributor to seismic action on a building is vertically propagating, horizontally polarized shear waves. To analyze site response, engineers use the relationship

$$G_{MAX} = \rho_{soil} \cdot v_s^2 = \frac{\gamma_{soil}}{g} \cdot v_s^2 \qquad (6.1)$$

where

G_{MAX} Shear modulus of the soil at low strain amplitudes, e.g. during a field seismic test (kPa)

ρ_{soil} mass density of the soil

v_s shear wave velocity in soil (m/sec)

γ_{soil} unit weight of the soil (kN/m^3)

g acceleration due to gravity ≈ 9.807 m/sec^2

The S-wave velocities can be measured via different methods, such as borehole tests or multichannel analysis of surface waves (MASW). S-wave velocities will depend on soil density, grain size, confining stress, void ratio, pre-consolidation history, fabric, cementation, age, and method of deposition. Soil classification and correlation studies have been conducted by many researchers who have published values for dynamic properties of various soil formations based on age (Table 6.2), specific structure (Table 6.3) or placement (Table 6.4). Many researchers have published their insights into the use of the 30-m profile approach to earthquake hazard assessment (Paoletti, 2012) (Kanli, et al., 2006) (Bauer, et al., 2007).

6.2 Table: Geomechanical properties for first 10 m of subsurface *(Carvalho, et al., 2009)*

Poisson's coefficient and V_P/V_S ratios for shallow layers in western Algarve calculated from seismic refraction studies

Geology	Profile	Velocity (m/s) 1st layer		VP1/VS1	Poisson's coefficient	Velocity (m/s) 2nd layer		VP2/VS2	Poisson's coefficient
		P wave	S wave			P wave	S wave		
Holocenic deposits	PN1	265	108	2.45	0.40	1902	301	6.32	0.49
	ALV1	541	166	3.26	0.45	2038	291	7.00	0.49
Odiáxere Gravels	OD1	325	188	1.73	0.25	1396	885	1.58	0.16
	FRA2	499	331	1.51	0.11	905	520	1.74	0.25
Ludo Formation	LG2	285	189	1.51	0.11	736	457	1.61	0.19
	LGA1	365	250	1.46	0.06	816	495	1.65	0.21
	POR1	529	307	1.72	0.25	826	472	1.75	0.26
Mem Moniz fossiliferous limestones	TUN1	255	111	2.30	0.38	724	340	2.13	0.36
Lagos–Portimão Formation[a]	ALV2	249	113	2.20	0.37	736	376	1.96	0.32
	ALB1	311	193	1.61	0.19	582	334	1.74	0.25
	LG1	365	179	2.04	0.34	1152	665	1.73	0.25
	FRA1	308	121	2.55	0.41	1795	1222	1.47	0.07

[a] Carbonates, sandstones and silts.

6.3 Table: Predictive equations for soil shear-wave velocities *(Nottis, 2001)*

Predictive Equations For Shear-Wave Velocity As A Function Of Depth For Surficial Materials Of The Lower Hudson Valley

Surficial Material	No. of Borings	No. of Data Points	Predictive Equation*	r**	Recommended Depth Range for Equation (feet)
Alluvium and Alluvial Fans	5	15	$V_S = 564.41*D^{0.1377}$	0.39	0 – 50
Glacial Kames	5	12	$V_S = 106.87*D^{0.664}$	0.97	0 – 60
Glacial Lake Delta	4	9	$V_S = 520.02*D^{0.1623}$	----	0 – 30
Glacial Lake Sands	5	11	$V_S = 244.69*D^{0.3468}$	0.88	0 – 50
Glacial Lake Silts and Clays	8	28	$V_S = 619.81*D^{0.1561}$	----	0 – 100
Glacial Outwash Sand and Gravel	5	27	$V_S = 301.52*D^{0.3225}$	0.45	0 – 100
Glacial Tills	5	21	$V_S = 626.38*D^{0.2239}$	0.41	0 – 100

* D = Depth in feet, and Vs = Shear-wave velocity in feet/second

** r = correlation coefficient. No value is listed if equation was determined with only a subset of available data points.

Predictive equations, based on soil type, confining stress and deposition have also been published and appear in Tables 6.3 and 6.4. Researchers determine predictive equations for soil shear-wave velocities to generate the required soils map for hazard analysis, that is, equations

that could predict shear-wave velocity as a function of the different factors mentioned above. (Matsuoka, et al., 2005)

For this study, ranges of values of v_s were determined for each unit because of lateral and vertical variations in geological material types and their physical properties: a worst-case (based on the lower v_s value) and a best-case (based on the higher value) presented in a later section.

6.4 Table: Stratigraphic units and range of v_s *(Perrin, et al., 2010)*

Unit	Description	Vs (min) (m/sec)	Vs (max) (m/sec)	Typical location
I	Hydraulic Fill	50	150	Aotea Quay
	Rock Fill	125	250	Railway yards/ Te Papa
	Other Fill	200	300	Subdivisions
II	Holocene lake silt, swamp, peat	50	200	Thorndon (rare)
	Holocene sand/gravel, loose	150	300	small stream channels
	Holocene sand/gravel, med dense	250	350	
	Holocene sand/gravel, dense	350	450	
	Holocene sand/gravel, very dense	400	500	
	Historical beach sand/gravel	150	250	Under reclamation, thin
III	Holocene silt/clay, soft-firm	100	200	
	Holocene silt/clay, firm-stiff	200	350	
	Older Silt/clay, v stiff	400	700	Paleosols (v thin) - in unit D
IV	Pleistocene gravel/sand/silt, dense	250	400	Thorndon/Te Aro
	Pleistocene, deeper, v dense	400	700	
	Pleistocene, deepest, v dense	700	1000	(effective bedrock – e.g. Te Papa)
V	Bedrock CW	200	700	Terrace Tunnel
	Bedrock, crushed (fault breccia)	500	900	
	Bedrock HW	600	1000	
	Bedrock MW	700	1100	
	Bedrock SW	900	1300	
	Bedrock UW	1200	1750	
	Bedrock, deep, UW	1500	2000	

Engineering codes have simplified these site effects into a single parameter: the average shear-wave velocity in the upper 30 m at a site, $v_{s,30}$ and soil classes are then assigned to different average values. The codes then use the simplified profiles as input to determine response spectra for design. However, in many cases this is not enough and detailed shear-wave velocity profiles are necessary for accurate ground motion modeling and application to building response analysis.

DOI: 10.15477/SZE.MMTDI.2015.002

6.5 Table: Ground types of EC8 *(European Committee for Standardization, 2013)*

Type	Description of stratigraphic profile	$v_{s,30}$ (m/s)
A	Rock or other rock-like geological formation, including at most 5 m of weaker material at the surface.	> 800
B	Deposits of very dense sand, gravel, or very stiff clay, at least several tens of meters in thickness, characterized by a gradual increase of mechanical properties with depth.	360 – 800
C	Deep deposits of dense or medium dense sand, gravel or stiff clay with thickness from several tens to many hundreds of meters.	180 – 360
D	Deposits of loose-to-medium cohesionless soil (with or without some soft cohesive layers), or of predominantly soft-to-firm cohesive soil.	< 180
E	A soil profile consisting of a surface alluvium layer with v_s values of type C or D and thickness varying between about 5 m and 20 m, underlain by stiffer material with v_s > 800 m/s.	
S_1	Deposits consisting, or containing a layer at least 10 m thick, of soft clays/silts with a high plasticity index (PI > 40) and high water content.	< 100 (indicative)
S_2	Deposits of liquefiable soils, of sensitive clays, or any other soil profile not included in types A – E or S_1.	

One goal of this research was to determine the shear-wave profile for the different sites of Győr according to hydrogeological registers using MASW and CPT measurements.

6.2.1. MASW technique

The multichannel analysis of surface waves (MASW) adopts the conventional seismic refraction mode of survey using an active seismic source such as hammers, weight drops, or explosives. The maximum depth of investigation is 20-30 m depending on site and source and is determined by the longest wavelength of the surface waves generated by the impact power of the source. A greater impact power means a longer wavelength and greater depth of penetration. Metallic plates placed on the ground surface are conventionally used for impact source locations. (Park Seismic LLC., 1990).

Vertical low-frequency geophones (< 4.5 Hz) are recommended as receivers. The length of the receiver spread usually limited to 50-100 m is directly related to longest wavelength detected and receiver spacing (distance between receivers) relates to the shortest wavelength detected. The source and receiver spread distance is one of the variables that affect the horizontal resolution of the dispersion curve (Park, et al., 2001).

A long recording time can increase the chance of recording ambient noise, so the use of more channels with a shorter recording time can increase the signal-to-noise ratio, eliminating

the influence of signals from ambient sources Twenty four or more geophones are typically laid out in a linear array and connected to a multi-channel seismograph which collects data simultaneously from all geophones.

Different types of waves are recorded through multichannel array. The dispersive nature of different types of waves is imaged through wave-field transformation of seismic record by frequency wavenumber (f-k) or slowness-frequency (p-f) transform. From the dispersion image, a dispersion curve of the fundamental mode of Rayleigh waves is selected, which is then inverted for a 1D v_s profile. Figure 6.6 shows a typical schematic of active MASW field survey.

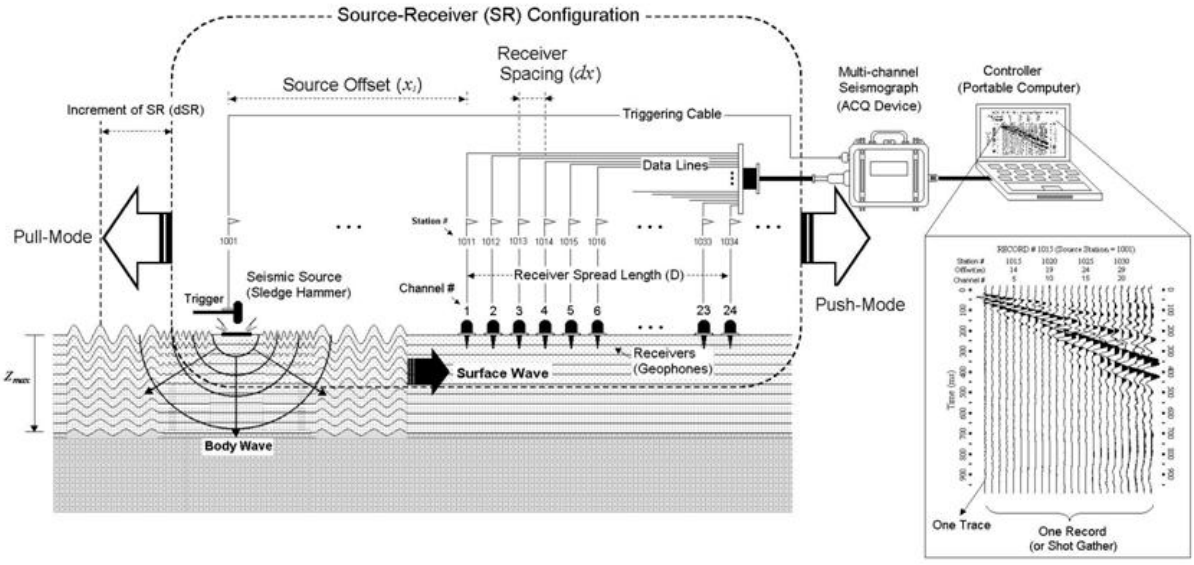

6.4. Figure: Schematic of active MASW field survey (Park Seismic LLC., 1990)

6.2.2. MASW measurements performed in Győr

The measurements were performed with DAQ Link3 instruments (manufacturer: Seismic Source, US), which was guided with a field PC using a special data collecting software. Features of the instrument:

- Number of channels: 24
- Frequency range: 0-15 kHz
- ADC: 24 bit Delta-Sigma
- Sampling: 62.5 μs-16 msec
- Recording length: 512–16384 samples

A basic requirement concerning the choice of source, geophones and geometry of spreading was to enable the detecting of low frequency (i.e. long wavelength) components of the spectrum. These are important in order to determine the velocity parameters of the upper 30 m strata. The following parameters and instrument were used to meet the requirements:

DOI: 10.15477/SZE.MMTDI.2015.002

- Sampling time 1 ms
- Sampling length 2000
- Used geophones 2,3 Hz
- Interval of geophones 4 m
- Number of channels 24
- Length of spreading 92 m
- Source hammer, SR-II drop weight

6.5. Figure: The used hammer and spacing of geophones

The SR-II is a specialized falling weight seismic source developed and manufactured by ELGI (Eötvös Loránd Geophysical Institution), using the energy of 8g gunpowder filled cartridge for generating vibration. (Kanli, et al., 2006)

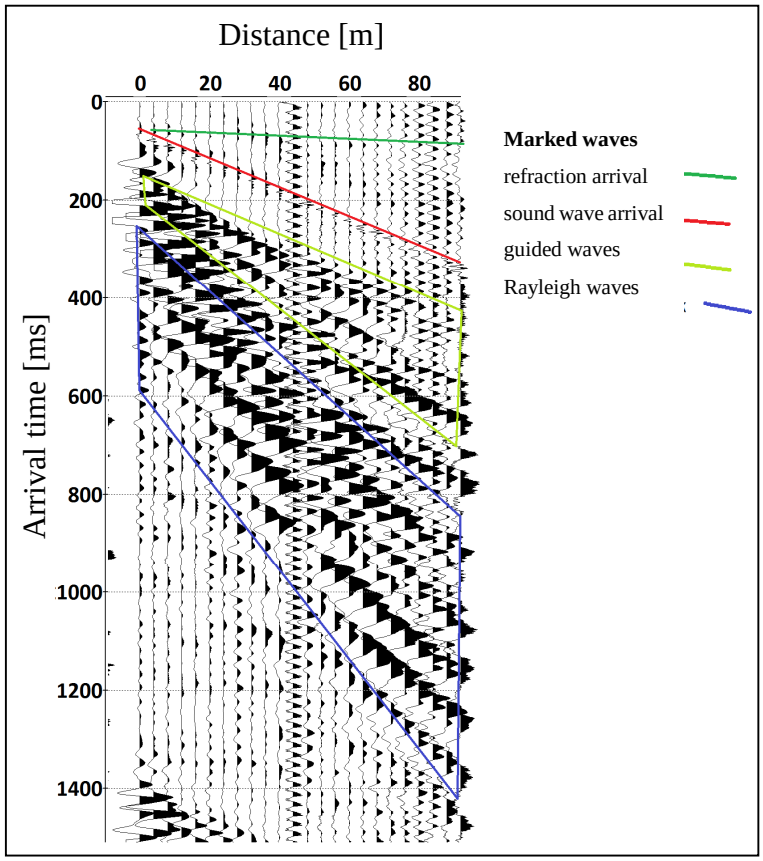

6.6. *Figure: Recording made with SR-II source*

DOI: 10.15477/SZE.MMTDI.2015.002

6.7. Figure: Field PC using a special data collecting software

The work was carried out with the Russian program package called Deco Geophysical Software Company RadexPro. The raw footage geometry and recording parameters were given first. After that a few simple processing steps were required, which subsequently served to improve the signal-to-noise ratio (DC member removal, tuning mute, summary). The program obtained the frequency-phase velocity image (Figure 6.8) due to phase-shift method, the dispersion curves were appointed immediately on the image (Park, et al., 1998).

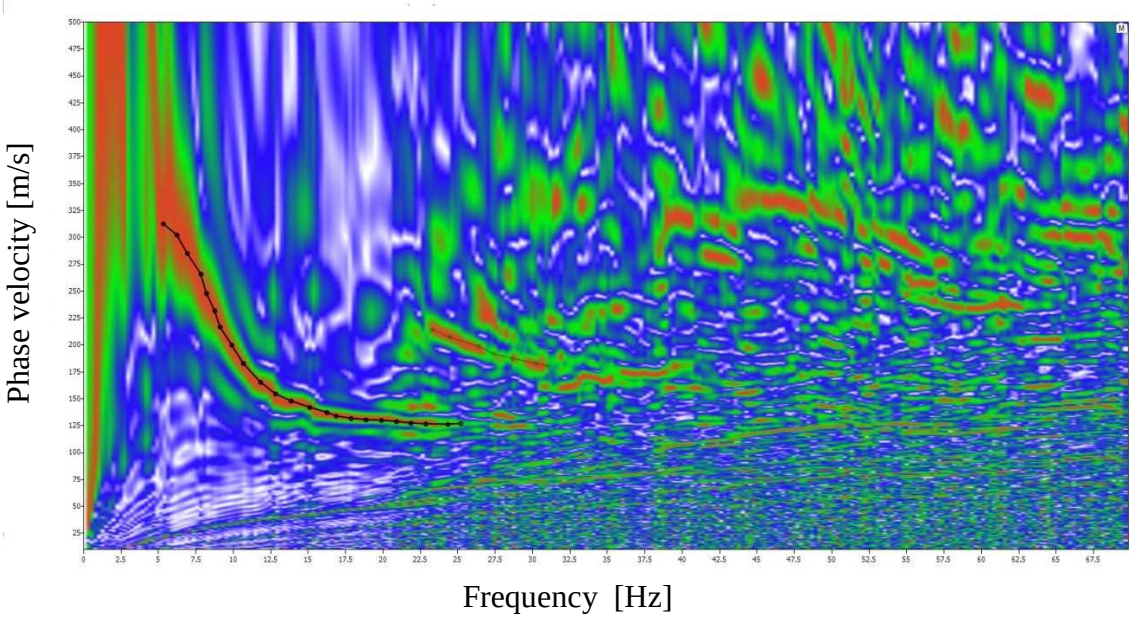

6.8. Figure: Dispersion image of the recording based on phase shift

Layer models were determined by the measured dispersion curves based on an inversion procedure according to Thomson-Haskell algorithm (Park, et al., 1999). This means practically, that the software is varying layer parameters of the initial model (layer thickness, P-wave velocity, S-wave velocity, and bulk density) due to some algorithm, until the measured and calculated theoretical dispersion curve based on parameters fit properly.

A typical field recording can be seen on Figure 6.7, frequency phase velocity images with marked dispersion curves are presented on Figure 6.8. The black and green dotted line shows the selected dispersion curves (fundamental and first mode). On Figure 6.9 the calculated theoretical curves from model parameters marked with red and the dispersion curves appear partially overlapped. The current model parameters appear in the lower left-hand table.

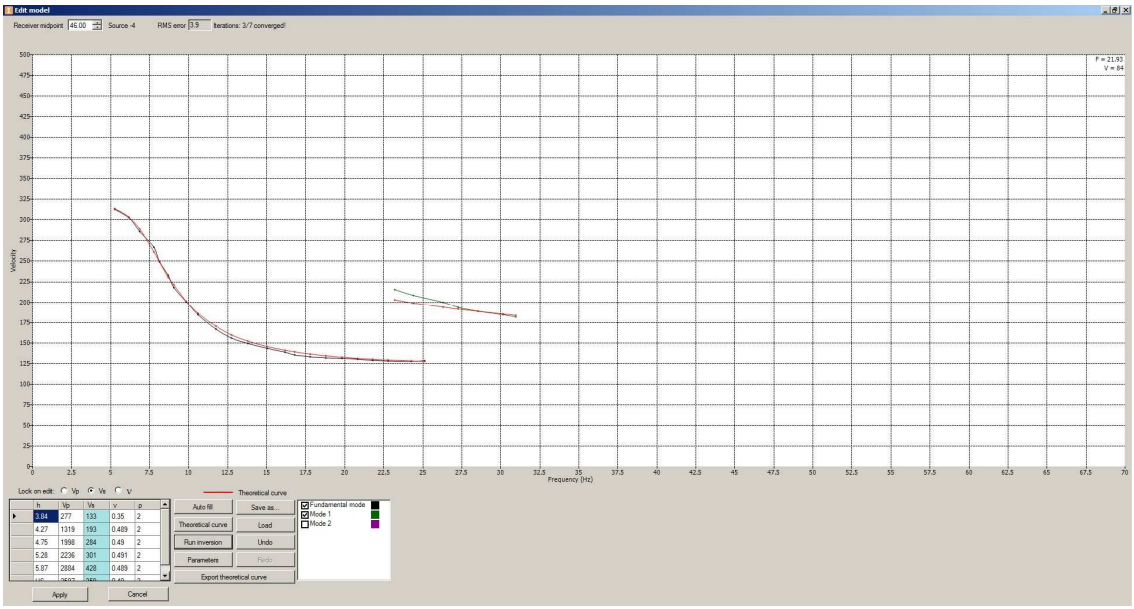

6.9. Figure: The regression of the dispersion curve with RadexPro software

6.2.3. Results from MASW measurements

Average shear-wave velocities were calculated for each site with the results shown in Table 6.6 and one of the plotted v_s profiles can be seen in Figure 6.10.

6.6 Table: MASW results about $v_{s,30}$ and soil profile category (MWSW measurements and evaluation were performed together with P. Tildy, scientific fellow of Hungarian Geological and Geophysical Institute)

Name	EOV_Y	EOV_X	Number of layers	Depth [m]	Half-space velocity [m/s]	$v_{s,30}$ [m/s]	Soil category
G01	544308	261421	6	27.511	390.548	286.4549	C
G02	543048	261704	6	25.300	461.292	297.2294	C
G03	544744	262852	6	26.411	365.185	292.3333	C
G04	545477	261477	6	26.400	426.092	323.4684	C
G05	544000	260260	6	24.211	405.335	319.5227	C
G06	543661	258115	6	19.800	344.000	304.1050	C
G07	546539	258250	6	30.800	521.232	322.9800	C
G08	545861	260003	6	18.689	336.016	294.3853	C
G09	546931	261918	6	28.600	400.071	311.3672	C
G10	543290	261956	5	20.900	326.404	270.1813	C
G11	546803	256010	7	33.000	644.761	467.2865	B

DOI: 10.15477/SZE.MMTDI.2015.002

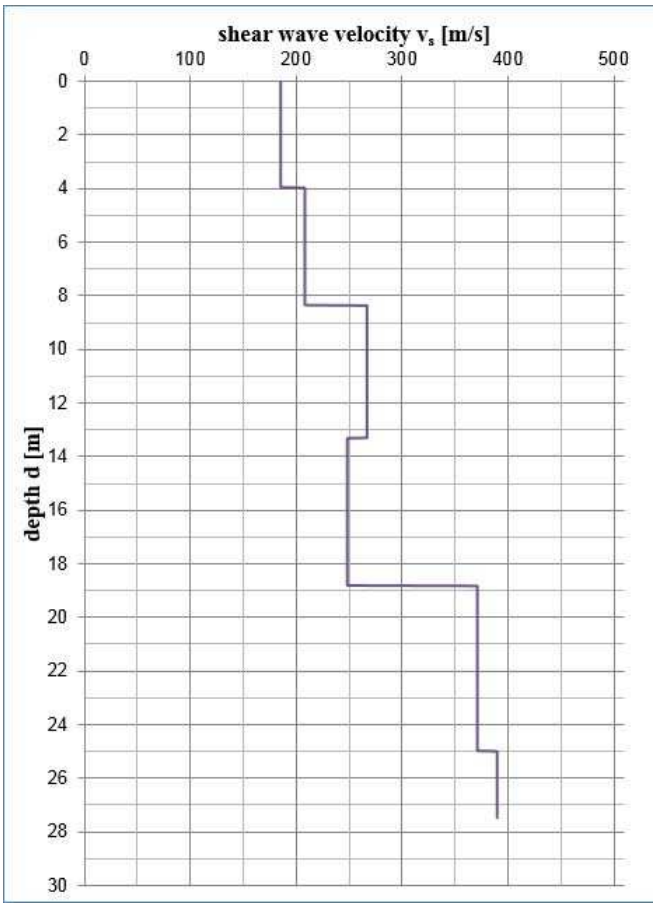

6.10. Figure: The v_s soil profile from MASW measurement (at Dunakapu square)

6.2.4. CPT technique

The cone penetration test involves advancing an instrumented cone penetrometer into the ground and measuring the cone tip resistance (q_t) and sleeve friction (f_s) at selected intervals (typically 1 to 5 cm). CPT systems used for geotechnical site investigation are the conventional CPT, the Piezo-CPT (CPTu), and the Seismic CPT (SCPT or SCPTu). The SCPT is performed in the same manner as the CPT with the addition of a geophone or accelerometer located in the CPT tip. The v_s is measured at selected intervals (typically 1 to 2 m) by striking a steel or wood beam pressed firmly against the ground and calculated based on the difference in travel time of the shear wave between the source and the geophone at two consecutive depth positions. CPTu incorporates a pore pressure transducer to measure the dynamic pore water pressure located behind the cone tip allowing the correction of the tip resistance due to pore pressures acting on unequal areas of the cone, and can be calculated by

$$q_t = q_c + (1 + a_n) \cdot u_2 \tag{6.2}$$

where q_c is the measured tip resistance and a_n is the net area ratio. The CPT does not retrieve actual soil samples for classification. Soil classification estimation is typically based in interpreted Soil Behavior Type (SBT) presented in Figure 6.11. (Robertson & Cabal, 2012)

DOI: 10.15477/SZE.MMTDI.2015.002

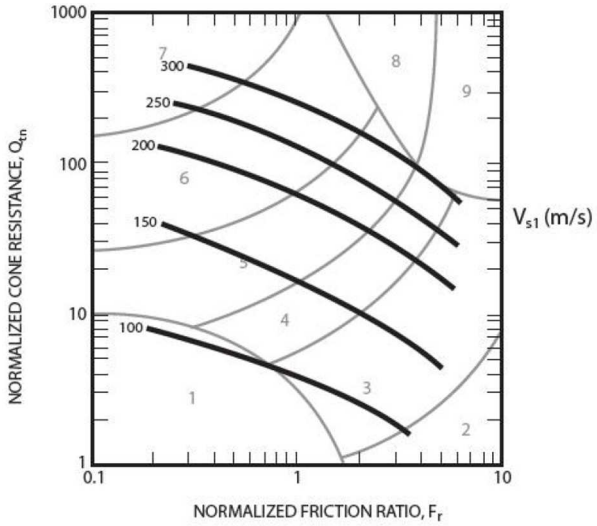

6.11. Figure: Normalizes CPT Soil Behavior Type (SBT) chart (Robertson & Cabal, 2012)

Shear wave velocity can be obtained by the equation based on Robertson & Cabal:

$$v_s = (\alpha_{vs}(q_t - \sigma_v)/p_a)^{0.5} \text{ [m/s]} \quad (6.3)$$

where $$\alpha_{vs} = 10^{(0.55 \cdot I_c + 1.68)} \quad (6.4)$$

and the vertical total stress is σ_v, atmospheric pressure is $p_a = 100$ kPa, and

soil behavior type index $$I_c = \lceil (3.47 - \log Q_t)^2 + (\log F_r + 1.22)^2 \rceil^{0.5} \quad (6.5)$$

normalized cone penetration resistance (dimensionless) $$Q_t = (q_t - \sigma_{v0})/\sigma'_{v0} \quad (6.6)$$

normalized friction ratio (%) $$F_r = (f_s/(q_t - \sigma_{v0})) \times 100\% \quad (6.7)$$

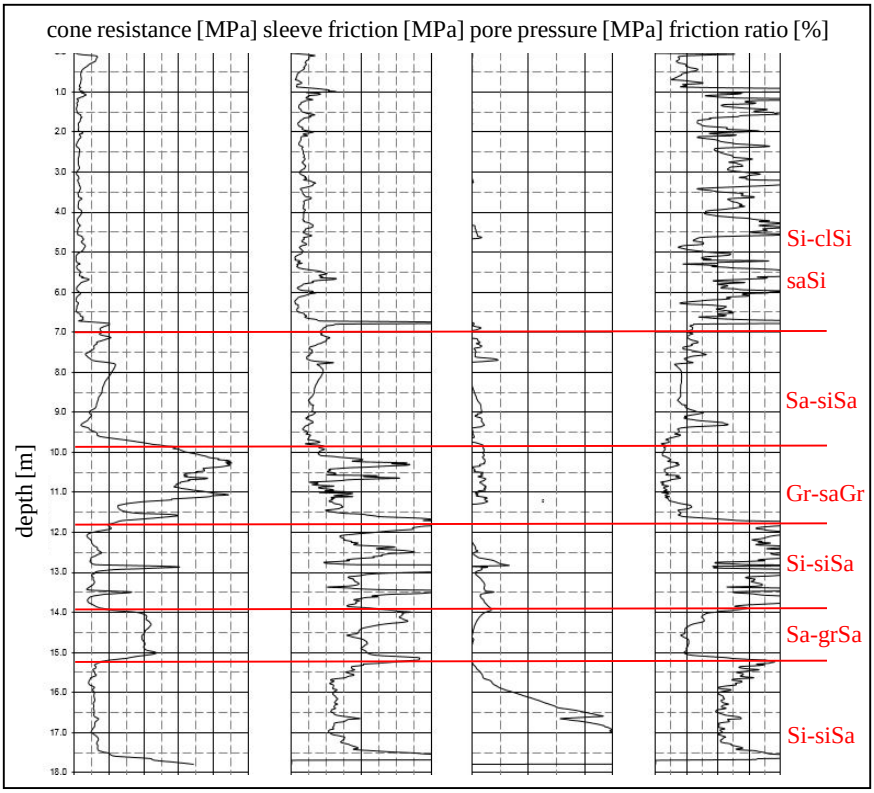

6.12. Figure: Plot of cone resistance, sleeve friction, pore pressure and friction ratio with identified soil layers based on SBT chart

6.2.5. CPT measurements around Győr

Raw CPT data were offered by geotechnical companies at four locations, which ensured the verification of the results. The first step was to plot the cone resistance, sleeve friction, friction ratio and pore pressure illustrated in Figure 6.12. The soil layers were identified based on SBT chart of Robertson & Cabal. Shear wave velocities were calculated. Average v_s values were determined for each soil layer.

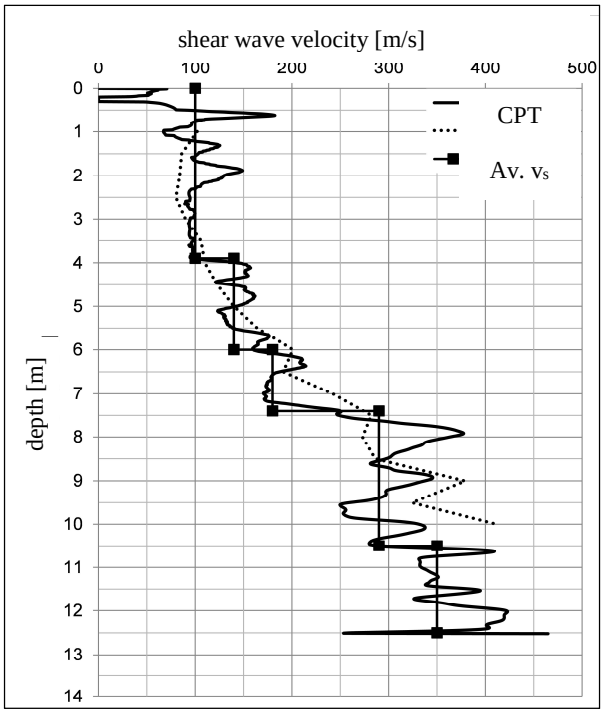

6.13. Figure: Average v_s values for soil layers

6.2.6. Results from CPT measurement

Figure 6.13 show the shear-wave velocities. The v_s is usually increasing with depth, so correction of the v_s values should be done according to

$$v_{s1} = v_s \left(\frac{p_a}{\sigma'_{v0}}\right)^{0.25} \tag{6.8}$$

This correction results in the increase of values in the upper 8-10 m of strata, while below that a slight decrease of the values of v_s.

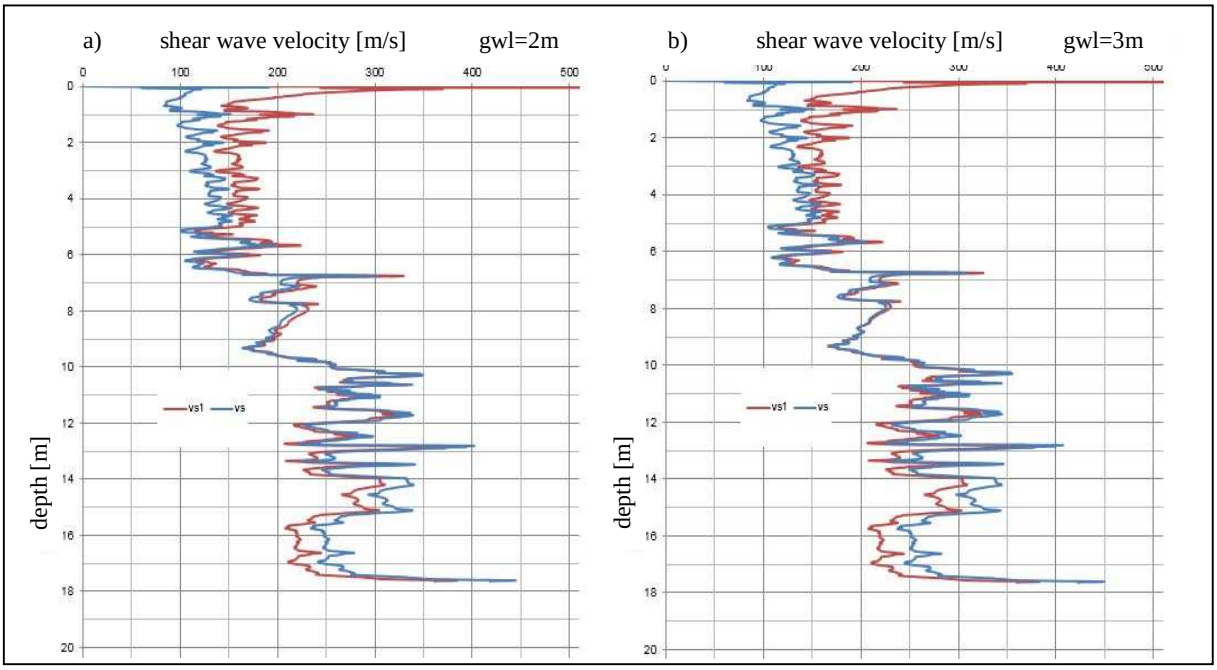

6.14. Figure: Plotted v_s and v_{s1} taking into account different ground water level

Taking into account the usual ground water level (Section 4.2.2) the v_s values were defined for several cases: ground water level of 2 m, 3 m and 4 m (Cs. Deseő, 1989). The difference between $v_{s,30}$ values referred to ground level is less than 1%, and has no significant influence on the average shear-wave velocity, so for further calculations the ground water level was assumed to be 3 m.

6.2.7. MASW and CPT correlation

MASW results and CPT results were correlated to at four places: Dunakapu Square in Downtown, on the two sides of Jedlik Bridge in Sziget and Révfalu city districts, and in Gyárváros. For the reached depth of CPT, average shear-wave velocities were calculated and compared to the average shear-wave velocities obtained from MASW measurements for the same depth. Compared to each other it can be clearly seen a quite good match with a difference ranging between 0.35 – 5.26 %, except one case, with a difference of 18.04 %, that can be explained by a layer of higher shear-wave velocities, that was partially examined by CPT measurements. Fig. 6.15 presents one of the results from the correlation (further are in Annex).

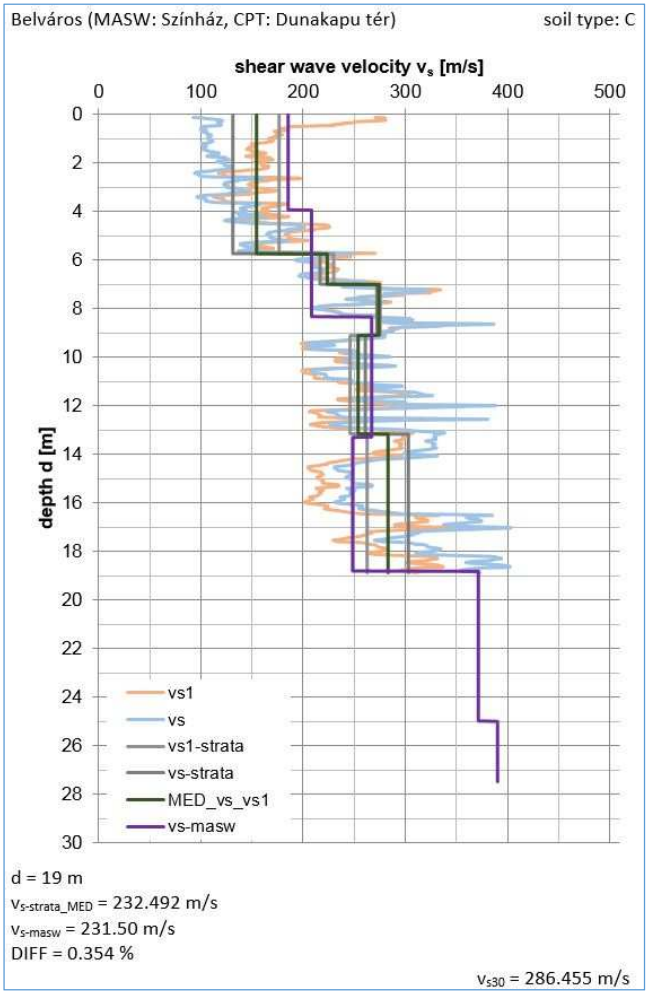

6.15. Figure: Correlated result of CPT and MASW measurements

DOI: 10.15477/SZE.MMTDI.2015.002

6.2.8. Identification of v_s properties and determination of $v_{s,30}$

CPT results were used only for validation purposes. The v_s values for each soil type were defined from MASW measurements. First, the approximate v_s range determination and $v_{s,30}$ calculations for the 60 borings required the reorganization of previously delineated groupings and categorization of soil types presented in Section 6.1.2, because on one hand it was obvious that previously determined soil layers could have similar shear-wave velocities, and on the other hand differences were found based on more detailed categorization. The following soil categories were defined: Ss (sandstone), Cls (claystone), clay (Cl), silt (Si), clayey sand (clSa), silty sand (siSa), sand (Sa), gravelly sand (grSa), sandy gravel (saGr), gravel (Gr), silty clay (siCl), sandy clay (saCl), and two stiffer soil types found in Kismegyer with higher shear-wave velocities. (Whole table is presented in Annex.)

Predictive equations were defined by finding a regression for each MASW measured v_s profile in the following form:

$$v_{s,i} = a \cdot D^b \tag{6.9}$$

where a can be interpreted as a basic v_s value for each soil category, and b is the depth correlation coefficient. Minimizing the error by varying a and b values of the equation, the computed v_s values and the measured values could be matched accurately (Figure 6.16). (Calculations for each site are attached to Annex.)

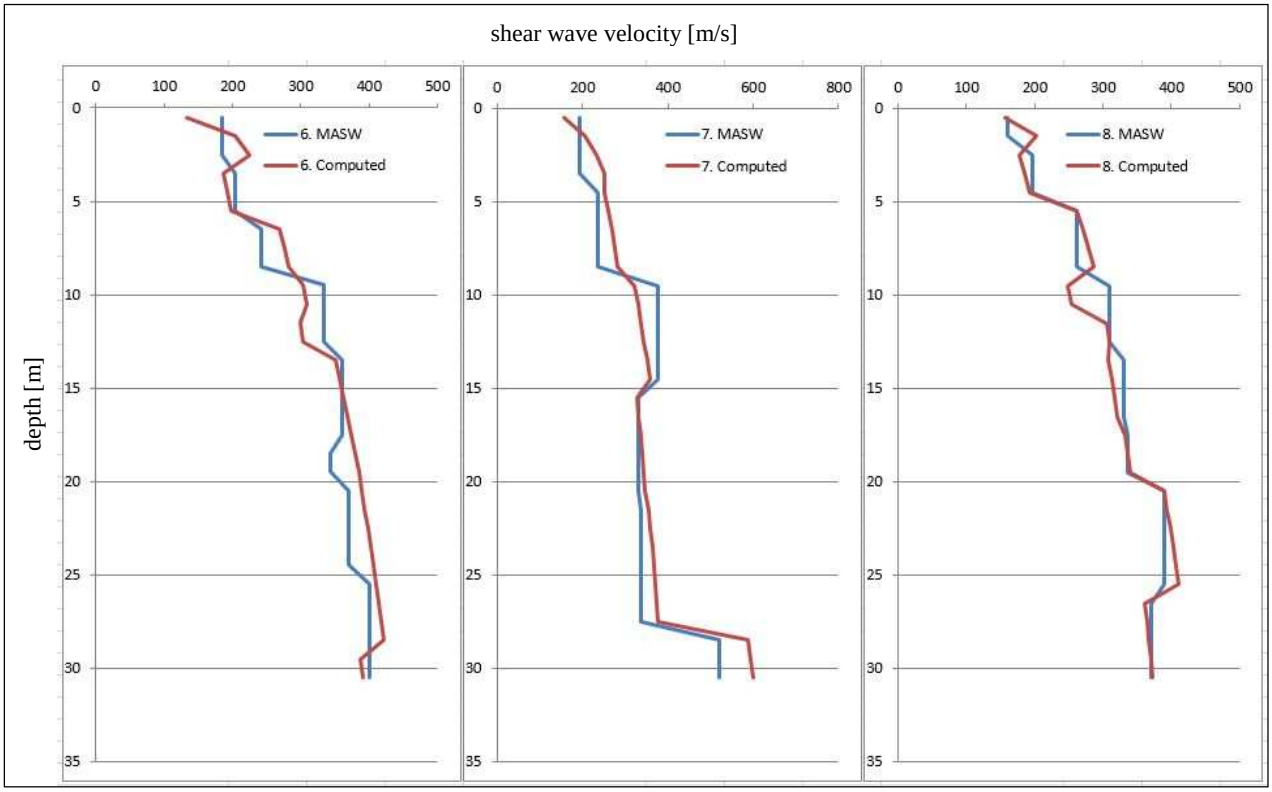

6.16. Figure: Correlation of computed and measured v_s profiles

For each layer noted on MASW recordings, an average shear-wave velocity was determined, and the depth of the mid-point of each layer was also recorded. The predictive equations for each kind of surficial material were then created by plotting the mid-point depth values and corresponding shear-wave velocity values from the appropriate MASW record on a graph, and then best-fitting the equation (13). Equations of this form are usually used to relate shear-wave velocity and depth. Correlation coefficients for the determined equations ranged from r = 0.39 to 0.97. The predictive equations are presented in Table 6.7.

6.7 Table: Predictive equations for different soil types in Győr

Based on MASW measurements		Based on literature and optimization	
Soil type	**Predictive equation**	**Soil type**	**Predictive equation**
Cl	$v_{s,i} = 190 \cdot D^{0.1858}$	Ss	$v_{s,i} = 250 \cdot D^{0.3500}$
Si	$v_{s,i} = 180 \cdot D^{0.1181}$	Cls	$v_{s,i} = 200 \cdot D^{0.2700}$
siSa	$v_{s,i} = 155 \cdot D^{0.2087}$	clSa	$v_{s,i} = 185 \cdot D^{0.2136}$
Sa	$v_{s,i} = 185 \cdot D^{0.2186}$	Gr	$v_{s,i} = 180 \cdot D^{0.2200}$
grSa	$v_{s,i} = 155 \cdot D^{0.1461}$	saGr	$v_{s,i} = 195 \cdot D^{0.1900}$
siCl	$v_{s,i} = 185 \cdot D^{0.2046}$	stiffCl	$v_{s,i} = 200 \cdot D^{0.3219}$
saCl	$v_{s,i} = 185 \cdot D^{0.2463}$	stiffclSa	$v_{s,i} = 195 \cdot D^{0.3388}$

Some soil types were underrepresented in MASW measurements, in those cases the values for equation were obtained by literature and optimization. Shear-wave velocity intervals were defined for each soil type varying with depth by 5 m steps (Table 6.8).

6.8 Table: Shear-wave velocity intervals for soil types in Győr

Depth [m]	MED v_s [m/s]				MIN vs [m/s]				MAX vs [m/s]			
	169.79	178.69	183.09	162.89	131.44	140.07	131.44	134.13	204.00	193.09	215.58	201.31
	190.93	233.00	185.86	207.79	159.80	202.15	163.31	200.57	222.73	257.04	208.40	215.00
	194.36	212.11	-	-	194.36	167.04	-	-	236.49	251.27	-	-
	-	-	192.94	235.83	-	-	183.68	212.15	-	-	202.20	259.50
1-5	203.81	256.09	191.80	192.67	187.06	160.00	159.80	155.97	270.82	324.59	215.58	251.86
	193.06	219.23	321.33	275.30	169.22	198.83	309.66	247.95	210.43	285.95	333.00	302.66
	220.10	276.33	208.40	224.35	218.34	268.57	208.40	220.15	222.73	287.41	208.40	228.37
	238.85	273.87	324.49	295.74	236.49	260.82	324.49	292.23	242.00	282.80	324.49	299.26
	263.29	282.74	220.79	274.50	261.61	262.21	183.68	221.22	266.20	293.23	267.23	299.09
5-10	316.22	381.09	345.64	319.17	270.82	346.25	329.40	313.37	384.32	412.86	378.12	322.07
	235.65	223.98	292.98	275.04	210.43	218.53	264.63	253.18	252.47	229.08	333.00	309.35
	-	-	264.69	262.04	-	-	248.55	244.79	-	-	309.66	309.66
	315.20	294.06	324.49	311.59	248.55	246.86	324.49	305.72	333.00	312.30	324.49	317.33
	284.93	305.51	267.23	312.45	261.61	294.12	267.23	304.83	333.77	319.73	267.23	319.74
10-15	428.67	453.03	359.21	345.87	384.32	426.38	329.40	330.11	463.43	473.08	378.12	357.42
	252.47	232.38	264.63	278.17	252.47	231.32	264.63	274.62	252.47	233.44	264.63	281.66
	381.49	354.19	Kismegy	538.58	523.98	371.71	354.19	Kismegy	538.58	514.32	391.27	354.19	Kismegy	538.58	533.53
	318.27	328.74	249.32	250.97	312.05	316.20	248.55	246.86	330.72	339.71	250.28	254.07
	343.64	334.25	329.97	335.73	326.40	324.12	329.97	328.24	378.52	339.71	329.97	342.88
15-20	450.55	486.62	370.98	375.66	424.77	483.34	344.00	363.34	463.43	493.17	443.05	384.47
	-	-	-	-	-	-	-	-	-	-	-	-
	381.49	358.08	Kismegy	538.58	551.38	371.71	358.08	Kismegy	538.58	542.64	391.27	358.08	Kismegy	538.58	560.03
	337.35	341.76	364.84	361.40	312.05	336.02	338.41	356.31	350.00	346.57	391.27	366.39
	369.25	349.69	417.52	353.16	326.40	343.20	329.97	346.15	378.52	355.95	461.29	358.08
20-25	656.53	556.38	396.72	398.12	656.53	552.64	370.00	389.24	656.53	560.11	370.00	389.24
	-	-	-	-	-	-	-	-	-	-	-	-
	392.91	380.98	-	-	390.55	375.59	-	-	400.00	387.74	-	-
	362.22	352.21	365.81	375.10	360.00	346.85	338.41	369.53	370.00	356.37	391.27	381.22
	369.47	365.00	-	-	365.19	358.88	-	-	370.00	369.74	-	-
25-30	617.87	584.07	416.12	417.29	521.23	567.37	390.00	410.73	656.53	594.62	430.00	425.74

DOI: 10.15477/SZE.MMTDI.2015.002

Calculation of $v_{s,30}$ for each boring were performed, based on three different method: first using the determined v_s intervals for each soil type (Table 6.9) based on the Table 6.8, then applying the values of predictive equations, finally with the help of Hardin & Black's formula (14). (Hardin & Black, 1968) In terms of its maximum value G_{max} in small strain ranges, will depend on several factors, such plasticity index of the soil, over consolidation ratio, normal stress, void ratio, etc.

$$G_{max} = 625 \cdot \frac{OCR^K}{0.3+0.7e^2} \cdot p_a^{0.5} \cdot \sigma^{0.5} \tag{6.10}$$

where OCR is the over consolidation ratio, σ is the normal stress, e is the void ratio.

Value of v_s can then be obtained by

$$v_s = \left(\frac{G_{max}}{\rho}\right)^{0.5} \tag{6.11}$$

where ρ is density obtained from the total unit weight of the soil divided by gravity (9.81 m/s^2).

6.9 Table: Shear-wave velocity intervals for each soil type by a step of 5 m

Correlations for program		Depth	v_s Low	v_s Med	v_s High	Expon. term	Void Ratio	Plasticity Index
	Ss	5	250	300	350	0.3050	0.100	0
		10	350	400	450	0.3050	0.100	0
		15	450	500	550	0.3050	0.100	0
		20	550	600	650	0.3050	0.100	0
		25	600	650	700	0.3050	0.100	0
		30	650	700	750	0.3050	0.100	0
	Cls	5	200	250	300	0.2700	0.100	0
		10	350	400	450	0.2700	0.100	0
		15	390	400	410	0.2700	0.100	0
		20	410	420	430	0.2700	0.100	0
		25	430	450	470	0.2700	0.100	0
		30	470	500	530	0.2700	0.100	0
	Cl	5	185	210	235	0.1858	0.475	30
		10	260	270	280	0.1858	0.500	30
		15	270	290	310	0.1858	0.525	30
		20	310	325	340	0.1858	0.550	30
		25	335	340	345	0.1858	0.575	30
		30	345	350	355	0.1858	0.600	30
	Si	5	195	205	215	0.1181	0.650	10
		10	220	225	230	0.1181	0.675	10
		15	245	260	275	0.1181	0.700	10
		20	255	265	275	0.1181	0.725	10
		25	270	280	290	0.1181	0.750	10
		30	290	290	300	0.1181	0.775	10

DOI: 10.15477/SZE.MMTDI.2015.002

Correlations for program		Depth	v_s Low	v_s Med	v_s High	Expon. term	Void Ratio	Plasticity Index
	clSa	5	175	185	195	0.2136	0.625	5
		10	290	295	300	0.2136	0.600	5
		15	300	310	320	0.2136	0.575	5
		20	335	345	355	0.2136	0.550	5
		25	355	360	365	0.2136	0.525	5
		30	370	375	380	0.2136	0.500	5
	siSa	5	130	165	200	0.2087	0.850	5
		10	250	275	300	0.2087	0.825	5
		15	255	280	305	0.2087	0.800	5
		20	275	285	295	0.2087	0.775	5
		25	290	300	310	0.2087	0.750	5
		30	310	330	350	0.2087	0.725	5
	Sa	5	205	230	255	0.2186	0.575	0
		10	265	275	285	0.2186	0.550	0
		15	310	330	350	0.2186	0.525	0
		20	350	355	360	0.2186	0.500	0
		25	355	360	365	0.2186	0.475	0
		30	375	380	385	0.2186	0.450	0
	Gr	5	190	195	200	0.2200	0.650	0
		10	200	220	240	0.2200	0.625	0
		15	240	280	320	0.2200	0.600	0
		20	320	330	340	0.2200	0.575	0
		25	340	370	400	0.2200	0.550	0
		30	405	415	425	0.2200	0.525	0
	saGr	5	210	230	250	0.1900	0.575	0
		10	245	265	285	0.1900	0.600	0
		15	295	300	305	0.1900	0.625	0
		20	320	330	340	0.1900	0.65	0
		25	340	350	360	0.1900	0.675	0
		30	350	360	370	0.1900	0.700	0
	grSa	5	160	175	190	0.1461	0.850	0
		10	195	215	235	0.1461	0.875	0
		15	220	225	230	0.1461	0.900	0
		20	230	235	240	0.1461	0.925	0
		25	240	260	280	0.1461	0.950	0
		30	280	300	320	0.1461	0.975	0
	siCl	5	170	190	210	0.2046	0.450	20
		10	265	280	295	0.2046	0.475	20
		15	290	305	320	0.2046	0.500	20
		20	330	335	340	0.2046	0.525	20
		25	340	350	360	0.2046	0.550	20
		30	360	365	370	0.2046	0.575	20
	saCl	5	155	190	225	0.2463	0.475	30
		10	315	320	325	0.2463	0.450	30
		15	330	345	360	0.2463	0.425	30
		20	365	375	385	0.2463	0.400	30
		25	390	400	410	0.2463	0.375	30
		30	405	415	425	0.2463	0.350	30

DOI: 10.15477/SZE.MMTDI.2015.002

Correlations for program		Depth	v_s Low	v_s Med	v_s High	Expon. term	Void Ratio	Plasticity Index
	stiffCl	5	230	255	280	0.3219	0.010	30
		10	345	380	415	0.3219	0.010	30
		15	435	455	475	0.3219	0.010	30
		20	480	485	490	0.3219	0.010	30
		25	550	555	560	0.3219	0.010	30
		30	575	585	595	0.3219	0.010	30
	stiffclSa	5	170	200	230	0.3388	0.100	5
		10	280	320	360	0.3388	0.100	5
		15	360	375	390	0.3388	0.100	5
		20	510	520	530	0.3388	0.100	5
		25	540	550	560	0.3388	0.100	5
		30	570	580	590	0.3388	0.100	5

The values of the Table 6.8 were used to determine the v_s profile for the given 60 borings and to calculate $v_{s,30}$ values in each case. Average shear-wave velocity for the upper 30 m were defined based on minimum, medium and maximum values of the v_s intervals, the predictive equation, and Hardin & Black's formula (Figure 6.17).

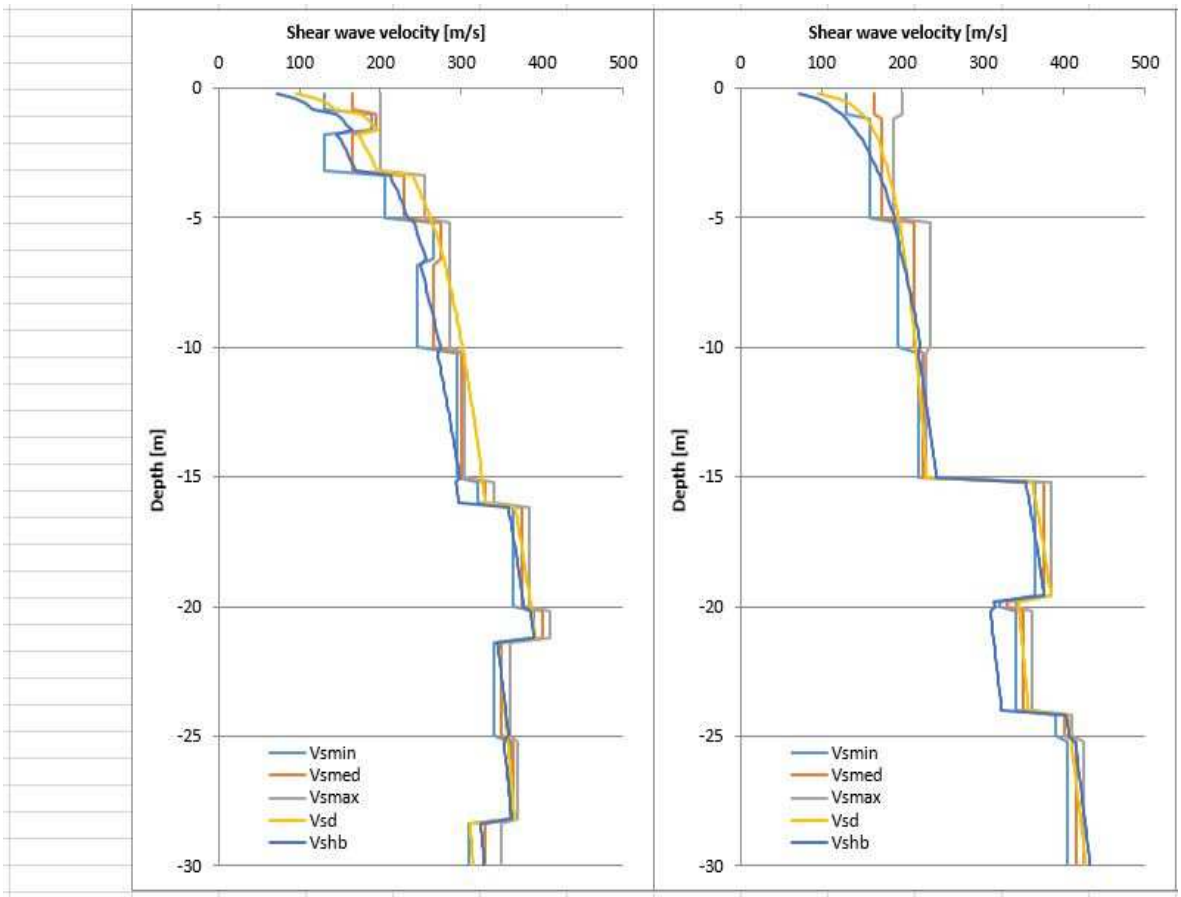

Vs30 time-average	258.37	277.65	297.10	288.53	262.09		248.09	265.38	282.10	266.97	249.14
Vs30 weighted-average	281.87	297.53	314.07	306.33	284.09		286.57	299.80	313.17	297.64	276.00
MASW 297.23						297.23					
Difference [%]	13.07	6.59	0.04	2.93	11.82		16.53	10.71	5.09	10.18	16.18
Difference [%]	5.17	0.10	5.66	3.06	4.42		3.59	0.86	5.36	0.14	7.14

6.17. Figure: Shear-wave velocity profiles and comparison with measured data

Both time-average and weighted-average method (Wair, et al., 2012) was used in each calculation to determine $v_{s,30}$ values. A comparison was made between the computed average shear-wave velocities computed, and reported field measurements of shear-wave velocities in surficial materials. Best match was obtained by weighted-average of the medium values of the shear-wave velocity intervals. The error, i.e. the average of the differences at sites, where MASW data were available, is 0.64 %, which offers an appropriate accuracy for further calculations. The determined v_s intervals can be used in response analysis.

6.2.9. Zonation and mapping

Previous grouping based on strata and former geomorphological studies proved to be adequate, reassignment of only one or two borings were needed based on $v_{s,30}$. The final grouping is presented in Figure 6.18, soil profiles are numbered from I to XV. In case of four profiles only one boring formed the basis of examination, and in three cases even measured data is not available. The reliability of the SPI, SPXIII and SPXIV are questionable, further investigations should be done using the presented method.

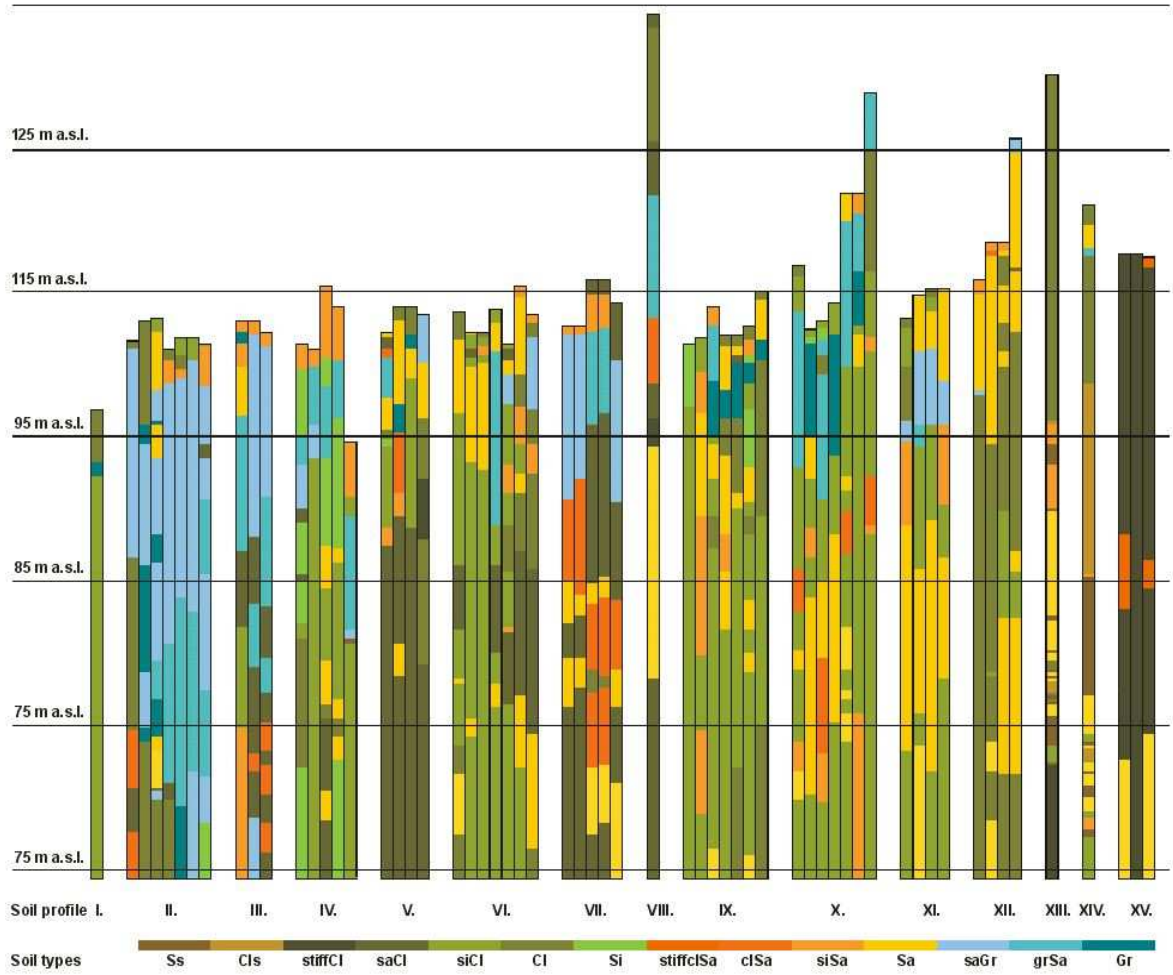

6.18. Figure: Soil profiles of Győr numbered from I to XV

DOI: 10.15477/SZE.MMTDI.2015.002

The intervals of $v_{s,30}$ can be found in Table 6.10, and the delineation of the zones is presented in Figure 6.19. There are some spots in the map, where the zone is not specified due to the lack of boring data. Soil categories according to EC8 are indicated in the Table 6.10.

6.10 Table: Intervals of $v_{s,30}$ and soil categories according to EC8 in Győr

Soil profile	Intervals of $v_{s,30}$ [m/s]	Soil category according to EC8
I	~300	C
II	275-285	C
III	295-300	C
IV	285-295	C
V	320-325	C
VI	300-310	C
VII	305-315	C
VIII	~330	C
IX	290-300	C
X	295-305	C
XI	295-305	C
XII	290-300	C
XIII	~315	C
XIV	~415	B
XV	445-450	B

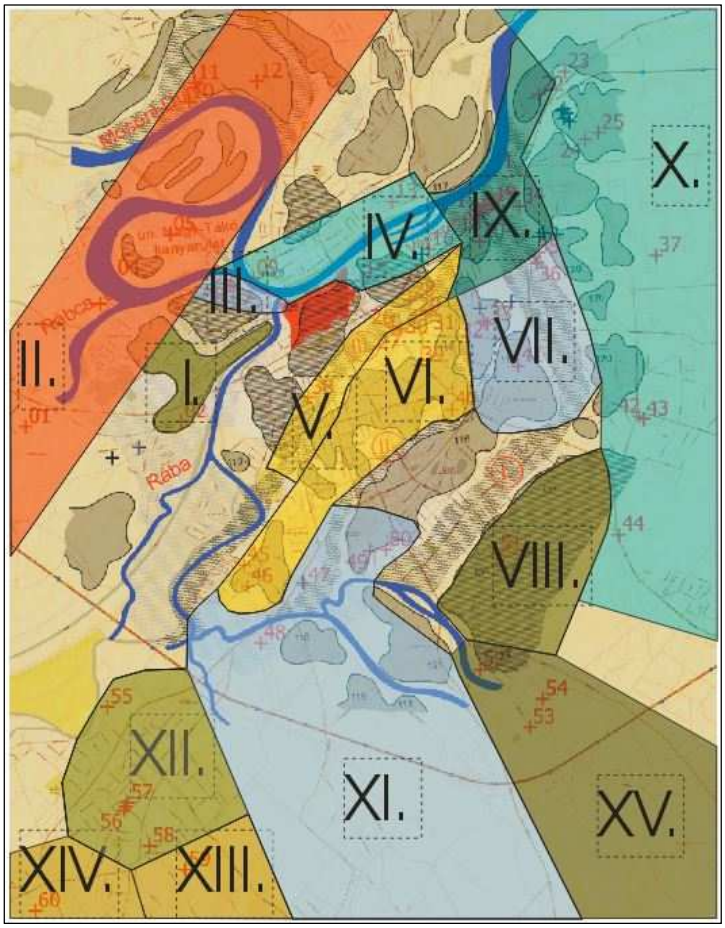

6.19. Figure: Zones with different soil profiles in Győr

DOI: 10.15477/SZE.MMTDI.2015.002

6.3. Response analysis

Seismologists and engineers divide the problem of seismic wave transmission into four stages: source, geologic path through rock layers, near surface path through soil and surficial rock layers, and interaction between shallow soil and structure (Figure 6.20). For risk assessment, all of these stages are important; however, this study will focus on the near-surface path through soil and surficial rock. This segment of the problem is commonly called site response analysis. It normally involves estimating an input motion at "bedrock" and computing the resulting surface ground motion.

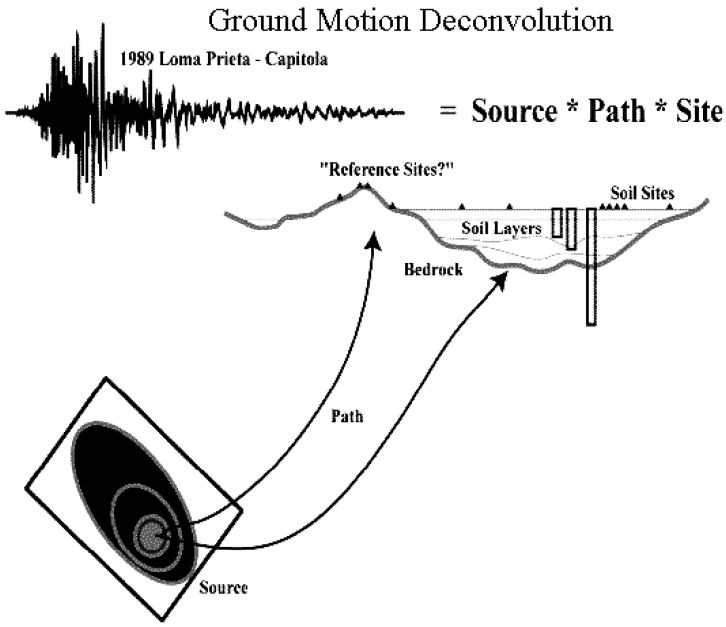

6.20. Figure: Considering ground motion at a site as contributions from the source, path and the site from Steidl (Boore, 2004)

The main parameters involved in the analysis are the intensity and duration of the input base motion and the dynamic properties of the soil layers leading up to the surface. Earlier sections discussed the measurement of dynamic soil properties, mainly shear wave velocity over the upper 30 m of soil ($v_{s,30}$), but other soil properties, and a method to select appropriate input base motions are still necessary.

Simplifications to site response analysis often reduce the problem to 1-dimension and a single type of wave: horizontally-polarized vertically-propagating shear wave. This corresponds to the most damaging wave for buildings. The horizontal motion imparts lateral inertia loads on the building which are generally more difficult to resist than vertical loads. The vertical propagation is a reasonable approximation as well since the pathway for seismic waves becomes more vertical as it moves through material that is less stiff (lower v_s) as it moves toward the surface.

6.3.1. REXEL software

The method chosen to select base motions was a magnitude scaling technique implemented in the software package REXEL (Iervolino, et al., 2010). Strong motion records are selected from a database (European Strong-Motion Database, ESD) and compared to a desired set of criteria. If the record meets the criteria it is copied into a “bin” of motions that will be used later. For many typical low to moderate seismic actions, the database will contain many suitable records. However, if the criteria are not met, REXEL will scale the earthquake motion (increase or decrease acceleration amplitude) so that it will meet the criteria. Other parameters affect the suitability of an earthquake for scaling and relocation. Distance from epicenter, frequency content, and type of faulting that initiated the motion all have an impact on the final behavior in the response analysis.

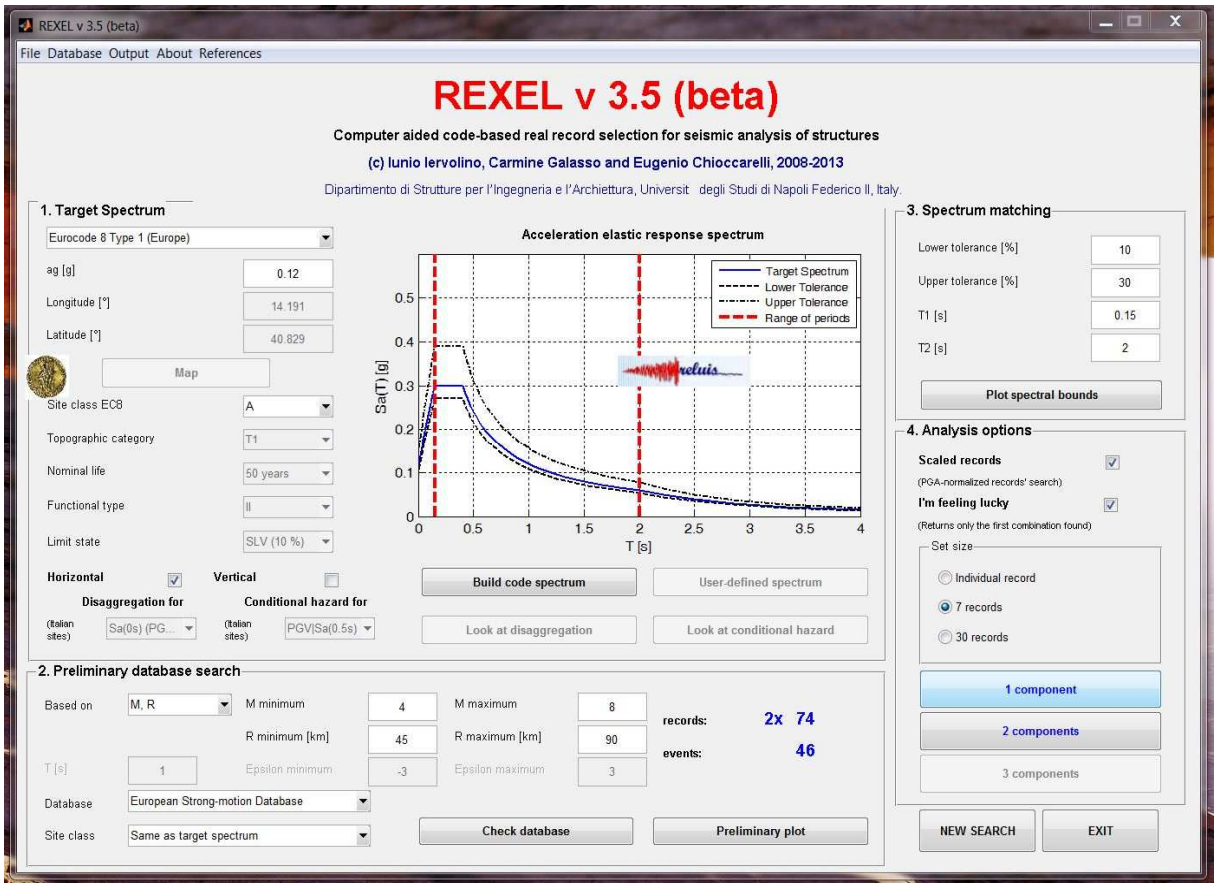

6.21. Figure: Main window of REXEL software, parameters can be selected according to the chosen target spectrum, used database, intensity and distance of earthquake, spectrum matching criterions, and possible analysis options (Iervolino, et al., 2010)

REXEL evaluates these parameters by asking the user for appropriate degrees of variation in these parameters and searches out those records that will meet these criteria. Naturally, as the criteria become less rigorous, more records (scaled and shifted in frequency or time) will meet the criteria.

DOI: 10.15477/SZE.MMTDI.2015.002

The most common set of criteria are those described by Eurocode 8 or other building code standards. Design spectra from these codes are easily input to the program and default values of allowed variability are often enough to produce a bin of 7 earthquake records that are subsequently used in the soil response analysis program.

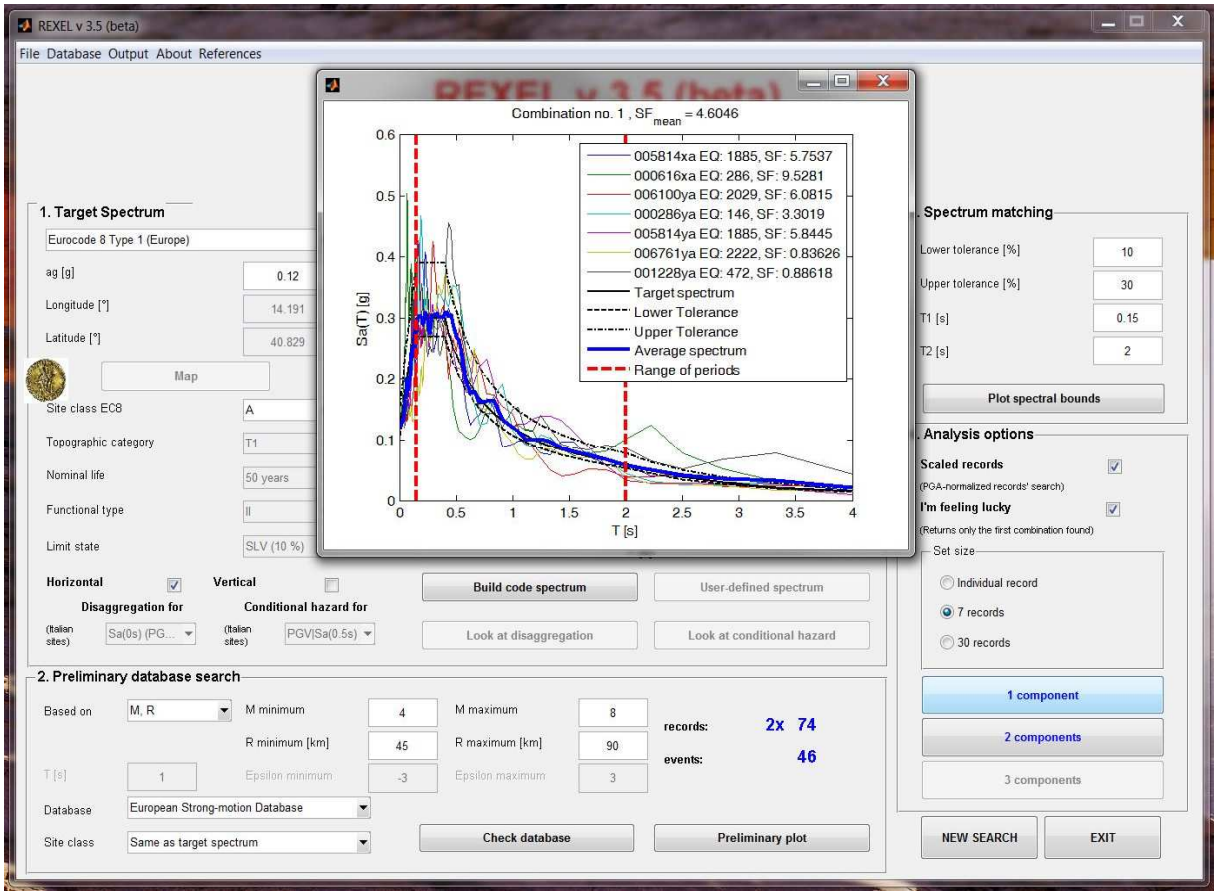

6.22. Figure: First combination of a set of 7 earthquake records that meet the selected parameters (Iervolino, et al., 2010)

6.3.2. Strong motion selection based on REXEL software

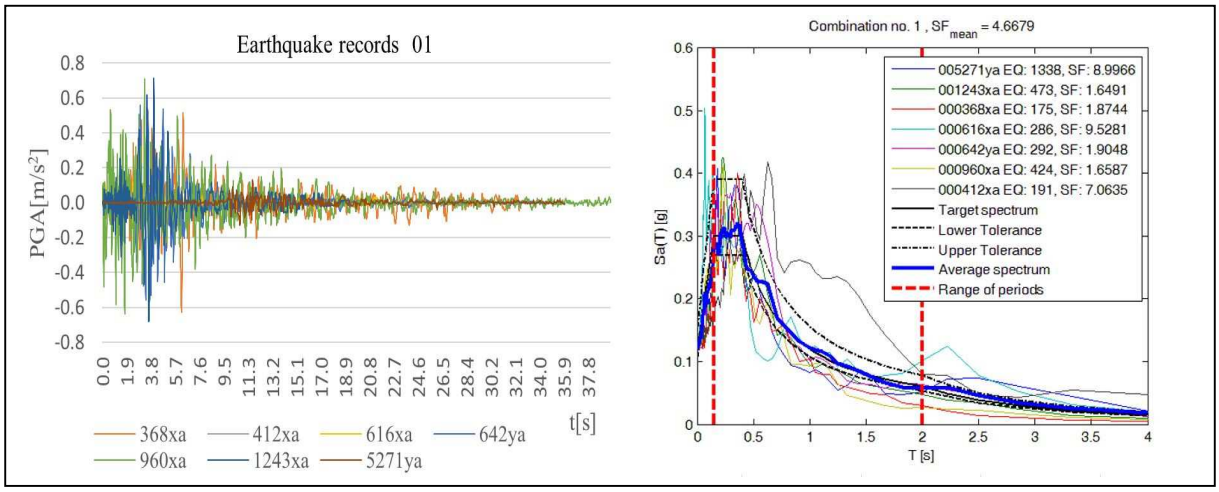

6.23. Figure: Set of 7 earthquake records and their match to the selected EC 8 T1

DOI: 10.15477/SZE.MMTDI.2015.002

Earthquake records were selected for site class A, for both EC 8 Type 1 and 2 spectra. The varied parameters were the intensity (M 3-4, 4-5, 5-6, 6-7) and epicentral distance (0-50, 0-100 km) of the earthquakes. Table 6.11 gives the characteristics and Figure 6. 23 illustrates the set of 7 earthquake records from European Strong-Motion Database (Ambraseys, et al., 2002) and their match to the selected Eurocode 8 Type 1 spectrum in case of site class A, 0.12 g PGA, magnitude values ranging between 5 and 6, and epicentral distance between 0 to 100 km. (Further records can be found in Annex.)

6.11 Table: Characteristics of the 7 set earthquake records

T1_012_A_5-6_0-100_01													
Waveform ID	**Earthquake ID**	**Station ID**	**Earthquake Name**	**Date**	**Mw**	**Fault Mechanism**	**Epicentral Distance [km]**	**Local geology**	**PGA_X [m/s²]**	**PGA_Y [m/s²]**	**PGV_X [m/s]**	**PGV_Y [m/s]**	**EC8 Site class**
5271	1338	ST2483	Mt. Vatnafjoll	1987.05.25	6.00	oblique	42	rock	0.1378	0.1308	0.0095	0.012	A
1243	473	ST575	Izmit (aftersh.)	1999.09.13	5.80	oblique	15	rock	0.714	3.112	0.055	0.145	A
368	175	ST143	Lazio Abruzzo	1984.05.07	5.90	normal	22	rock	0.6280	0.671	0.056	0.038	A
616	286	ST134	Umbria Marche	1997.09.26	6.00	normal	59	rock	0.124	0.200	0.011	0.014	A
642	292	ST225	Umbria Marche	1997.10.14	5.60	normal	23	rock	0.524	0.618	0.051	0.052	A
960	424	ST296	Sicilia-Orientale	1990.12.13	5.60	strike slip	50	rock	0.710	0.639	0.044	0.036	A
412	191	ST161	Golbasi	1986.06.06	5.80	strike slip	34	rock	0.167	0.309	0.025	0.038	A

DOI: 10.15477/SZE.MMTDI.2015.002

6.3.3. STRATA software

The next step in the response analysis is to determine the effect of the soil profile on surface response. Several software packages will compute this response, the program STRATA was used in this study due to its ease of use, allowance for many realizations of soil profiles, and low cost (freely available with user manual and sample problems). (Kottke & Rathje, 2013)

For linear elastic, one-dimensional wave propagation, the soil is assumed to behave as a Kelvin-Voigt solid, in which the dynamic response is described using a purely elastic spring and a purely viscous dashpot (Kramer, 1996). The solution to the one-dimensional wave equation for a single wave frequency (ω) provides displacement (u) as a function of depth (z) and time (t)

$$u(z,t) = A\exp[i(\omega t + k^* z)] + B\exp[i(\omega t - k^* z)] \tag{6.12}$$

where A and B represent the respective amplitudes of the upward ($+z$) and downward ($-z$) waves, respectively (Figure 6.24).

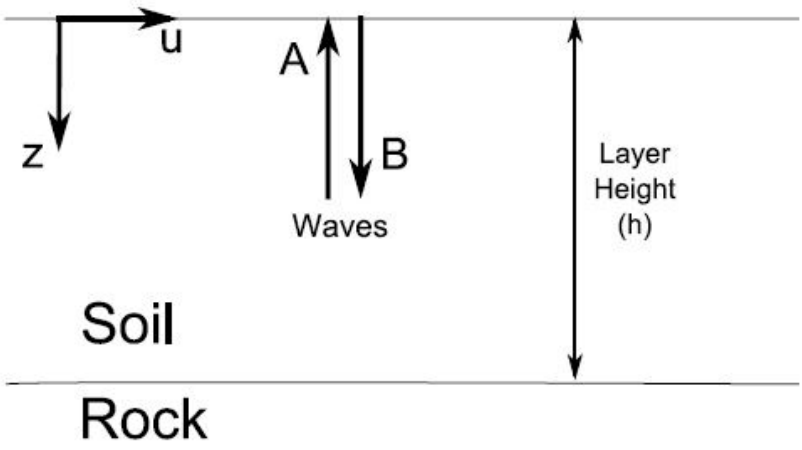

6.24. Figure: Waves in one layer (Kottke & Rathje, 2013)

Strata uses the complete definition of the complex shear-modulus, not the approximation, in the calculations

$$G^* = G\left(1 - 2D^2 + i2D\sqrt{1 - D^2}\right) \cong G(1 + i2D) \tag{6.13}$$

For a layered system, shown in Figure 6.25, the wave amplitudes are calculated by maintaining compatibility of displacement and shear stress at the layer boundaries, based on recursive formulas developed by Kramer (Kramer, 1996):

$$A_{m+1} = \frac{1}{2}A_m(1 + \alpha_m^*)\exp(ik_m^* h_m) + \frac{1}{2}B_m(1 - \alpha_m^*)\exp(-ik_m^* h_m) \tag{6.14}$$

$$B_{m+1} = \frac{1}{2}A_m(1 - \alpha_m^*)\exp(ik_m^* h_m) + \frac{1}{2}B_m(1 + \alpha_m^*)\exp(-ik_m^* h_m) \tag{6.15}$$

where *m* is the layer number, h_m is the layer height and α_m^* is the complex impedance ratio.

DOI: 10.15477/SZE.MMTDI.2015.002

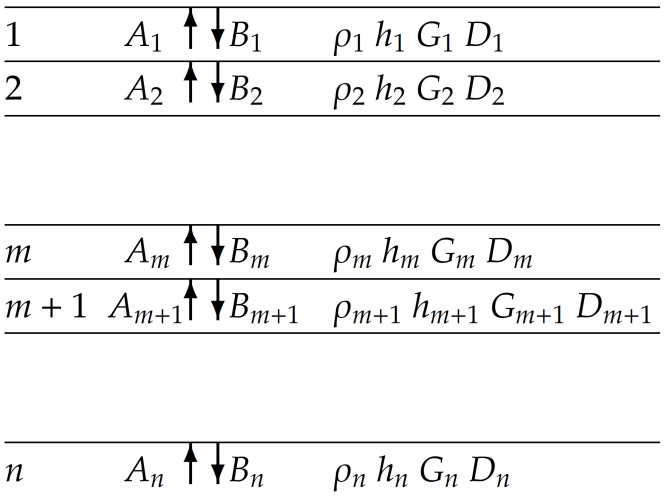

6.25. Figure: Layered system (Kottke & Rathje, 2013)

At the surface of the soil column (m=1), the shear stress must equal zero, therefore the amplitudes of the upward and downward waves must be equal ($A_1 = B_1$). The wave amplitudes (A and B) within the soil profile are calculated at each frequency (assuming known stiffness and damping within each layer) and used to compute the response at the surface of a site.

The transfer function between the motion in the layer of interest (m) and in the rock layer (n) at the base of the deposit is defined as:

$$TF_{m,n}(\omega) = \frac{u_m(\omega)}{u_n(\omega)} = \frac{A_m + B_m}{A_n + B_n} \tag{6.16}$$

where ω is the frequency of the harmonic wave.

The response at the layer of interested is computed by multiplying the Fourier amplitude spectrum of the input rock motion by the transfer function:

$$Y_m(\omega) = TF_{m,n}(\omega) \cdot Y_n(\omega)$$

where Y_n is the input Fourier amplitude spectrum at layer n and Y_m is the Fourier amplitude spectrum at the top of the layer of interest.

The dynamic properties of soil (shear modulus, G, and damping ratio, D) vary with shear strain, and thus the intensity of shaking. In equivalent-linear site response analysis, the nonlinear response of the soil is approximated by modifying the linear elastic properties of the soil based on the induced strain level, and are iteratively calculated based on the computed strain. A transfer function is used to compute the shear strain in the layer based on the outcropping input motion. (Kottke & Rathje, 2013)

The maximum strain within the layer is derived from this Fourier amplitude spectrum – either through conversion to the time domain or through RVT methods. An effective strain (γ_{eff}) is calculated from the maximum strain ($\gamma_{eff} = 0.65\gamma_{max}$).

DOI: 10.15477/SZE.MMTDI.2015.002

Equivalent-linear site response analysis requires that the strain dependent nonlinear properties (i.e. G and D) be defined. The initial (small strain) shear modulus (Gmax) is calculated by:

$$G_{max} = \rho v_s^2 \tag{6.17}$$

where ρ is the mass density of the site, and v_s is the measured shear wave velocity. Characterizing the nonlinear behavior of G and D is achieved through modulus reduction and damping curves that describe the variation of $G/G_{max}$and D with shear strain (Figure 6.26).

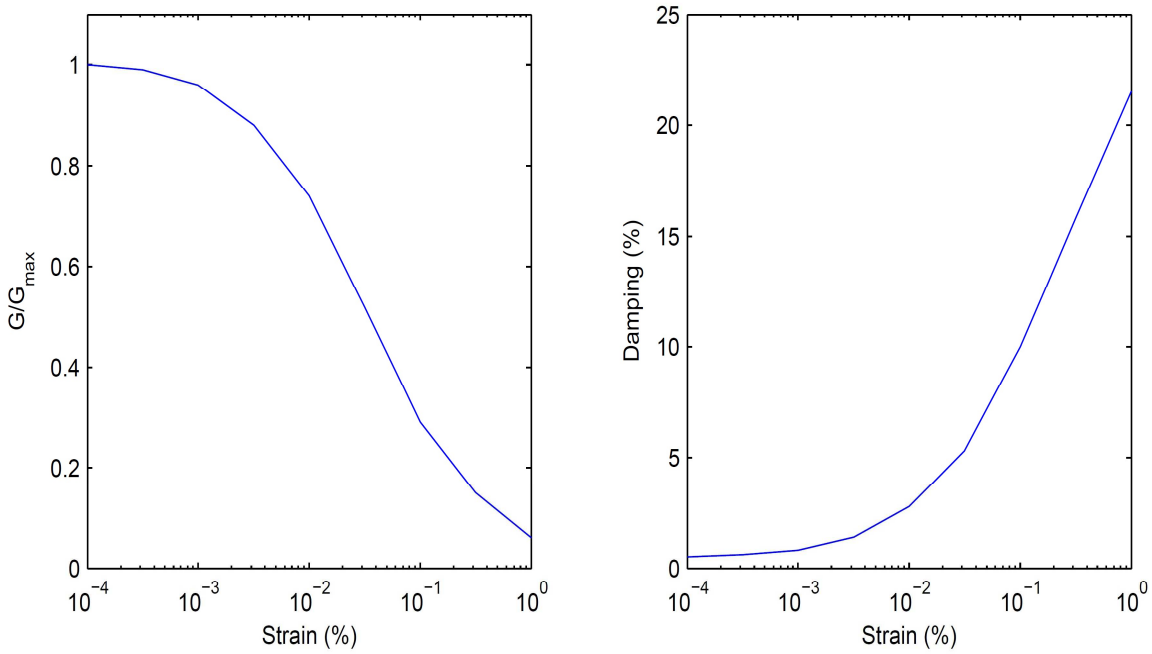

6.26. Figure: Modulus reduction and damping curves (Kottke & Rathje, 2013)

The calculation is carried out in the frequency domain. The time history records of acceleration, velocity, and displacement are generated by inverse FFT.

Other, more advanced software codes have been developed to study 2- and 3-dimensional site response. Due to the nature of the site data, the uncertainty in distribution of soil properties in 2- and 3-dimensions, these methods require significant amount of time for even a single realization.

The computational method of STRATA is very efficient; a large number of soil profiles, earthquakes and soil nonlinear conditions can be examined. Soil profiles can be varied by specifying mean and standard deviation values for each soil layer. Many earthquake motions can be specified initially and their magnitudes can be varied over a small range. The software will collect all the results and compute mean profile data, high and low percentile, as well as response spectra envelopes with similar results for mean and standard deviation. The impact of the variability of input data on site response can be quantified.

DOI: 10.15477/SZE.MMTDI.2015.002

6.3.4. Site response based on STRATA software

Response analysis was performed in case of each previously defined 15 soil profiles for Győr (Section 6.2.9) taking into account different PGA values according to different Limit Stages (Chapter 6).

Selected earthquake records were imported to STRATA from European Strong-Motion Database according to REXEL selections. The motion location input was defined in bedrock, using a scale factor for each record to obtain same PGA values.

Method of analysis is based on equivalent linear method, using time series approach. The nonlinear properties of the soil, and site profile were taken into account, reaching 100 realizations in each case. (Figure 6.27)

Soil properties were defined based on tables used for design. G/G_{max} model and damping model of Vucetic & Dobry was used (Vucetic & Dobry, 1991). (Figure 6.28)

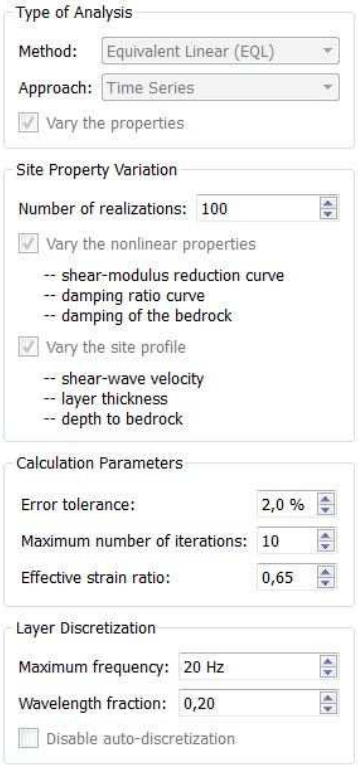

6.27. Figure: Method used for response analysis

	Name	Unit Weight (kN/m³)	G/G_max Model	Damping Model	Notes	Varied
1	Gr	22.00	Vucetic & Dobry, PI = 0	Vucetic & Dobry, PI = 0		☑
2	saGr_ grSa	21.00	Vucetic & Dobry, PI = 0	Vucetic & Dobry, PI = 0		☑
3	Sa	19.00	Vucetic & Dobry, PI = 0	Vucetic & Dobry, PI = 0		☑
4	Cl	20.00	Vucetic & Dobry, PI = 30	Vucetic & Dobry, PI = 30		☑
5	siCl	19.50	Vucetic & Dobry, PI = 15	Vucetic & Dobry, PI = 15		☑
6	saCl	20.50	Vucetic & Dobry, PI = 30	Vucetic & Dobry, PI = 30		☑
7	Alluvium_Sa (D>30m)	20.00	Vucetic & Dobry, PI = 0	Vucetic & Dobry, PI = 0		☑
8	Alluvium_grSa_saGr (D>30m)	22.00	Vucetic & Dobry, PI = 0	Vucetic & Dobry, PI = 0		☑
9	Alluvium_Cl (D>30m)	21.00	Vucetic & Dobry, PI = 30	Vucetic & Dobry, PI = 30		☑
10	Alluvium_saCl (D>30m)	21.50	Vucetic & Dobry, PI = 30	Vucetic & Dobry, PI = 30		☑
11	Alluvium_siCl (D>30m)	20.50	Vucetic & Dobry, PI = 15	Vucetic & Dobry, PI = 15		☑
12	siSa_clSa	20.00	Vucetic & Dobry, PI = 0	Vucetic & Dobry, PI = 0		☑
13	Si	19.50	Vucetic & Dobry, PI = 0	Vucetic & Dobry, PI = 0		☑
14	stiffCl	21.00	Vucetic & Dobry, PI = 30	Vucetic & Dobry, PI = 30		☑
15	Cls	23.00	Vucetic & Dobry, PI = 0	Vucetic & Dobry, PI = 0		☑
16	Ss	25.00	Vucetic & Dobry, PI = 0	Vucetic & Dobry, PI = 0		☑

6.28. Figure: Applied soil properties for examination of SP I to XV in Győr

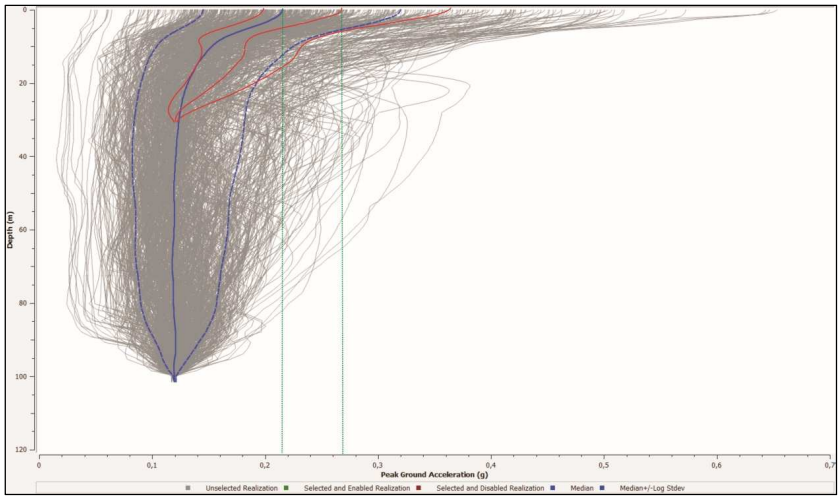

6.29. Figure: Peak ground acceleration [g] profile versus depth [m]

Different total depths were examined to decide the depth used for response analysis in case of Győr. Figure 6. 29 presents the differences between total depth of 30 m (red line), 100 m and 200 m (purple line). It is obvious that results of the analysis considering only the upper 30 m is not appropriate for the purposes of the research. The results of the examinations considering 100 or 200 m total depth match adequately. The depth of most of the examined borings ranges between 100 and 200 m (Table 5.1), and only 13 exceeds 200 m, so the total depth of the examinations were set to 100 m.

File Edit Tools Window Help

General Settings | Soil Types | Soil Profile | Motion(s) | Output Specification | Compute | Results

Site Profile

	Depth (m)	Thickness (m)	Soil Type	Vs (m/s)	Minimum (m/s)	Maximum (m/s)	Varied
1	0.00	1.50	saCl	205.00	☑ 185.00	☑ 225.00	☑
2	1.50	2.00	saGr_ grSa	180.00	☑ 155.00	☑ 205.00	☑
3	3.50	1.50	Sa	190.00	☑ 170.00	☑ 210.00	☑
4	5.00	1.50	Sa	250.00	☑ 235.00	☑ 275.00	☑
5	6.50	3.50	siCl	265.00	☑ 250.00	☑ 280.00	☑
6	10.00	2.50	siCl	300.00	☑ 280.00	☑ 320.00	☑
7	12.50	1.50	Sa	330.00	☑ 310.00	☑ 350.00	☑
8	14.00	1.00	saCl	350.00	☑ 340.00	☑ 360.00	☑
9	15.00	5.00	saCl	380.00	☑ 370.00	☑ 390.00	☑
10	20.00	5.00	saCl	400.00	☑ 390.00	☑ 410.00	☑
11	25.00	5.00	saCl	415.00	☑ 405.00	☑ 425.00	☑
12	30.00	15.00	Alluvium_saCl (D>30m)	455.00	☐ 0.00	☐ 0.00	☑
13	45.00	5.00	Alluvium_Sa (D>30m)	430.00	☐ 0.00	☐ 0.00	☑
14	50.00	5.00	Alluvium_saCl (D>30m)	495.00	☐ 0.00	☐ 0.00	☑
15	55.00	20.00	Alluvium_Sa (D>30m)	460.00	☐ 0.00	☐ 0.00	☑
16	75.00	25.00	Alluvium_Cl (D>30m)	390.00	☐ 0.00	☐ 0.00	☑
17	100.00	Half-Space	Bedrock	800.00	☐ 0.00	☐ 0.00	☑

6.30. Figure: One of the site profiles in Győr

Values of v_s were set according to Table 6.9 in the upper 30 m, below that the predictive equations were used from Table 6.7. Figure 6.30 represents one of the site profiles in Győr.

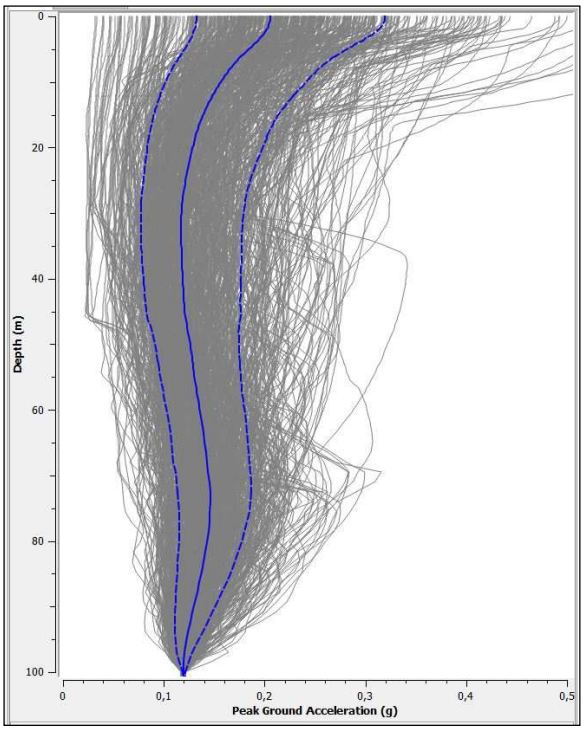

6.31. Figure: Peak ground acceleration profile

Peak ground acceleration profile results obtained from site response analysis can be seen on Figure 6.31. Spectral acceleration and transfer functions were plotted for each soil profile. (Plotted PGA, S_a and transfer functions for each soil profiles can be found in Annex.)

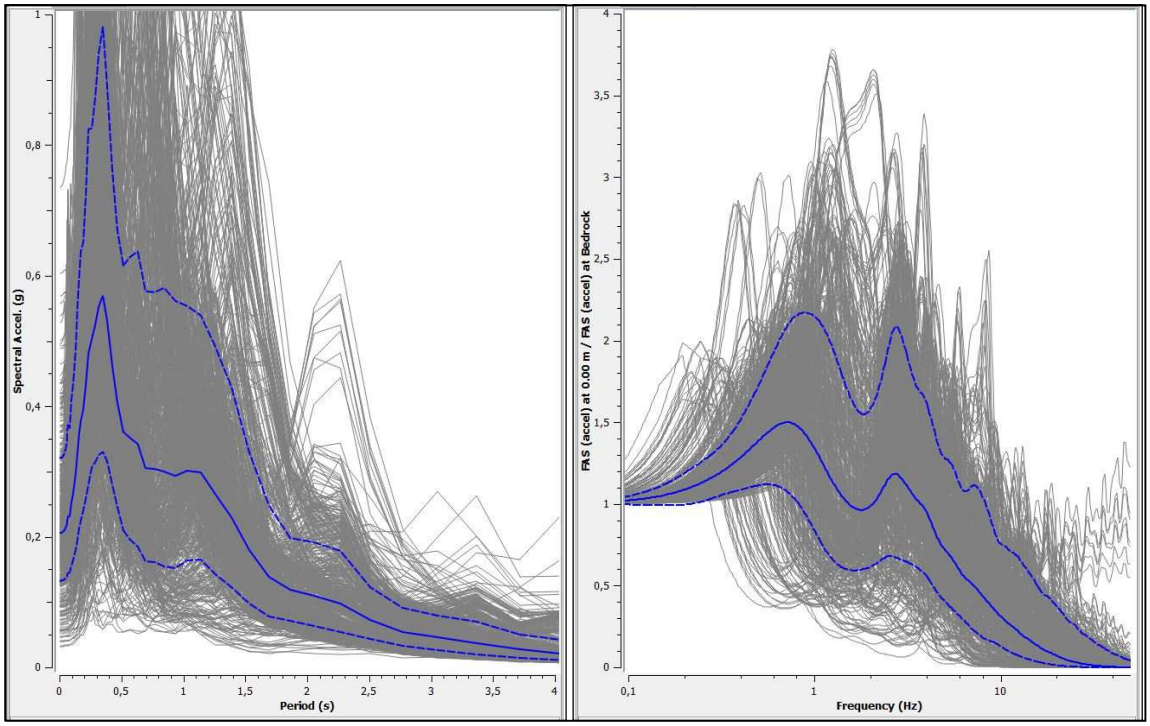

6.32. Figure: Spectral acceleration and transfer function

DOI: 10.15477/SZE.MMTDI.2015.002

Soil amplification was estimated for 15 soil profiles based on response analysis. Table 6.12 contains the amplification values and the dominant first and second frequencies of the transfer functions for each soil profile for the return period of 475 years.

6.12 Table: PGA median values and standard deviation, and amplification factors

Soil profile	PGA [0.12 g]		Amplification	Data from median values of transfer function					
	Median	Log Stdev	m	m_1	f_1 [Hz]	T_1 [s]	m_2	f_2 [Hz]	T_2 [s]
I.	0.192	0.447	1.601	1.570	0.652	1.533	1.219	2.262	0.442
II.	0.214	0.374	1.782	1.937	0.767	1.304			
III.	0.234	0.413	1.949	1.714	0.915	1.093			
IV.	0.199	0.363	1.660	1.806	0.727	1.376			
V.	0.206	0.440	1.715	1.499	0.717	1.395			
VI.	0.197	0.462	1.642	1.610	0.644	1.554	1.201	1.976	0.506
VII.	0.216	0.492	1.797	1.591	0.843	1.186			
VIII.	0.212	0.437	1.768	1.680	0.757	1.321			
IX.	0.210	0.419	1.754	1.599	0.788	1.269	1.286	2.356	0.424
X.	0.191	0.405	1.595	1.729	0.727	1.376	1.207	2.003	0.499
XI.	0.197	0.378	1.639	1.711	0.727	1.376	1.277	2.030	0.493
XII.	0.211	0.457	1.761	1.618	0.799	1.252			
XIII.	0.322	0.452	2.680	1.879	1.231	0.812			
XIV.	0.296	0.416	2.471	1.660	1.019	0.981	1.294	3.129	0.320
XV.	0.243	0.535	2.029	1.433	0.832	1.202	0.906	4.758	0.210

Table 6.13 compares the amplification factors for different earthquake intensities.

6.13. Table: amplification factors for different earthquake intensities and return periods

Soil profile	Amplification		
	PGA [0.09 g]	PGA [0.12 g]	PGA [0.21 g]
	225 years return period	475 years return period	2475 years return period
I.	1.811	1.601	1.244
II.	2.064	1.782	1.674
III.	2.192	1.949	1.605
IV.	1.883	1.660	1.411
V.	2.172	1.715	1.500
VI.	1.862	1.642	1.158
VII.	2.146	1.797	1.552
VIII.	1.880	1.768	1.473
IX.	1.967	1.754	1.466
X.	1.765	1.595	1.311
XI.	1.758	1.639	1.255
XII.	1.803	1.761	1.533
XIII.	2.904	2.680	2.162
XIV.	2.894	2.471	2.191
XV.	2.153	2.029	1.603

DOI: 10.15477/SZE.MMTDI.2015.002

6.3.5. Hazard compared to Eurocode 8 response spectra

The site response analysis determines the main frequencies and amplification that the surface of the ground will experience. Site response analysis was performed based on a one dimensional analysis of STRATA software, with an earthquake input motion introduced at bedrock and the waves travelled vertically up through the soil column. Acceleration time histories were generated with help of REXEL software, compatible to Eurocode Type 1 and 2 spectra (T1 and T2). Seven different acceleration time histories for site response analyses were used in case of each soil profile with 100 realizations, varying the soil properties, taking into account different scenarios for different return periods: 225, 475 and 2475 years.

Figure 6.33 shows the median values and the logarithmic standard deviation of the spectral acceleration for different bins of earthquakes in case of one of the previously-defined soil profiles in Section 6.2.9. On the Figure 6.33 a) the return period is the same for both median values (475 years), but one represents the median values generated from the bin of earthquakes fitting T2 spectra, and the line shifted to the right represents the median values generated from the bin of earthquakes fitting T2 spectra. These median lines are very close to each other in case of every soil profiles, the two lines almost overlap each other, only a little shift to the right can be observed in case of spectral acceleration calculated based on T1 compatible earthquake bin.

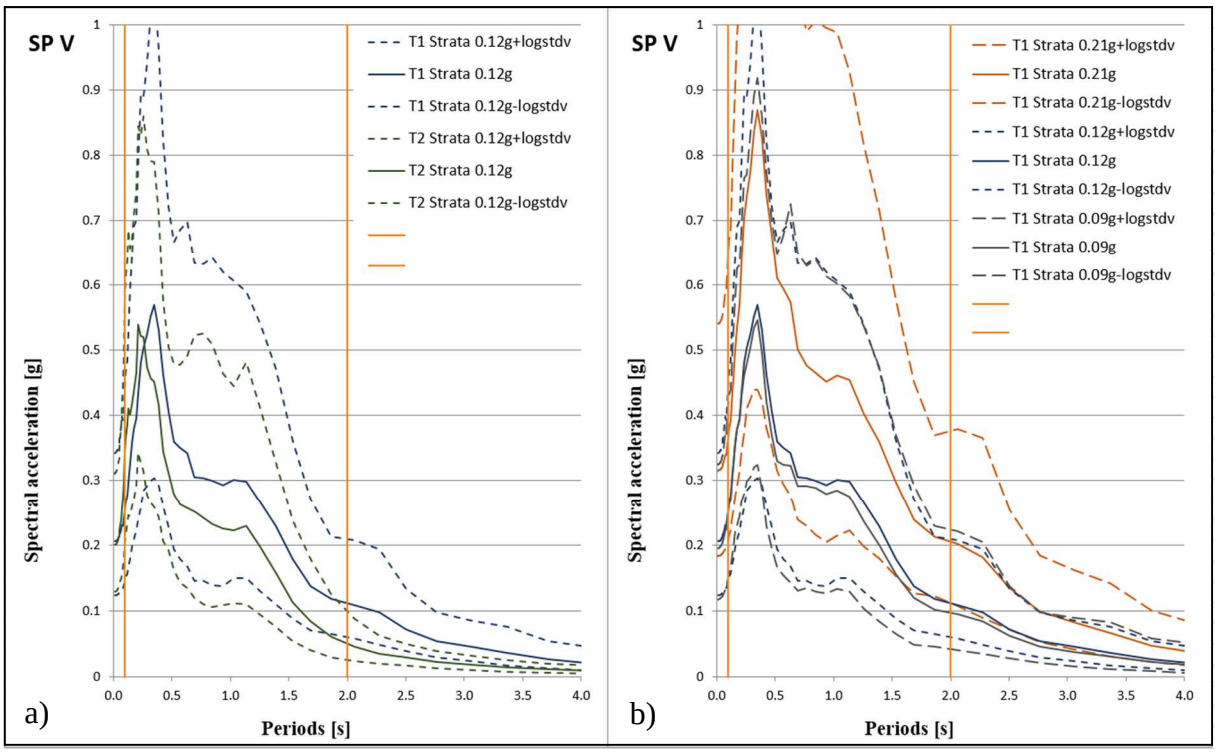

6.33. Figure: Spectral acceleration results for one soil profile

Results of acceleration spectra for different return periods can be seen for soil class C on the Figure 6.33 b). In the case of 225 years return period the median values of the

acceleration spectra are almost as high as the median values of the acceleration spectra obtained for 475 years return period. The local deposits amplify more the outcrop acceleration resulting from minor earthquakes, than in case of higher intensities. Buildings should be controlled in case of Limit State of Damage Limitation assuming 225 years return period, corresponding to a probability of exceedance of 20% in 50 years according to Eurocode 8. That means that these buildings should remain in operational state, but they were designed against seismic loads assuming 475 years return period referred to Limit State of Significant Damage.

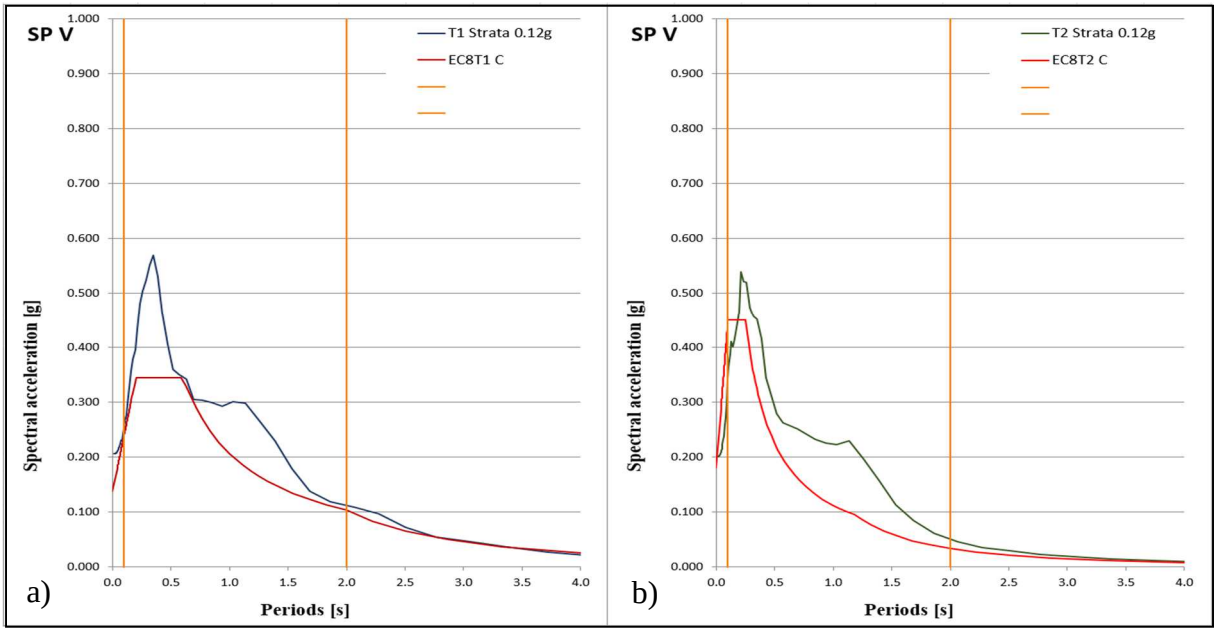

6.34. Figure: Spectral acceleration results compared to acceleration spectra of EC8

On Figure 6.34 a) and b) are presented the compared results of the median values of spectral acceleration obtained from the bin of earthquakes fitting code-based T1 and T2 spectra respectively. The code-spectra do not cover the expected values of the acceleration spectra obtained from one dimensional site response analysis. The peak values are much higher than the plateau of the two code spectra, even considering acceptable risk, especially in the first case. Buildings with frequency range between 1.33 Hz and 0.8 Hz (period between 0.75-1.25 s) designed due to EC8 in Győr might be designed underestimating the actual earthquake forces. This second "bump" on each diagram should be considered to be a result of the second dominant frequency shown on transfer functions (Figure 6.32) specific to almost all soil profiles in Győr.

Spectral acceleration is different for buildings with different importance factors. Buildings are classified in 4 importance classes, depending on the consequences of collapse for human life, on their importance, and on the social and economic consequences of collapse.

During the analysis of local site effects the results were compared to different levels of safety due to importance classes and importance factors given in Table 6.13 according to EC8.

6.14. Table: Importance classes for buildings according to EC8 *(European Committee for Standardization, 2013)*

Importance class	Buildings
I	Buildings of minor importance for public safety, e.g. agricultural buildings, etc.
II	Ordinary buildings, not belonging in the other categories.
III	Buildings whose seismic resistance is of importance in view of the consequences associated with a collapse, e.g. schools, assembly halls, cultural institutions etc.
IV	Buildings whose integrity during earthquakes is of vital importance for civil protection, e.g. hospitals, fire stations, power plants, etc.

During the analysis of local site effects the results were compared to different levels of safety due to importance classes and importance factors given in Table 6.13 according to EC8. Different level of safety represented with different response spectra taking into account importance factor II, III and IV respectively, can be seen on the Figure 6.35 a). The figure shows that not even the buildings with highest importance factor (1.4) meet the expected median values (without importance factor) of spectral acceleration specific to the site. The plots shown here and corresponding plots in the appendix point out the importance of understanding local site response. Effects of layered soils that do not conform to code profiles can produce significant amplification of seismic actions that are not accounted for in the code. Logarithmic standard deviation on Figure 6.33 a) highlights that the variability of actions is very large for even fairly simple soil profiles and "typical" earthquake records. It is for these two observations that the engineer should be cautious in selecting a single number for PHA and applying it blindly to every analysis.

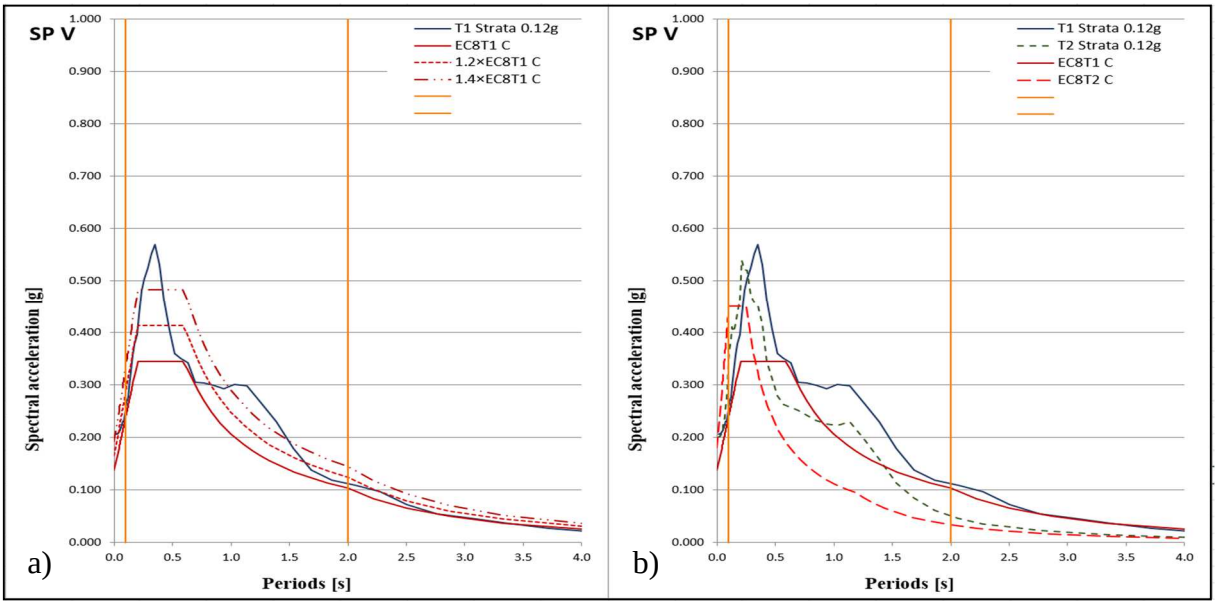

6.35. Figure: Spectral acceleration results compared to different acceleration spectra of EC8

DOI: 10.15477/SZE.MMTDI.2015.002

Chapter 7. Vulnerability of buildings in Győr

Győr has a large number of masonry and reinforced concrete buildings. They range in age from less than 5 years to over 100 years. Some of the older ones have been renovated and rebuilt several times, meaning that parts of the building may be new while other parts are still quite old. Many of the buildings would be impossible to analyze quickly by typical structural engineering software and methods; the buildings are too irregular and have such a wide variety of material properties, that an expert would be needed to fully understand the heterogeneous mix of components. Because of this, and due to limitations in computational resources, personnel and time, alternate methods of evaluating building vulnerability are appropriate. This also true in a zone of moderate seismicity where static overdesign in the past may provide enough stability for low to moderate shaking of low and smaller buildings. This chapter will examine methods to evaluate building vulnerability by visual screening and pushover methods. Both of these approaches have many variations, and this study examines only a few.

7.1. Visual screening method

Visual classification worked out by researchers and agencies (Grünthal ed., 1998) (Vaseva, 2002) is largely based on inspections of structural systems, possibly the time of construction and the proximity to earthquakes. This study attempts to develop a more precise method, which takes more factors into consideration such as the regularity in the layout, the direction of earthquake wave propagation to the building, etc.

Evaluation of building response requires characteristic material properties and loading without the application of partial factors. Since the goal is to estimate performance, dimensions, and properties should reflect actual conditions. A simplified model often neglects some of the positive influence of structural elements because they may only be present in some buildings and not others of the same classification. A total of 26 screened zones were examined more deeply. The zones differ from each other not only in location, but also in types of building and their age. Building data were gathered with the help of a questionnaire and the screening evaluation of trained staff. The checklist consists of questions about:

- General data of each building (age and function of the buildings, regularity in plan and elevation, position of the building, changes in function, previous damages, etc.);
- Structural data of each building (construction system, quality of materials, workmanship);
- Other specific items to check are listed in the Checklist of Building Data (Annex).

7.1.1. Methods of classifications

For each type of data that must be collected, a classification system has to be defined. It is an essential step in a risk analysis to ensure a uniform interpretation of data and results. Dealing with vulnerability models, the classification system should group together structures that would be expected to behave similarly during a seismic event. Usually, buildings have been grouped in terms of vulnerability classes when used with observed vulnerability models applying macroseismic scales (e.g. MSK).

The need for a deeper diversification of building behaviors has led to more elaborate classification systems, where consideration is given to primary parameters affecting building damage and loss characteristics such as the basic structural system, the seismic design criteria (code level) the building height (low-rise, midrise, high-rise) as well as non-structural elements affecting non-structural damage. From the general classification, subcategories can be eventually recognized, if more detailed or a regionalized classification is required. Further refinement of visual screening can correlate estimated performance to a level of shaking. EMS (Grünthal ed., 1998) and FEMA (FEMA, 2002) classifications systems were the base of this research.

For masonry constructions EMS classification considers seven typologies, various materials, techniques of installation and construction particulars. FEMA 155 classifies masonry structures according to reinforcement only. The detailed EMS classification was not needed in this research because the masonry buildings in Győr would fall into the category unreinforced masonry either wooden or reinforced concrete floors of EMS.

For reinforced concrete, EMS differentiates the construction only in relation to the seismic resistant system (frame or shear wall), but FEMA also determines one more category for RC: concrete frame with unreinforced masonry infill, which is typical to this region as well. For construction in steel or in wood, only one category is considered in EMS and does not make reference to prefabricated constructions. These differences favored the use of FEMA 155 for this research tailored to the most-used building construction of the area and creating a checklist.

7.1.1. Classification procedure of investigated area

The previously presented checklist (Section 5.2.1) was created based on literature concerning inventories for score assignment, and the knowledge about the most-used building construction of the area. The classification of more than 5000 buildings was performed based on the main construction structure and material and the city district where they were built. (Fig. 7.1). It can be clearly seen that loadbearing masonry represents the largest structural group.

DOI: 10.15477/SZE.MMTDI.2015.002

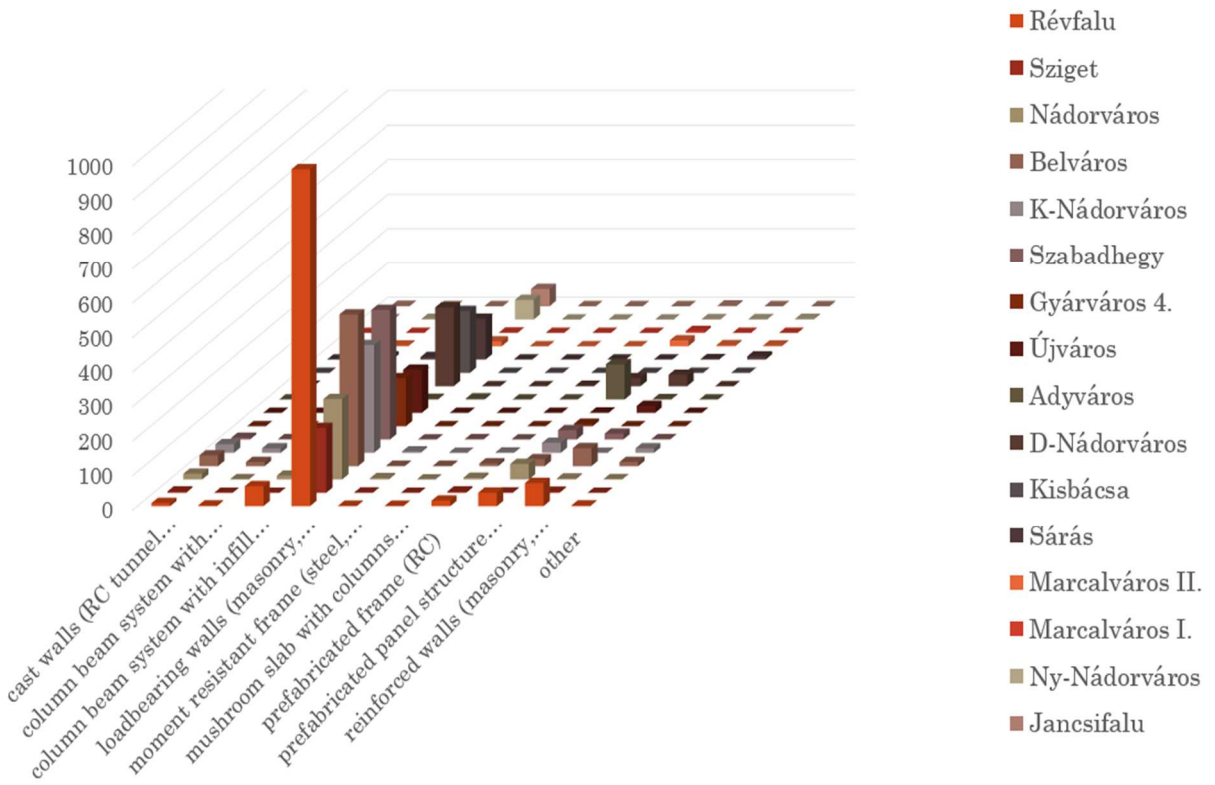

7.1. Figure: Number and type of structures in different districts of the town

Figure 7.2 shows the number of loadbearing structures compared to other building structures in different city districts.

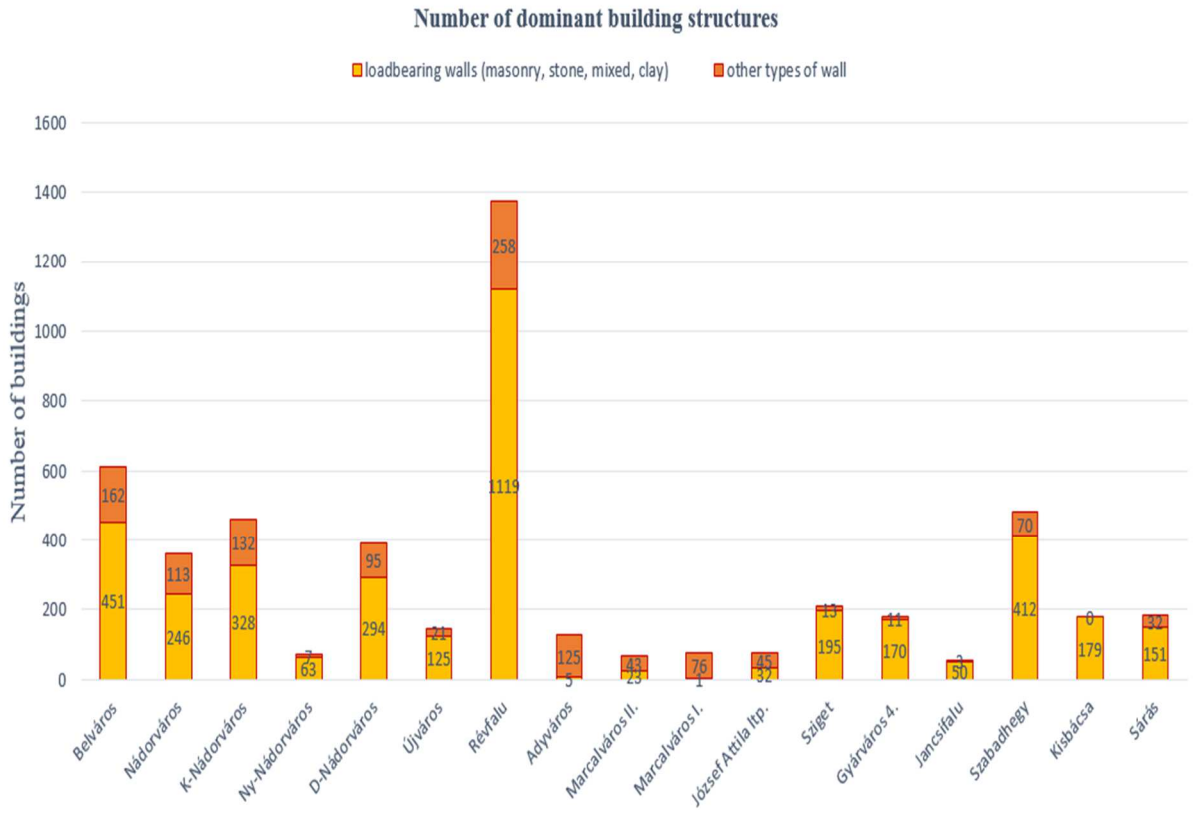

7.2. Figure: Number of loadbearing wall structures compared to other structures

DOI: 10.15477/SZE.MMTDI.2015.002

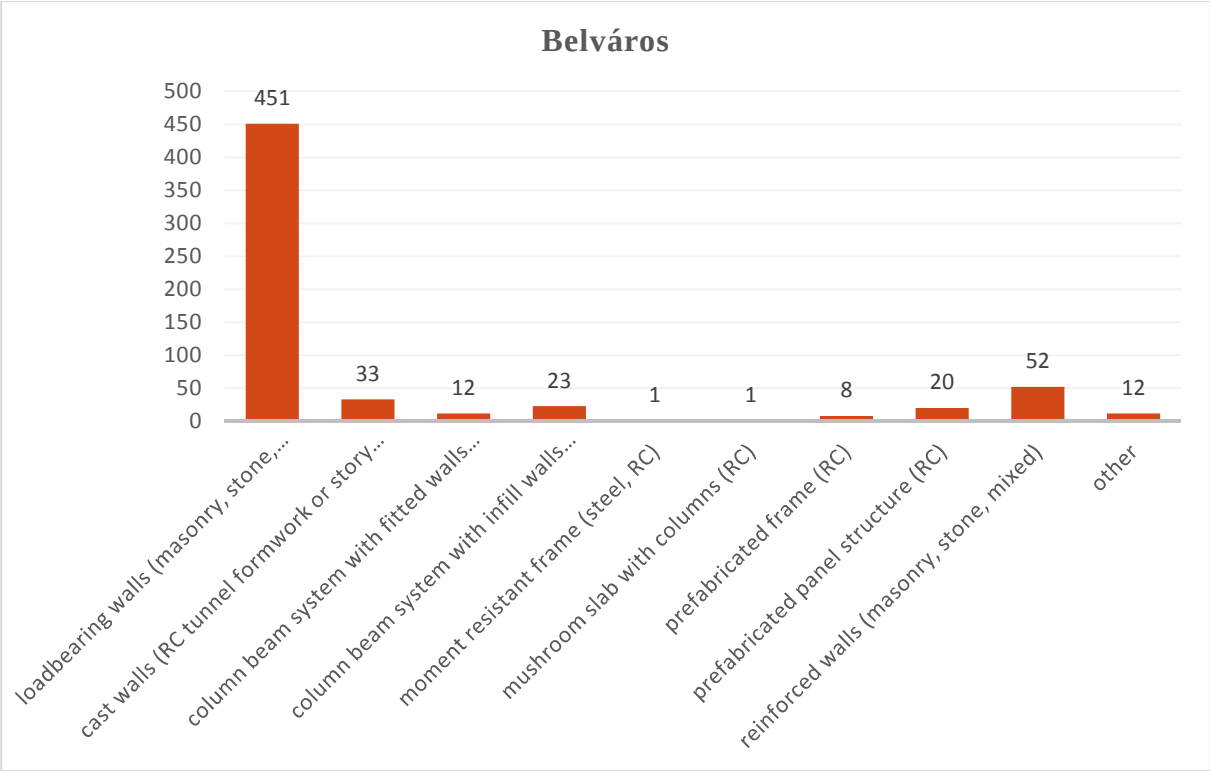

7.3. Figure: Number of building structures in Downtown

3367 building data were collected in four city districts: Belváros (Downtown), Adyváros, Nádorváros and Révfalu. These districts were inspected so that more than 95% of the buildings were recorded on the checklists. Structural distribution and later score assignment have been performed in these city parts as a model for analysis. (Fig. 7.3, 7.4 and Annex)

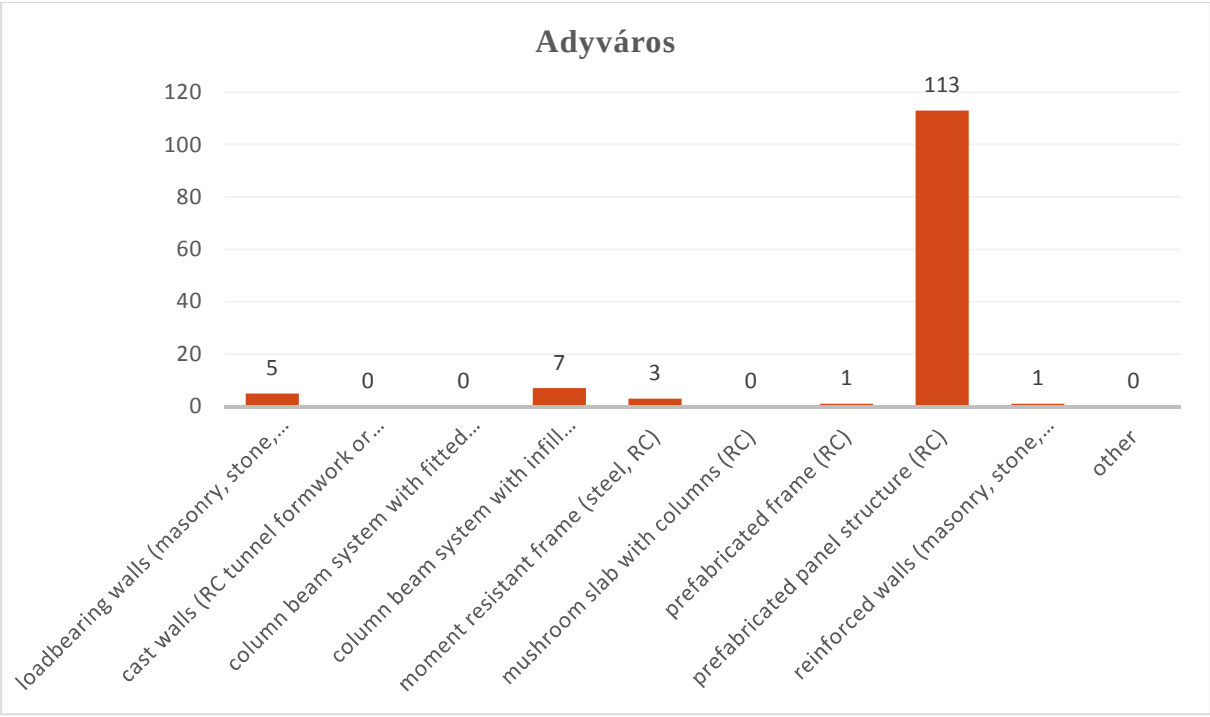

7.4. Figure: Number of building structures in Adyváros

7.1.2. Method of score assignment

For every category, a different score is given (Table 7.1). There may be several questions or items to check in a category, but it usually works on a demerit basis. That is, a score is lowered for having poor seismic resistance features. If a structure scores below a threshold, further evaluation may be required. If the evaluation is during an emergency, occupancy may be restricted or forbidden or the structure torn down. As a pre-earthquake assessment tool, the score assignment may be used to evaluate the relative vulnerability of structures in the same vicinity.

7.1 Table: Visual Checklist of Specific Building Features

Item To Visually Check	Comments on Evaluation
Lateral load path	The structure contains a complete load path for seismic force effects from any horizontal direction that serves to transfer inertial forces from the building to the foundation.
Building configuration	The building is regular with regards to the plan and the elevation.
Roof construction	The roof diaphragm is considered to be rigid and it is expected that the roof structure will maintain its integrity, i.e. shape and form, during an earthquake of intensity expected in this area.
Floor construction	The floor diaphragm(s) are considered to be rigid and it is expected that the floor structure(s) will maintain its integrity, during an earthquake of intensity expected in this area.
Foundation performance	There is no evidence of excessive foundation movement (e.g. settlement) that would affect the integrity or performance of the structure in an earthquake.
Wall proportions	Height-to-thickness ratio of the shear walls at each floor level is: 1) Less than 25 (concrete walls); 2) Less than 30 (reinforced masonry walls); 3) Less than 13 (unreinforced masonry walls).
Foundation- wall connection	Vertical load-bearing elements (columns, walls) are attached to or concrete columns and walls are doweled into the foundation.
Wall-roof connections	Exterior walls are anchored for out-of-plane seismic effects at each diaphragm level with metal anchors or straps.
Wall openings	The total width of door and window openings in a wall is: 1) for brick masonry construction in cement mortar: less than 1/2 of the distance between the adjacent cross walls; 2) for adobe masonry, stone masonry and brick masonry in mud mortar: less than 1/3 of the distance between the adjacent cross walls; 3) for precast concrete wall structures: less than 3/4 of the length of a perimeter wall.

Quality of building materials	Quality of building materials is considered to be adequate per requirements of national codes and standards (an estimate).
Quality of workmanship	Quality of workmanship is considered to be good (per local construction standards).
Maintenance	Buildings of this type are generally well maintained and there are no visible signs of deterioration of building elements (concrete, steel, timber).

Other features may influence building vulnerability or skew the assessment process. Usually, modernizations of apartments have been introduced. In the case where the ground floor is used for a commercial purpose, the ground floor windows are often enlarged and interior walls are replaced by columns of steel or reinforced concrete.

With regard to the design level, the EMS distinguishes three different Earthquake Resistant Design (ERD) levels referring to different amount of design lateral load usually prescribed by the codes of different European regions, depending on the seismicity. On the other hand, FEMA distinguished four code levels accounting not only for the increase in the horizontal design load, but also for the advancements in aseismic codes providing ductility, drift and deformation capacity to designed buildings: pre-code, low-code, medium-code and high-code. What appears to be relevant in FEMA classification system is the subdivision by class of height: three classes are distinguished depending on the number of floors.

7.1.3. Score assignment of investigated area

Four districts were examined more closely. The zones differ from each other not only in location, but also in types and ages of buildings. Data from cca. 3367 building were analysed, and buildings are classified based on these results. For each building class, a vulnerability function is assigned. The following figures give an overview about the analysed building-stock.

For each building a base score was determined due to structure based on FEMA 155. Score modifiers were taken into account, such as:

- vertical irregularity score modifier,
- construction code score modifier,
- score modifier concerning the height of the building,
- and soil score modifier.

The construction time determined the level of seismic design used at the construction of each building. Based on the height of buildings two categories were taken into account: low-rise building with no modifier and mid-rise buildings. Vertical irregularity was based on the questionnaire.

DOI: 10.15477/SZE.MMTDI.2015.002

Two sets of histograms represent first the score of the buildings (with code, height and irregularity modifier) (Fig. 7.5) and secondly the score with the soil modifier (Fig. 7.6) differentiating the most dominant building types.

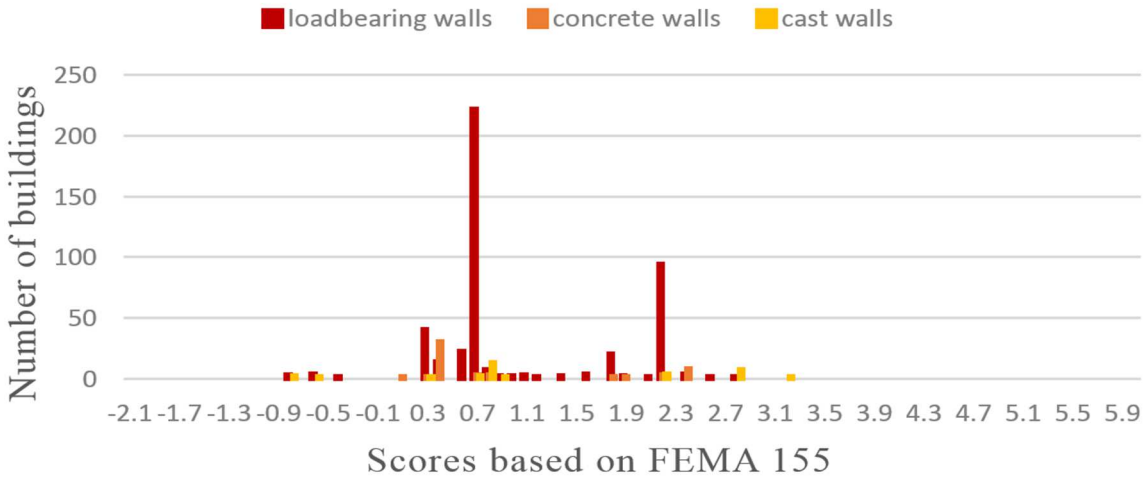

7.5. Figure: Scores of the buildings with soil modifier in Belváros

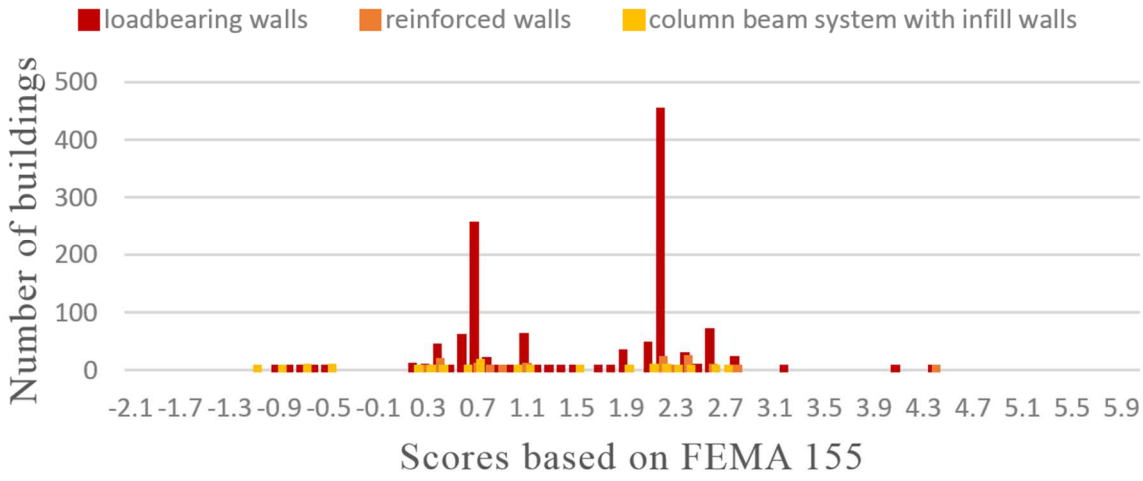

7.6. Figure: Scores of the buildings with soil modifier in Révfalu

Masonry buildings dominate the final scores of the districts with two peaks: the lower score for the irregular buildings and higher for regular buildings. Lower scores represent higher risk for the. Figure 7.2 presents the average scores and standard deviation of the examined for city districts and the score of the most typical building for the same district offering an estimate for the districts.

7.1. Table: Average score of city districts

	Belváros	Révfalu
Average score	1.85	2.42
St. deviation	1.04	1.6
Score of typical building	0.7	2.1

DOI: 10.15477/SZE.MMTDI.2015.002

7.2. Pushover method

The method for determination of vulnerability functions is a non-linear static analysis using a simple model with the bilinear approximation of the capacity curve, assuming first mode force distribution and linear first mode shape thus linear strength distribution. From the curve of the seismic demand and the shear capacity of the building, the vulnerability function of the building can be obtained. These vulnerability functions should be derived for typical layouts, offering a family of curves allowing the experts to decide the vulnerability category of a specific building on-site based on visual screening.

7.2.1. Pushover Method of Analysis

Pushover analysis has become more popular due to several shortcomings with conventional linear elastic or equivalent linear (with reduction in stiffness) analysis. In a typical elastic analysis, material and component behavior is considered linear with easily applied stiffness reduction factors or penalty methods to imitate loss of stiffness and strength in the structure. The idea is straightforward, but suffers from several shortcomings. (Papanikolaou, et al., 2005)

- The force reduction factors recommended in codes of practice are derived for general cases and must be approximate. They will not represent the specific structure under consideration.
- Inelastic behavior occurs in very specific zones of the structure. Therefore when some zones become inelastic, forces and deformations redistribute themselves to a significantly different pattern. Global or general reductions cannot represent these changes.
- Collapse or ultimate limit states are almost never predicted by elastic actions. This should especially be true for properly designed structures that have more than one system of energy absorption and can sustain local failure in several places.
- Global and local inelastic deformations will distribute themselves differently than if they were purely elastic. Of course the magnitudes of deformation may also be quite different as well.

All this has led to an increased dependence on inelastic incremental analysis. To better appreciate the trade-off between a static pushover and fully nonlinear dynamic analysis, one must consider the differences and similarities. They both use the same material constitutive relationships, some adjustment between viscous damping (time dependent) and hysteretic damping (essentially no time dependence) may be necessary.

This is a small difference since most high amplitude damping is hysteretic and viscous damping may be (partially) hysteretic as well. Introducing damping as viscous is often only due to modeling convenience. Static analysis requires no unloading/reloading definition. Static and dynamic analyses require equilibrium and geometric compatibility, with dynamic equilibrium requiring inertia and damping forces as well. Numerical models for both approaches require iteration with static methods perhaps more computationally stable. Finally, the differences that may impact computational effort and resources can be summarized as

1. Static monotonic analysis requires only (simpler) monotonic constitutive models.
2. Dynamic analysis requires treatment of structural damping and mass distribution.
3. Static analysis to collapse computational cycles will equal the number of stages desired of deformation to collapse divided by the displacement increment necessary for convergence of each stage; this is likely to be in the tens of steps.
4. Dynamic analysis is an equilibrium analysis repeated as many times as the duration of the earthquake divided by the time step for response history analysis; this is likely to be in the thousands of time increments.

Due to the relative ease of computation, pushover has become more used by industry, and it has been included as an accepted inelastic method in assessment guidance documents (e.g. FEMA 273/274 and sequels) as well as Eurocode 8.

7.2.2. Conventional pushover analysis formulation

Conventional pushover analysis is the nonlinear incremental-iterative solution of the equilibrium equation $\mathbf{KU} = \mathbf{P}$ in a finite element analysis, matrix structural analysis, or simplified formulation. $\mathbf{K}$ is the nonlinear stiffness matrix, $\mathbf{U}$ is the displacement vector and $\mathbf{P}$ is a predefined load vector applied laterally over the height of the structure in relatively small increments (Papanikolaou, et al., 2005).

This lateral load can be a set of forces or displacements that have a necessarily constant ratio throughout the analysis (fixed pattern). At the end of each iteration, the reaction vector ($\mathbf{P_e}$) of the structure is calculated from the assemblage of all finite element contributions. The out-of-balance forces are iteratively re-applied until convergence to a specified tolerance is reached:

$$\Delta\mathbf{U} = [\mathbf{K}_T]^{-1} \cdot (\lambda \cdot \mathbf{P}_0 - \mathbf{P}^e) \tag{7.1}$$

where :

$\Delta\mathbf{U}$ is the calculated displacement increment within an iteration;

$\mathbf{K}_T$ is the current nonlinear (tangent) stiffness matrix;

λ is the load factor within the corresponding load increment;

$\mathbf{P}_0$ is the initial load;

$\mathbf{P}^e$ is the equilibrated load (reaction) of the previous iteration.

Work in the literature, with very few exceptions, has focused on developing pushover techniques without assessing their performance comprehensively. This would require application of static pushover to a wide range of structures, ranging from low to high rise, from regular to highly irregular, subjected to a large number of earthquake records covering a wide range of magnitudes, distance, site condition and source mechanism. Due to the requirements for an exhaustive set of analyses to cover all possible scenarios for this study, applying full, comprehensive pushover analyses to determine vulnerability functions of all building stock was considered to be beyond the resources of this study. Future research in this area for typical buildings in Győr (and Hungary) would certainly be a worthy effort.

In order to demonstrate the concepts of pushover and vulnerability, the following sections demonstrate these calculations by more simplified methods.

7.2.3. Pushover in Masonry and Reinforced Concrete Structures

All structural elements, which contribute to the loadbearing capacity of the building should be taken into account. This means that walls thicker than 12 cm are considered. The non-structural elements add to the weight only. The walls are joined by floors and spandrels, these elements transfer horizontal forces.

The equivalent horizontal earthquake forces act at the floor levels, where the mass is the highest. The vertical forces imply self-weight of all elements and live loads.

The piers transfer all forces to the ground, this way it is the most critical part of the building. The height of the piers is equal to the height of the adjacent opening. Early cracking of the spandrels reduces the stiffness of the spandrels.

As the walls are joined by spandrels a coupling effect will take place. It depends on the extent of spandrels. The frame model can be used to demonstrate the effect of coupling walls. Figure 7.7 presents three cases of bending moment distributions. In the first case, where the walls are joined only by the floors the coupling effect is negligible. In the third case the coupling is strong; the overturning moment is carried by high normal forces on the outer walls.

The extent of coupling effect can be expressed by the height of zero moment (h_0) and the value of zero moment depends on the ratio of the flexural stiffness of the spandrel to the flexural stiffness of the pier:

$$\frac{EI_{sp}}{EI_p} \cdot \frac{h_{st}}{l_0} \tag{7.2}$$

DOI: 10.15477/SZE.MMTDI.2015.002

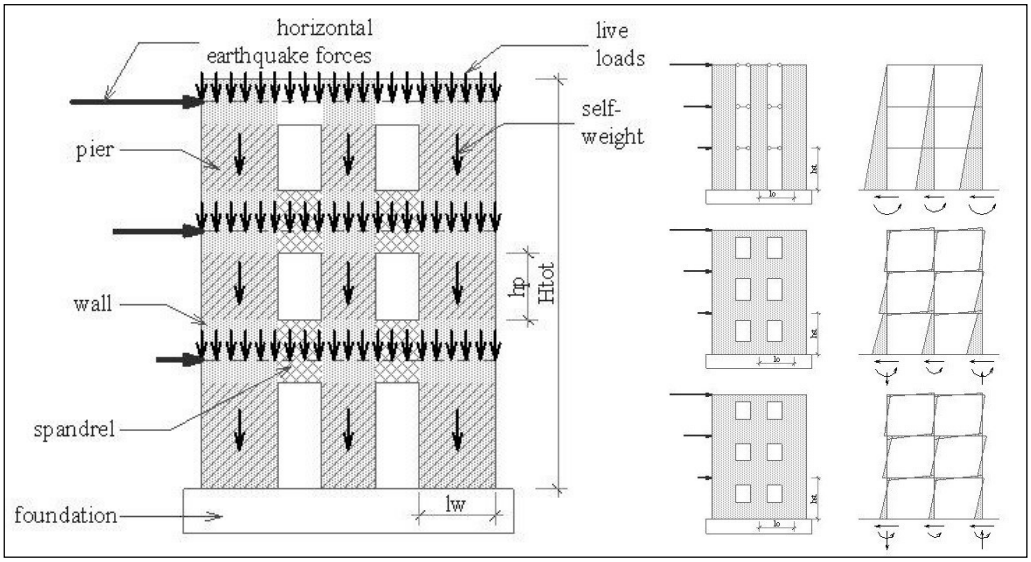

7.7. Figure: The structural model and coupling effect

With identification of potential collapse mechanisms yielding the equivalent shear capacity the vulnerability can be obtained. The critical acceleration causing the mechanism to take place can be determined depending on boundary conditions. Two types of collapse mechanisms can occur: in-plane and out-of-plane mechanisms. Calculating the equivalent shear which results in the collapse mechanism the expected damage grade can be calculated.

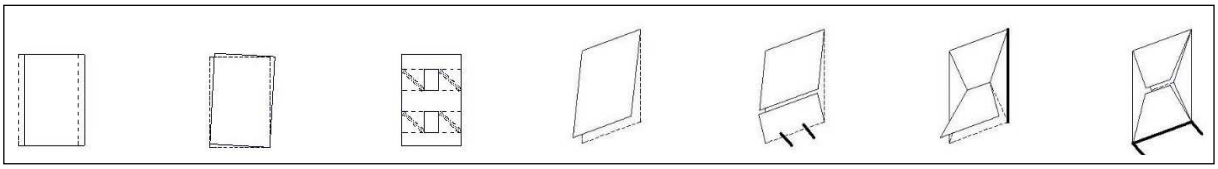

7.8. Figure: In-plane (a: sliding at joints, b: global overturning, c: crushing of the compressed edge) and out-of plane mechanism (a: the free standing wall, b: the wall with ties at the top, c: transverse walls, d: the wall with ring beam) (D'Ayala, et al., 1997)

In the region *A* due to tensile stresses normal to bed joints causes a horizontal crack resulting in sliding horizontally along the bed joints. In the region *B* the increased shear is carried by compressed masonry. Final failure occurs by the overturning of the wall and the crushing of the compressed corner. In the region *C* diagonal cracks occur due to shear failure. If the mortar is weak the crack forms in the mortar bed, if the strength of the bricks are rather low, than more regular crack forms. The two parts of the wall slide downwards on each other. The in-plane loaded wall plane can undergo three different local failures depending on the condition of biaxial stresses (Page, 1995).

The stress distribution in masonry is rather complex depending on the quality of brick and the mortar, the workmanship, the boundary conditions and the applied forces. There exist different failure criterions, the flexural failure is calculated from ultimate stress distribution, and shear failure is defined by the diagonal tension capacity by principal stresses relationship.

To obtain the shear capacity of a wall element the lower bound theorem of plasticity is used. For this a statically adequate stress field should comply with the equilibrium and material conditions. The capacity curve of a wall element can be calculated increasing the shear gradually until one of the three material conditions is violated. The base shear can be plotted as a function of top displacement.

The horizontal deformation (δ) is calculated with the principle of virtual work. A constant drift over the building height is hypothesized. The drift corresponds to the first mode shape assuming a linear distribution of the force. The drift can be calculated with the following formula:

$$\delta = \frac{d}{h_p}, \tag{7.3}$$

where h_p is the height of the pier, d is the horizontal deformation.

The displacement can be obtained as a ratio of the drift and the total height of the building:

$$\Delta = \delta \cdot H_{tot}. \tag{7.4}$$

According to the bilinear approximation the capacity curve of a wall element can be characterized by three elements: the maximum shear strength of the wall element, the nominal yield displacement (Δ_y) at the top of the wall and the ultimate displacement (Δ_u) at the top of the wall. The transition between the linear elastic and perfectly plastic region is called the yield point even if masonry structures do not yield.

$$\Delta_y = V_m \cdot H_{tot} \cdot \left(\frac{h_p \cdot (3h_0 - h_p)}{6 \cdot E \cdot I_{eff}} + \frac{\kappa}{G \cdot A_{eff}} \right) \tag{7.5}$$

$$\Delta_u = \mu_w \cdot \Delta_y \tag{7.6}$$

Full detailed calculations are presented in the appendix. Summarizing the shear capacities of the separate walls the shear capacity of the whole building can be obtained (Figure 7.9).

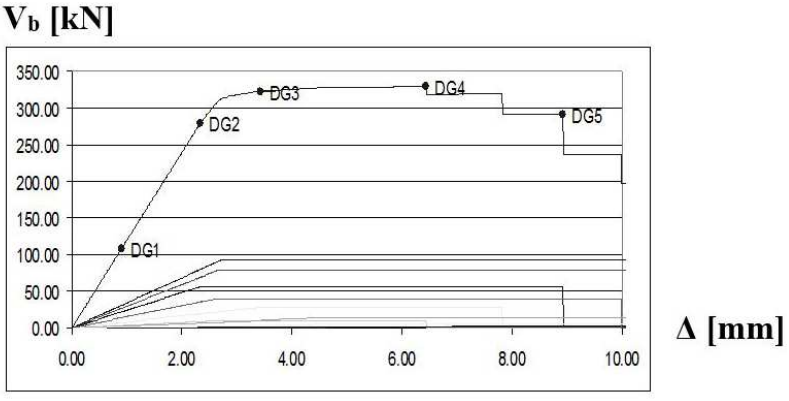

7.9. Figure: Shear capacity of the building with identification of damage grades

DOI: 10.15477/SZE.MMTDI.2015.002

The main task is to obtain the vulnerability function of the building. This requires the identification of the damage grades. In the European Macroseismic Scale (Grünthal ed., 1998) five grades are differentiated from slight damage to total destruction allowing the identification of the points were the capacity curve of the building enters the next damage grade. The damage grades given in EMS 98 are related to the displacements at the top of the building. These points are given in the next table.

7.2. Table: Damage grades according to EMS and modified by Lang *(Lang & Bachmann, 2000)*

DG	EMS 98	after Lang
1	negligible to slight damage	point of onset cracking
2	moderate damage	yield of the first wall
3	substantial to heavy damage	yield of the last wall
4	very heavy damage	failure of the first wall
5	destruction	drop of the base shear capacity below 2/3 of maximum V_{bm}

The seismic demand is determined using an elastic acceleration response spectrum. It represents the maximum response of equivalent single degree of freedom system as a function of their frequencies. The displacement demand can be calculated from the following equations:

fundamental frequency of the equivalent SDOF system

$$f = \frac{1}{2\pi} \cdot \sqrt{\frac{k_E}{m_E}} \qquad (7.7)$$

modal participation factor

$$\Gamma = \frac{\sum m_i \cdot \phi_i}{\sum m_i \cdot \phi_i^{\,2}} \qquad (7.8)$$

spectral displacement

$$\Delta = \Delta_{by} \cdot \frac{1}{2} \cdot \left(\left(\frac{k \cdot \Gamma \cdot S_d}{V_{bm}} \right) + 1 \right) \qquad (7.9)$$

displacement demand

$$S_d(f_1) = \frac{S_a(f_1)}{(2\pi \cdot f_1)^2} \qquad (7.10)$$

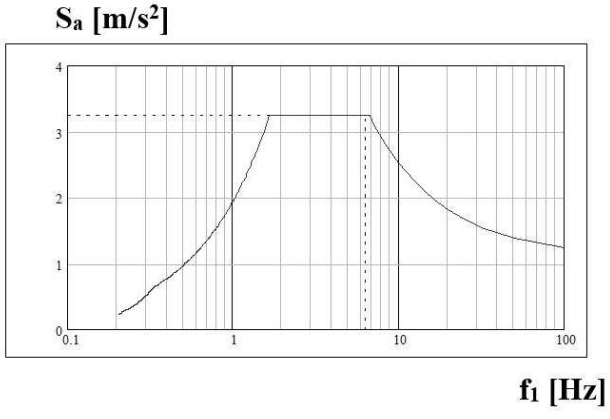

7.10. Figure: Seismic demand

DOI: 10.15477/SZE.MMTDI.2015.002

The spectral displacement should be then compared with the displacement capacity of the building.

From the figure of the shear capacity of the building and the seismic demand, the third curve about the vulnerability function can be plotted. Varying the intensity of seismic demand for every case the displacement of the building can be plotted. With increasing displacement demand the top displacement of the building increases as well. Plotting the damage grades on the figure will provide the vulnerability function of the building shown in Figure 7.11.

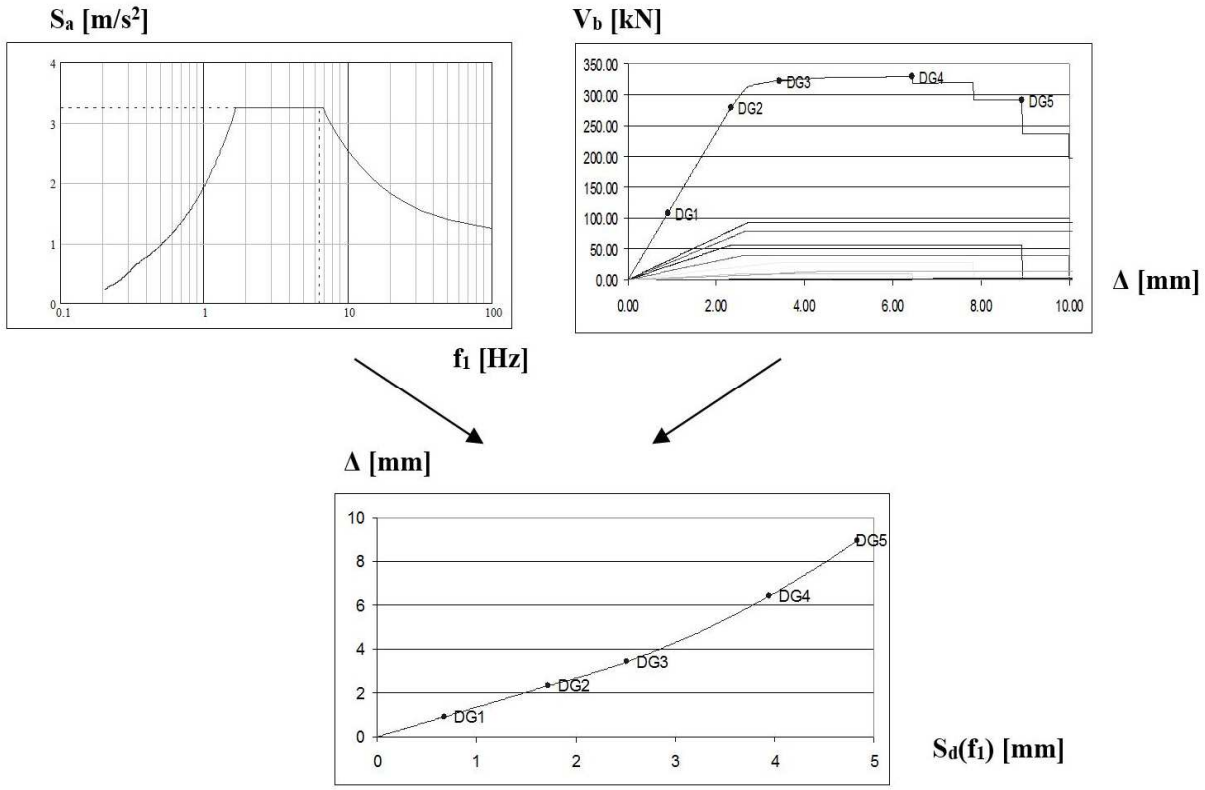

7.11. Figure: Obtaining vulnerability functions

Based on the known PGA value the top displacement of the building can be determined. From the vulnerability function it can be read the level of damage the building would suffer in case of seismic event.

Vulnerability functions were determined for typical layouts in case of masonry and reinforced concrete buildings. The steps of the pushover analysis have the same order in case of both masonry and reinforced concrete building taking into account building material features respectively. With the given value of possible PGA the expectable damage can be estimated.

DOI: 10.15477/SZE.MMTDI.2015.002

Chapter 8. Seismic risk

This research assessed the seismic risk based on local site affects and building vulnerability, scoring those factors contributing strongly to the physical damages of buildings. Local soil effects were evaluated based on 6000 realizations of response analysis and presented in Chapter 6. Vulnerability of buildings were investigated according to FEMA 155 taking into account a building inventory with more than 5000 buildings presented in Chapter 7. Level of seismic risk can be determined overlapping the two sets of data.

8.1. Microzonation of Győr based on local soil effect (Ch. 6)

One alternative to determine the effects of soil layers is to use the values of $v_{s,30}$, the equivalent shear wave velocity that is the weighted average of shear wave velocities in the upper 30 meters. Based on shear wave profiles 15 zones were determined in Győr. The basic intention in assessing the ground shaking intensity is to estimate the effects of local site conditions. This decision should be made on all the available results from site identifications from average of shear wave velocity to results of site response analysis. The main objective is to estimate more accurately the ground motion characteristics during possible earthquakes taking into account all the main controlling factors.

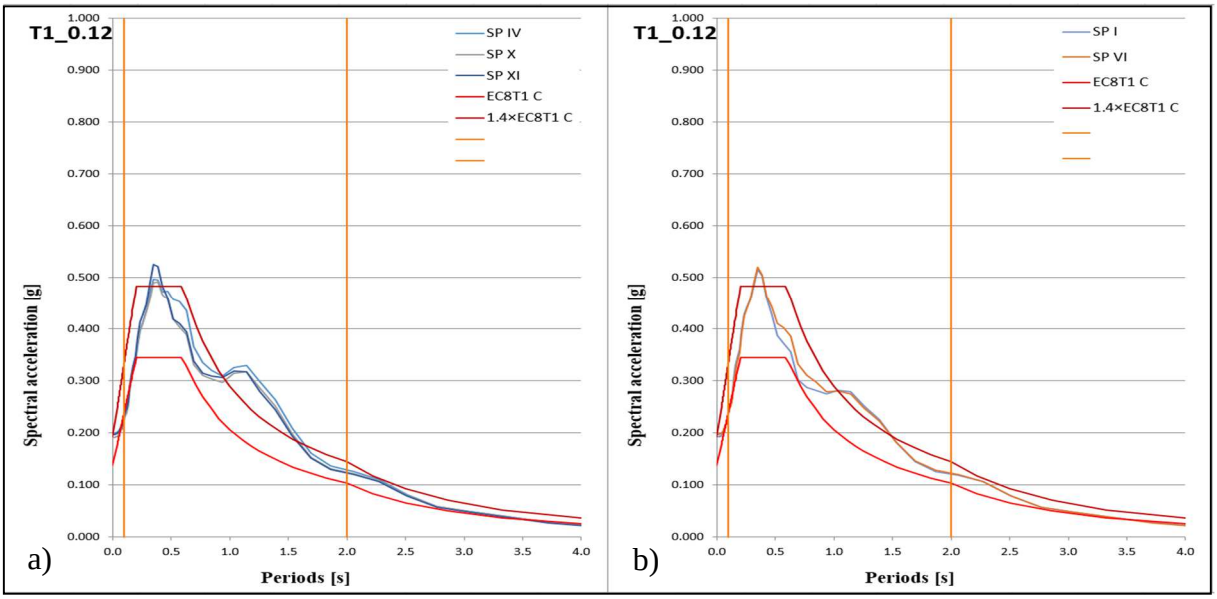

8.1. Figure: Zones of Győr marked with C1 and C2

The results of response analysis for each soil profile can be found in Annex, and these were compared to each other. Based on the careful examinations of spectral accelerations, shear wave velocities, amplification factors and geomorphology eight zones (C1-C6 and B1-B2) were defined in Győr. Two zones of Győr are presented on Figure 8.1 a) and b) marked with C1 and C2 respectively. The spectral accelerations are compared to the elastic response spectra of EC

DOI: 10.15477/SZE.MMTDI.2015.002

8 taking into account importance factor II and IV. Note that they are quite similar in shape, but do show some differences. Three of the soil profiles fit well together to form zone C1, while two others were closely related and designated zone C2. Similar arguments can be made for the remaining zones. These zones will later be assigned different soil effect factors in the evaluation of risk. The zonation with respect to spectral accelerations was mapped (Figure 8.2). Soft transition boundaries were used to show the variation of the mapped parameters. More defined clear boundaries are not recommended. This allows some flexibility to the urban planners and avoids misinterpretation of clear boundaries as accurate estimations of the different zones.

8.2. Figure: Microzonation of Győr

8.2. Zonation of building structures based on RVS scores (Ch. 7)

The city districts provide a good way to categorize building structures, in general, since each district has a predominant building type and construction era. As shown earlier, there are over 5000 buildings that have received scores, and it would be possible to map every single one. From an administrative view, this would be problematic since evaluation, retrofit, repair, and planning efforts would be applied by district, or perhaps sub-district.

Using a district approach is quite common in risk analysis; however some decisions are necessary about how to assign a district score. One may pick a dominant structure type, either

by building count (small residential buildings would have more influence) or total resident occupancy (apartment houses would have more influence). The average score for the dominant structure would then be applied to the district. Another approach is to use an unweighted or weighted average of all the buildings in the district. Statistical methods could be applied to the results as well to better describe the distribution of scores and the influence of different components of the hazard and vulnerability studies. For this study, both the dominant building approach and the average score approach produced essentially the same result.

8.3. Figure: City districts of Győr with different urban structure

8.3. Overall risk

Figure 8.4 shows the relative seismic risk associated with each city district. The level of risk is represented by color where low risk is blue and increasing risk shifts to light blue, blue-green, green, tan, light red, and finally red.

As the figure demonstrates, highest risk is centered in Belváros and gradually reduces as one moves outward. Newer districts, with better construction, and variations in soil conditions are responsible for the reduction and pattern of risk values shown. Lowest risk

DOI: 10.15477/SZE.MMTDI.2015.002

factors are in the Gyárváros district where there are substantial buildings constructed according to newer codes and single free-standing homes having regular configurations.

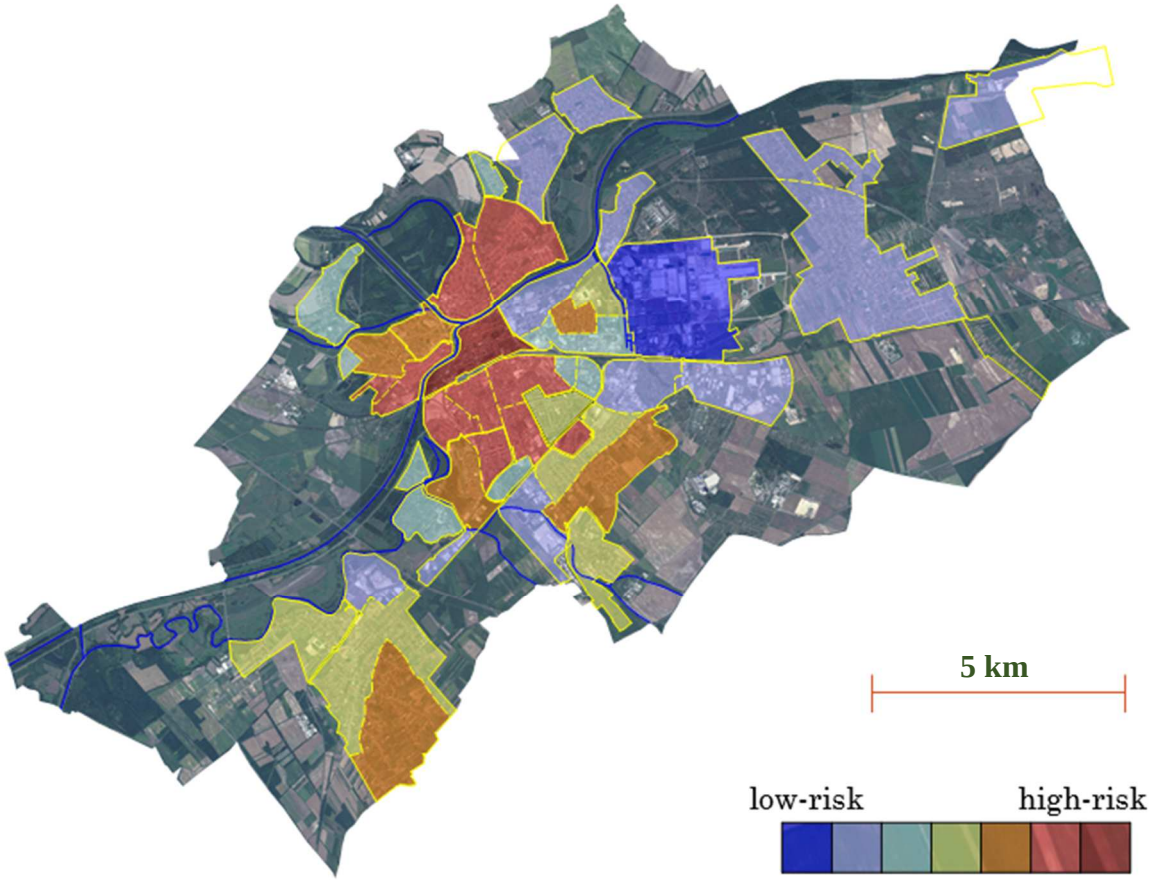

The risks shown are relative since the evaluation by rapid visual screening uses a score/demerit system. Based on the results cited earlier, a building score below 2.0 would normally indicate that further analysis and/or building improvement is needed. However, in order to “anchor” these numbers and give definite recommendations, further detailed analyses of selected building types would be necessary.

As a comparison, FEMA 155 scores used in the RVS were cross-verified through detailed evaluation of 500 buildings after the Northridge California earthquake, then further refined by examination of several thousand U.S. Army buildings by the Corps of Engineers. Since there are some differences in materials and construction methods between Hungary and the U.S., a direct application of the method would require slight modification. Nevertheless, relative risks from this study will not change significantly.

DOI: 10.15477/SZE.MMTDI.2015.002

Chapter 9. Conclusion

This study presents a comprehensive approach for assessing seismic risk in a small city. The area is considered a moderate earthquake risk with past events estimated up to M=6.5. It is a typical situation for many cities in Hungary and throughout Europe where the seismic hazard is not great, but cannot be ignored. In order to make the best use of limited resources, this methodology used existing soil data, rapid visual building assessment, a limited number of field tests and free, but sophisticated software.

Variation in seismic hazard was evaluated mainly as a function of soil type. Starting with historical soil data, field testing by MASW was performed in strategic locations. Based on the results and correlations with the historical data, soil profile zones were delineated through the city. Using 1-dimensional site response software with 6000 realizations, the impact of the different soil zones was evaluated and compared to the more uniform approach by soil type profile from Eurocode 8. While there was very general agreement with EC-8, there was also a great deal of variation in the level of seismic action due to the different soil profiles. The different seismic actions could be mapped in a manner similar to the soil profiles.

The rapid visual evaluation of buildings was performed on over 5000 structures in Győr. The evaluation method was developed from well-known approaches, but modified to account for typical building designs found here. The reliability of the visual evaluations performed by trained non-experts was verified by experts over a significant percentage of all buildings. Further evaluation of building vulnerability was performed by pushover analyses by simplified methods. The analyses showed that the vulnerability assessments were consistent and reasonable.

Estimates of seismic risk were computed using seismic hazard results and building vulnerability functions. As one would expect, since the hazards and vulnerabilities were not uniformly distributed around Győr, there were zones of higher and lower risk. Based on these risk assessments, engineers and planners can decide where to improve buildings, whether to permit further development, and formulate emergency response plans in case of a seismic event. Other aspects of risk include economic evaluation of building repair or retrofit, assessment of insurance premiums, or redesigning infrastructure systems to better tolerate hazards.

The method developed for Hungarian context can be directly used to evaluate the earthquake risk of other cities. The research can be even carried on to determine the earthquake risk of the whole city of Győr.

DOI: 10.15477/SZE.MMTDI.2015.002

9.1. New scientific results

The under- and over- estimation of risk has a great social and economic effect, so the used method should fulfil strict requirements. Stress should be laid on planning and prevention. By assessing the buildings it can be determined which may require additional evaluation, and a priority list of interventions can be established. This can decrease the expected damage during an earthquake.

9.1.1. Theses

Thesis I

I determined and mapped the local soil effect for seismic hazard determination in the area of Győr.

I determined the shear wave velocity profiles for different soil categories in Győr using MASW.

I correlated the measured MASW data to CPT and soil boring data and developed empirical relationships between soil types, soil depth and shear wave velocity.

Using the correlations I was able to create a soil profile map for the Győr area.

I performed seismic site response analysis for 15 different averaged soil profiles. Based on the response analyses, I was able to differentiate between regions of the city.

Even though the soil in the city area is classified as soil type C according to EC8 (European Committee for Standardization, 2013), I determined that the hazard is not uniform.

Thesis II

I performed building vulnerability assessment for the designated area.

I defined a simplified methodology for rapid evaluation of dynamic analysis of buildings and created a checklist. Based on the checklist I led the evaluation of more than 5000 buildings in area of Győr.

I determined the vulnerability of the building stock based on score assignment.

I determined the vulnerability of masonry and reinforced concrete buildings typical to Győr by pushover methods.

Thesis III

I designed the method for seismic risk analysis using a rapid assessment method based on available data with limited resources.

I delineated the zones for the designated area with different seismic vulnerability.

I determined the districts with different vulnerability level of the buildings.

I applied the risk assessment methodology over discrete areas making it ideal for GIS implementation. The method is directly applicable to other towns in Hungary.

DOI: 10.15477/SZE.MMTDI.2015.002

9.1.2. Zones and classification

In seismic microzonation the variation of earthquake ground motion was studied taking into account the seismic hazard of the country completed with geological and geotechnical site conditions conducting research concerning the local soil effect because earthquake zonation maps prepared at small scales do not yield the necessary information for risk mitigation at a city level. Figure 8.2 presents the microzonation of Győr in Section 8.1.

The need for a deeper diversification of building behaviors led to more elaborate classification systems, where consideration was given to primary parameters affecting building damage and loss characteristics such as the basic structural system, the seismic design criteria (code level) the building height (low-rise, midrise, high-rise) as well as non-structural elements affecting non-structural damage. Figure 8.3 presents the districts with different building types of Győr in Section 8.2.

Structural and non-structural damages are the root cause of many of the other losses expected after an earthquake. Direct economic losses, consequences to buildings and their content, consequences to inhabitants can be estimated after physical damage has been determined. Seismic risk was evaluated overlapping the microzonation and building vulnerability data based on scoring system of FEMA presented in Figure 9.1 determining the low-risk, medium-risk and high-risk areas of the city.

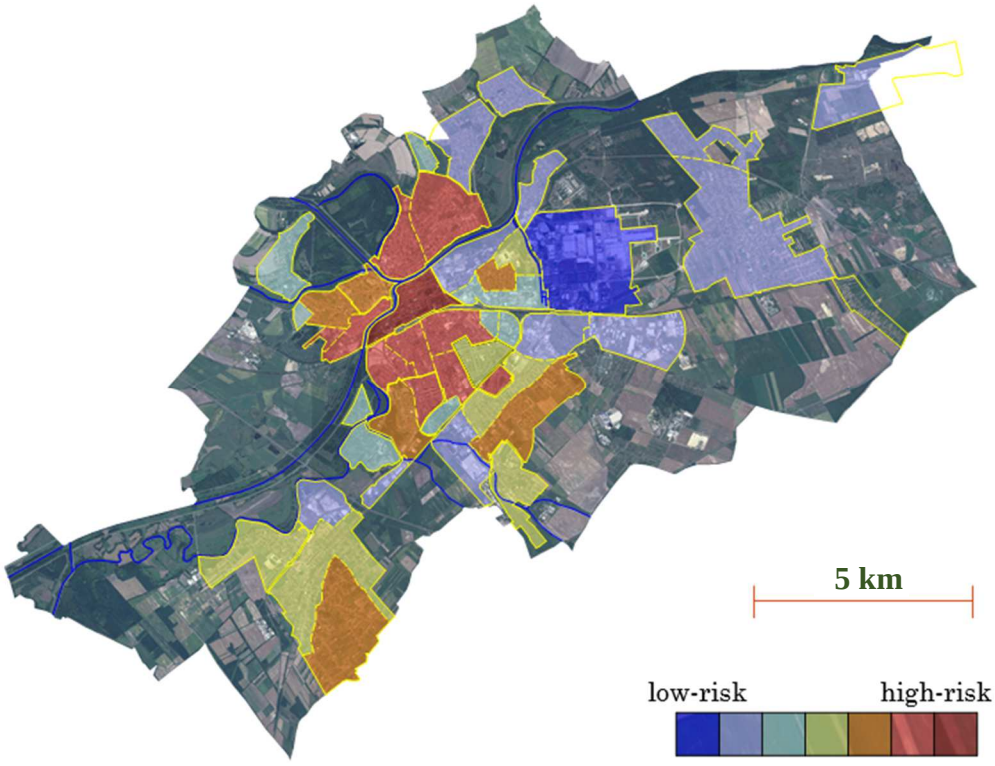

9.1. Figure: Low-risk, medium-risk and high-risk areas of Győr in case of LS of Significant Damage a probability of exceedance of 10% in 50 years

DOI: 10.15477/SZE.MMTDI.2015.002

9.2. Usability of research and possibilities for further research

Earthquake risk is a public safety issue that requires appropriate risk management measures and means to protect citizens, properties, infrastructures and the built cultural heritage. The aim of a seismic risk analysis is the estimation and the hypothetical, quantitative description of the consequences of seismic events of an investigated area, on a regional or state level. The effects to be predicted are the physical damage to buildings and other facilities.

Based on damage pattern, further studies can determine the possible number and type of casualties, the potential economic losses due to the direct cost of damage and to indirect economic impacts (loss of the productive capacity and business interruption), the loss of function in lifelines and critical facilities (such as hospitals, fire stations, communication system, transportation networks, water supply, etc.) and also social, organizational and institutional impact.

This research gives a good overview about seismic hazard of the city of Győr, the vulnerability of the building stock and the seismic risk concerning building damages of residential buildings in the designated area. The results provided by a seismic risk analysis could be regarded as helpful guidelines on respect to all the phases of the risk management: during normal periods, during crisis periods, as well as in the recovery and post-emergency periods, and can be directly applied into development plans, emergency planning, insurance calculation, etc. The method developed for Hungarian context can be directly used to evaluate the earthquake risk of other cities. The research can be even carried on to determine the earthquake risk of the whole city of Győr.

The results of site response analysis reveals the fact, that in areas with diverse soil conditions, especially in case of alluvium further analysis is needed for creating elastic response spectrum for design purposes.

Future work related to this research is recommended in several directions:

- Seismic risk of the whole city could be performed based on the methodology.
- Societal and economical aspects could be incorporated to be able to estimate the cost of the different events.
- The seismic risk analysis of infrastructures could be evaluated, because damages of this structures can have an effect on the buildings.
- Based on detailed building analysis, further simplifications could be implemented concerning visual screening, which does not worsen the results, in order to reduce the man-hours needed for field survey.

References

Alexander, E. D., 2002. *Principles of Emergency Planning and Management.* Oxford: University Press.

Alföldi, L., 2009. Hungary in Maps. In: K. Kocsis & F. Schweitzer, szerk. *Hydrography.* Budapest: Geographical Research Institute Hungarian Academy of Sciences, pp. 51-56.

Ambraseys, N. et al., 2002. *Internet-Site for European Strong-Motion Data, European Commission, Research-Directorate General, Environment and Climate Programme.* [Online] Available at:http://www.isesd.hi.is/ESD_Local/frameset.htm [Accessed 15 01 2014].

Applied Technology Council, 1985. *ATC-13: Earthquake Damage Evaluation Data for California.* Redwood City, CA: Applied Technology Council.

Austrian National Archives & Arcanum Adatbázis Kft., *2014. Historical Maps of the Habsburg Empire. Available at:http://mapire.staatsarchiv.at/en/map/mkf_hun/?zoom=13&lat=47.6818&lon=17.64292 [Accessed: 23 03 2014].*

Bada, G., 2005. *Pannon-medence jelenkori geodinamikája: vizsgálati módszerek és kutatási eredmények. Elektronikus jegyzet a hasonló című PhD kurzushoz. (Contemporary Geodinamics of Pannonian Basin: Testing Methods and Research Results.).* [Online] Available at: http://geophysics.elte.hu/dolgozok/bada.htm#oktatas

[Accessed 30 04 2014].

Bard, P.-Y., 1997. *Local Effects on Strong Ground motion: Basic Physical Phenomena and Estimation Methods for Microzoning Studies.* Thessaloniki, Greece, Proceedings of SERINA-Seismic risk: An Integrated Seismological, Geotechnical and Structural Approach.

Bard, P.-Y. & Gariel, J.-C., 1986. The Seismic Response of Two-dimensional Sedimentary Deposits with Large Vertical Velocity Gradients. *Seismological Society of America,* Volume Vol. 76 No. 2, pp. 343-366.

Bauer, R. A., Su, W.-J., Counts, R. C. & Karaffa, M. D., 2007. *Shear Wavw Velocity, Geology and Geotechnical Data of Earth Materials in the Central US Urban Hazard Mapping Areas, Final Technical Report,* Champaign, Illinois: Illinois State Geological Survey.

Bauer, R. A., Wen-June, S., Counts, R. C. & Karaffa, M. D., 2007. *Shear Wave Velocity, Geology and Geotechnical Data of Earth Materials in the Central U.S. Urban Hazard Mapping Areas,* Champaign, Illinois: Final Technical Report Illinois State Geological Survey.

Benedetti, D. & Pezzzoli, P., 1996. *Shaking Table Tests on Masonry Buildings, Results and Comments : Experimental Evaluation of Technical Interventions to Reduce the Seismic Vulnerability of Masonry Buildings.* Bergamo, Italy: IMSES.

Bisztricsány, E., 1974. *Mérnökszeizmológia (Engineering Seismology).* Budapest: Akadémiai Kiadó.

Bommer, J. J., 2002. Deterministic vs. Probabilistic Seismic Hazard Assessment: an Exaggerated and Obstructive Dichotomy. *Journal of Earthquake Engineering,* Volume Volume 6, Supplement 001, pp. 43-73.

Boore, D. M., 2004. Can Site Response Be Predicted?. *Journal of Earthquake Engineering,* Volume Vol. 8, Special Issue 1, pp. 1-41.

Boore, D. M., 2007. *Predicting Earthquake Ground Motion in North America.* Ottawa, Ontario, Canada, Proceedings, Ninth Canadian Conference on Earthquake Engineering.

Borbíró, V. & Valló, I., 1956. *Győr városépítéstörténete (History of Town Construction of Győr).* Budapest: Akadémiai Kiadó.

Borcherdt, R. D., 1970. Effects of Local Geology on Ground Motion Near San Francisco Bay. *Bulletin of Seismological Society of America,* Volume Vol. 60, pp. 29-61.

Bouchon, M. & Barker, J. S., 1996. Seismic Response of a Hill: The Example of Tarzana, California. *Bulletin of the Seismological Society of America,* Volume Vol. 86, p. 66–72.

Caltrans, 2007. *Soil and Rock Logging, Classification, and Presentation Manual.* hely nélk.:State of California Department of Transportation Division of Engineering Services Geotechnical Services.

Calvi, G. M. et al., 2006. Development of Seismic Vulnerability Assessment Methodologies Over the Past 30 Years. *ISET Journal of Earthquake Technology,* Volume Vol. 43, No. 3, pp. 75-104.

Calvi, M. G., 1999. A Displacement-Based Approach for Vulnerability Evaluation of Classes of Buildings. *Journal of Earthquake Engineering,* Volume Vol. 3, No. 3, pp. 411-438.

Carvalho, J. et al., 2009. Seismic velocities and geotechnical data applied to the soil microzoning of western Algarve, Portugal. *Journal of Applied Geophysics,* Volume Vol. 68 Issue 2, pp. 249-258.

Castano, J. C. & Zamarbide, J. L., 1992. *A Seismic Risk Reduction Program for Mendoza City, Argentina.* Tenth World Conference on Earthquake Engineering, Madrid, Spain, International Association for Earthquake Engineering.

Civertan,2014.[Online] Available at: http://www.civertan.hu/legifoto/galery_image.php?id=2551[Accessed 30 04 2014].

Coburn, A. W. & Spence, R., 2002. *Earthquake Protection.* West Sussex, England ed. s.l.:John Wiley & Sons.

Committee on National Earthquake Resilience, 2011. *National Earthquake Resilience: Research, Implementation, and Outreach.* Washington, D.C.: National Academies Press.

Cs. Deseő, É., 1989. Surface and Groundwaters. In: L. Balásházy & S. Somogyi, eds. *National Atlas of Hungary*. Budapest: MTA Földrajztudományi Kutatóintézet, pp. 62-76.

D'Ayala, D., Spence, R., Oliveira, C. & Pomonis, A., 1997. Earthquake Loss Estimation for Europe's Historic Town Centres. *Earthquake Spectra,* Vol. 13(No. 4), pp. 773-793.

Dolce, M., Kappos, A., Zuccaro, G. & Coburn, A. W., 1995. *Report of the EAEE Working Group 3: Vulnerability and Risk Analysis, Proceedings of 10th European Conference on Earthquake Engineering.* Vienna, A. A. Balkema.

Dulácska, E., 2009. *Földrengés elleni védelem, egyszerű tervezés az Eurocode 8 alapján, Gyakorlati útmutató (Protection Against Earthquakes, Simple Design According to Eurocode 8, Practical Guide).* Budapest: Mérnöki Kamara Nonprofit Kht..

Erdélyi, M., 1990. A Kisalföld hidrógeológiája a vízlépcsők megépítése előtt és után (The Hidrogeology of the Little Hungarian Plain Before and After the Construction of Dams). *Földrajzi értesítő,* Volume Vol. XXXIX. Nr. 1-4., pp. 7-27.

ETH Zurich, 2013. *European Facility for Earthquake Hazard and Risk.* [Online] Available at:http://portal.share-eu.org:8080/jetspeed/portal/ [Accessed 13 05 2014].

European Committee for Standardization, 2002. *Geotechnical Investigation and Testing - Identification and Classification of Soil - Part 1: Identification and Description (ISO 14688-1:2002).* Brussels: s.n.

European Committee for Standardization, 2013. *Eurocode 8: Design of Sturctures for Earthquake Resistance MSZ EN 1998-1:2004/A1:2013.* Brussels: s.n.

Faccioli, E., 2006. Seismic Hazard Assessment for Derivation of Earthquake. *Bulletin of Earthquake Engineering,* Volume Vol. 4, pp. 341-364.

Fäh, D., Kind, F., Lang, K. & Giardini, D., 2001. Earthquake scenarios for the city of Basel. *Soil Dynamics and Earthquake Engineering*, Volume Volume 21, Issue 5, pp. 405-413.

FEMA, 1988. *FEMA 154: Rapid Visual Screening of Buildings for Potential Seismic Hazard.* 2002 szerk. Washington D.C.: Federal Emergency Management Agency.

FEMA, 2002. *FEMA 155: SECOND EDITION Rapid Visual Screening of Buildings for Potential Seismic Hazards: Supporting Documentation.* 2002 ed. Washington D.C.: Federal Emergency Management Agency.

FEMA, 2013. *"Earthquake Model." Hazus-MH 2.1 Technical Manual.* s.l.:Federal Emergency Management Agency.

Foerster, E. et al., 2009. Del. 1.1.1: Methodologies to Assess Vulnerability of Structural Systems. In: *ENSURE (Enhancing Resilience of Communities and Territories Facing Natural and Na-tech Hazards) Project WP1: State-of-the Art on Vulnerability Types.* s.l.:European Commission Seventh Framework Programme, pp. 1-139.

Földvary, G. Z., 1988. *Geology of the Carpathian Region.* ISBN 9971-50-344-1 ed. Singapore: World Scientific Publishing Co Pte Ltd..

Fukuyama, H., Tumialan, G. & Matsuzaki, Y., 2001. *Outline of the Japanese Guidelines for Seismic Retrofitting of RC Buildings using FRP Materials.* Cambridge, UK, No-nmetallic reinforcement for Concrete Structures - FRPRCS-5.

GeoRisk Earthquake Engineering Ltd., 2006. *Seismic Hazard Map of Hungary.* [Online] Available at:http://georisk.hu/ [Accessed 03 05 2014].

Giardini, D. et al., 2013. *Seismic Hazard Harmonization in Europe (SHARE).* [Online] Available at: http://www.share-eu.org/node/90 [Accessed 13 05 2014].

Giovinazzi, S., 2009. Geotechnical Hazard Representation for Seismic Risk Analysis. *Bulletin of the New Zealand Society for Earthquake Engineering*, Volume Vol. 42, No. 3, pp. 221-234.

GoogleMap,2014. [Online] Available at: https://maps.google.hu/maps?oe=utf-8&client=firefox-a&q=gy%C5%91r&ie=UTF-8&hq=&hnear=0x476bbf87407ea035:0x400c4290c1e11e0,Gy%C5%91r&gl=hu&ei=FVtiU5 qyKYextAbcj4HYAw&ved=0CJYBELYDMBA [Accessed 30 04 2014].

Göcsei, I., 2005. 2.1 Győr természeti adottságai (Natural Endowments of Győr). In: *Győr Megyei Jogú településrendezési eszközeinek felülvizsgálata - 2003-2005 (Evaluation of Settlement Assets in Győr).* Győr: Győr Megyei Jogú Város Önkormányzata.

Gribovszki, K., 2005. *Földrengések geofizikai és geológiai környezetének valamint Debrecen földrengésveszélyezettségének vizsgálata térinformatikai eszközökkel (Studying the Geophysical and Geological Environment of Earthquakes and Deterministic Seismic Hazard of Debrecen).* Sopron: PhD Dissertation - University of West Hungary Kitaibel Pál Environmental Doctoral School Geoenvironmental Sciences Program.

Gribovszki, K. & Panza, G. F., 2004. Seismic microzonation with the use of GIS - Case study for Debrecen, Hungary. *Acta Geodaetica et Geophysica Hungarica,* Volume Vol. 39, No. 4, pp. 177-190.

Gribovszki, K., Schulek-Tóth, F. & Varga, P., 2010. Deterministic Seismic Hazard Assessment of the Inner Town of Budapest. *Acta Geodaetica et Geophysica Hungarica,* Volume Vol. 45, No. 3, pp. 372-387.

Grünthal ed., G., 1998. *European Macroseismic Scale 1998.* Luxembourg: European Seismological Commission.

Gyenes, Z., 2011. *Nemzeti katasztrófa kockázat értékelés (National Disaster Risk Assessment).* Hungary: Belügyminisztérium, Országos Katasztrófavédelmi Főigazgatóság (National Directorate General for Disaster Management, Ministry of Interior).

Győri , E., Mónus, P., Tóth, L. & Zsíros, T., 2004. *Talajfolyosódás veszélyeztetettség Magyarországon (Liquefaction hazard in Hungary).* Győr, Széchenyi István Egyetem, Magyarország Földrengésbiztonsági Konferencia.

Győr-Moson-Sopron County Emergency Directorate, 2014. *Győr-Moson-Sopron Katasztrófavédelmi Igazgatóság (Győr-Moson-Sopron County Emergency Directorate).* [Online]

Available at: http://gyor.katasztrofavedelem.hu/a-megye-veszelyeztetettsegenek-elemzese [Accessed 28 04 2014].

Haas, J., 1989. Geological Sectionss. In: K. Brezsnyánszky & J. Haas, eds. *National Atlas of Hungary.* Budapest: MTA Földrajztudományi Kutatóintézet, pp. 34-50.

Haas, J., 2009. Geology. In: K. Kocsis & F. Schweitzer, eds. *Hungary in Maps.* Budapest: Geographical Research Institute, Hungarian Academy of Sciences, pp. 34-37.

Haddar, F. N., 1992. *Urban Seismic Vulnerability Analysis: The Case of Algeria, Proceedings of the.* Tenth World Conference on Earthquake Engineering, Madrid, Spain, International Association for Earthquake Engineering.

Hardin, B. O. & Black, W. L., 1968. Vibration Modulus of Normally Consolidated Clay. *Journal of the Soil Mechanics and Foundation Division, ASCE,* Volume Vol 95. No. 2, pp. 353-369.

Hazard Mitigation Unit, 2014. *New York City Hazard Mitigation Plan 2014.* Brooklyn, New York: New York City Office of Emergency Management.

HHP Contact Tanácsadó Kft., Győri Építész Műhely, Győri Mérnök Műhely & MTA RKK Nyugat-magyarországi Tudományos Intézete, 2011. Győr Megyei Jogú Város középtávú integrált városfejlesztési stratégiája (Medium-term Strategy for Integrated Urban Development of Győr County Town). In: Győr: Győr Megyei Jogú Város Önkormányzata.

Horvát, F. & Bada, G., 2003. *A Pannon-medence recens tektonikája (Recent Tectonics of Pannonian Basin).* Győr, Széchenyi István Egyetem - Conference on Earthquake Safety of Hungary, pp. 25-39.

Horváth, F., Dombrádi, L. & Tóth, L., 2009. Geophysics. In: F. Kocsis & F. Schweitzer, eds. *Hungary in Maps.* Budapest: Geographical Research Institute, Hungarian Academy of Sciences, pp. 29-33.

Hungarian Central Statistical Office, 2012.01.01.[Online]
Available at: http://www.ksh.hu/interaktiv/terkepek/mo/nepesseg.html?mapid=WNT001
[Accessed 30 04 2014].

Iervolino, I., Galasso, C. & Cosenza, E., 2010. REXEL: Computer Aided Record Selection for Code-based Seismic Structural Analysis. *Bulletin of Earthquake Engineering,* Volume Vol. 8, pp. 339-362.

Inel, M., Senel, S. M., Toprak, S. & Manav, Y., 2008. Seismic Risk Assessment of Buildings in Urban Areas: a Case Study for Denizli, Turkey. *Natural Hazards,* Volume 46., pp. 265-285.

Inter, 1993. Seismic Hazard in Hungary. In: R. K. McGuire, ed. *The Practice of Earthquake Hazard Assessment.* Denver, Colorado USA: International Association of Seismology and Physics of the Earth's Interior, pp. 135-138.

Japan Meteorological Agency, 1996. *Explanation Table of JMA Seismic Intensity Scale.* [Online] Available at:http://www.jma.go.jp/jma/en/Activities/inttable.html
[Accessed 15 03 2014].

Jibson, R. W., 1987. *Summary of Research on the Effects of Topographic Amplification of Earthquake Shaking on Slope Stability USGS Open-File Report: 87-268,* s.l.: US Geological Survey.

Kanli, A. I. et al., 2006. Vs30 Mapping and Soil Classification for Seismic Site Effect Evaluation in Dinar Region, SW Turkey. *Geophysical Journal International,* Volume Vol. 165, pp. 223-235.

Katona, T., 2001. *Seismic Safety Evaluation and Enhancement at the Paks Nuclear Power Plant.* Ispra, Italy, Nuclear Energy Agency, Committee on the Safety on Nuclear Instalations Workshop Proceedings.

Kegyes-Brassai, O., 2003. *Épületek osztályozása földrengéskockázat szempontjából (Classification of Buildings in Terms of Earthquake Risk).* Sopron, DOSz, Tavaszi Szél Konferencia.

Kegyes-Brassai, O., 2004a. Evaluation of Vulnerability of Masonry Buildings Based on the Shear Capacity of the Walls. *Bulletin: Faculty of Architectural Engineering Budapest University of Technology and Economics,* pp. 125-134.

Kegyes-Brassai, O., 2004b. *Evaluation of Building Structures to Obtain Vulnerability Function in Order to Determine Earthquake Risk.* Delft, Fifth International PhD Symposium in Civil Engineering.

Kegyes-Brassai, O., 2006. *The Vulnerability Study of Masonry Structures in Hungary.* Geneva, First European Conference on Earthquake Engineering and Seismology joint event of the Thirteenth European Conference on Earthquake Engineering.

Kegyes-Brassai, O., 2006. *The Vulnerability Study of Masonry Structures in Hungary.* Geneva, Switzerland, 13th ECEES 2006.

Kegyes-Brassai, O., 2007. *Risk Analysis and Building Vulnerability.* Győr, Széchenyi István Egyetem - Conference on Earthquake Safety of Hungary.

Kegyes-Brassai, O. & Ray, R. P., 2013. *Earthquake Risk Analysis Method Applied to a Town in Hungary.* Tokyo, Japan, Tenth International Conference on Urban Earthquake Engineering.

Kircher, C. A., Nassar, A. A., Kustu, O. & Holmes, W. T., 1997. Development of Building Damage Functions for Earthquake Loss Estimation. *Earthquake Spectra,* Volume Vol. 13 No. 4, pp. 663-682.

Kottke, A. & Rathje, E. M., 2013. *NEEShub - Resources: Strata.* [Online] Available at:https://nees.org/resources/strata [Accessed 10 12 2013].

Kramer, S. L., 1996. *Geotechnical Earthqauke Engineering.* Upper Saddle River, New Jersey: Prentice Hall.

Lacave, C., Bard, P.-Y. & Koller, M. G., 1999. Microzonation: Techniques and Examples. *Naturgefahren-Endbebenrisiko,*Vol. 22 (http://www.ndk.ethz.ch/downloads/publ/publ_Bl15/Koller.pdf), pp. 1-23.

Lang, K. & Bachmann, H., 2000. *Erdbebenverletzbarkeit bestehender Gebäude aus unbewehrtem Mauerwerk.* Zürich: Schweizer Gesellschaft für Erdbebeningenieurwesen und Baudynamik (SGEB), ETH Zürich, 7./8.09.2000, Dokumentation SIA DO162, Schweizer Ingenieur- und Architekten-Verein.

Lang, K. & Bachmann, H., 2004. On the Seismic Vulnerability of Existing Buildings: A Case Study of the City of Basel. *Earthquake Spectra,* Volume Vol. 20, No. 1, pp. 43-66.

Lantada, N. et al., 2010. Seismic Hazard and Risk Scenarios for Barcelona, Spain, Using the Risk-UE Vulnerability Index Method. *Bulletin of Earthquake Engineering,* Volume Vol. 8. Issue 2., pp. 201-229.

Lee, K. et al., 2000. *Potential Seismic Risk Assessment of Urban Cities in Japan Considering their Regional Characteristics.* 12th World Conference on Earthquake Engineering, Auckland, New Zealand, Upper Hutt, N.Z. : New Zealand Society for Earthquake Engineering. Lemoine, A., Douglas, J. & Cotton, F., 2012. *Seismic Hazard Harmonization in Europe (SHARE).*[Online] Available at:http://www.share-eu.org/node/90 [Accessed 13 05 2014].

Luco, N. et al., 2007. *Risk-Targeted versus Current Seismic Design Maps for the Conterminous United States.* Squaw Creek, California, SEAOC Convention.

Marosi, S. & Somogyi, S., 1990. *Magyarország kistájainak katasztere I-II. (Microregions in Hungary I-II.).* Budapest: MTA Földrajztudományi Kutatóintézet.

Martinez, M.,2014.*CNN:Six things we've learned since 1994 Northridge Earthquake.* [Online] Available at: http://edition.cnn.com/2014/01/16/us/northridge-earthquake-things-learned/ [Accessed 30 04 2014].

Matsuoka, M., Wakamatsu, K., Fujimoto, K. & Midorikawa, S., 2005. Average Shear-wave Velocity Mapping Using Japan Engineering Geomorphologic Classification Map. *Journal of Structural Mechanics and Earthquake Engineering,* Volume Vol. 23, No. 1, pp. 239-251.

Mouroux, P. et al., 2004. *The European RISK-UE Project:an Advanced Approach to Earthquakes Risk Scenarios.* Vancouver, B.C., Canada, 13th World Conference on Earthquake Engineering.

Nakamura, Y., 1989. A Method for Dynamic Characteristics Estimations of Subsurface Using Microtremors on the Ground Surface. *Railway Technical Research Institute, Quarterly Reports,* Volume Vol. 30, pp. 25-33.

NERIES, 2006-2010. *Network of Research Infrastructures for European Seismology.* [Online] Available at: http://www.neries-eu.org/ [Accessed 10 11 2013].

Nigbor, R. L., Swift, J. N. & Diehl, J. G., 2001. *Resolution of Site Response Issues in the Northridge Earthquake (ROSRINE),* Los Angeles, California: University of Southern California School of Engineering Department of Civil Engineering.

Nottis, G. N., 2001. *Multidisciplinary Center for Earthquake Engineering Research.* [Online] Available at: http://mceer.buffalo.edu/education/reu/01presentations/swvlwrhudson.htm [Accessed 12 02 2014].

NRC, 1994. *Practical Lessons from the Loma Prieta Earthquake.* Geotechnical Board, National Research Council ed. Washington, DC: The National Academies Press.

Oliveira, C. S., 2008. Lisbon earthquake scenarios: A review on uncertainties, from earthquake source to vulnerability modelling. *Soil Dynamics and Earthquake Engineering,* Volume 28, pp. 890-913.

Oliveira, C. S. & Campos-Costa, A., 2006. Overview on Earthquake Hazard Assessment - methods and new trends. In: C. S. Oliveira, A. Roca & X. Goula, eds. *Assessing and Managing Earthquake Risk.* Dordrecht, The Netherlands: Springer, pp. 15-47.

Oropeza, M., Michel, C. & Lestuzzi, P., 2010. *A Simplified Analytical Methodology for Fragility Curves Estimation in Existing Buildings.* Ohrid, Macedonia, Fourtenth European Conference on Earthquake Engineering.

Page, A. W., 1995. *Unreinfoced Masonry Structures - an Australian Overview.* Melbourne, Australia, PCEE 95.

Paoletti, V., 2012. Remarks on Factors Influencing Shear Wave Velocities and Their Role in Evaluating Susceptibilities to Earthquake-triggered Slope Instability: Case Study for the Campania Area. *Natural Hazards and Earth System Sciences,* Volume Vol. 12, pp. 2147-2158. Papanikolaou, V. K., Elnashai, A. S. & Pareja, J. F., 2005. *Limits of Applicability of Conventional and Adaptive Pushover Analysis for Seismic Response Assessment.* Report Mid-America Earthquake Center Civil and Environmental Engineering Department University of Illinois at Urbana-Champaign March ed. s.l.:s.n.

Papp, F., 2008. *Online EOV>>WGS84 Transformation.*[Online]
Available at: http://pf-prg.hu/trafo/trafo-4.php?mod=-3 [Accessed 10 03 2014].
Park Seismic LLC., 1990. *Multichannel Analysis of Surface Waves (MASW).* [Online] Available at: http://www.masw.com/DataAcquisition.html [Accessed 04 05 2014].
Park, C. B., Miller, R. D. & Xia, J., 1998. *Imaging Dispersion Curves of Surface Waves on Multi-channel Record.* New-Orleans, Louisiana, Technical Program with biographies, SEG, 68th Annual Meeting.
Park, C. B., Miller, R. D. & Xia, J., 1999. Multichannel Analysis of Surface Waves (MASW). *Geophysics,* Volume Vol. 64, pp. 800-808.
Park, C. B., Miller, R. D. & Xia, J., 2001. *Offset and resolution of Dispersion Curve in Multichannel Analysis of Surface Waves (MASW).* Denver, Proceedings of the SAGEEP.
Perrin, N. D., Stepheenson, W. R. & Semmens, S., 2010. *Site Class Determinations (NZS 1170.5) in Wellington Using Borehole Data and Microtremor Techniques.* Wellington, New Zealand, New Zealand Society for Earthquake Engineering Conference Proceedings. Pitilakis, K. et al., 2011. D3.2 Fragility Functions for Common Masonry Building Types in Europe. In: *SYNER-G Systemic Seismic Vulnerability and Risk Analysis for Buildings, Lifeline Networks and Infrastructures Safety Gain.* s.l.:European Commission Seventh Framework Programme, pp. 1-177.
Porro, B. & Schraft, A., 1989. Investigation of Insured Earthquake Damage. *Natural Hazard,* Volume Vol. 2, pp. 173-184.
Porro, B. & Schraft, A., 1989. Investigation of Insured Earthquake Damage. *Natural Hazards,* Volume Vol. 2, pp. 173-184.
Rechnitzer, J. et al., 2014. Győr-Moson-Sopron Megye területfejlesztési koncepciója (Regional Development Plan of Győr-Moson-Sopron County). In: Győr: Universitas-Győr Nonprofit Kft.. Robertson, P. K. & Cabal, K., 2012. *Guide to Cone Penetration Testing for Geotechnical Engineering.* 5th Edition ed. Signal Hill,California: Gregg Drilling & Testing, Inc.. Robertson, P. K. & Cabal, K. L., 2012. *Guide to Cone Penetration Testing for Getechnical Engineering.* California: Gregg Drilling and Testing Inc..
Roca, A., Oliveira, C. S., Ansal, A. & Figueras, S., 2006. Local Site Effects and Microzonation. In: C. S. Oliveira, A. Roca & X. Goula, eds. *Assesssing and Managing Earthquake Risk.* Dordrecht, The Netherlands: Springer, pp. 67-91.

Scharek, P., ed., 1990. South Győr. In: *The Geological Map Series of the Little Hungarian Plain.* Budapest: Magyar Állami Földtani Intézet.

Scharek, P., ed., 1991. North Győr. In: *The Geological Map Series of the Little Hungarian Plain.* Budapest: Magyar Állami Földtani Intézet.

Scharek, P. & Tóth, G., 1994. *A természetvédelmi területek földtani és hidrogeológiai elemzése (Geological and Hydrogeological Analysis of the Natural Reservation Areas),* Budapest: Magyar Állami Földtani Intézet.

Schweitzer, F., 2009. Relief and Landscapes. In: K. Kocsis & F. Schweitzer, eds. *Hungary in Maps.* Budapest: Geographical Research Institute Hungarian Academy of Sciences, pp. 38-44. Seed, H. B. & Idriss, I. M., 1971. Simplified Procedure for Evaluating Soil Liquefaction Potential. *Journal of the Soil Mechanics and Foundations Division,* Volume Vol. 97 No. 9, pp. 1249-1273.

Southern California Earthquake Center, 2001. *A Comparison of the February 28, 2001, Nisqually, Washington, and January 17, 1994, Northridge, California Earthquakes.* [Online] Available at: http://www.scec.org/news/01news/feature010313.html [Accessed 30 04 2014].

Spence, R., Coburn, A. W. & Pomonis, A., 1992. *Correlation of Ground Motion with Building Damage: The Definition of a New Damage-Based Seismic Intensity Scale.* Madrid, Spain, Tenth World Conference on Earthquake Engineering.

Srbulov, M., 2003. An Estimation of the Ratio between Horizontal Peak Accelerations at the Ground Surface and at Depth. *European Earthquake Engineering,* Volume Vol. XVII No. 1, p. 59–67.

Stewart, J. P. et al., 2001. *Ground Motion Evaluation Procedures for Performance-Based Design PEER Report 2001/09,* Berkeley: Pacific Earthquake Engineering Research Center, University of California.

SYNER-G, 2009-2012. *Systemic Seismic Vulnerability and Risk Analysis for Buildings, Lifeline Networks and Infrastructures Safety Gain.*[Online] Available at: http://www.vce.at/SYNER-G/ [Accessed 25 10 2013].

Szabó, M., 2005. *Vizes élőhelyek tájökológiai jellemvonásai a Szigetköz példáján (Szigetköz as an Example of the Ecological Characteristics of Wetland Landscapes).* Doctoral Dissertation ed. Budapest: s.n.

Szentendrei,L.,2013.*Példátlan földrengések várhatók Európában-HetiVálasz (Unprecedented earthquakes are expected in Europe).*[Online]

Available at: http://hetivalasz.hu/vilag/uj-meresi-eredmenyekre-tamaszkodnak-67624 [Accessed 15 04 2014].

Tate, E., Cutter, S. L. & Berry, M., 2010. Integrated Multihazard Mapping. *Environment and Planning B: Planning and Design,* Volume Vol. 37 No. 4, p. 646 – 663.

TCG, 2001. *Seismic retrofitting of existing buildings: Summary of the 1st phase of the.* Athens: Technical Chamber of Greece.

Tetra Tech, Inc., 2014. *New Jersey State Hazard Mitigation Plan 2014.* West Trenton, New Jersey: New Jersey Office of Emergency Management.

Teves-Costa, P., Almeida, I. M. & Silva, P. L., 2001. Microzonatiion of Lisbon: 1-D Theoretical Approach. *Pure and Applied Geophysics,* Volume Vol. 158, pp. 2579-2596.

Timár, G., Molnár, G. & Márta, G., 2003. A budapesti sztereografikus, ill. a régi magyarországi hengervetületek és geodéziai dátumaik paraméterezése a térinformatikai gyakorlat számára (Parameters of the Hungarian Stereographic and Old Zonal Cylindric Projections and Their Datums for the GIS). *Geodézia és Kartográfia,* Volume Vol. 53 No. 3, pp. 16-21.

Tóth, L., Győri, E. & Zsíros, T., 2006. Seismic Hazard in the Pannonian Region. In: N. Pintér, ed. *The Adria Microplate: GPS Geodesy, Tectonics and Hazards.* Netherlands: Springer, pp. 369-384..

Tóth, L. & Mónus, P., 2011. A földrengések és megfigyelőik (Earthquakes and their observers). *História,* Volume Vol. 04, pp. 13-16.

Tóth, L., Mónus, P. & Zsíros, T., 1996-2013. *Hungarian Earthquake Bulletin.* Budapest: GeoRisk Ltd..

Tóth, L., Mónus, P., Zsíros, T. & Kiszely, M., 2002. Seismicity in the Pannonian Region – Earthquake Data. *European Geosciences Union Stephan Mueller Special Publication Series,* Volume Vol. 3, pp. 9-28.

Trifunac, M. D. & Hudson, D. E., 1971. Analysis of the Pacoima Dam Accelerograms – San Fernando Earthquake of 1971. *Bulletin of the Seismological Society of America,* Volume Vol. 61, p. 1393–1411.

UNDRO, 1979. Natural Disasters and Vulnerability Analysis. In: *Report of Expert Group Meeting,.* Geneva: United Nations Disaster Relief Coordinator, pp. 1-49.

US Geological Survey,2014.Earthquake HazardProgram. [Online] Available at:http://earthquake.usgs.gov/earthquakes/?source=sitenav [Accessed 20 04 2014].

Varga, P., 2001. Budapest földrengés-veszélyeztetettsége (Seismic Hazard of Budapest). *Természet Világa,* Volume Vol. 132. Nr. 1., pp. 15-18.

Varga, P., 2011. Földrengések előrejelzése. *Magyar Tudomány (Hungarian Science),* Volume Vol. 7., pp. 843-860.

Varga, P., 2014. Az 1763. évi komáromi földrengés (The Komárom Earthquake of 1763). *Természet Világa,* Volume Vol. 145. Nr. 2..

Varga, P., Szeidovitz, G. & Gutdeutsch, R., 2001. Isoseismal Map and Tectonical Position of the Komárom Earthquake of 1763. *Acta Geod. Geoph. Hung.,* Volume Vol. 36 (1)., pp. 97-108..

Vaseva, 2002. *Seismic Vulnerability Assessment of Buildings in a Given Region According to EMS 98.* London, 12th ECEE.

Vaseva, E. & Kostov, M., 2002. *Seismic Vulnerabilty Assessment of Buildings in a Given Region According to EMS 98.* s.l., Elsevier Science Ltd..

Vidale, J. E. & Helmberger, D. V., 1988. Elastic Finite-difference Modeling of the 1971 San Fernando, California Earthquake. *Bulletin of the Seismological Society of America,* Volume Vol. 78 No. 1, pp. 122-141.

Villagrán De León, J. C., 2006. Vulnerability – A Conceptual and Methodological Review. *Publication Series of United Nations University - Institute for Environment and Human Security,* Volume No. 4.

Vucetic, M. & Dobry, R., 1991. Effect of Soil Plasticity on Cyclic Response. *Journal of the Geoechnical Engineering Division, ASCE,* Volume Vol. 117, No. 1, pp. 89-107.

Wair, B. R., DeJong, J. T. & Shantz, T., 2012. *Guidelines for Estimation of Shear Wave Velocity Profiles PEER Report 2012/8.* Berkeley, California: Pacific Earthquake Engineering Research Center Headquarters at the University of California.

Wenk, T. & Fäh, D., 2012. *Seismic Microzonation of the Basel Area.* Fifteenth World Conference on Earthquake Engineering, Lisbon, Portugal, International Association for Earthquake Engineering.

Western Transdanubia Water Authority, 2014. *A Mosoni-Duna és a Lajta folyó térségi vízgazdálkodási rehabilitációja (The Regional Water Management Rehabilitation of Moson-Danube and Leitha River).*[Online]

Available at:http://www.keopmosoniduna.hu/ [Accessed 02 05 2014].

Whitman, R. V., Reed, J. W. & Hong, S.-T., 1974. *Earthquake Damage Probability Matrices.* Rome, Fifth World Conference on Earthquake Engineering.

Winkler, G., Auer, J., Kottmayer, T. & Németh, I., 2006. 5.7.2. Győr - örökségvédelmi hatástanulmány a városrendezési tervek felülvizsgálatához (Heritage Impact Study for Urban

Planning - Győr). In: *Győr Megyei Jogú településrendezési eszközeinek felülvizsgálata - 2003-2005 (Evaluation of Settlement Assets in Győr).* Győr: Győr Megyei Jogú Város Önkormányzata.

Wood, H. & Neumann, F., 1933. The Modified Mercalli Intensity Scale of 1931. *Bulletin of the Seismological Society of America,* Volume Vol. 2, pp. 277-283.

Zeevaert, L., 1986. Consolodation in the Intergranular Viscosity of Highly Compressible Soils. In: R. N. Yong & F. C. Townsend, eds. *Consolodation of Soils: Testing and Evaluation, ASTM STP 892.* American Society for Testing and Materials, Philadelphia: American Society for Testing, pp. 257-281.

Zeevaert, L., 1991. Seismosoil Dynamics of Foundations in Mexico City Earthquake, September 19, 1985. *Journal of Geotechnical Engineering,* Volume Vol. 117, No. 3, pp. 376-428.

Zsíros, T., 2000. *A Kárpát-medence szeizmicitása és földrengés veszélyessége: Magyar földrengés katalógus (456-1995) (The Seismicity and Hazard of Carpathian Basin: Hungarian Earthquake Catalogue).* Budapest: MTA Földtudományi Kutatóközpont Geodéziai és Geofizikai Kutatóintézet.

DOI: 10.15477/SZE.MMTDI.2015.002

Annexes

EMS Building Classification

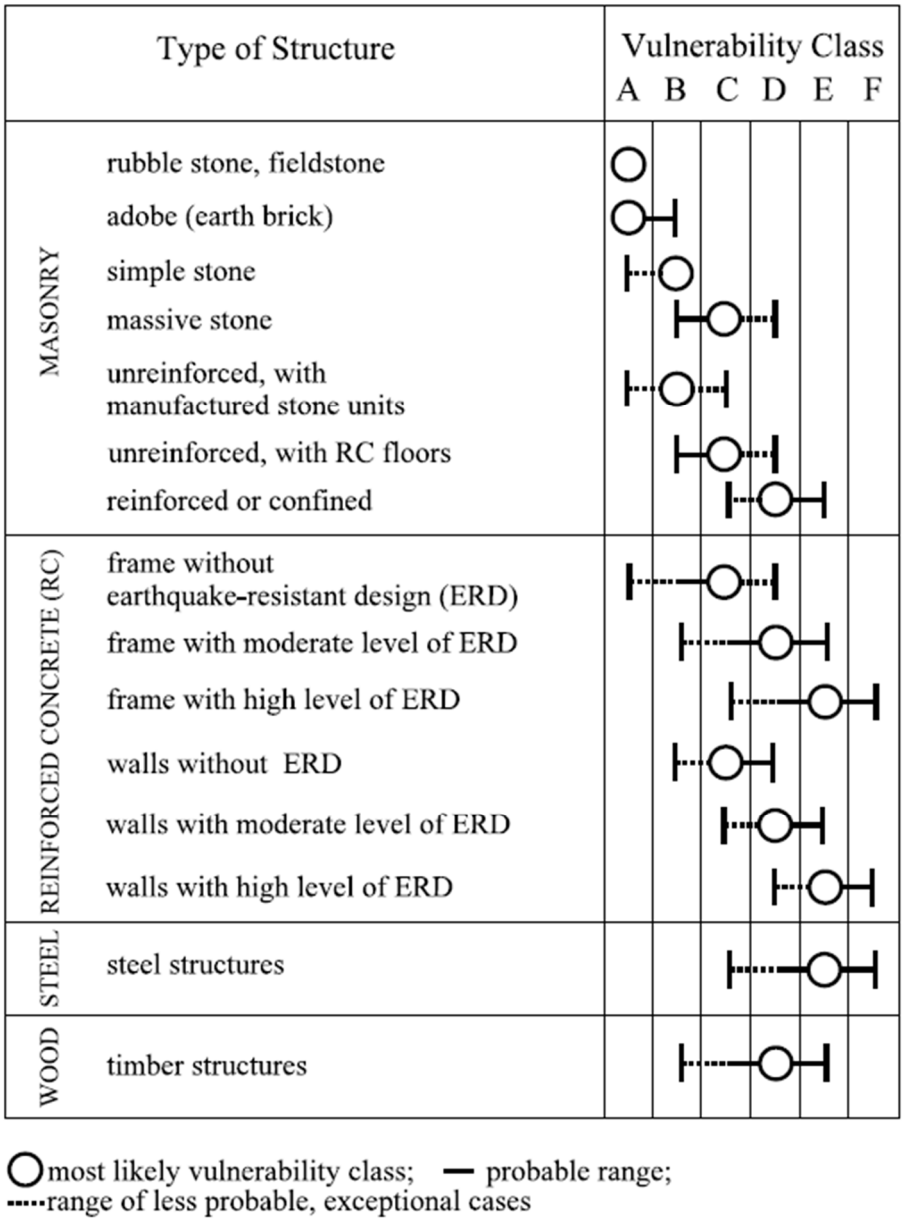

DOI: 10.15477/SZE.MMTDI.2015.002

Layout Map of Geological Observation Sites

Hungarian Geological Institute (Scharek, 1990) (Scharek, 1991)
Compiled North and South Győr – Geological Variant

Compiled by Síkhegyi F., 1982.
Scientific editor: dr. Scharek P.
Responsible editor: dr. Hámori G.

A TÉRKÉPEZÉS SORÁN LEMÉLYÍTETT FÚRÁSOK

149 Sekélyfúrás (10—15 m mély) sorszámmal

9 Kismélységű fúrás (30—40 m mély) sorszámmal

2 A fúrás megfigyelőkúttá kiépítve, sorszámmal

507 Mérnökgeofizikai szondázás helye és száma

146 Paraméter szondázás sekélyfúrási ponton, a fúrás és a szondázás sorszámával

JELENTŐSEBB TERMÉSZETES ÉS MESTERSÉGES FELTÁRÁSOK

4006 Feltárás jele és száma

DOI: 10.15477/SZE.MMTDI.2015.002

Thickness of the Quaternary Deposits

Hungarian Geological Institute (Scharek, 1990) (Scharek, 1991)
Compiled North and South Győr – Geological Variant

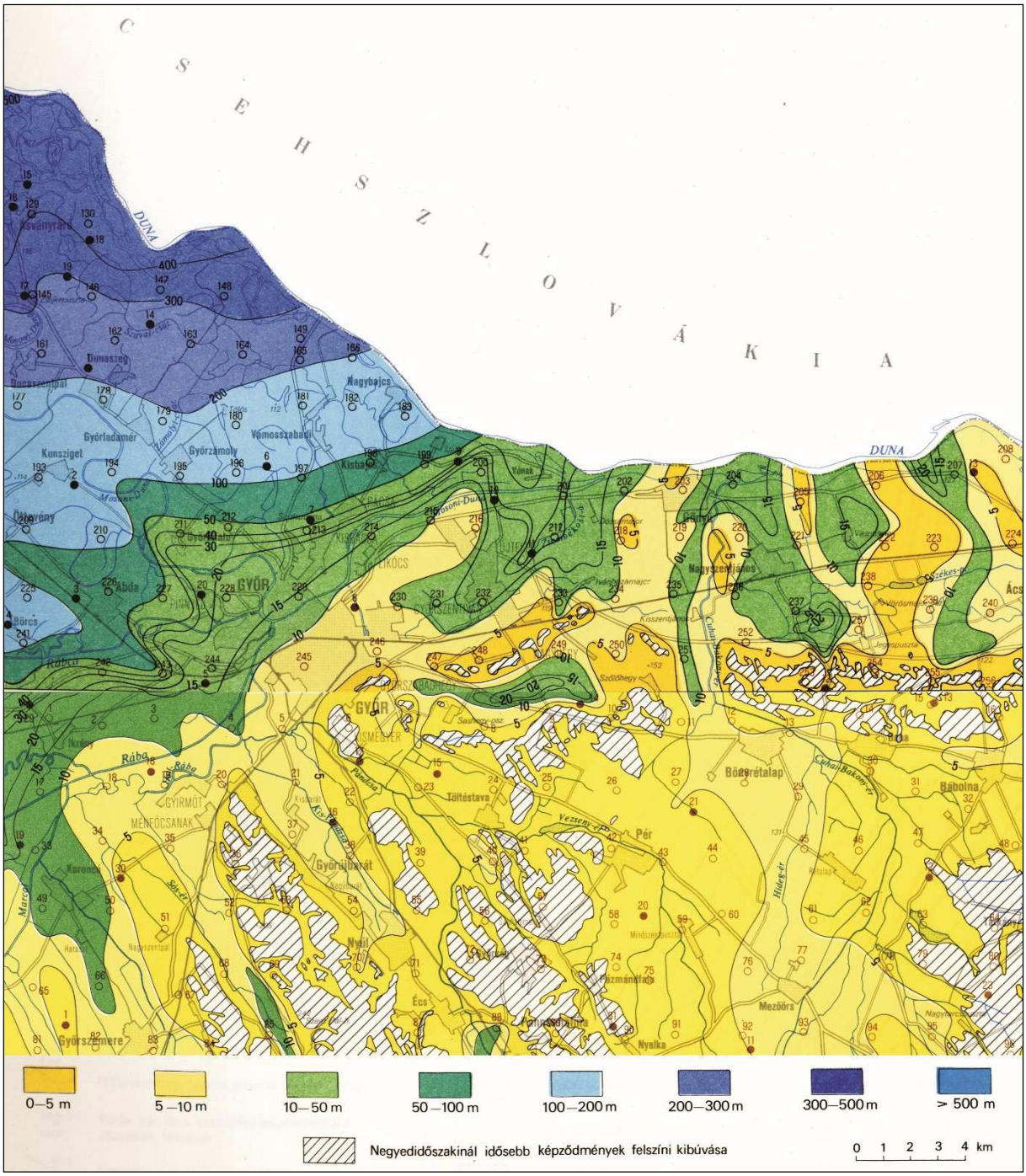

Compiled by Don Gy. and Dudás J., 1986.
Scientific editor: dr. Scharek P.
Responsible editor: dr. Hámori G.

DOI: 10.15477/SZE.MMTDI.2015.002

Position of the Basement of Pannonian Deposits

Hungarian Geological Institute (Scharek, 1990) (Scharek, 1991)
Compiled North and South Győr – Geological Variant

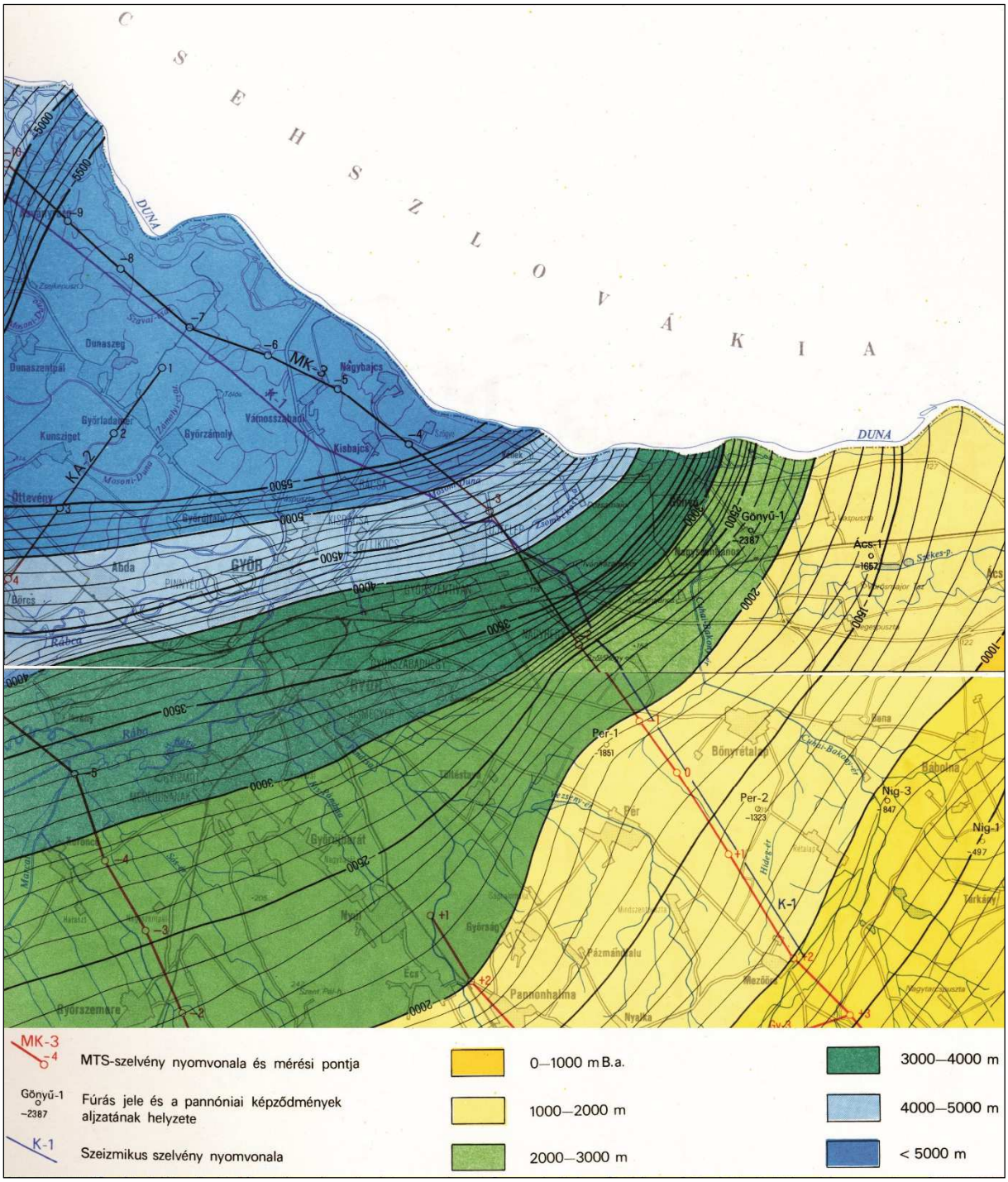

Compiled by Don Gy.,1990.
Scientific editor: dr. Scharek P.
Responsible editor: dr. Gaál G.

DOI: 10.15477/SZE.MMTDI.2015.002

Number of Residents in Different City Districts of Győr

HISTORICAL URBAN					TOTAL
Function of the area	**Belváros**	**Nádorváros**	**Újváros**	**Révfalu**	
special (cultural, educational, ecclesiastic)	69.79%	14.72%	5.94%	9.57%	
Total area [ha]	90.49	256.37	117.39	263.81	*728*
Number of residents	**10,358**	**20,130**	**4,397**	**6,640**	***41,525***

HOUSING ESTATES					TOTAL
Function of the area	**Adyváros**	**Marcal-város I.**	**Marcal-város II.**	**József A. lt.**	
urban residential	44.70%	32.46%	15.99%	47.16%	
Total area [ha]	57.81	38.68	92.49	25.53	*215*
Number of residents	**17,156**	**11,423**	**6,841**	**4,508**	***39,928***

GARDEN CITIES						TOTAL
Function of the area	**Gorkij-város**	**Sziget**	**Gyárváros 4.**	**Jancsifalu**	**Szabad-hegy**	
rural residential	100.00%	7.55%	51.56%	54.40%	47.17%	
garden city residential	-	44.02%	23.91%	7.34%	26.94%	
Total area [ha]	10.74	55.13	38.61	15.73	297.04	*417*
Number of residents	**892**	**4,556**	**4,898**	**1,727**	**8,121**	***20,194***

ATTACHED VILLAGES					
Function of the area	**Pinnyéd**	**Kisbácsa**	**Bácsa**	**Győrszentiván**	
rural residential	58.45%	84.38%	85.82%	66.20%	
Total area [ha]	95.74	130.47	76.13	634.24	
Number of residents	**646**	**3,045**	**2,378**	**8,172**	

ATTACHED VILLAGES					TOTAL
Function of the area	**Likócs**	**Kismegyer**	**Gyirmót**	**Ménfőcsanak**	
rural residential	66.75%	55.37%	54.09%	75.19%	
Total area [ha]	61.12	110.47	176.20	560.80	*1,845*
Number of residents	**1,365**	**1,344**	**1,273**	**6,964**	***25,187***

DOI: 10.15477/SZE.MMTDI.2015.002

Checklist for Building Data

Buildings – points of data collection

1. IDENTIFICATION OF THE BUILDING

1.1. Number of the building (Generated from the sign of the territory, name of the street and number of the house)

1.2. Function
- residential
- public
- other

1.3. Two picture of the building should be uploaded illustrating
- mass of the building
- relationship to adjacent buildings

2. GENERAL DATA

2.1. Construction date
- before 1910
- 1910-1945
- 1945-1990
- 1990-2006
- after 2006

2.2. State of the building
- good (recently built of renovated)
- good from structural point, minor restoration needed
- significantly degraded with noticeable structural damages

2.3. Relationship to adjacent buildings
- free standing
- on one site built together with same height
- on one site built together with different height
- on two site built together with same height
- on two site built together with different height
- other

2.4. Mass or elevation
- compact
- irregular

2.5. Layout
- regular
- irregular

2.6. Form of the roof
- flat roof
- low-pitched roof
- high roof
- other
  - bound by gables
    - yes
    - no
    - cannot be defined

2.7. Basement
- yes
- no
- subsequently buried
- cannot be defined

2.8. Number of stories (without basements and attic)
- F (ground floor)
- F + 1 E (ground floor and one story)
- F + 2 E
- F + 3 E
- F + 4 E
- F + 5 E
- F + 6 E
- F + 7 E
- F + 8 E
- F + 9 E
- F + 10 E

2.9. Attic is used for living space
- yes
- no
- cannot be defined

3. STRUCTURAL DATA

3.1. Structural system
- prefabricated frame (RC)
- prefabricated panel structure (RC)
- moment resistant frame (steel, RC)
- column beam system with infill walls (steel, RC, wood)
- column beam system with fitted walls (steel, RC, wood)
- cast walls (RC tunnel formwork or story high formwork)
- mushroom slab with columns (RC)
- loadbearing walls (masonry, stone, mixed, clay)
- reinforced walls (masonry, stone, mixed)
- other

3.2. Later conversions
- there was not any
- cannot be defined
- there was
  - redemption on ground floor, joint spaces
  - redemption in attic, joint spaces
  - structural reconstruction of the elevation (e.g. altering the openings, new openings)
  - posterior strengthening

3.3. Direction of structural system
- parallel to the plain of street elevation
- perpendicular to the plain of street elevation
- bidirectional
- mixed: various direction in different parts of the building

3.4. Orientation (of the plain of street elevation)
- N
- NE
- E
- SE
- S
- SW
- W
- NW

3.5. Type of foundation
- strip foundation
- base plate
- pile foundation
- mixed
- cannot be defined

3.6. Material of vertical structure (column, wall, etc.)
- clay
- masonry
- stone
- wood
- steel
- reinforced concrete
- slag concrete
- aerated concrete
- other

3.7. Material of horizontal structure, type of the slab
- timber (closely placed joists, beam slab, covered slab, plank slab)
- brick vault (Prussian vault, other vaults)
- reinforced concrete slab (ribbed or plain)
- prefabricated beam and fillers
- other

3.8. Material of roof
- wood
- steel
- reinforced concrete (beam or coffin slab)
- other

3.9. Type of shell
- easy (bit. shingles, metal roofing)
- heavy (slate, tile)
- other

The questionnaire should be filled online at se.sze.hu.

DOI: 10.15477/SZE.MMTDI.2015.002

Further Examined Areas of Győr

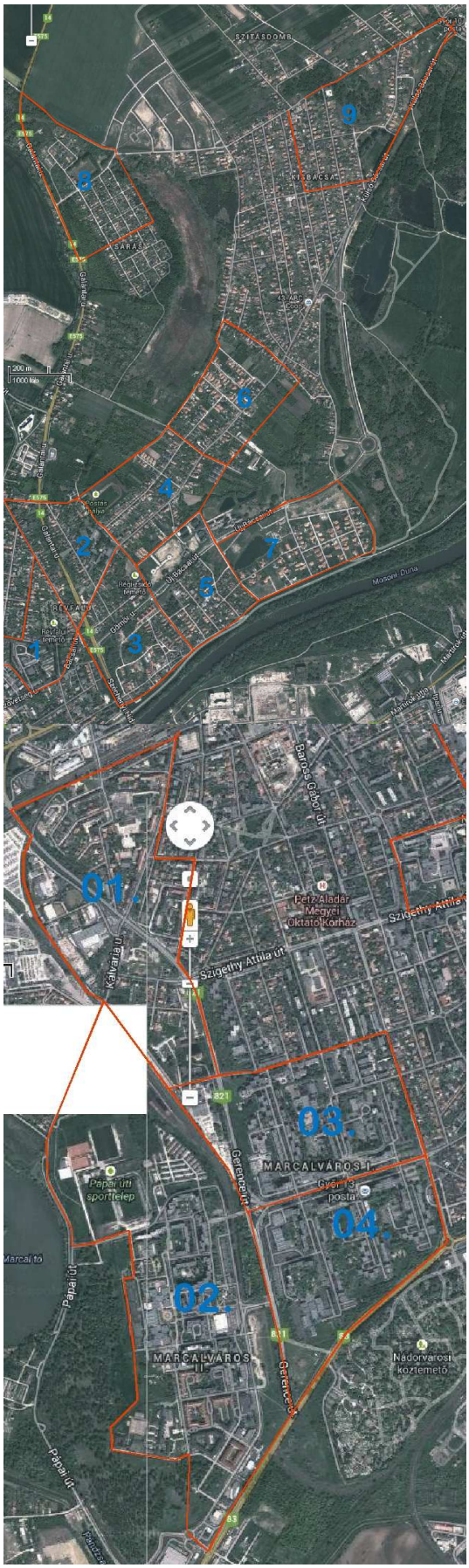

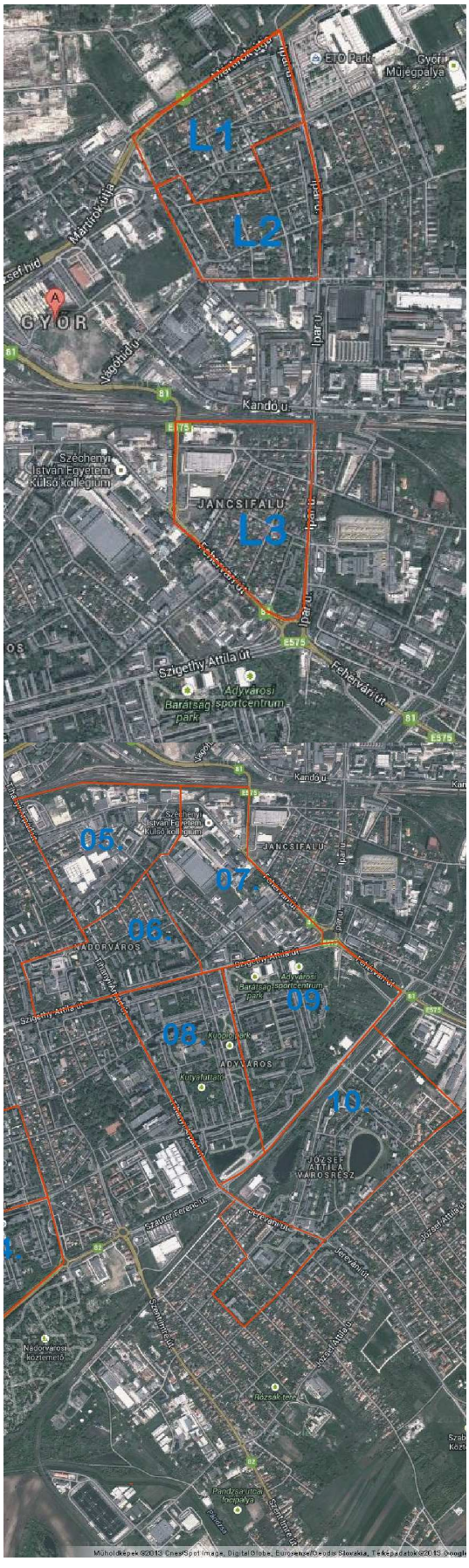

DOI: 10.15477/SZE.MMTDI.2015.002

Number of earthquakes within 100 km radius around Győr

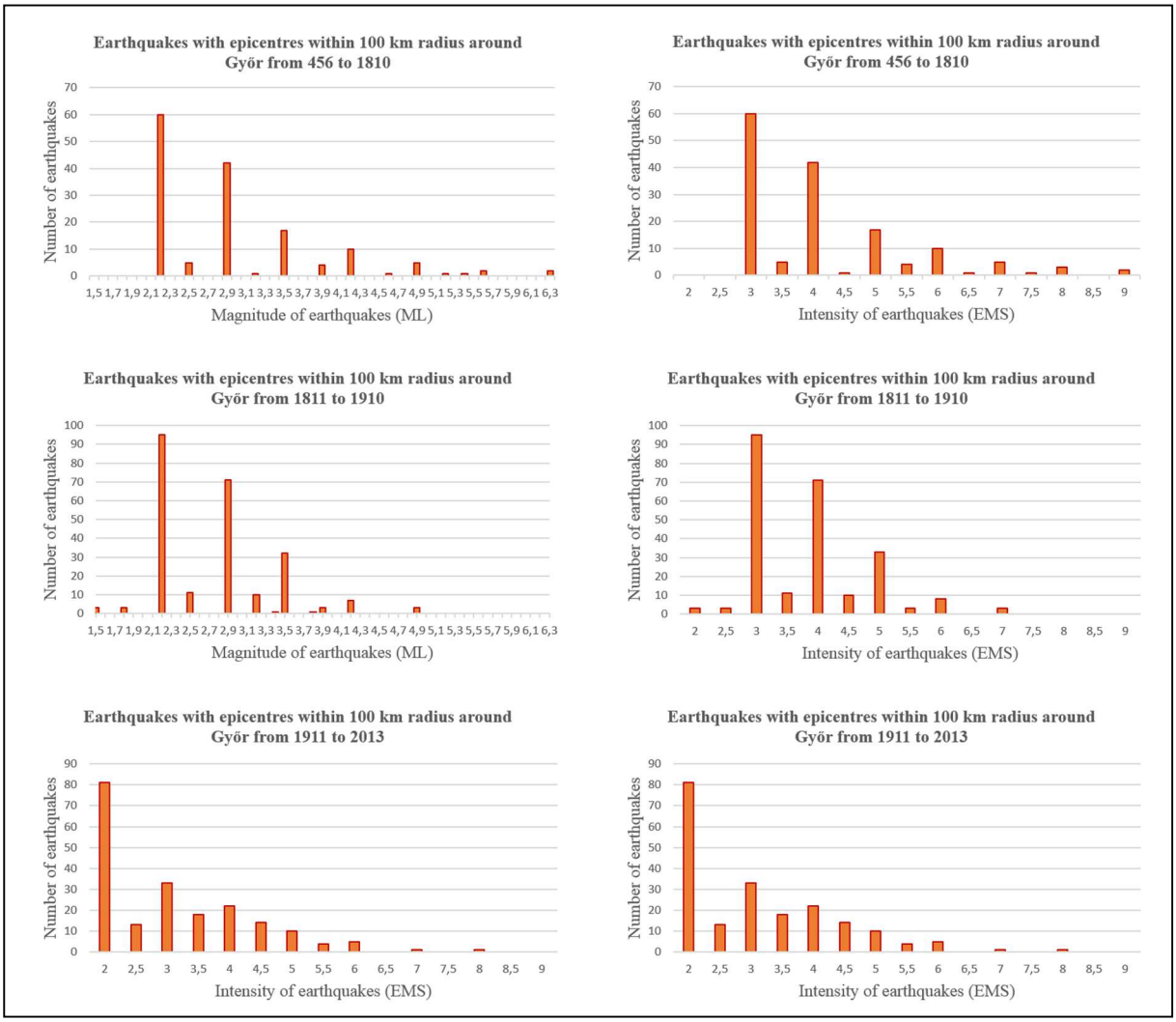

DOI: 10.15477/SZE.MMTDI.2015.002

MASW and CPT Correlations

Belváros (MASW: Színház, CPT: Dunakapu tér) soil type: C

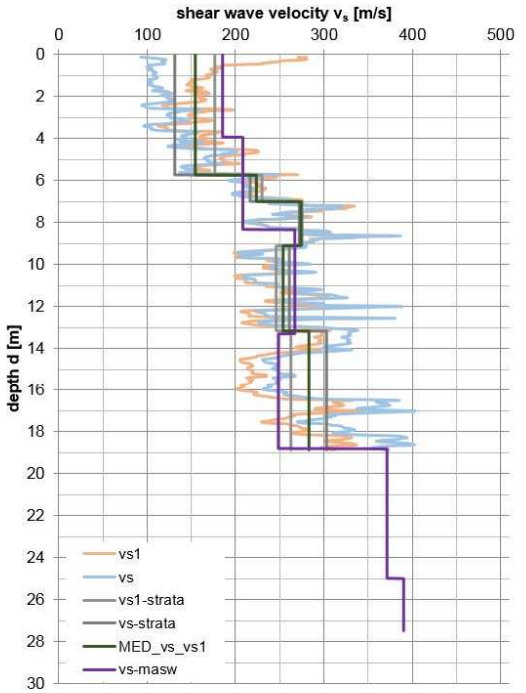

d = 19 m
$v_{s\text{-}strata\_MED}$ = 232.492 m/s
$v_{s\text{-}masw}$ = 231.50 m/s
DIFF = 0.354 %

v_{s30} = 286.455 m/s

Gyárváros (MASW: Rába Gépgyár, CPT Audi) soil type: C

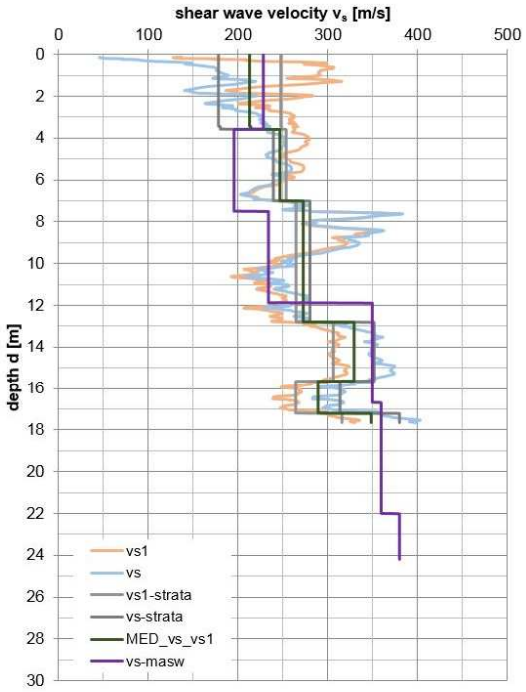

d = 17.68 m
$v_{s\text{-}strata\_MED}$ = 268.382 m/s
$v_{s\text{-}masw}$ = 262.738 m/s
DIFF = 5.266 %

v_{s30} = 307.67 m/s

Jedlik-híd Sziget (MASW: Kekszgyár, CPT: Jedlik-híd) soil type: C

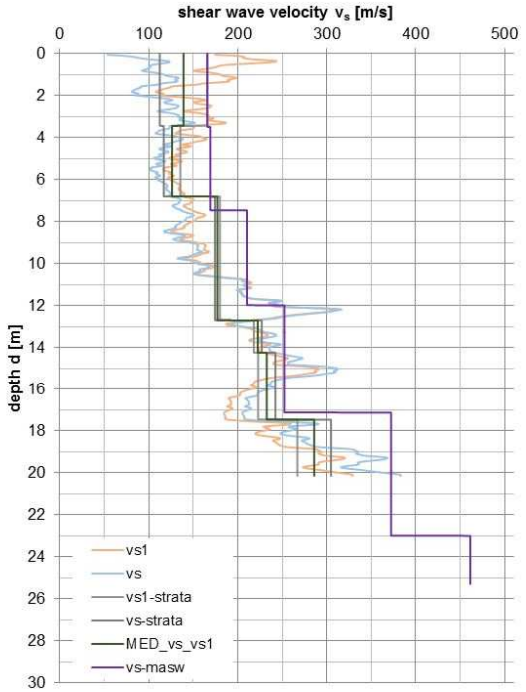

d = 20.15 m
$v_{s\text{-}strata\_MED}$ = 189.074 m/s
$v_{s\text{-}masw}$ = 229.688 m/s
DIFF = 18.043 %

v_{s30} = 297.229 m/s

Jedlik-híd Révfalu (MASW: Aranypart, CPT: Jedlik-híd) soil type: C

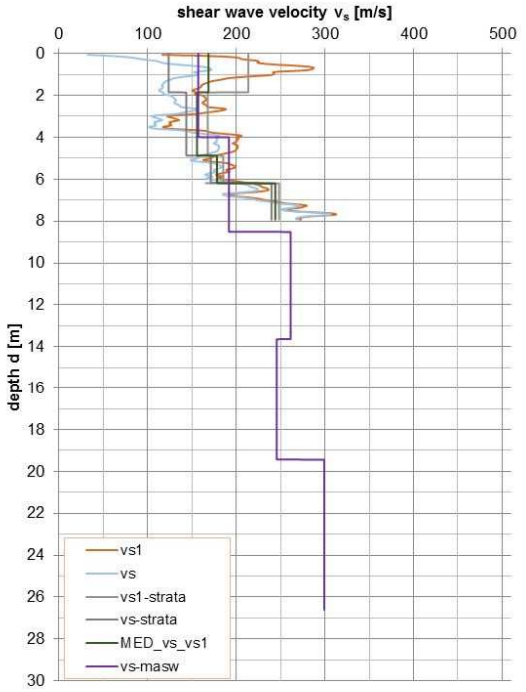

d = 7.93 m
$v_{s\text{-}strata\_MED}$ = 182.105 m/s
$v_{s\text{-}masw}$ = 174.483 m/s
DIFF = 4.242 %

v_{s30} = 258.628 m/s

DOI: 10.15477/SZE.MMTDI.2015.002

Soil Categorization of Upper 15 m in Case of Each Boring (A3 print)

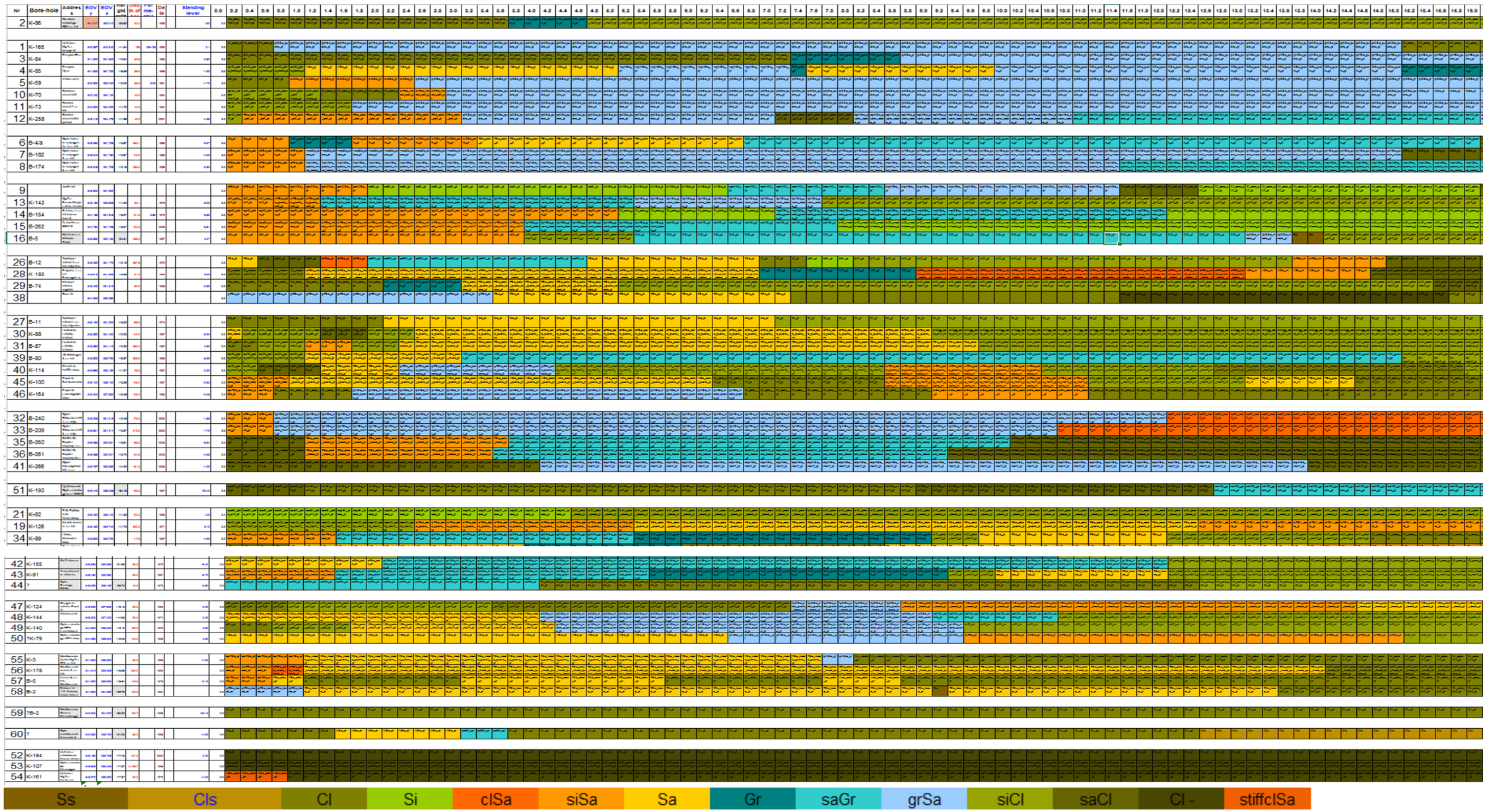

DOI: 10.15477/SZE.MMTDI.2015.002

Identification of v_s Values for Each Soil Category Varied by Depth (A3 print)

total error: 393,097

	Ss	Cls	Cl	Sl	olSa	slSa	Sa	Gr	saGr	grSa	slCl	saCl	stiffCl	stiffclSa
	1	2	3	4	5	6	7	8	9	10	11	12	13	14
alpha	250	200	190	180	185	155	185	180	195	155	185	185	200	195
beta	0.305	0.27	0.1858351	0.1181184	0.213631281	0.2086823	0.2186484	0.22	0.19	0.1460761	0.2045977	0.2462681	0.321949917	0.3388447
MidDepth	1. Battyányi tér	Soil type III.			2. Kékszigyár	Soil type II.			3.Víztükör ltp.	Soil type III.			4. OBI mellett	Soil type IV.
(m)	Soil	Vs	Vs Comp	Error^2	Soil	Vs	Vs Comp	Error^2	Soil	Vs	Vs Comp	Error^2	Soil	Vs	Vs Comp	Error^2
0.5	ogrCl_calc_pl	185.35	134.12572	2623.9264	bFSa_calc_pl	165.844	134.12572	1006.049	clFSa_calc_quartz_soft_pl	131.443	134.12572	7.1970111	Cl_mcalc_mstiff_pl	170.964	167.0366	15.42444859
1.5	ogrCl_calc_pl	185.35	168.66891	277.69176	fgrMSa_quartz_musc_lo	165.844	164.45778	1.9216137	clFSa_mcalc_quartz_loose_pl	131.443	164.45778	1089.9758	clFSa_mcalc_quartz_loos	170.964	202.15003	972.5683346
2.5	ogrCl_calc_pl	185.35	187.6613	5.3420964	fgrMSa_quartz_musc_lo	165.844	177.19898	128.93548	fgrMSa_quartz_loose_pl	131.443	177.19898	2093.6093	clFSa_mcalc_quartz_loos	170.964	226.0376	3033.101342
3.5	ogrCl_calc_pl	185.35	201.31171	254.77625	fgrMSa_quartz_musc_lo	165.844	186.12599	411.35904	fgrMSa_quartz_loose_pl	131.443	186.12599	2990.2292	clFSa_mcalc_quartz_loos	170.964	243.29397	5231.62508
4.5	Cl_calc_pl	208.4	214.99528	43.497704	fgrMSa_quartz_musc_lo	169.223	193.08583	569.43481	fgrMSa_quartz_loose_pl	194.17	193.08583	1.1754178	clFSa_mcalc_quartz_loos	218.341	257.03698	1497.379254
5.5	Cl_calc_pl	208.4	220.15217	138.11341	fgrMSa_quartz_musc_lo	169.223	198.82957	876.54876	fgrMSa_quartz_loose_pl	194.17	198.82957	21.711557	clFSa_mcalc_quartz_loos	218.341	268.5659	2522.540467
6.5	Cl_calc_pl	208.4	224.53939	260.4798	fgrMSa_quartz_musc_lo	169.223	203.74121	1191.5068	fgrMSa_quartz_loose_pl	194.17	203.74121	91.608059	clFSa_mcalc_quartz_loos	218.341	278.55692	3625.957402
7.5	Cl_calc_pl	208.4	228.367	398.68101	fgrMSa_quartz_musc_lo	210.433	208.04496	5.7027275	fgrMSa_quartz_loose_pl	194.17	208.04496	192.51456	clFSa_mcalc_quartz_loos	218.341	287.41041	4770.583827
8.5	mgrCSa_calc_quartz_pl	267.23	292.83583	655.6583	fgrMSa_quartz_musc_lo	210.433	211.8837	2.1045411	clCl_calc_stiff_pl	266.204	286.63467	417.41246	clFSa_mcalc_quartz_loos	324.487	292.22992	1040.519015
9.5	mgrCSa_calc_quartz_pl	267.23	299.09014	1015.0688	fgrMSa_quartz_musc_lo	210.433	215.35438	24.22	clCl_calc_stiff_pl	266.204	293.23226	730.52707	clFSa_mcalc_quartz_loos	324.487	299.25683	636.5613725
10.5	mgrCSa_calc_quartz_pl	267.23	304.83202	1413.9116	fgrMSa_quartz_musc_lo	210.433	218.52595	65.495787	clCl_calc_stiff_pl	266.204	299.29863	1095.2549	clFSa_mcalc_quartz_loos	324.487	305.72412	352.045601
11.5	mgrCSa_calc_quartz_pl	267.23	310.14673	1841.8454	fgrMSa_quartz_musc_lo	210.433	221.44927	121.35831	clCl_calc_stiff_pl	266.204	304.92153	1499.0473	clFSa_mcalc_quartz_loos	324.487	311.7238	162.899191
12.5	mgrCSa_calc_quartz_pl	267.23	315.09935	2291.4751	fgrMSa_quartz_musc_lo	252.468	224.16303	801.17115	clCl_calc_stiff_pl	266.204	310.16802	1932.8353	clFSa_mcalc_quartz_loos	324.487	317.32626	51.27613497
13.5	mgrCSa_calc_quartz_pl	267.23	319.74078	2757.3818	fgrMSa_quartz_musc_lo	252.468	226.69733	664.12744	clCl_calc_stiff_pl	333.768	315.0906	348.8453	MSa_ml	264.628	266.81626	4.788483931
14.5	Cl_calc_pl	248.547	246.86041	2.8446017	fgrMSa_quartz_musc_lo	252.468	229.07609	547.18141	clCl_calc_stiff_pl	333.768	319.73117	197.03254	MSa_ml	264.628	270.8249	38.40153391
15.5	Cl_calc_pl	248.547	248.81272	0.0706084	fgrMSa_quartz_musc_lo	252.468	231.31866	447.29462	clCl_calc_stiff_pl	333.768	324.12377	93.01111	MSa_ml	264.628	274.6204	99.84806676
16.5	Cl_calc_pl	248.547	250.65696	4.4519187	fgrMSa_quartz_musc_lo	252.468	233.44091	362.03032	clCl_calc_stiff_pl	333.768	328.29644	29.937965	MSa_ml	264.628	278.22682	184.9278342
17.5	Cl_calc_pl	248.547	252.40513	14.885147	saCl_ml	372.378	374.36248	3.9381452	clCl_calc_stiff_pl	333.768	332.27257	2.2363227	MSa_ml	264.628	281.66422	290.2326635
18.5	Cl_calc_pl	248.547	254.06732	30.473921	saCl_ml	372.378	379.52087	51.020628	clCl_calc_stiff_pl	378.523	336.07188	1802.0972	saCl_calc_mstiff_ml	443.049	379.52087	4035.822978
19.5	MSa_calc_pl	371.714	354.18957	307.10561	saCl_ml	372.378	384.47319	146.29368	clCl_calc_stiff_pl	378.523	339.71121	1506.3552	saCl_calc_mstiff_ml	443.049	384.47319	3431.125222
20.5	MSa_calc_pl	371.714	358.08378	185.7829	saCl_ml	372.378	389.23763	284.24719	clCl_calc_stiff_pl	378.523	343.20498	1247.3623	saCl_calc_mstiff_ml	443.049	389.23763	2895.66334
21.5	saCl_calc_pl	371.714	346.56572	632.43586	saCl_ml	372.378	393.82998	460.18762	clCl_calc_stiff_pl	378.523	346.56572	1021.2676	saCl_calc_mstiff_ml	443.049	393.82998	2422.511527
22.5	saCl_calc_pl	371.714	349.80434	480.03313	saCl_ml	372.378	398.26405	670.08774	clCl_calc_stiff_pl	378.523	349.80434	824.76133	saCl_calc_mstiff_ml	443.049	398.26405	2005.691483
23.5	saCl_calc_pl	371.714	352.93042	352.82284	mgrMSa_quartz_musc_lo	461.292	355.2528	11244.313	clCl_calc_stiff_pl	378.523	352.93042	654.98011	saCl_calc_mstiff_ml	443.049	402.55198	1640.008669
24.5	saCl_calc_pl	371.714	355.95242	248.42742	mgrMSa_quartz_musc_lo	461.292	358.07679	10653.38	clCl_calc_stiff_pl	365.185	355.95242	85.240546	saCl_calc_mstiff_ml	426.092	406.7045	375.8750525
25.5	Msa_calc_pl	390.548	375.58612	223.85799	fsaCl_ml	420	410.73117	85.91115	clCl_calc_stiff_pl	365.185	358.87785	39.780191	saCl_calc_mstiff_ml	426.092	410.73117	235.9549999
26.5	Msa_calc_pl	390.548	378.75834	138.99612	fsaCl_ml	420	414.64052	28.723984	clCl_calc_stiff_pl	370	361.7134	68.667758	saCl_calc_mstiff_ml	426.092	414.64052	131.136304
27.5	Msa_calc_pl	390.548	381.83836	75.857758	clFSa_ml	380	375.54174	19.876076	clCl_calc_stiff_pl	370	364.46508	30.635348	saCl_calc_mstiff_ml	426	418.44021	57.15037632
28.5	Cl_pl	370	354.09101	253.0959	clFSa_ml	380	378.41827	2.5018618	clCl_calc_stiff_pl	370	367.13829	8.1894015	saCl_calc_mstiff_ml	426	422.13714	14.92166855
29.5	Cl_pl	370	356.36758	185.84294	fsaCl_ml	430	425.73755	18.168441	clCl_calc_stiff_pl	370	369.7379	0.0686969	saCl_calc_mstiff_ml	426	425.73755	0.068877594
30.5	Cl_pl	370	358.58216	130.36718	fsaCl_ml	430	429.24712	0.5668329	clCl_calc_stiff_pl	370	372.26834	5.1453518	saCl_calc_mstiff_ml	426	429.24712	10.54376857
31.5																

	5. Bem tér	Soil type IV.			6. Marcalliváros, Iskola	Soil type V.			7. Szabadh. TV tower 2.	Soil type VII.			8. Ifjúság körút	Soil type VII.			9. Rába Gépgyár 2.
	Soil	Vs	Vs Comp	Error^2	Soil	Vs	Vs Comp	Error^2	Soil	Vs	Vs Comp	Error^2	Soil	Vs	Vs Comp	Error^2	Soil
0.5	grFSa_pl	153.621	140.07429	183.51342	clFSa_calc_pl	185	134.12572	2588.1919	csaCL_stiff_pl	193.857	155.96877	1435.5176	saCl_loose_pl	159.797	155.96877	14.655332	Cl_mcalc_pl
1.5	grFSa_pl	153.621	164.45778	117.43574	CL_calc_pl	185	204.86961	394.80149	csaCL_stiff_pl	193.857	204.42659	111.71622	FSa_calc_quartz_loose_pl	159.797	202.15003	1793.779	FSa_calc_loose_pl
2.5	grFSa_pl	153.621	177.19898	555.92095	CL_calc_pl	185	225.27077	1621.7347	csaCL_stiff_pl	193.857	231.83107	1442.0303	grFSa_calc_quartz_loose_pl	197.513	177.19898	412.65957	FSa_calc_loose_pl
3.5	FSa_ol	222.73	243.29397	422.87701	grMSa_mcalc_quartz_pl	204	186.12599	319.48031	csaCL_stiff_pl	193.857	251.86949	3364.2886	grFSa_calc_quartz_loose_pl	197.513	186.12599	129.66404	FSa_calc_loose_pl
4.5	FSa_ol	222.73	257.03698	1176.9692	grMSa_mcalc_quartz_pl	204	193.08583	119.11904	clMSa_mstiff_pl	236.492	251.27162	218.4372	grFSa_calc_quartz_loose_pl	197.513	193.08583	19.599806	csaCGr_calc_loose_pl
5.5	FSa_ol	222.73	268.5659	2100.9296	grMSa_mcalc_quartz_pl	204	198.82957	26.733396	clMSa_mstiff_pl	236.492	260.81887	591.79655	siCl_mcalc_mstiff_ml	262.167	262.2094	0.0017974	csaCGr_calc_loose_pl
6.5	FSa_ol	222.73	278.55692	3116.6453	Cl_calc__pl	242	269.04286	731.31626	clMSa_mstiff_pl	236.492	269.04286	1059.5585	siCl_mcalc_mstiff_ml	262.167	271.32634	83.893456	csaCGr_calc_loose_pl
7.5		263.948	279.38769	238.38413	Cl_calc__pl	242	276.29354	1176.0471	clMSa_mstiff_pl	236.492	276.29354	1584.1628	siCl_mcalc_mstiff_ml	262.167	279.38769	296.55228	csaCGr_calc_loose_pl
8.5		263.948	286.63467	514.6862	Cl_calc__pl	242	282.79537	1664.2625	clMSa_mstiff_pl	236.492	282.79537	2144.0024	siCl_mcalc_mstiff_ml	262.167	286.63467	598.6671	clFSa_calc-loose_pl
9.5		263.948	293.23226	857.56813	siSa_calc_pl	333	302.65512	920.75112	clMSa_mstiff_pl	378.12	322.07264	3141.3064	siFSa_calc_quartz_loose_pl	309.658	247.95066	3807.7964	clFSa_calc-loose_pl
10.5		263.948	299.29863	1249.6674	siSa_calc_pl	333	309.35217	559.21995	clMSa_mstiff_pl	378.12	330.10952	2305.0063	siFSa_calc_quartz_loose_pl	309.658	253.18372	3189.3441	clFSa_calc-loose_pl
11.5	aiCl_pl	424.767	439.05768	204.22352	Cl_calc_pl	333	299.1359	1146.7773	clMSa_mstiff_pl	378.12	337.58857	1642.7965	siCl_calc_mstiff_ml	309.658	304.92153	22.434126	clFSa_calc-loose_pl
12.5	aiCl_pl	424.767	451.00368	688.36328	Cl_calc_pl	333	303.80718	852.22089	clMSa_mstiff_pl	378.12	344.59236	1124.1028	siCl_calc_mstiff_ml	309.658	310.16802	0.2601234	clFSa_calc-loose_pl
13.5	aiCl_pl	424.767	462.31806	1410.0821	saCl_calc_pl	361	351.18572	725.45556	clMSa_mstiff_pl	378.12	351.18572	725.45556	siCl_calc_mstiff_ml	330.724	308.18347	508.07558	saCl_calc_mstiff_pl
14.5	aiCl_pl	424.767	473.07754	2333.9081	saCl_calc_pl	361	357.42061	12.812065	clMSa_mstiff_pl	378.12	357.42061	428.46493	Cl_mcalc_mstiff_ml	330.724	312.30331	339.32176	saCl_calc_mstiff_pl
15.5	aiCl_pl	424.767	483.34495	3431.3765	saCl_calc_pl	361	363.33934	5.4724992	saMGr_quartz_pl	329.97	328.24463	2.9768908	Cl_mcalc_mstiff_ml	330.724	316.19796	211.00568	saCl_calc_mstiff_pl
16.5	saCl_ml	312.048	328.29644	264.01181	saCl_calc_pl	361	368.97688	63.630571	saMGr_quartz_pl	329.97	332.16706	4.8270665	Cl_mcalc_mstiff_ml	330.724	319.89312	117.3079	saCl_calc_mstiff_pl
17.5	saCl_ml	312.048	332.27257	409.03307	saCl_calc_pl	361	374.36248	178.55577	saMGr_quartz_pl	329.97	335.90142	35.181751	siCl_mcalc_mstiff_ml	336.016	332.27257	14.013298	saCl_calc_mstiff_pl
18.5	saCl_ml	312.048	336.07188	577.14703	saCl_calc_pl	344	379.52087	1261.7324	saMGr_quartz_pl	329.97	339.46675	90.188219	siCl_mcalc_mstiff_ml	336.016	336.07188	0.0031231	saCl_calc_mstiff_pl
19.5	saCl_ml	312.048	339.71121	765.25306	saCl_calc_pl	344	384.47319	1638.0793	saMGr_quartz_pl	329.97	342.87924	166.6484	siCl_mcalc_mstiff_ml	336	339.71121	13.773062	FSa_pl
20.5	saCl_ml	312.048	343.20498	970.75757	saCl_calc_pl	370	389.23763	370.08648	clFSa_mstiff_pl	329.97	346.1528	261.88291	Cl_calc_mstiff_ml	390	389.23763	0.5812052	FSa_pl
21.5	saCl_ml	312.048	346.56572	1191.4732	saCl_calc_pl	370	393.82998	567.86814	clFSa_mstiff_pl	338.41	356.30528	320.24119	Cl_calc_mstiff_ml	390	393.82998	14.668778	clFSa_calc__pl
22.5	aiCl_pl	405.335	398.26405	49.998292	saCl_calc_pl	370	398.26405	798.85669	clFSa_mstiff_pl	338.41	359.78265	456.78999	Cl_calc_mstiff_ml	390	398.26405	68.294571	clFSa_calc__pl
23.5	aiCl_pl	405.335	402.55198	7.7452044	saCl_calc_pl	370	402.55198	1059.6314	clFSa_mstiff_pl	338.41	363.14052	611.59864	Cl_calc_mstiff_ml	390	402.55198	157.55218	clFSa_calc__pl
24.5	aiCl_pl	405	406.7045	2.9053294	saCl_calc_pl	370	406.7045	1347.2205	clFSa_mstiff_pl	338.41	366.38788	782.75983	Cl_calc_mstiff_ml	390	406.7045	279.04041	clFSa_calc__pl
25.5		420	410.73117	85.91115	saCl_calc_pl	400	410.73117	115.15808	clFSa_mstiff_pl	338.41	369.53256	968.61361	Cl_calc_mstiff_ml	390	410.73117	429.78154	clFSa_calc__pl
26.5		420	414.64052	28.723984	saCl_calc_pl	400	414.64052	214.34494	clFSa_mstiff_pl	338.41	372.58174	1167.7078		370	361.7134	68.667758	Cl_calc_pl
27.5		420	418.44021	2.4329348	saCl_calc_pl	400	418.44021	340.04146	clFSa_mstiff_pl	338.41	375.54174	1378.7662		370	364.46508	30.635348	Cl_calc_pl
28.5		420	422.13714	4.5673776	saCl_calc_pl	400	422.13714	490.05308	saCl_stiff_pl	521.232	588.05396	4465.1742		370	367.13829	8.1894015	clFSa_calc__pl
29.5		420	425.73755	32.919533	MSa_calc_loose_pl	400	387.74482	150.18947	saCl_stiff_pl	521.232	594.6194	5385.7101		370	369.7379	0.0686969	clFSa_calc__pl
30.5		420	429.24712	85.509172	MSa_calc_loose_pl	400	390.5814	88.710049	saCl_stiff_pl	521.232	601.03561	6368.6168		370	372.26834	5.1453518	clFSa_calc__pl
31.5									FSa_loose_pl								

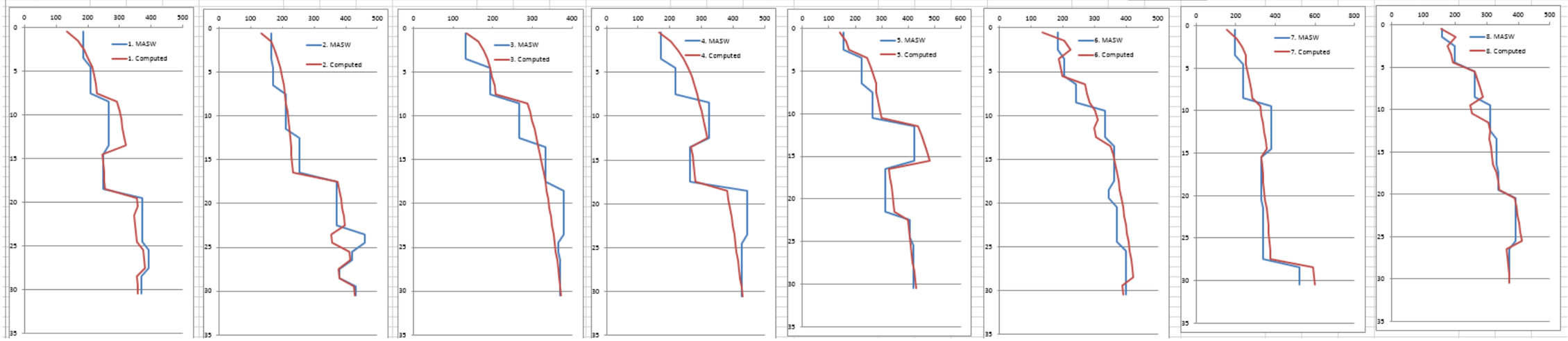

DOI: 10.15477/SZE.MMTDI.2015.002

Shear-wave profiles I to VI in Győr (A3 print)

SPI

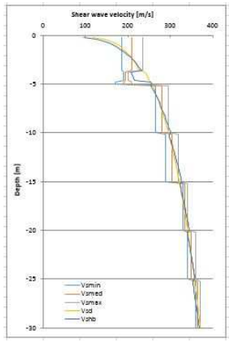

SPII

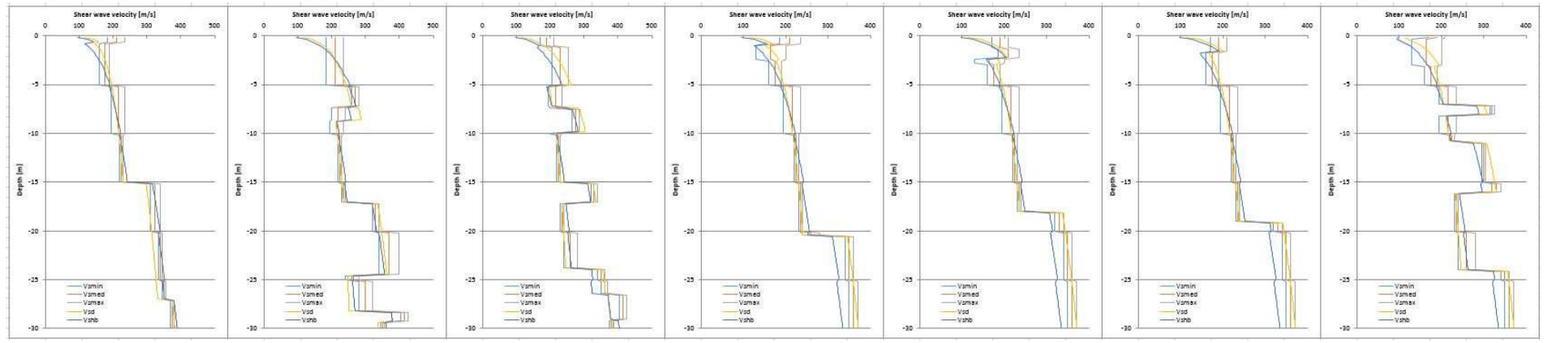

SPIII

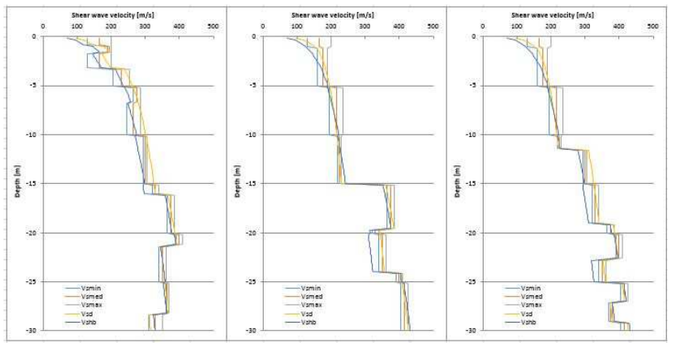

SPIV

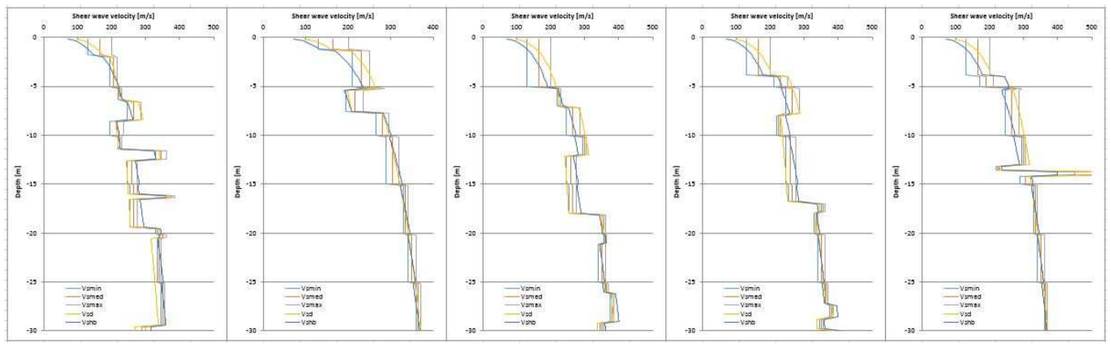

SPV

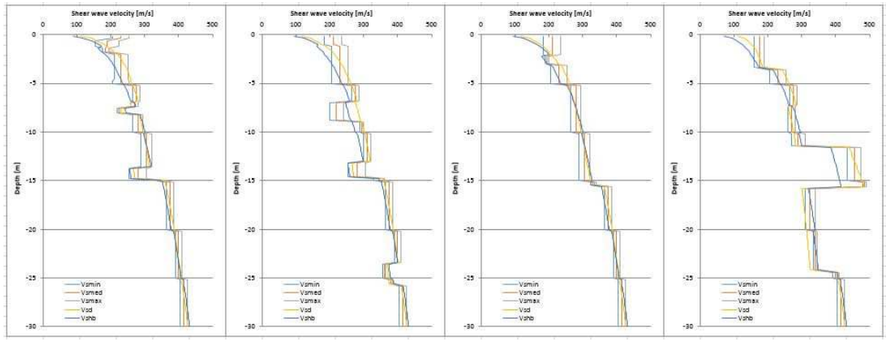

SPVI

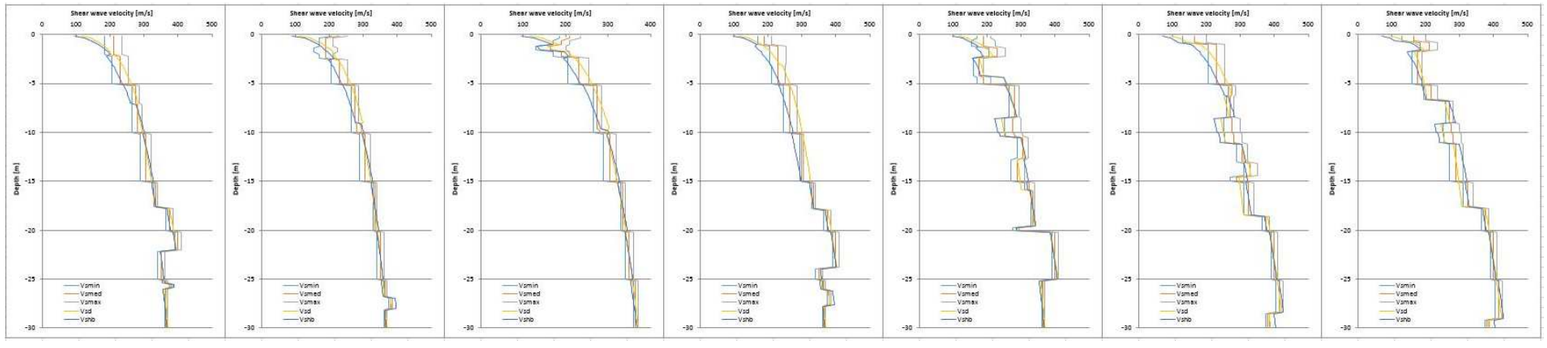

DOI: 10.15477/SZE.MMTDI.2015.002

Shear-wave profiles VII to XII in Győr (A3 print)

SPVII

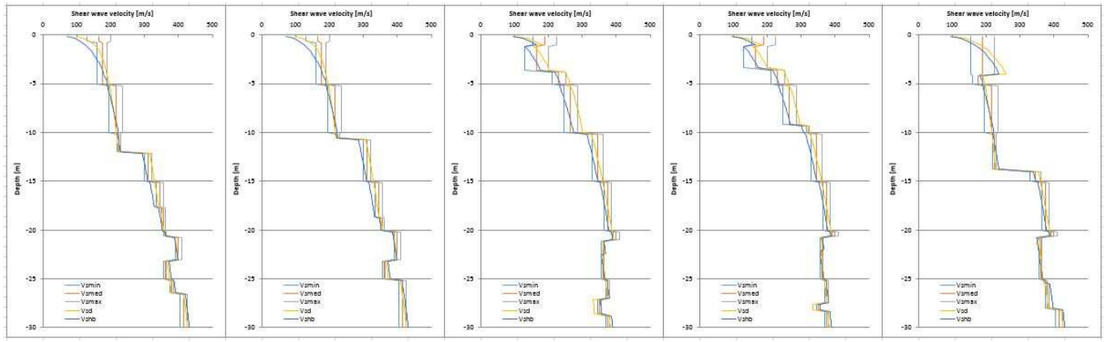

SPVIII

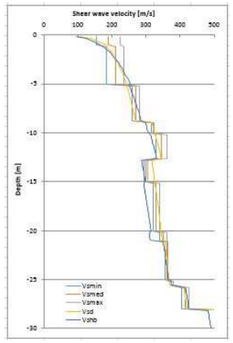

SPIX

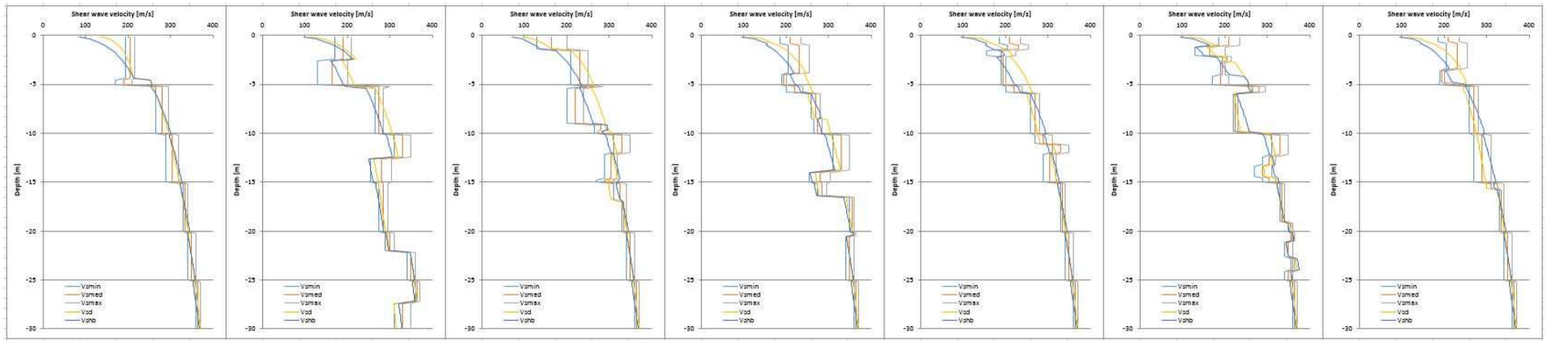

SPX

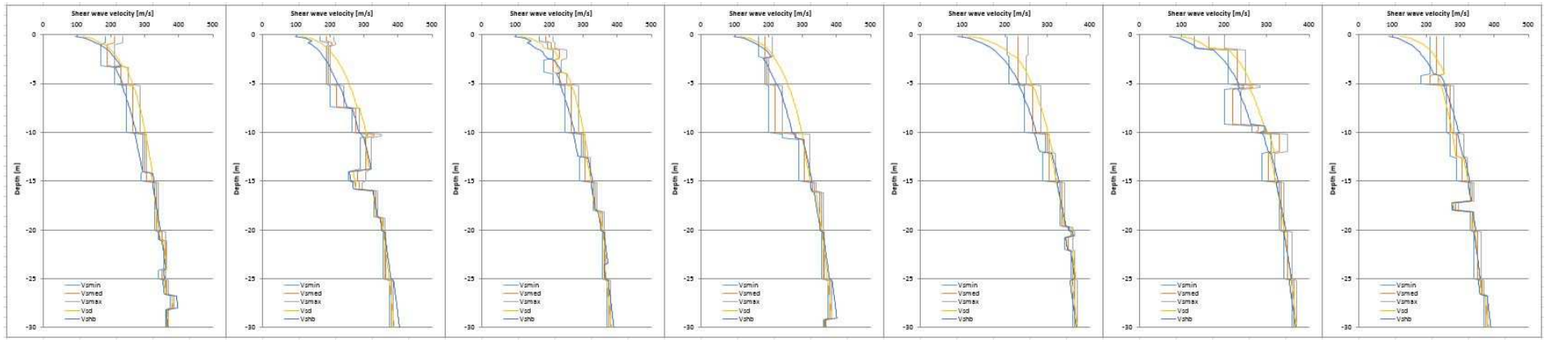

SPXI SPXII

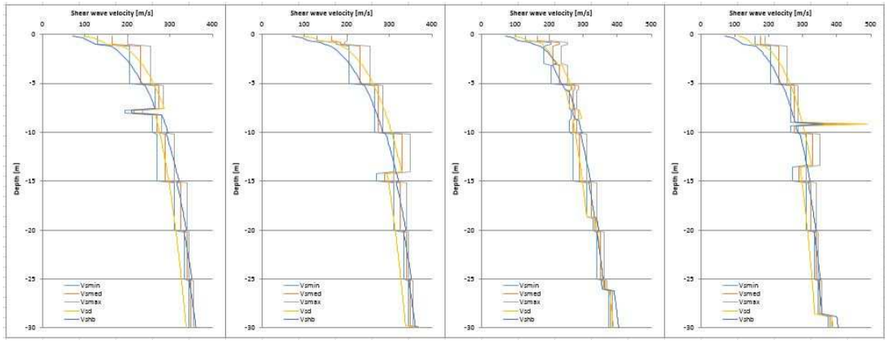

DOI: 10.15477/SZE.MMTDI.2015.002

Some sets of 7 earthquake records based on ESD and REXEL (A3 print)

T1_012_A_5-6_0-100_01

Date	Mw	Fault Mechanism	Epicentral Distance [km]	Local geology	PGA_X [m/s^2]	PGA_Y [m/s^2]	PGV_X [m/s]	PGV_Y [m/s]	EC8 Site class
1987.05.25	6.00	oblique	42	rock	0.1378	0.1308	0.0095	0.0115	A
1999.09.13	5.80	oblique	15	rock	0.7138	3.112	0.0551	0.1454	A
1984.05.07	5.90	normal	22	rock	0.628	0.6706	0.0563	0.0385	A
1997.09.26	6.00	normal	59	rock	0.1236	0.2004	0.0109	0.0144	A
1997.10.14	5.60	normal	23	rock	0.524	0.618	0.0507	0.0522	A
1990.12.13	5.60	strike slip	50	rock	0.7097	0.6395	0.0443	0.0358	A
1986.06.06	5.80	strike slip	34	rock	0.1667	0.3089	0.025	0.0382	A
	5.81		35		0.43	0.81	0.04	0.05	

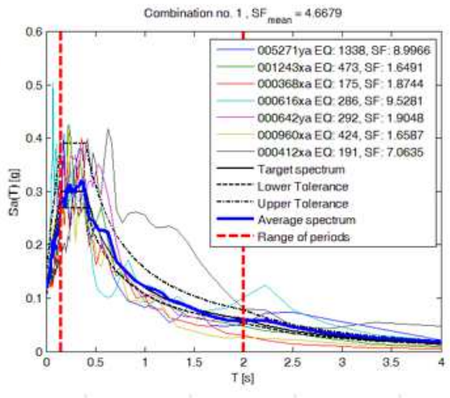

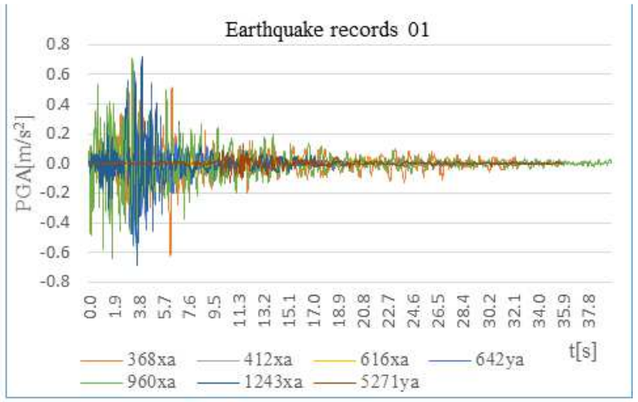

T1_012_A_5-6_0-100_02

Date	Mw	Fault Mechanism	Epicentral Distance [km]	Scaling Factor	PGA_X [m/s^2]	PGA_Y [m/s^2]	PGV_X [m/s]	PGV_Y [m/s]	EC8 Site class
1987.05.25	6.00	oblique	42		0.1378	0.1308	0.0095	0.0115	A
1999.09.13	5.80	oblique	15		0.7138	3.112	0.0551	0.1454	A
1984.05.07	5.90	normal	22		0.628	0.6706	0.0563	0.0385	A
1997.09.26	6.00	normal	59		0.1236	0.2004	0.0109	0.0144	A
1997.10.14	5.60	normal	23		0.524	0.618	0.0507	0.0522	A
1987.05.25	6.00	oblique	24		0.3222	0.243	0.0168	0.0228	A
1986.06.06	5.80	strike slip	34		0.1667	0.3089	0.025	0.0382	A
	5.871		31.29		0.37	0.75	0.03	0.05	

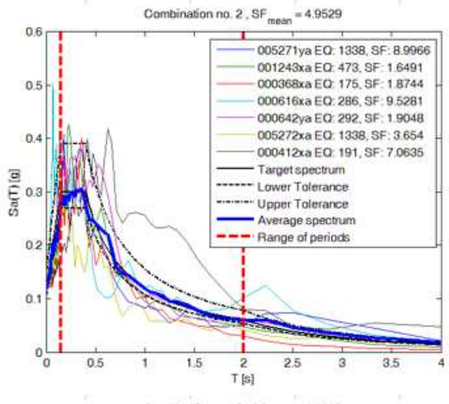

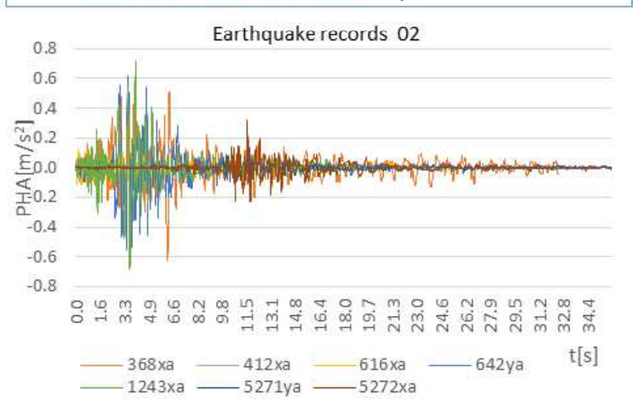

T1_012_A_5-6_0-100_03

Date	Mw	Fault Mechanism	Epicentral Distance [km]	Scaling Factor	PGA_X [m/s^2]	PGA_Y [m/s^2]	PGV_X [m/s]	PGV_Y [m/s]	EC8 Site class
1987.05.25	6.00	oblique	42		0.1378	0.1308	0.0095	0.0115	A
1999.09.13	5.80	oblique	15		0.7138	3.112	0.0551	0.1454	A
1984.05.07	5.90	normal	22		0.628	0.6706	0.0563	0.0385	A
1997.09.26	6.00	normal	59		0.1236	0.2004	0.0109	0.0144	A
1997.10.14	5.60	normal	23		0.524	0.618	0.0507	0.0522	A
1997.10.14	5.60	normal	23		0.524	0.618	0.0507	0.0522	A
1986.06.06	5.80	strike slip	34		0.1667	0.3089	0.025	0.0382	A
	5.814		31.14		0.40	0.81	0.04	0.05	

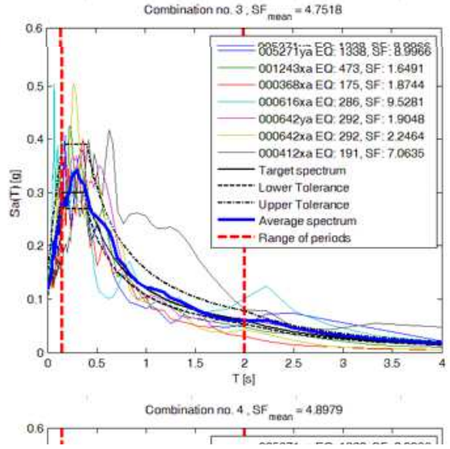

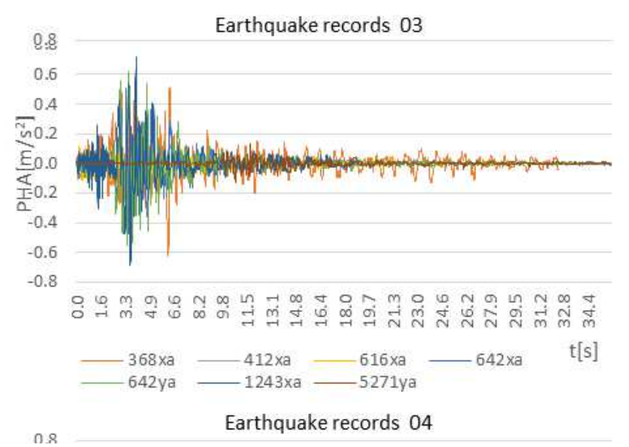

T1_012_A_5-6_0-100_04

DOI: 10.15477/SZE.MMTDI.2015.002

STRATA Results: PGA Profiles and Transfer Functions (A3 print)

II.	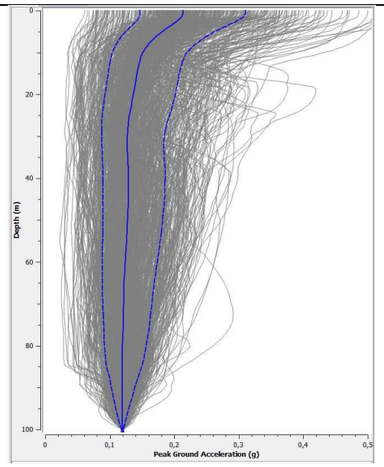	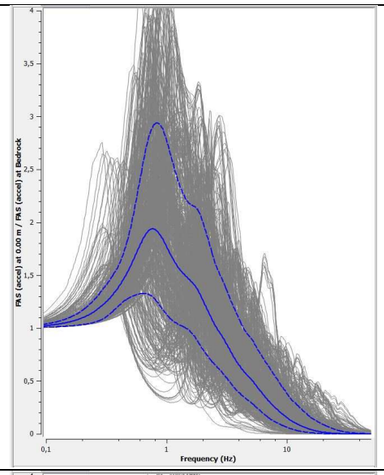	V.	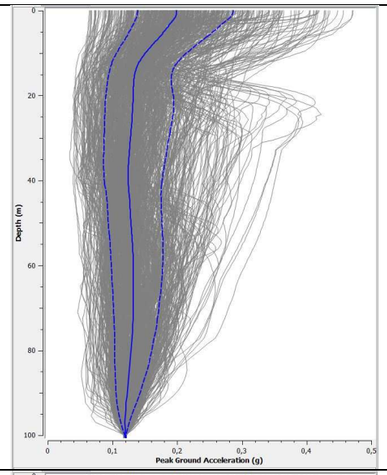	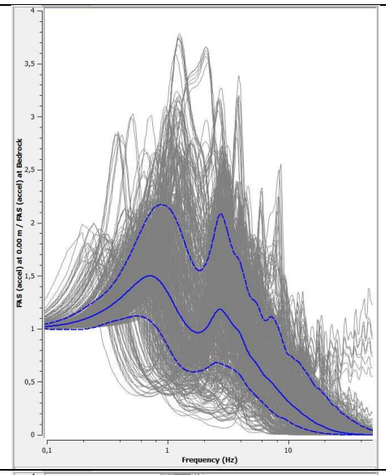
III.	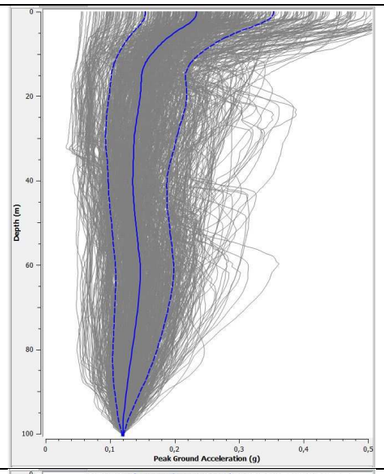	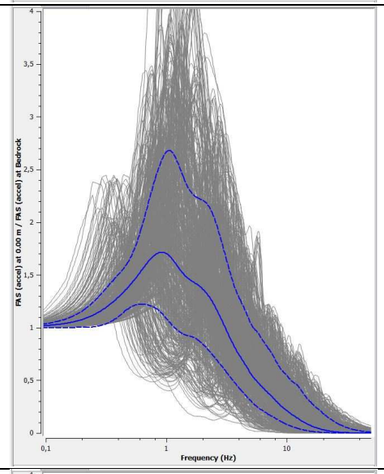	VI.	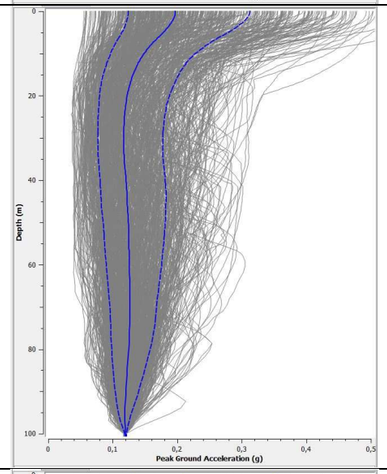	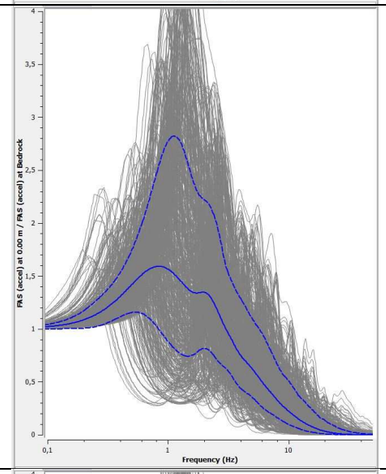
IV.	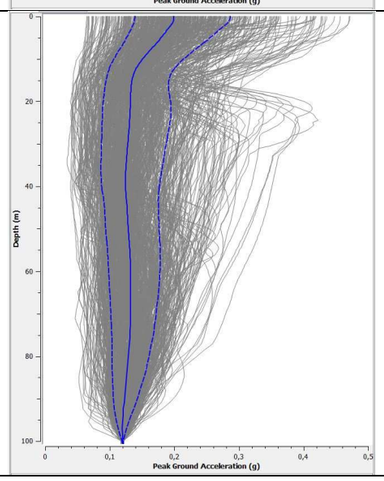	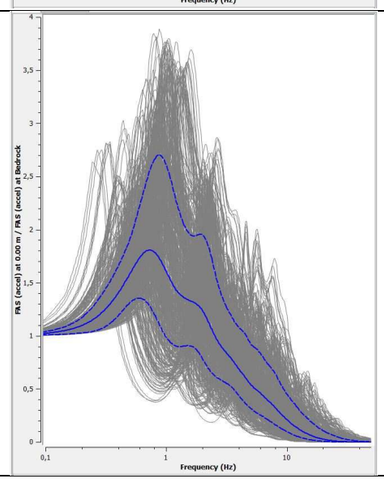	VII.	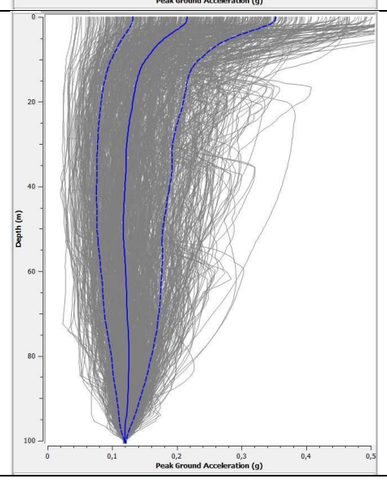	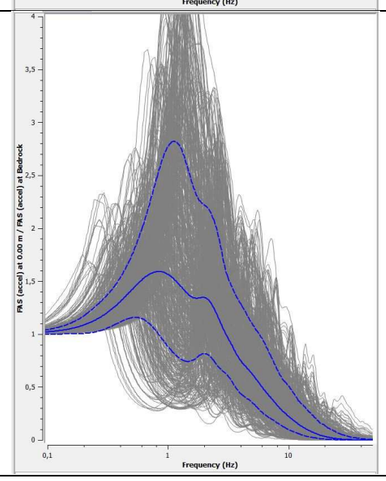

DOI: 10.15477/SZE.MMTDI.2015.002

STRATA Results: Comparison of Response Spectrum to Design Spectrum (A3 print)

II.

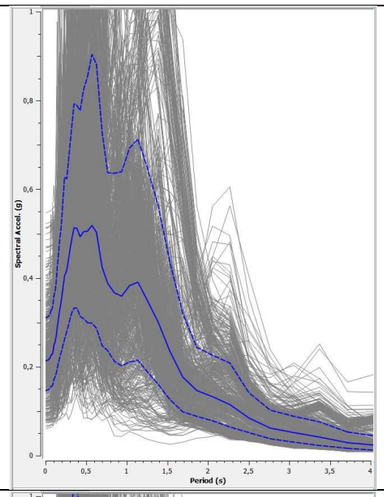

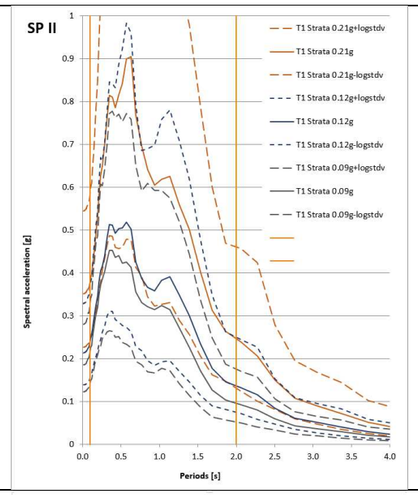

V.

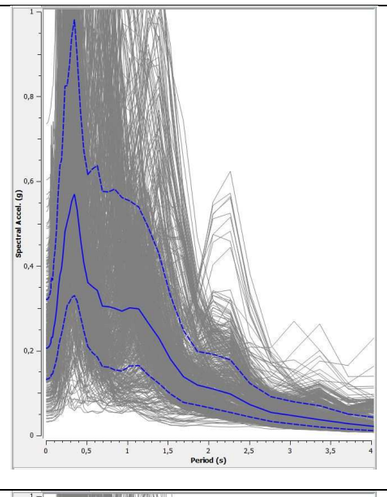

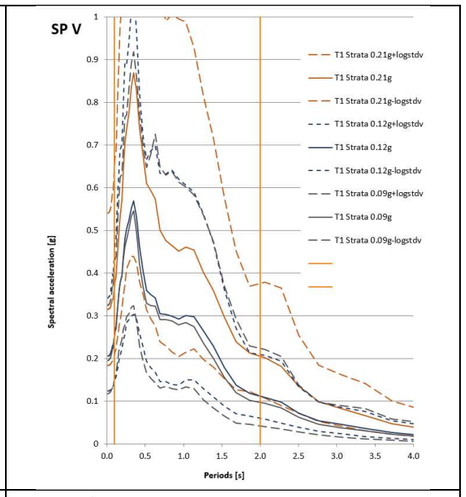

III.

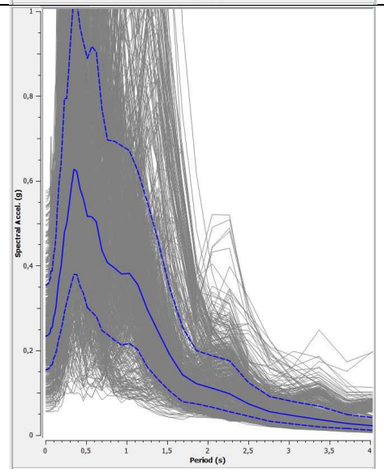

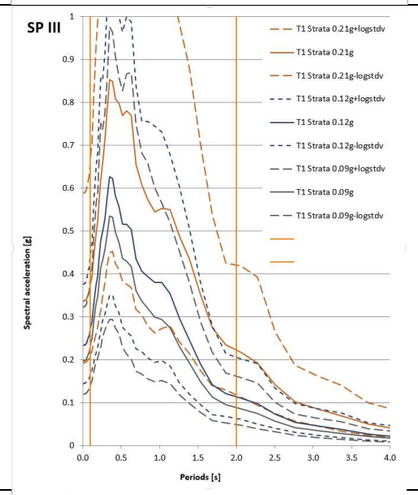

VI.

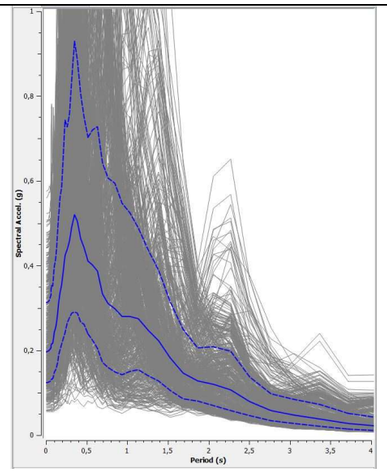

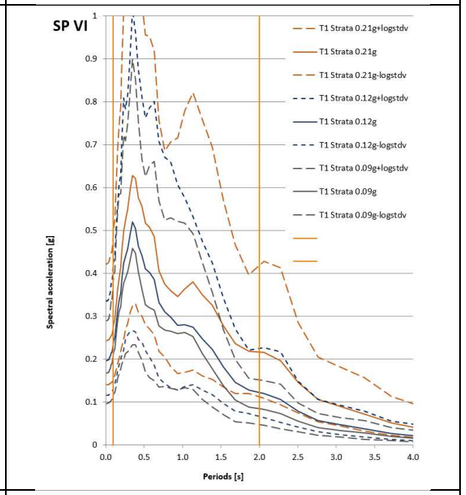

IV.

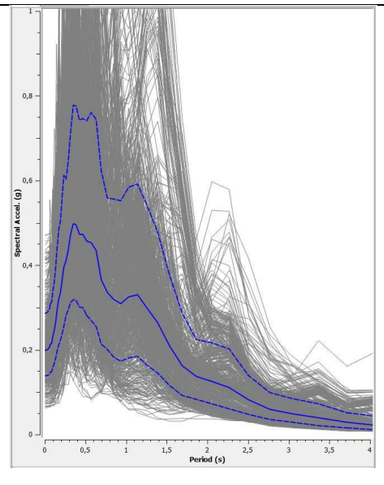

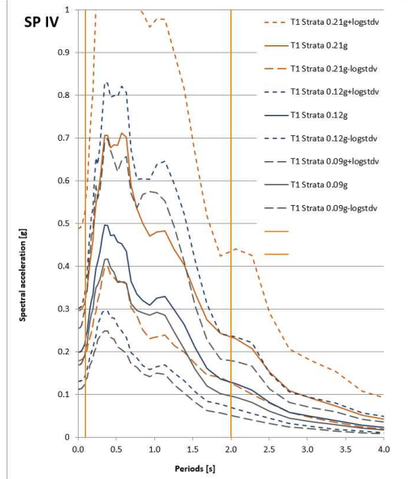

VII.

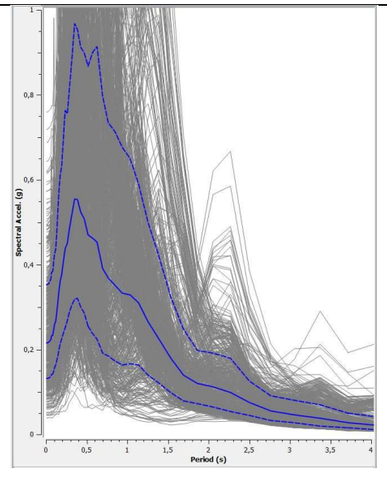

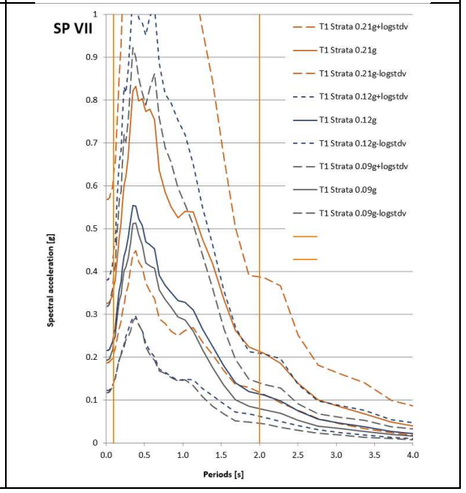

DOI: 10.15477/SZE.MMTDI.2015.002

STRATA Results: Response Spectra Based on Different Parameters (A3 print)

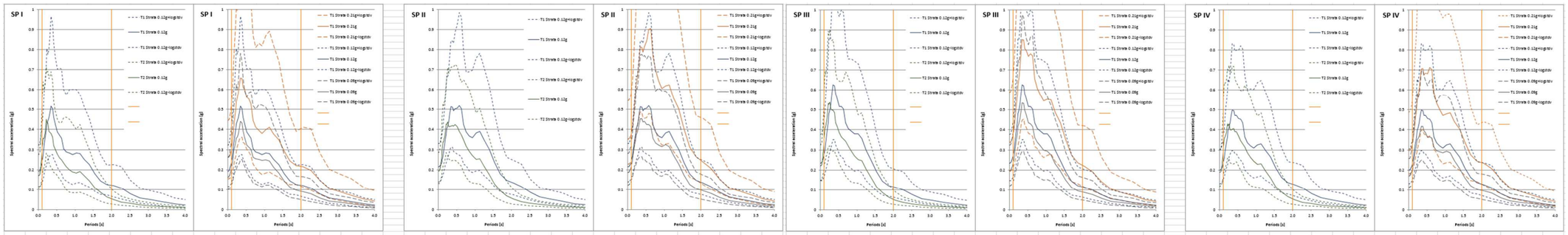

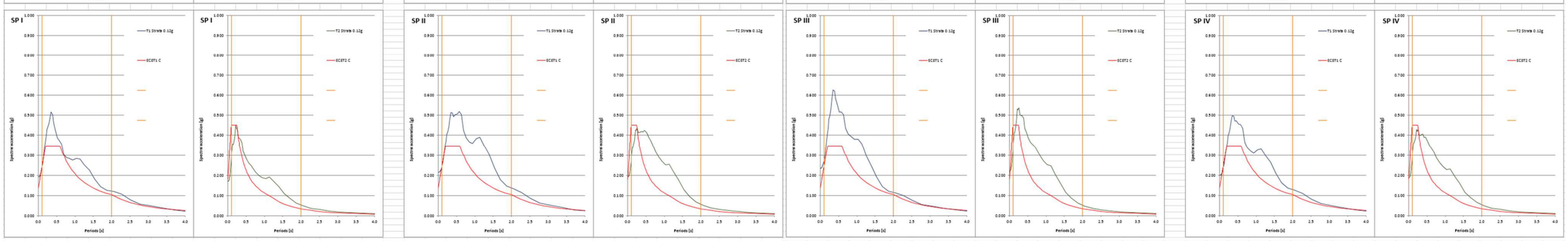

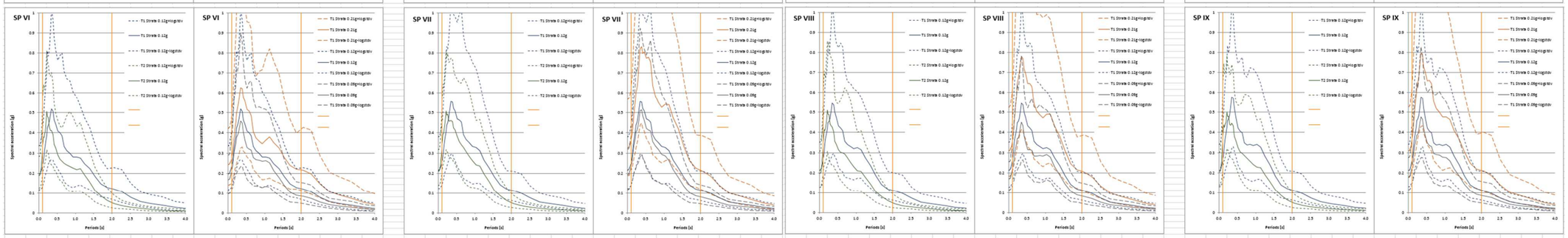

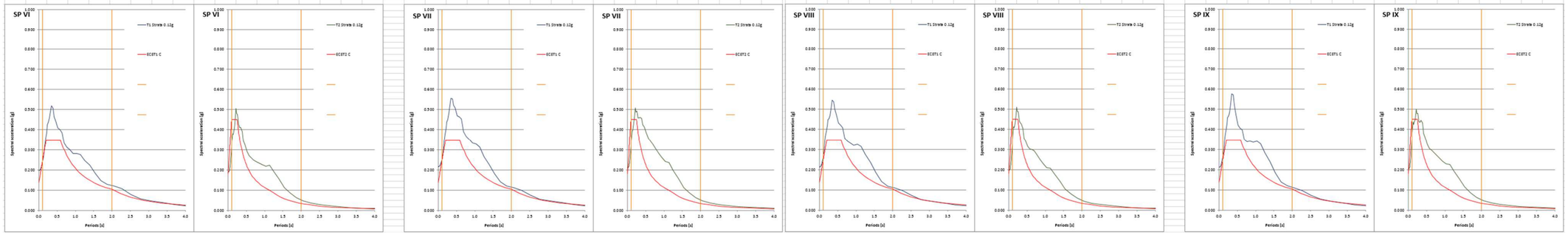

DOI: 10.15477/SZE.MMTDI.2015.002

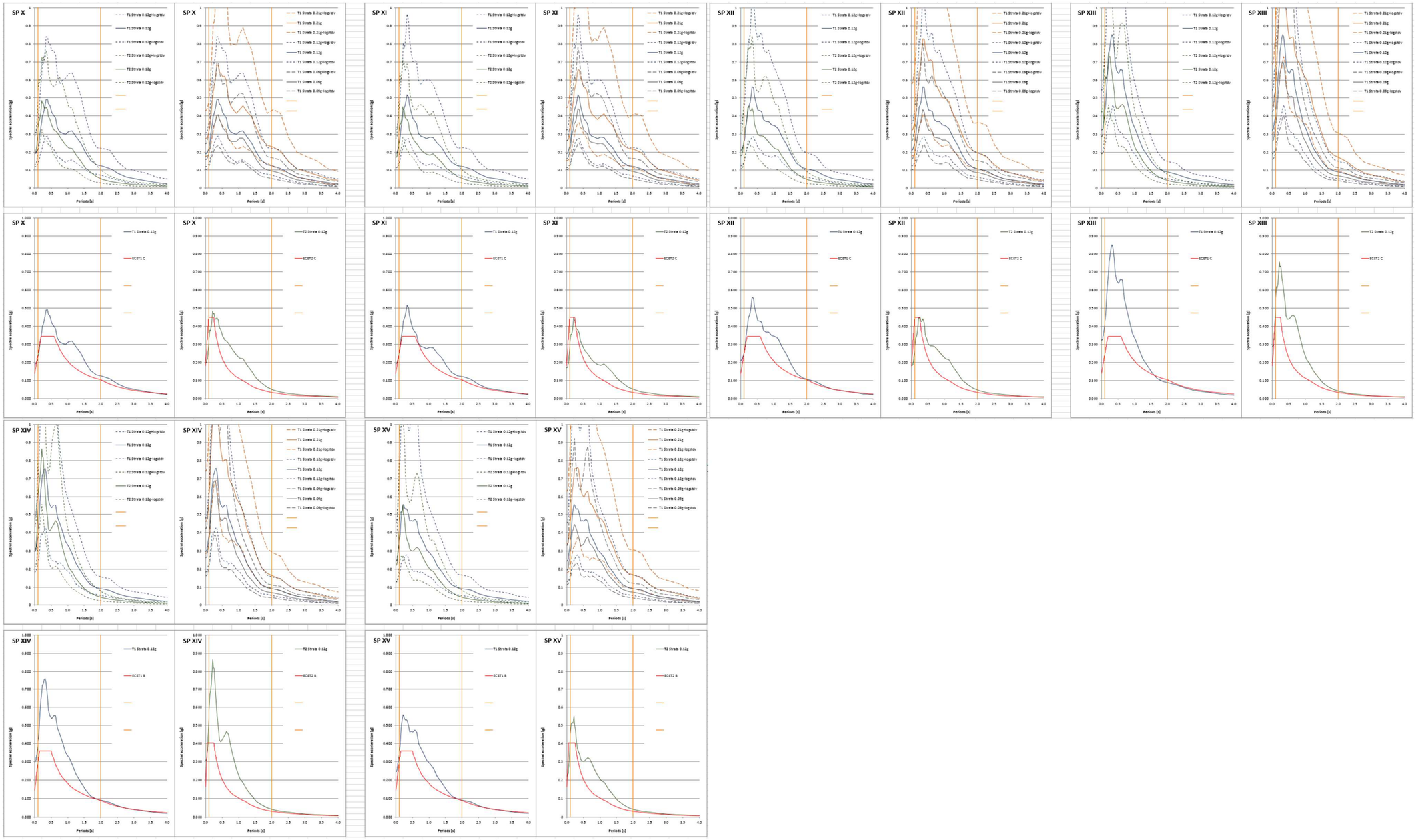

DOI: 10.15477/SZE.MMTDI.2015.002

Properties of Zones in Győr (A3 print)

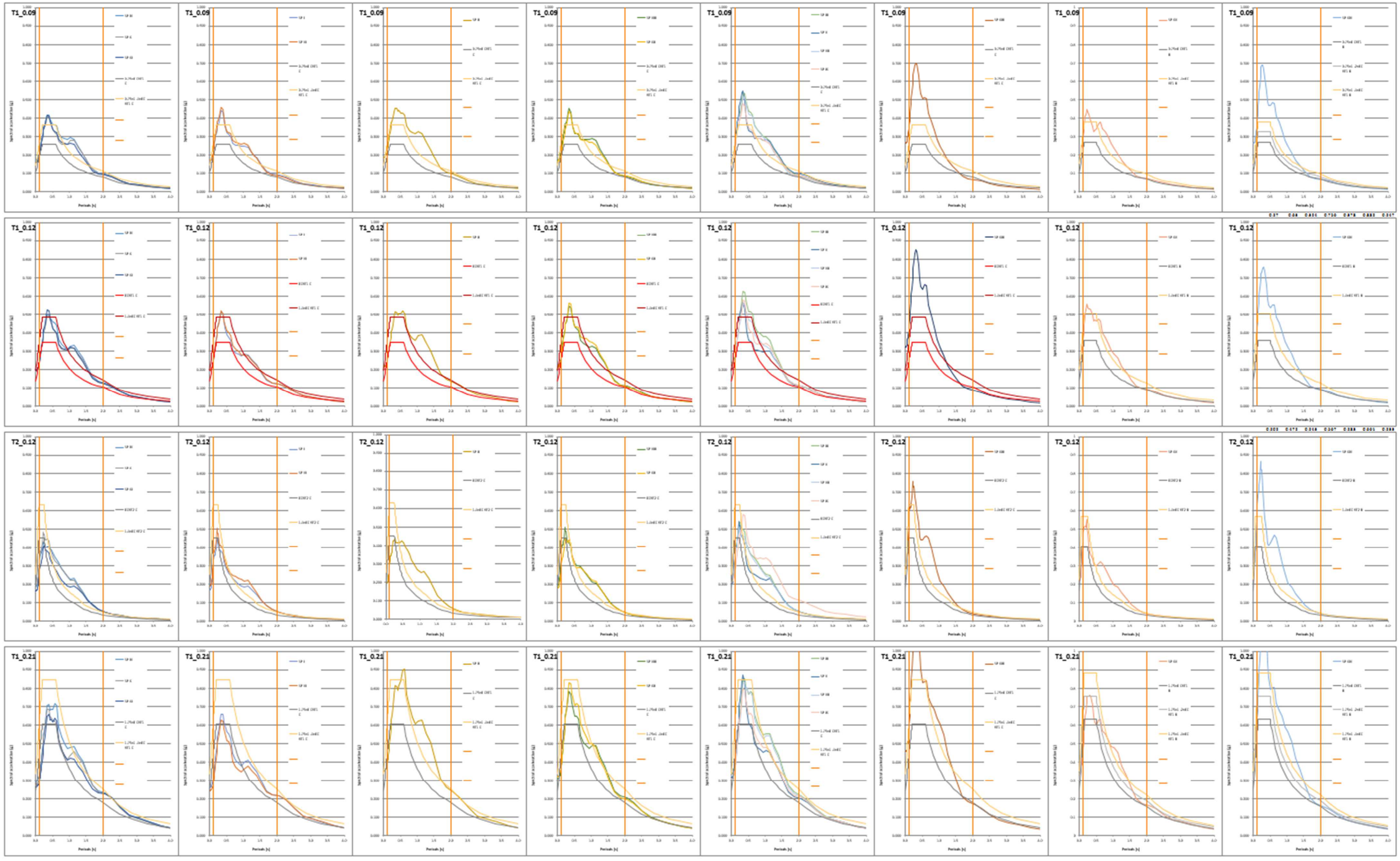

DOI: 10.15477/SZE.MMTDI.2015.002

Number of Different Building Structures in Two City Districts

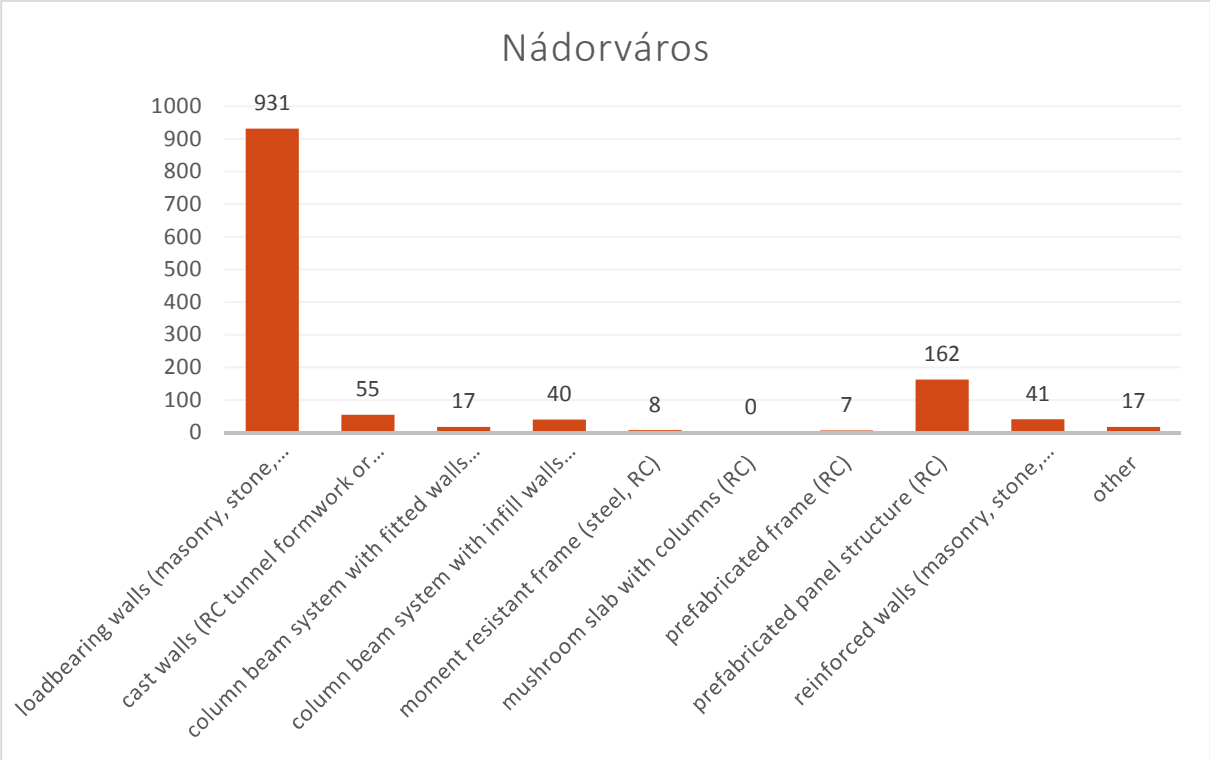

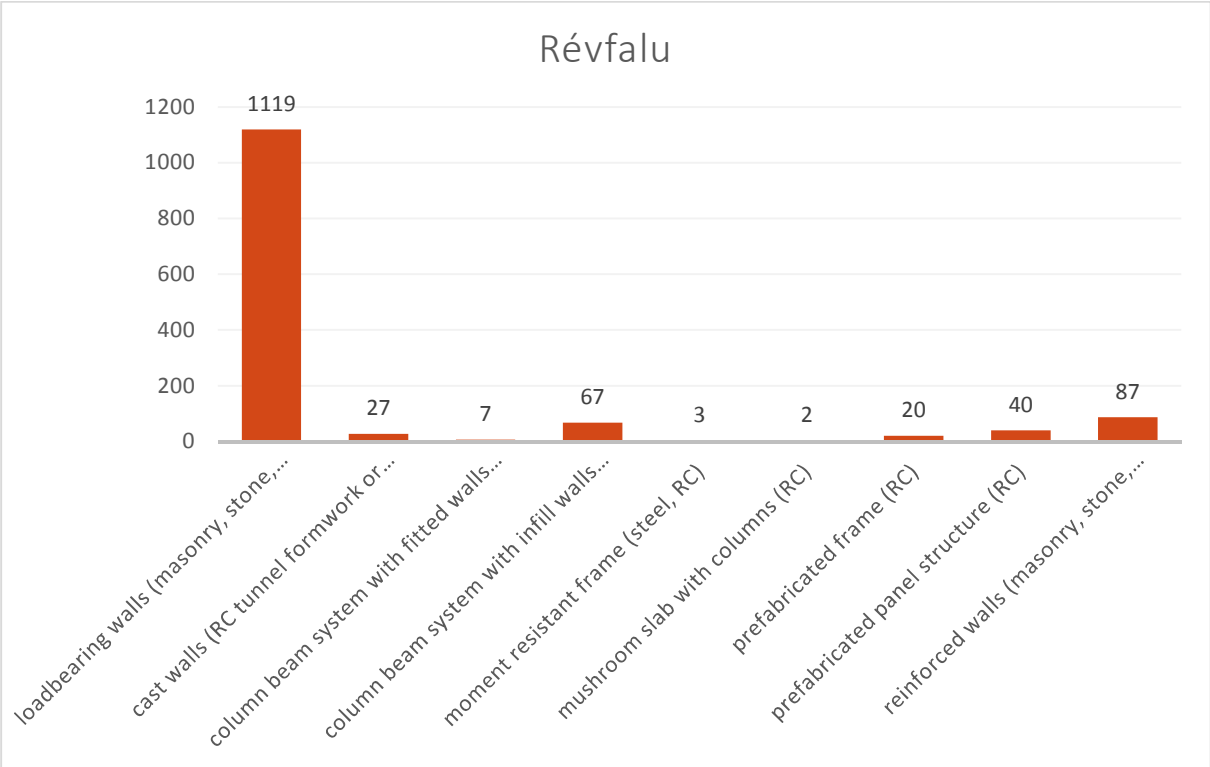

DOI: 10.15477/SZE.MMTDI.2015.002

FEMA Scores of Belváros without and with Soil Modification Factor

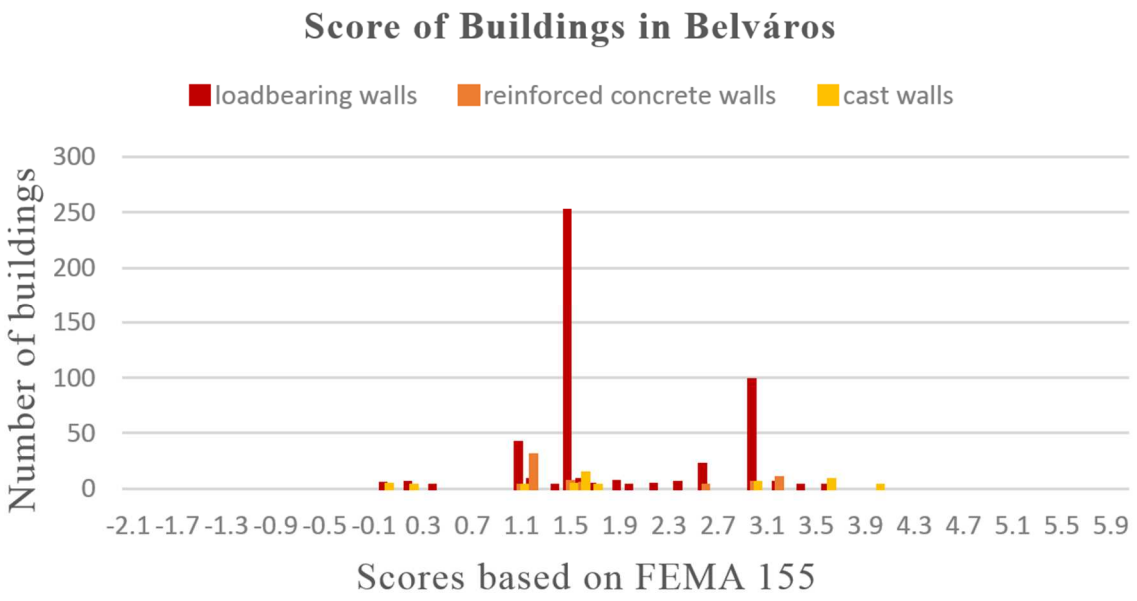

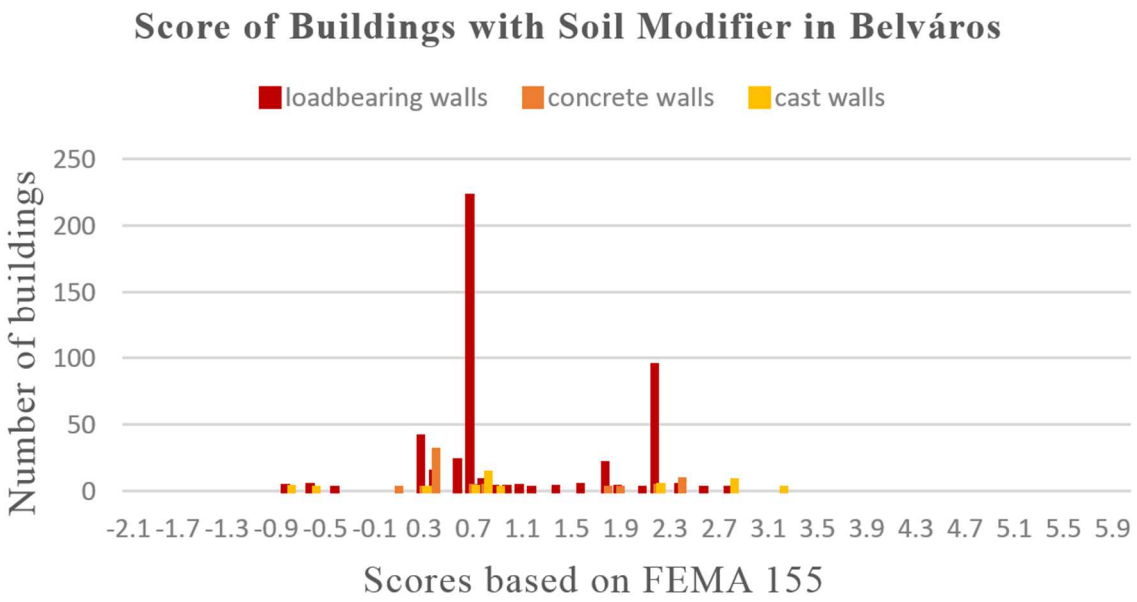

DOI: 10.15477/SZE.MMTDI.2015.002

FEMA Scores of Belváros without and with Soil Modification Factor

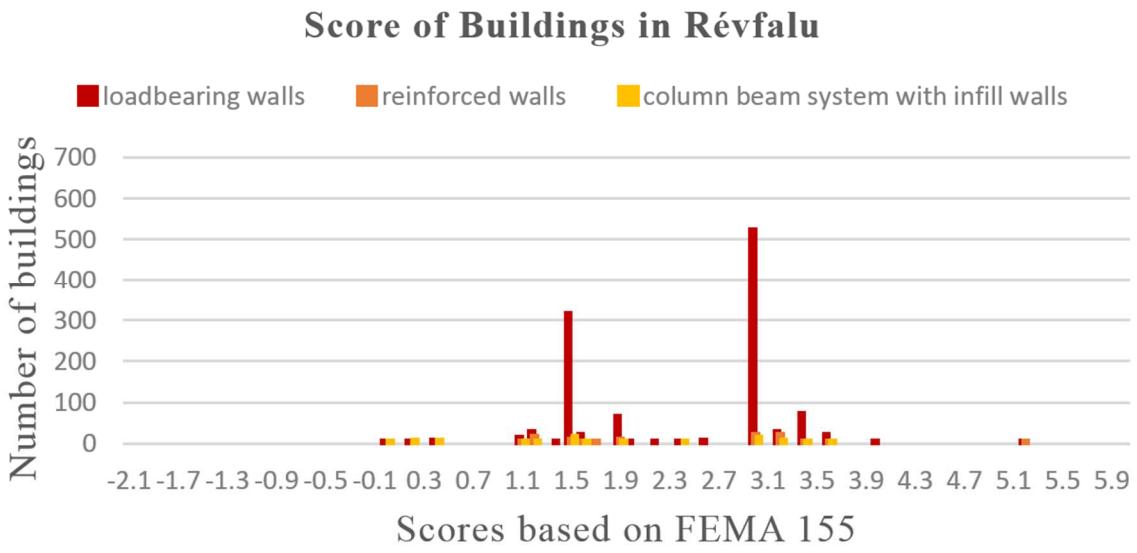

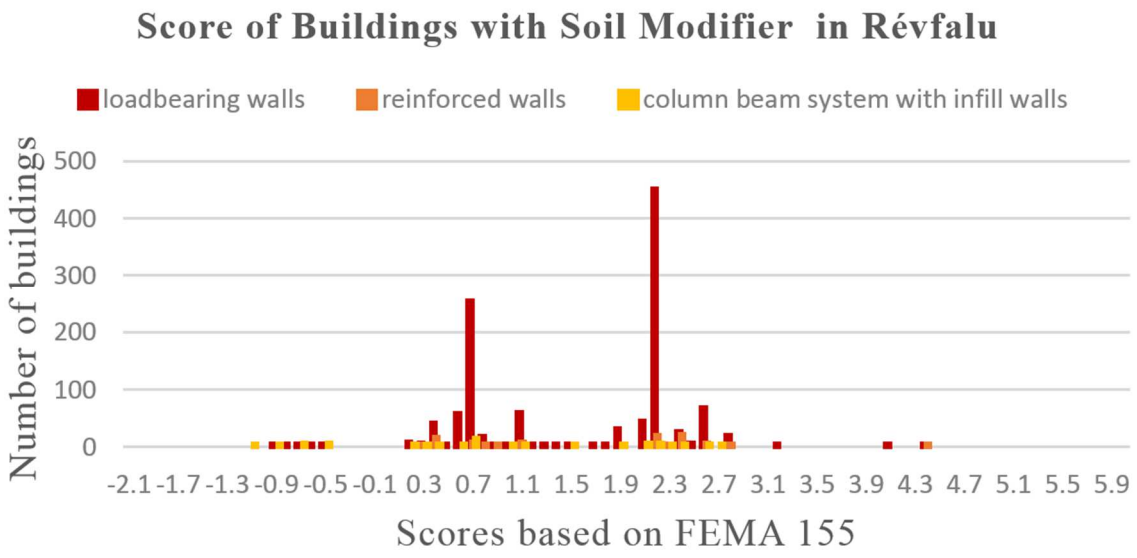

DOI: 10.15477/SZE.MMTDI.2015.002

FEMA Structural Scores in Different City Districts Taking into Account Two Scenarios

TOWN PARTS					TOTAL
Function of the area	Belváros	Nádorváros	Újváros	Révfalu	
economic, commercial, industrial	2.51%	30.23%	8.34%	1.49%	
special (cultural, educational, ecclesiastic)	69.79%	14.72%	5.94%	9.57%	
rural residential	-	7.69%	50.25%	36.97%	
garden city residential	-	29.74%	15.11%	34.49%	
urban residential	4.89%	12.46%	0.40%	0.14%	
Total area [ha]	90.49	256.37	117.39	263.81	*728*
Number of residents	10,358	20,130	4,397	6,640	*41,525*
Soil profile	C1	C1/C2/C5	C2/C5	C1/C3	
Basic Structural Hazard Score	2.7	4.2	4.2	4.2	
Modifier of soil	-0.4	-0.6	-0.6	-0.5	
Structural Hazard Scores Scenario I.	2.3	3.6	3.6	3.7	
Structural Hazard Scores Scenario II.	0.7	2.0	2.0	2.1	

HOUSING ESTATES					TOTAL
Function of the area	Adyváros	Marcalváros I.	Marcalváros II.	József A. lt.	
economic, commercial, industrial	1.98%	10.42%	8.28%	7.44%	
special (cultural, educational, ecclesiastic)	20.41%	22.56%	14.85%	-	
rural residential	0.24%	-	-	8.63%	
garden city residential	2.32%	6.83%	2.33%	1.17%	
urban residential	44.70%	32.46%	15.99%	47.16%	
Total area [ha]	57.81	38.68	92.49	25.53	*215*
Number of residents	17,156	11,423	6,841	4,508	*39,928*
Soil profile	C2	C2/C5	C1/C5	C2/C5	
Basic Structural Hazard Score	4.8	4.8	4.8	4.8	
Modifier of soil	-0.9	-1.1	-1.0	-1.1	
Structural Hazard Scores Scenario I.	3.9	3.7	3.8	3.7	
Structural Hazard Scores Scenario II.	2.3	2.1	2.2	2.1	

GARDEN CITIES						TOTAL
Function of the area	Gorkijváros	Sziget	Gyárváros 4.	Jancsifalu	Szabadhegy	
economic, commercial, industrial	-	4.56%	3.54%	27.21%	6.43%	
special (cultural, educational, ecclesiastic)	-	7.48%	1.81%	2.93%	3.71%	
rural residential	100.00%	7.55%	51.56%	54.40%	47.17%	
garden city residential	-	44.02%	23.91%	7.34%	26.94%	
urban residential	-	9.15%	15.78%	8.12%	1.76%	
Total area [ha]	10.74	55.13	38.61	15.73	297.04	*417*
Number of residents	892	4,556	4,898	1,727	8,121	*20,194*
Soil profile	C2	C5	C5	C2/C5	C4/C5	
Basic Structural Hazard Score	4.6	4.6	4.6	4.6	4.6	
Modifier of soil	-0.5	-0.8	-0.8	-0.6	-0.7	
Structural Hazard Scores Scenario I.	4.1	3.8	3.8	4.0	3.9	
Structural Hazard Scores Scenario II.	2.5	2.2	2.2	2.4	2.3	

ATTACHED VILLAGES								
Function of the area	Pinnyéd	Kisbácsa	Bácsa	Likócs	Kismegyer	Győrszentiván	Gyirmót	Ménfőcsanak
economic, commercial, industrial	0.41%	-	1.84%	17.51%	4.18%	2.47%	3.05%	2.01%
special (cultural, educational, ecclesiastic)	1.98%	-	2.40%	0.49%	2.15%	1.42%	0.90%	1.74%
rural residential	58.45%	84.38%	85.82%	66.75%	55.37%	66.20%	54.09%	75.19%
garden city residential	30.30%	1.16%	2.45%	-	6.92%	2.30%	1.73%	5.04%
urban residential	-	-	-	-	-	-	-	-
Total area [ha]	95.74	130.47	76.13	61.12	110.47	634.24	176.20	560.80
Number of residents	646	3,045	2,378	1,365	1,344	8,172	1,273	6,964
Soil profile	C3	C1	C1	C1	C4/B2	C1	C4/B1	C4/C6
Basic Structural Hazard Score	4.6	4.6	4.6	4.6	4.6	4.6	4.6	4.6
Modifier of soil	-0.6	-0.4	-0.4	-0.4	-0.7	-0.4	-0.7	-0.8
Structural Hazard Scores Scenario I.	4.0	4.2	4.2	4.2	3.9	4.2	3.9	3.8
Structural Hazard Scores Scenario II.	2.4	2.6	2.6	2.6	2.3	2.6	2.3	2.2

DOI: 10.15477/SZE.MMTDI.2015.002

Detailed Results of a Typical Masonry Structure "*A*"

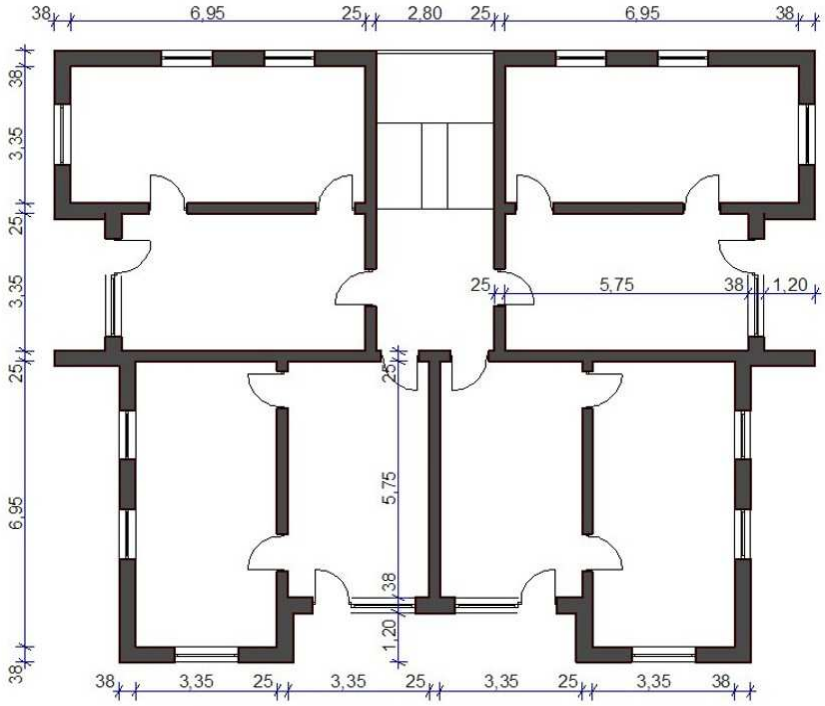

A.1. Figure: Layout of the building A (Kegyes-Brassai, 2006)

A.1. Table: Comparison of shear forces and shear capacities in the case of building A

Wall	Shear force (x)	Shear capacity	Wall	Shear force (y)	Shear capacity
			1	92,1665	190
11	10,54961	97,28	2	10,19288	91,2
12	8,692607	91,2	3	9,69168	89,68
13	**1502,844**	**384**	4	13,10335	99,18
14	34,41342	109	5	13,10335	99,18
15	114,0272	162,5	6	41,38643	110
16	32,00767	140,6	7	113,5644	154
17	16,38793	112,48	8	7,595304	62,5
18	18,82496	117,8	**9**	**588,8392**	**266,5**
			10	**1694,547**	**379**

DOI: 10.15477/SZE.MMTDI.2015.002

Detailed Results of a Typical Masonry Structure *"B"*

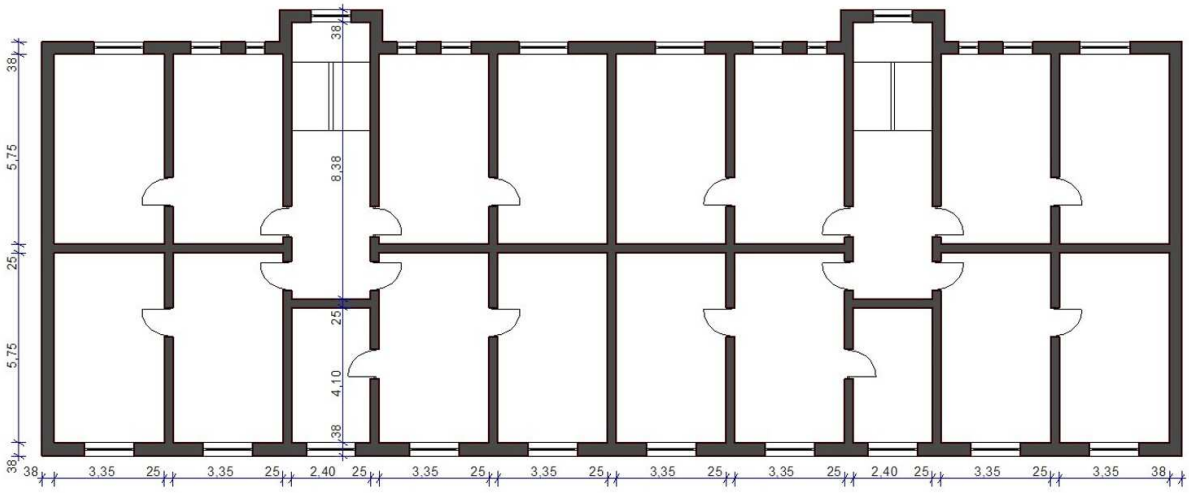

A.2. Figure: Layout of the building B (Kegyes-Brassai, 2006)

A.2. Table: Comparison of shear forces and shear capacities in the case of building B

Wall	Shear force (x)	Shear capacity	Wall	Shear force (y)	Shear capacity
9	8,361377	115,52	**1**	**1809,917**	**950,76**
10	15,82051	142,88	2	54,68616	224,00
11	13,42787	135,28	3	3,259549	87,50
12	21,73631	158,84	4	70,68108	244,00
13	21,11826	157,32	5	135,351	303,00
14	**683,294**	**379,00**	6	4,72106	99,00
15	**4933,02**	**732,50**	7	0,608196	50,00
16	5,247701	98,80	**8**	**1190,739**	**625,50**
17	13,24521	134,52			
18	22,43811	160,36			

DOI: 10.15477/SZE.MMTDI.2015.002

Detailed Computation of a Typical Reinforced Concrete Structure

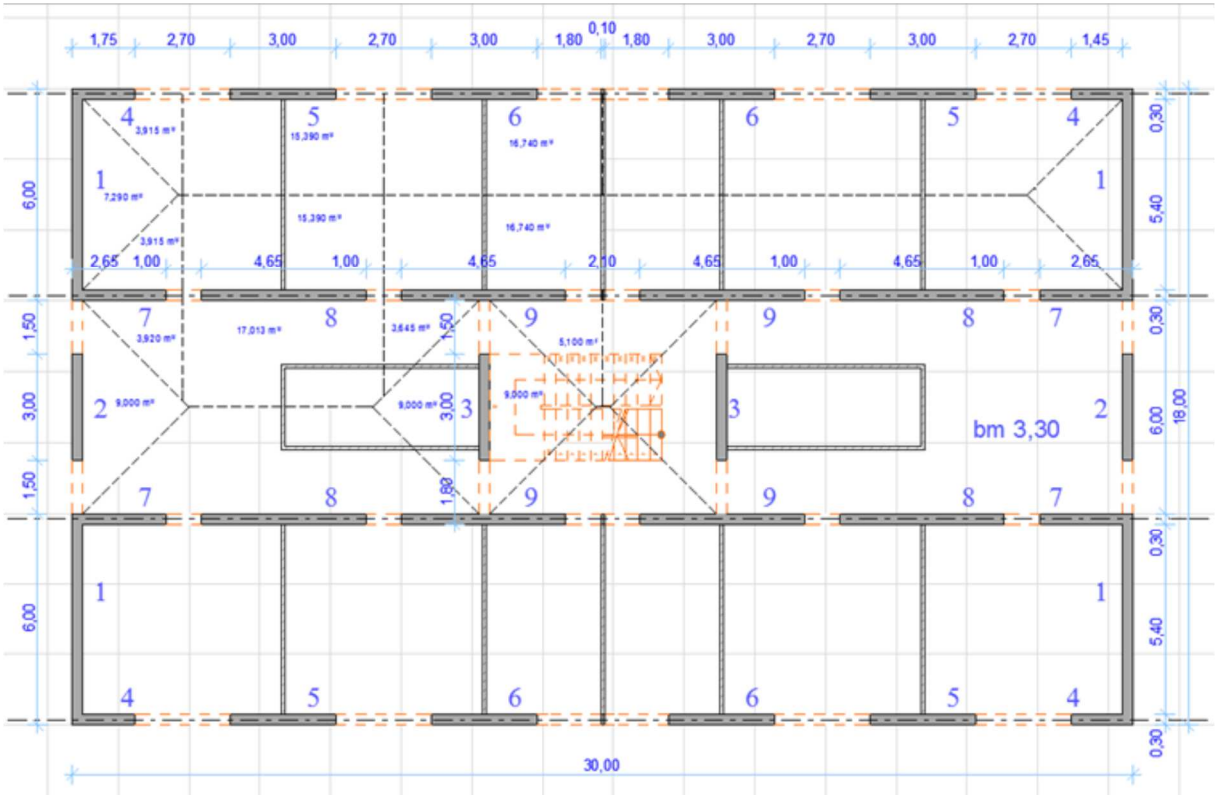

A.3. Figure: Layout of the typical reinforced building and the reinforcement

fy [kN/m2]	500000
fyh [kN/m2]	240000
fc0' [kN/m2]	33000
Es [kN/m2]	210000000
Ec [kN/m2]	30000000
ey	0.002381
esu	0.025000
ec	0.001100

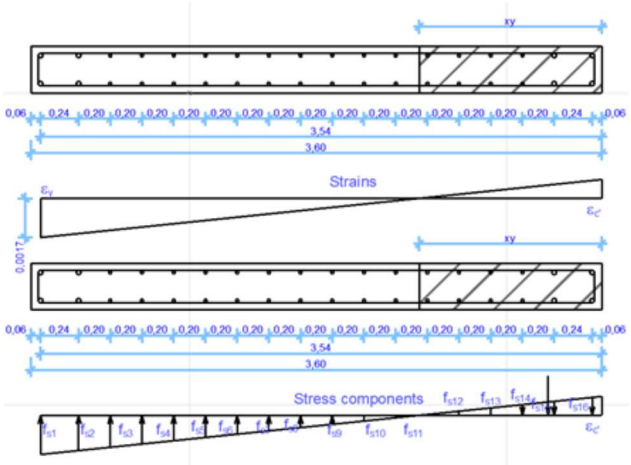

$$\phi'_y = \frac{\varepsilon_y}{(d - x_y)} \qquad \phi_u = \frac{\varepsilon_{cu}}{x_u} \qquad \phi_y = \phi'_y \cdot \frac{M_u}{M_y} \qquad \mu_\phi = \frac{\phi_u}{\phi_y}$$

$$EI_{eff} = \frac{M_y}{\phi'_y}$$

$$V_m = \frac{M_u}{h_0} \qquad V_c = t \cdot z \cdot k \cdot \sqrt{f'_c}$$

$$\Delta_y = V_m \cdot H_{tot} \cdot \left(\frac{h_p \cdot (3h_0 - h_p)}{6 \cdot EI_{eff}} + \frac{\kappa}{GA_{eff}} \right)$$

DOI: 10.15477/SZE.MMTDI.2015.002

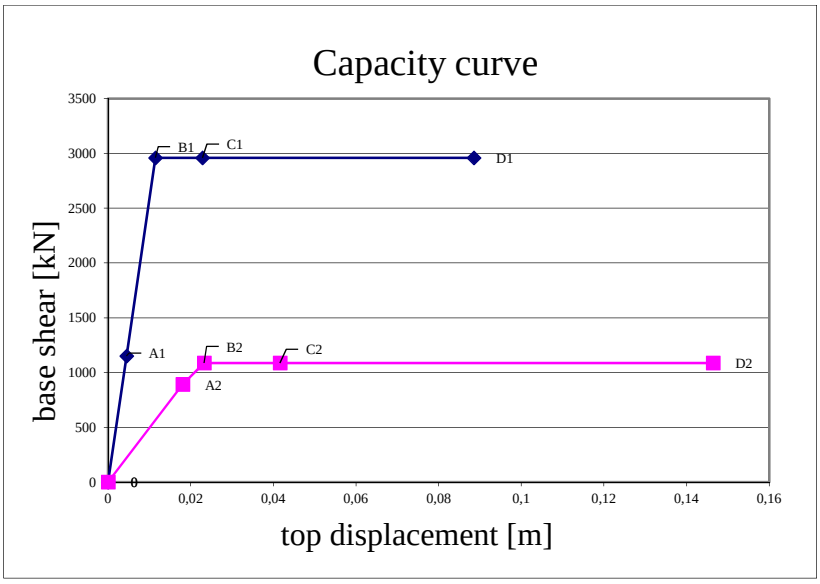

A.4. Figure: Capacity curves of wall elements

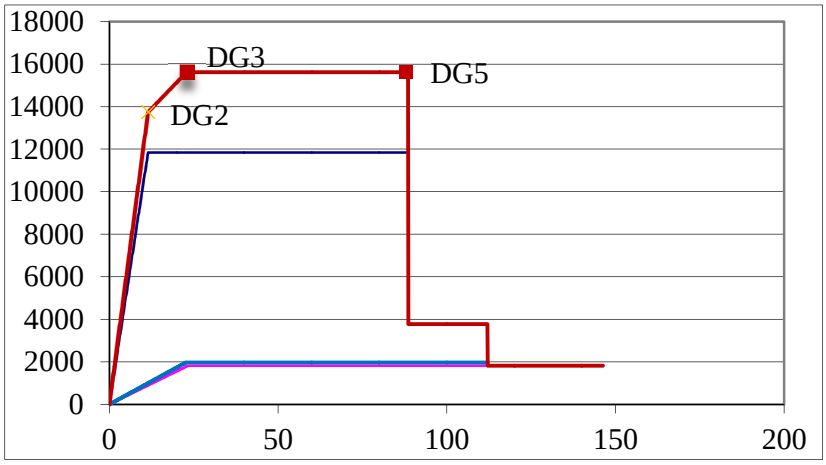

A.5. Figure: Shear capacity of the building

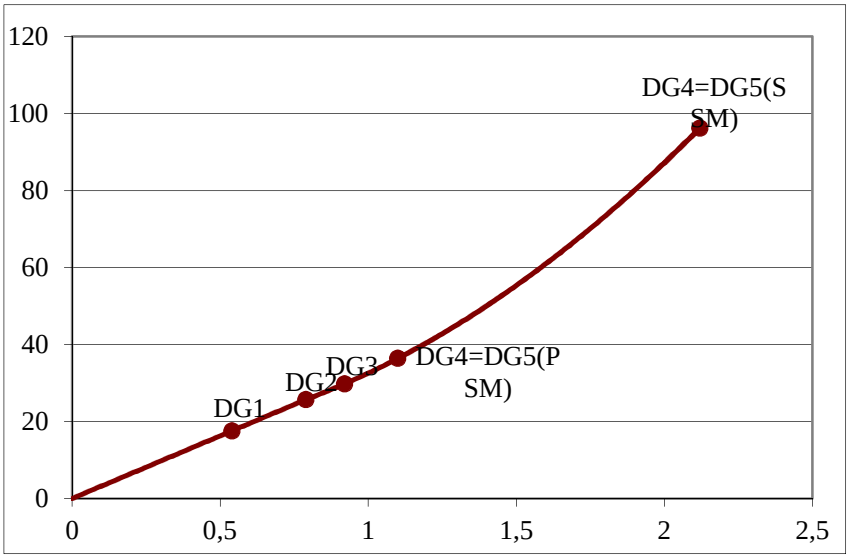

A.6. Figure: Vulnerability function of the building

DOI: 10.15477/SZE.MMTDI.2015.002

Lists

List of Symbols

EI_{sp}	flexural stiffness of the spandrel
EI_{p}	flexural stiffness of the pier
Δ_u	ultimate displacement
Δ_y	yield displacement
$v_{s,30}$	average shear-wave velocity in the upper 30 m
h_0	height of zero moment
h_p	height of the pier
$\mathbf{K}_T$	current nonlinear (tangent) stiffness matrix
$\mathbf{P}_0$	initial load
$\mathbf{P}^e$	equilibrated load (reaction) of the previous iteration
A_{m+1}, B_{m+1}	wave amplitudes
F_r	normalized friction ratio
G^*	complex shear-modulus, not the approximation, in the calculations
G_{MAX}	shear modulus of the soil at low strain amplitudes, e.g. during a field seismic test
H_{tot}	total height of the building
I_a	Arias Intensity
I_c	soil behavior type index
Q_t	normalized cone penetration resistance
S_a	Spectral Acceleration
S_d	Spectral Displacement
S_d	displacement demand
S_v	Spectral Velocity
Y_m	Fourier amplitude spectrum at the top of the layer of interest
Y_n	input Fourier amplitude spectrum at layer n
a_n	net area ratio
a_{rms}	RMS Acceleration
f_s	sleeve friction
p_a	atmospheric pressure
q_c	cone resistance

DOI: 10.15477/SZE.MMTDI.2015.002

u_2 pore pressure

v_s Shear wave Velocity in soil

v_{s1} Shear wave Velocity in soil taking into account different GWL

γ_{soil} unit weight of the soil (kN/m^3)

ρ_{soil} mass density of the soil

σ_v, vertical total stress

Δ displacement

$\mathbf{\Delta U}$ calculated displacement increment within an iteration

h_m layer height

α_m complex impedance ratio

Γ modal participation factor

D damping ratio

DM a Damage Measure representing the performance of the structure under consideration (e.g. displacement ductility for buildings/bridge, building settlement for foundations, slope displacement for waterfront structures).

DV a Decision Variable that can be understood and used by owners/policy makers (e.g. cost, down time, etc.).

G soil shear modulus

IM an Intensity Measure of the ground motion (e.g., spectral acceleration, duration).

d horizontal deformation

$dv(IM)$ Derivative with respect to IM of the Poisson rate of IM exceeding some threshold value.

f fundamental frequency of the equivalent SDOF system

g acceleration due to Gravity ≈ 9.807 m/sec^2

t time

u displacement

z depth

δ drift

λ load factor within the corresponding load increment

$v(DV)$ Poisson rate of DV exceeding some threshold value

ω wave frequency

DOI: 10.15477/SZE.MMTDI.2015.002

List of Abbreviations

a.B.s.l.	above Baltic Sea level
CGr	coarse gravel
Cl	clay
Cls	clay stone
clSa	clayey sand
CSa	coarse sand
D	dimensional
DIFF	difference
Eq.	equation
FGr	fine gravel
Fig.	figure
FSa	fine sand
grSa	gravelly sand
MGr	medium gravel
MSa	medium sand
P-wave	pressure wave
saCl	sandy clay
saGr	sandy gravel
Si	silt
siCl	silty clay
siSa	silty sand
Ss	sandstone
S-wave	shear wave
T1	type 1 spectra
T2	type 2 spectra
vs.	versus

DOI: 10.15477/SZE.MMTDI.2015.002

List of Acronyms

ADC	Analog to Digital Converter
ASI	Acceleration Spectrum Intensity
ATC	Applied Technology Council
CAV	Cumulative Absolute Velocity
CF	Confidence Factor
CF_{KF}	Confidence Factor of Full Knowledge level
CF_{KL}	Confidence Factor of Limited Knowledge level
CF_{KN}	Confidence Factor of Normal Knowledge level
CL	Class value of each city
CPT	Cone Penetration Test
CPTu	Cone Penetration Test gathering piezometer data
DC	Direct Current
DL	Damage Limitation
DMA	Disaster Mitigation Act of 2000
DPM	Damage Probability Matrices
DSHA	Deterministic Seismic Hazard Analysis
EC8	Eurocode 8: Design of Structures for earthquake resistance
EERC	Engineering Education and Research Center
ELGI	Eötvös Loránd Geophysical Institute
EMS	European Macroseismic Scale
ENSURE	Enhancing Resilience of Communities and Territories Facing Natural and Na-tech Hazards
EOV	Egységes Országos Vetületi rendszer (Unified National Projection System)
EPA	Effective Peak Acceleration
ERD	Earthquake Resistant Design
ESD	European Strong-Motion Database
ETH Zürich	Eidgenössische Technische Hochschule Zürich (Swiss Federal Institute of Technology in Zürich)
FEMA	Federal Emergency Management Agency
FFT	Fast Fourier Transform
FS	Factor Score of each city
GIS	Geographic Information System

DOI: 10.15477/SZE.MMTDI.2015.002

GWL	Ground Water Level
HAZUS	Hazards US
HMP	Hazard Mitigation Plan
IDNDR	International Decade for Natural Disaster Reduction
JBDPA	Japanese Seismic Index Method
JMA	Japan Meteorological Agency Seismic Intensity Scale
KF	Full Knowledge level
KL	Limited Knowledge level
KN	Normal Knowledge level
LS of DL	Limit State of Damage Limitation
LS of NC	Limit State of Near Collapse
LS of SD	Limit State of Significant Damage
LS	Limit State
MASW	Multichannel Analysis of Surface Waves
MB	Body wave Magnitude
ML	Local Magnitude
MMI	Modified Mercalli Intensity Scale
MS	Surface wave magnitude
MSK	Medvedev–Sponheuer–Karnik Scale
	MSZ EN 1998-1:2004/A1:2013
MW	Moment Magnitude
NC	Near Collapse
NEHRP	National Earthquake Hazards Reduction Program
NERIES	Network of Research Infrastructures for European Seismology
NRC	National Research Council
OCR	Over Consolidation Ratio
OD	Overall Damage
PBEE	Performance-Based Earthquake Engineering
PC	Personal Computer
PEER	Pacific Earthquake Engineering Research Center
PGA	Peak Ground Acceleration
PGD	Permanent Ground Deformation
PGV	Peak Ground Displacement
PGV	Peak Ground Velocity

DOI: 10.15477/SZE.MMTDI.2015.002

PHA	Peak Horizontal Acceleration
PHV	Peak Horizontal Velocity
PSHA	Probabilistic Seismic Hazard Analysis
PSI	Parameterless Scale of Intensity
PVA	Peak Vertical Acceleration
RISK-UE	Advanced Approach to Earthquake Risk Scenarios with Applications to Different European Towns
RMS	Root Mean Square
ROSRINE	Resolution of Site Response Issues in the 1994 Northridge Earthquake
RVS	Rapid Visual Screening
RVT	Random Vibration Theory
SBT	Soil Behavior Type
SCPT	Seismic Cone Penetration Test
SCPTu	Seismic Cone Penetration Test gathering piezometer data
SD	Significant Damage
SHARE	Seismic Hazard Harmonization in Europe
SP	Soil Profile
SYNER-G	Systemic Seismic Vulnerability and Risk Analysis for Buildings, Lifeline Networks and Infrastructures Safety Gain
TÁMOP	Társadalmi Megújulás Operatív Program (Social Renewal Operational Program)
TCG	Technical Chamber of Greece
UBC	Uniform Building Code
UNDRO	United Nations Disaster Relief Organization
VSI	Velocity Response Spectrum Intensity

DOI: 10.15477/SZE.MMTDI.2015.002

List of Tables

DOI: 10.15477/SZE.MMTDI.2015.002

List of Figures

DOI: 10.15477/SZE.MMTDI.2015.002